Examination of the Thermal Properties of Municipal Solid Waste and the Scalability of its Pyrolysis

by

Frances Louise Bradfield

Thesis presented in partial fulfilment

of the requirements for the Degree

of

MASTER OF ENGINEERING

(CHEMICAL ENGINEERING)

in the Faculty of Engineering

at Stellenbosch University

Supervisor

Prof. J. H. Knoetze

Co-Supervisor

Prof. J. Gorgens

April 2014

Declaration

By submitting this master's thesis, I declare that the entirety of the work contained therein is my own, original work, that I am the sole author thereof (save to the extent explicitly otherwise stated), that reproduction and publication thereof by Stellenbosch University will not infringe any third party rights and that I have not previously in its entirety or in part submitted it for obtaining any qualification.

Frances Louise Bradfield 26th February 2014

Abstract

Concerns surrounding the world's current dependence on quickly depleting fossil fuels and their negative environmental impacts have brought about much research into renewable and sustainable energy sources. With population and economic growth not only is this dependence increasing but there is an increasing production of waste by society in general. With space becoming a premium commodity and environmental protection a necessity, landfilling of the majority of the world's waste is no longer feasible. Thus, research is being carried out into waste-to-energy (WTE) processes and refuse derived fuels (RDF). This study focuses on thermochemical conversion, specifically pyrolysis of solid wastes as a means of energy product recovery.

Before a specific waste stream can be used in WTE or RDF contexts its composition and degradation behaviour needs to be investigated. For this reason, a full physical characterisation of the municipal solid waste (MSW) from the Stellenbosch municipality was carried out. It was found that the composition of waste differs between areas within the municipality but the composition of the waste in general compares well with international data. It was found that six main components present in the recyclables stream; namely high and low density polyethylene (HD/LDPE), poly(ethylene terephthalate) (PET), glossy paper, office paper and newspaper would be suitable for thermochemical conversion.

The thermal properties and pyrolytic degradation of these six components were investigated by multi heating rate thermogravimetric analysis (TGA) from which kinetic parameters (activation energy, pre-exponential factor and kinetic rate constants) were calculated by a differential isoconversional method. The volatiles released during degradation were identified by way of online mass spectrometry (TGA-MS) yielding six individual kinetic schemes.

In order to gauge to what extent milligram pyrolytic experimentation (TGA-MS) can be used to predict larger scale pyrolytic behaviour, runs were performed on one plastic (HDPE) and one paper (glossy paper) sample on a gram scale pyrolytic plant under both slow and vacuum conditions. It was found that, especially for high thermal conductivity samples, yields on gram scale experimentation can be accurately predicted on a milligram scale. Further, the compositions of slow pyrolysis oils from glossy paper, obtained by gas chromatography–mass spectrometry (GC-MS), were compared to TGA-MS results as well as off gases captured from TGA runs by thermal desorption (TGA/TD-GC-MS). It was found that TGA-MS and TGA/TD-GC-MS can be used to predict the main functional groups in pyrolysis oil produced on a gram scale. Thus small scale experimentation can be used to determine the suitability of different waste components for pyrolytic conversion.

Opsomming

Kommer oor die wêreld se huidige afhanklikheid van fossielbrandstowwe en die negatiewe uitwerking op die omgewing het baie navorsing oor hernubare en volhoubare energie bronne meegebring. Bevolking en ekonomiese groei veroorsaak 'n toename in hierdie afhanklikheid en in die produksie van afval deur die samelewing. Daar is baie min onbenutte grond oop en die beskerming van die omgewing het noodsaaklik geword. Dus is storting van die meeste van die wêreld se afval nie meer ‘n aanvaarbare opsie nie. As gevolg daarvan word daar tans navorsing in afval-tot-energie (ATE) prosesse en afval afgeleide brandstowwe (AAB) gedoen. Hierdie studie fokus op die termochemiese omskakeling van afval, spesifiek pirolise, as 'n methode vir energie-produk hernuwing.

Voordat 'n spesifieke afvalstroom gebruik kan word as 'n AAB moet die samestelling en afbrekings gedrag eers ondersoek word. Daarom is 'n volledige fisiese karakterisering van die munisipale afval (MA) van Stellenbosch munisipaliteit uitgevoer. Resultate het getoon dat daar ‘n verskil in die samestelling van afval tussen die gebiede binne die munisipaliteit is. Afgesien daarvan vergelyk die samestelling van die afval in die algemeen goed met internasionale data. Daar is gevind dat daar ses belangrike komponente teenwoordig is in die herwinbare stroom wat geskik sou wees vir termochemiese omskakeling, naamlik; hoë en lae digtheid poliëtileen (HD/LDPE), poli(etileen tereftelaat) (PET), glans, kantoor en koerant papier.

Die termiese eienskappe en termiese afbreking van hierdie ses komponente is ondersoek deur middel van multi-verhittimgs tempo termogravimetriese analise (TGA) waaruit kinetiese parameters (aktiveringsenergie, pre-eksponensiële faktor en kinetiese snelheidskonstantes) deur 'n differensiële omskakelings metode bereken is. Die vlugtige komponente wat tydens die afbreking vrygestel is, is geïdentifiseer deur aanlyn-massaspektrometrie (TGA-MS) wat ses individuele kinetiese skemas verskaf.

Om vas te stel tot watter mate milligram pirolitiese eksperimente (TGA-MS) gebruik kan word om op ‘n groter skaal die pirolitiese gedrag te kan voorspel, is eksperimentele lopies op een plastiek- (HDPE) en een papier (glans papier) monster op 'n laboratorium skaal pirolise opstelling onder stadige- en vakuum omstandighede uitgevoer. Daar is gevind dat, veral met hoë hitte geleiding komponente, die opbrengs op gram skaal eksperimente akkuraat voorspel kan word op ‘n milligram skaal. Verder was die samestelling van die stadige pirolise olies uit glans papier, wat verkry word deur gaschromatografie-massaspektrometrie (GC-MS), vergelyk met TGA-MS resultate sowel as af-gasse gevang van TGA lopies deur termiese desorpsie (TGA/TD-GC –MS). Daar is gevind dat TGA-MS en TGA/TD-GC-MS gebruik kan word om die belangrikste funksionele groepe in pirolise olie, wat op 'n gram skaal geproduseer word, te voorspel. Dus kan milligram eksperimente gebruik word om die geskiktheid van afval komponente vir pirolitiese omskakeling te bepaal.

Acknowledgements

I would like to thank my supervisor, Prof. Knoetze, and co-supervisor, Prof. Görgens, for the opportunity to do this study under them and for their insights and help over the last two years.

Thank you to Dr Marion Carrier for all her help and advice throughout my project, I could not have done it without her.

The financial assistance of the National Research Foundation (NRF) is hereby acknowledged. Opinions expressed and conclusions arrived at are those of the author and are not necessarily to be attributed to the NRF.

List of Abbreviations

GHG	greenhouse gas
MSW	municipal solid waste
RDF	refuse derived fuel
HDPE	high density polyethylene
LDPE	low density polyethylene
PET	poly(ethyl)terephthalate
GP	glossy paper
OP	office paper
NP	newspaper
Ea	activation energy
α	conversion
β	heating rate
Y	yield
MC	moisture content
VM	volatile matter
FC	fixed carbon
T	temperature
t	time
w	weight
K	rate constant
A	pre-exponential constant
R	universal gas constant
m/z	mass to charge ratio
TGA	thermogravimetric analysis
DTG	differential thermogravimetry
MSW	mass spectrometry
GC-MS	gas chromatography - mass spectrometry
TD	thermal desorption

Table of Contents

Chapter 1: Introduction

Global economic growth has led to increasing consumption by all members of society and, as such, has led to a growth in waste production, especially in plastics (UNEP, 2009). According to Troschinetz *et al.* (2008) an incremental increase in a household's income can lead to a relatively large increase in the amount of waste that household produces, the extent has been investigated in several studies (Medina (1997), Medina (2004), Sivaknmar *et al.* (2010)). This increase in consumption has increased the pressure on waste management and waste treatment processes finally increasing the amount of waste landfilled.

There is growing concern about the potential hazards and the environmental impacts of landfills. Increased waste means that more, larger, unsightly landfills are required bringing with them noise, smell and pollution. Release of methane from biological decomposition of organic materials in landfills also contribute to significant greenhouse gas (GHG) emissions (Kumar *et al.* (2004)), owing to methane having 20 times larger environmental impact than carbon dioxide (EPA, 2011). For this reason people, historically have adopted the 'NIMBY', or 'not in my backyard', approach to landfills (Tammemagi, 1999) but with urban expansion and a general shortage of space, as well as increased transport costs, this has become unrealistic. As a result, the general public is becoming less accepting of current waste disposal techniques (Tammemagi, 1999) and there is increasing pressure on government and industry to find alternatives to dumping.

Convenience of consumable goods has become greatly valued and expected by many members of society. This convenience, for example individually packaged ready meals, brings with it increased and more complex packaging, generally produced from virgin materials, that must be disposed of (Hopewell *et al.*, 2009). Globally, there have been many recycling initiatives but there is always a question of incentive both on the side of public and industry and eventual degradation due to ultra violet exposure and other physical factors (Hopewell *et al.*, 2009). At the end of their useful life recyclables, along with non-recyclables, are usually landfilled and left to degrade over extremely long periods of time. This waste, left to rot, still has a high calorific value that can be converted into useful energy.

Fears about the amount of remaining fossil fuel have come to the fore with many experts predicting that with the current usage rates, as well as the expected growth, the world will run out of traditional fuels in the near future. These fears have driven a movement both by industry and by academia to try and find alternative forms of energy to lessen the world's

dependence on fossil fuel, the main source of carbon dioxide, a known GHG (EPA, 2011 I). The focus of this movement is to find 'renewable' and 'sustainable' forms of energy.

The idea of a waste derived fuel is not a new one. Taking something that no one wants and that poses potential environmental and health risks and turning it into something extremely valuable seems ideal. There are, however, problems associated with this mostly due to the fact that waste, especially general municipal solid waste is an extremely heterogeneous substance (Speight, 2011). The composition is constantly changing (Brunner *et al.* (1986)). This heterogeneity and fluctuations in composition make it difficult to produce any homogeneous and consistent fuel or use directly in existing energy production processes (Speight, 2011). Thus, characterisation of municipal solid waste as well as the specific separation required for the production of a usable fuel is key to any potential site for a waste-to-fuel or energy application.

In this study the characterisation of municipal solid waste from the Stellenbosch area in the Western Cape of South Africa was carried out in the hopes of identifying a potential source(s) of a refuse derived fuel. The results of this characterisation are documented in Chapter 4 and the final composition of a potential refuse derived fuel (RDF) presented.

The versatility of thermochemical conversion processes specifically pyrolysis, as discussed in Chapter 2, makes it an attractive option and will be the focus of this study. However, in order to eventually commission a large-scale pyrolytic waste to energy plant, the behaviour of the potential feedstocks under various operating conditions must be known. Many studies into the kinetics of thermal degradation of the RDF components have been carried out but few studies exist on the kinetics of mixed source post-consumer components such as are found in separated recycling streams.

Products of the thermal degradation and the pathways postulated for the production of these products are usually found from gram or kilogram scale experimentation with offline chemical analysis and require purpose build plants that have a limited range of potential operating parameters. This can prove both expensive and time consuming and, as the chemical analysis of the products is done offline, the degradation pathways postulated are not necessarily based on the primary degradation products possibly limiting their reliability and usefulness. Thus small scale analysis of the suitability of different feedstocks to particular waste-to-energy applications will allow for better screening saving time and money on larger scale projects.

Kinetics are a vital consideration in reactor design and are found, usually, by milligram scale thermogravimetry, an extremely versatile method capable of a range of process parameters. This, coupled with online product analysis, gives a clearer picture of the primary degradation of the feedstock. The analysis of the products of selected gram scale pyrolytic experiments coupled with kinetic and degradation pathway analysis on a milligram scale, using thermogravimetric-mass spectrometry, will show to what extent milligram experimentation can be used to predict gram scale behaviour. This is the main aim of this study and could potentially reduce the need for intermediate laboratory scale pyrolytic experiments before pilot projects and provide a quick method for investigating the influences of differing process conditions and feedstock compositions.

Chapter 2: Literature Review

2.1. Refuse derived fuels

The composition of municipal solid waste (MSW) depends greatly on the society that produces it. Communities with a relatively large amount of disposable income will generally have more waste than their poorer counterparts (Thitame *at al.* (2010)). This is likely due to the amount of packaging (polyethylene films, hard plastics, packaging papers, glass and metals) associated with luxury goods as well as the sheer volume of purchased goods in comparison to less affluent neighbourhoods (Medina (1997), Medina (2004), Sivaknmar *et al.* (2010)).

Waste is generally collected from all areas in a certain radius and landfilled at one site. As a result the homogeneity of the MSW reporting to the landfills is low (Thitame *et al.* 2010). It is also extremely difficult to predict the composition of the MSW in a landfill without detailed studies on all the affected areas' waste. The composition of the MSW in each landfill in a country will be different and, as such, if it is desired to use the MSW for any waste to energy application, a study of the composition and the characteristics of the waste must be carried out for each site.

To date, there is no legal or internationally accepted definition of refuse derived fuel (RDF) (Gendebien *et al.*, 2003; Hernandez-Atonal *et al.*, 2007) and there exist both inter- and intra-country discrepancies in what can be classified as such. Historically, RDF has been used to describe raw, untreated municipal solid waste (MSW) as well as single shredded waste, with or without the removal of the magnetic fraction (Alter, 1978). For the most part, English speaking countries use the phrase to define a high calorific value fraction of MSW that has been separated from the inert and recyclable fractions by some mechanical means (Diaz *et al.*, 2005). There has been a movement by the European Standards Organisation (CEN) to correctly define and classify fuels from waste (Garg *et al.*, 2007). They use the phrase 'solid recovered fuels' (SRF), which can be used interchangeably with RDF in most cases, to refer to waste derived fuel with highly specified consumer quality requirements (Hernandez-Atonal *et al.*, 2007). In some cases the term RDF describes a fraction that has not only been separated but also undergone a biological treatment to remove the putrescible fraction, termed mechanical and biological pre-treatment (MBT) (Soyez *et al.*, 2002).

Part of the production of RDF is making the final product suitable for its end use (Caputo *et al.* (2002)). The moisture content in MSW, mostly due to a usually high organics

concentration, is one of the main factors affecting its usefulness to industry. Lower moisture content means a higher energy density, a desirable trait for a fuel, and thus the dewatering of waste is important.

The high moisture content (low energy density) inherent in the organic fraction of waste makes it unsuitable for use as a fuel without extensive mechanical drying or other moisture removal (UNEP 2005). Such processes are energy intensive and thus are unfeasible and environmentally unfriendly. An alternative to potentially expensive and energy intensive dewatering processes is to focus on separating out all components of the waste that have excessively high moisture contents. Most of these materials are biodegradable and could be biologically treated.

The biological treatment of MSW can take the two possible forms: anaerobic digestion and aerobic digestion or composting and can be done on a source (private) scale or on a larger scale at a centralised composting facility. Anaerobic digestion of waste produces an energy rich, mostly methane biogas fuel, that could be used directly for energy production (heating/electricity) or running crude engines, leaving a sludge that is greatly reduced in toxicity (Visvanathan *et al.* (2005)). The high nutrient sludge produced in this way thus has a much lower calorie content than the undigested waste and as such it seems that it would not make a suitable RDF. Chen *et al.* (1990), who saw RDF as just the mechanically treated high calorie fraction of MSW, used RDF as a feedstock for an anaerobic digester. It is recommended that the high calorie, non-digestible fraction be separated out and removed from the raw MSW prior to anaerobic digestion (Liekam *et al.*, 1999; Stegmann, 2005). Aerobic digestion can be used to 'biologically dry' waste removing excess moisture in an aerated environment without greatly depleting the energy content. This produces a good feedstock for a RDF production plant, provided that significant amounts of energy-bearing carbon and hydrogen remain in the RDF after biological treatment (Nicoletti *et al.* 2010; Soyez *et al.*, 2002). In general, the products of such bio-treatment could be utilised by the individual producing their own compost or collected by an interested party. Large scale composting could provide significant amounts of locally produced fertiliser for the large surrounding farming community. Such a composting facility could generate an income for the municipality or just save on the cost of collection and obviously landfilling.

By exposing all the waste to the composting process and sieving regularly, all biodegradable components will be composted and removed leaving only non-biodegradable components

which can then be recycled or converted to energy. This can thus form part of an integrated waste management process (Stegmann, 2005).

There are many different routes from waste to energy depending on the feedstock and the desired 'energy output' (product) suitable for a specific application. Thermochemical conversion can be used at any stage, including as the last step, in an integrated waste management system including recycling, anaerobic/aerobic digestion and composting. The non-biodegradable fraction that can no longer be recycled can be thermochemically treated by a pyrolytic process to harness the remaining energy into useful energy products.

2.2. Thermal treatment of MSW

There are three main pathways to energy application of municipal solid waste (MSW) and/or refuse derived fuel (RDF) via thermal treatment namely; combustion, gasification and pyrolysis. Below is an overview of each process with specific reference to MSW as a feedstock in each case.

2.2.1. Combustion

Incineration (high temperature combustion) of MSW has been used as a waste management strategy for many years with instances of controlled combustion found throughout history as far back as the 13th century (Petts, 1994). It has been used effectively to reduce both the mass and volume of waste by up to 70 and 90% respectively (Singh *et al.*, 2011).

In addition to the reduced pressure on the available land for landfilling there is an added benefit of energy recovery, usually in the form of electricity, from the process. Without the recovery of this energy recent studies have shown that traditional incineration plants are not financially viable (Lee *et al.*, 2007) due to the cost of meeting emissions requirements (gas clean up) in most countries as well as the high capital costs of incineration plants. Most incineration plants use the heat produced from combustion as a method of energy recovery as a way to make the process financially viable (Petts, 2004) e.g. to generate electricity through the use of steam and/or gas powered turbines. Due to the nature of the energy application product, heat, it must be converted immediately since no 'storage' is possible (Bridgwater, 2003). After the energy is recovered the flue gas is then subjected to a series of gas clean up procedures to remove harmful emissions including particulates, NOx, SOx, dioxins, HCl and HF (Wevers *et al.* 1992). Apart from the scrubbed gas and energy, incineration of MSW produces ash as a solid residue. Singh *et al.* (2011) stipulate that most

of the ash produced in this way is almost completely sterile while Malkow (2003) and Dalai *et al.* (2009) warn of potentially harmful residues found in small quantities. It can be used as a feedstock for cement production, giving additional income, or, depending on toxicity, dumped as waste as sterile/low toxicity residues pose little or no threat to the environment.

The incineration of MSW can be done on a bulk basis with no costly pre-treatment necessary as the system is able to cope with changes in composition as well as size in the waste. There are many different types of incinerators to suit the requirements of the installation with the most popular being water wall incinerators where raw MSW is loaded by crane into hoppers and then conveyed along the length of the incinerator (moving bed) before the solid residue (ash) is quenched in a water bath, the gas is used to produce electricity (Knox, 2005).

2.2.2. Gasification

Due to the environmental issues associated with incineration as a MSW disposal option, much research has gone into alternative forms of thermal treatment of MSW for energy production (Malkow (2004), Zevenhoven *et al.* (1997)). Gasification is one such alternative and, although not a new technology, has recently been receiving much attention with the surge in biofuels and quest for alternative energies (Belgiorno *et al.*, 2002).

Gasification is a thermochemical process that can basically be described as a hybrid between pyrolysis and combustion though there are many reactions occurring concurrently. The solid feedstock is heated to around 300 ºC at which point the substance undergoes devolatilisation producing a gas of hydrogen, light hydrocarbons and carbon monoxide and a solid char. This gas and char then react with a limited amount of oxygen (less than is required stoichiometrically for complete combustion) and together with the addition of the water gas shift reaction produce syngas, a mixture of hydrogen and carbon monoxide, water vapour, carbon dioxide and light hydrocarbons (Belgiorno *et al.* (2002) and Singh *et al*. (2011)).

Due to the incomplete combustion, the volume of gas produced by gasification is much lower than that in incinerators per volume of feedstock and thus smaller gas clean up operations are required for the removal of harmful substances reducing both capital and running costs (Belgiorno *et al.* (2002), Malkow (2004)). Although, in some cases, oxygen is required as a feedstock increasing the running costs the high temperatures reduce the production of dioxins and NOx again reducing costs associated with gas clean up (Arena,

2012, Belgiorno *et al.*, 2002 Malkow, 2004). Gasification processes are also said to be more efficient that incineration (Knox, 2005 and Phan *et al.*, 2007).

Gasification is also a versatile technology (Phan *et al.*, 2007) with numerous uses for the gas produced. Syngas is mainly used in South Africa as a feedstock for chemical processes most commonly the Fischer – Tropsch process used to produce liquid hydrocarbons. It can also be used as a fuel for gas engines and can be combusted to produce steam and/or heat for electricity production among others (Belgiorno *et al.* (2002) and Singh *et al.* (2011)). It does, however, have limitations where feedstock is concerned. Due to their nature, gasification processes are extremely sensitive to changes in feedstock and as such are not able to accept raw MSW due to its heterogeneous and inconsistent nature. Extensive pre-treatment including sorting, cutting, shredding, screening, classifying and removing all inerts and non-combustibles as well as ensuring the feedstock has the properties required for the efficient function of the process, is necessary before the MSW can be introduced into a gasifier. It is also advantageous to remove all high moisture biodegradables (Buah *et al.,* 2007). This can be expensive and energy intensive and thus is of concern when considering gasification as a waste management solution.

2.2.3. Pyrolysis

The thermal decomposition of an organic compound in the absence of oxygen is known as pyrolysis. Heating in the absence of oxygen causes volatiles to be driven off as a gas, mainly hydrogen, methane and tars (a portion of which can be condensed to a liquid bio-oil) leaving char as a solid residue. Pyrolysis of MSW has been suggested as an alternative to incineration as it addresses many of the drawbacks. Pyrolysis, like gasification, has been reported as producing fewer harmful emissions (Wang *et al.*, 2002) as well as being more efficient than incineration for energy applications (Phan *et al.*, 2007). Depending on the type and the final application of the produced fuel pyrolysis is also less sensitive to changing feed than gasification.

Pyrolysis produces three phases of fuel products, solid (char), liquid (pyrolysis/bio oil) and gas in different ratios depending on process conditions and process type (Miskolczi *et al.* 2010). Bridgwater (2003) states that the final process temperature and heating rate applied to the system influence the relative yields of the three products to the greatest extent. The production of three different fuel types that can be easily transported, stored and can be used

in a variety of applications makes pyrolysis a versatile and attractive process (Knox, (2005), Phan *et al.* (2007), Singh *et al.*, 2011, Williams *et al.* 1997).

Pyrolysis can also be used as an intermediate treatment step before combustion or gasification of waste. The pyrolytic products will be more consistent than raw MSW making them more suitable as a feed to a gasification set up. Knox (2005) states that the fuel produced from MSW via pyrolysis can be burnt in a more controlled and cleaner way than the raw MSW thereby reducing secondary pollution and, in turn, gas clean-up costs. The end gas flowrate is also smaller and hence, when compared with direct incineration, pyrolysis has lower capital and running costs (Singh *et al.*, 2011). There are operational plants pyrolysing MSW in existence like the 2.2 MW pyrolysis – combustion plant in Burgau-Unterknoringen, Germany (Malkow, 2004) proving that, in selected cases, this is a viable option.

Pyrolysis does, however, require that the feedstock remain consistent in order for a predictable fuel output in terms of volume and quality. This means that raw MSW as a feedstock is not entirely suitable and the MSW requires some form of pre-treatment before entering the process while this may increase the process cost, the quality of fuel will be increased (Phan *et al.* 2007).

There are two main types of pyrolysis: conventional (or slow) and fast pyrolysis. Vacuum pyrolysis is a hybrid between the two combining the low heating rates used in conventional pyrolysis with the very short volatiles residence times in fast pyrolytic set ups. Each has different process conditions and set ups and are used to achieve different end products. Demirbas (2009) compared the process variables of conventional and fast pyrolysis (Table 2.2.1 below) of different bio-feedstocks and gave an indication of typical yields. Vacuum pyrolysis and conventional pyrolysis are very similar in process set up, differing only in the process atmosphere and residence times, which are much shorter for vacuum conditions. The reduced residence times decreases the likelihood of undesirable secondary reactions whereby the primary pyrolysis products are further degraded. Thus vacuum pyrolysis produces more oil and less char and gas than conventional pyrolysis (Zhang *et al.*, 2007).

Table 2.2.1: Comparison of Parameters & Yields in General for Conventional & Fast Pyrolysis (Bridgwater (2003), Demirbas (2009) and Mohan *et al.* (2006))

Pyrolysis Type	Pyrolysis temperature	Heating Rate	Particle size	Residence time	Possible % yield *		
					Char	Liquid	Gas
Conventional / slow	470 – 950 K	1–60 K/min	5 – 50 mm	300 – 3600 s	25-91	12-33	2-54
Vacuum	470 – 950 K	1–60 K/min	5 – 50 mm	0.50-10 s	20-30	35-45	25-35
Fast	650-1250 K	60-12 000 K/min	<1 mm	0.50-10 s	9-34	46-76	12-24

*Dependent on process conditions (HR, upper T, residence time etc)

The set ups of fast pyrolysis plants require the feed to be very fine and homogeneous for effective operation (usually fluidised bed type operations). Due to the nature of waste, as discussed previously, much pre-treatment would be required before MSW could be introduced to such a system. The feed size requirements for slow and vacuum pyrolysis are less stringent (although particle size does play a role, Section 2.4.3) and thus make these technologies more suited to an inhomogeneous feed. For this reason these are the technologies focussed on in this study.

2.3. Fixed bed pyrolysis

There are many different types of pyrolysis reactor set ups possible for batch, semi batch and continuous operation; each with its own advantages and disadvantages. Set ups include rotary ovens, belt conveyer ovens, screw type conveyer ovens etc. However, the simplest form for a pyrolysis reactor is a fixed bed like the one depicted in Figure 2.3.1 operating on a static batch basis under an inert or vacuum atmosphere.

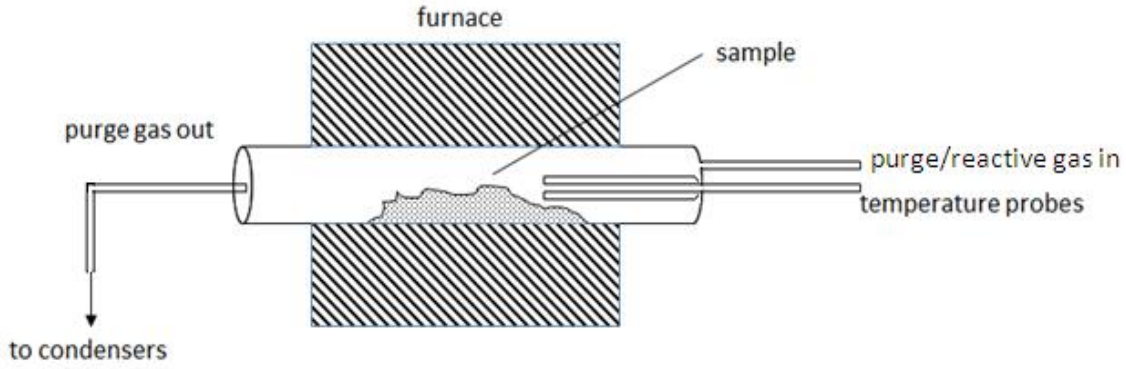

Figure 2.3.1: Basic Schematic of a Typical Batch Pyrolysis Reactor

One of the main problems with static – batch pyrolysis is very low heat transfer rates (Berrueco *et al.* (2005), Lopez *et al.* (2011), Williams *et al.* (1992), Yang *et al.* (2007)) between the furnace and the sample and then through the sample itself. Some efforts have been made to develop mathematic models that take into account not only the reaction

kinetics of the process but also the mass and heat transfer characteristics. Yang *et al.* (2007) designed a reactor with three different temperature probes; above the sample in the reactor, on the surface of the sample and in the middle of the sample. These three temperature probes together with the known furnace temperature at a given time gave a temperature profile for the system over the whole run. It was found that up to a 250°C difference in temperature between the set temperature of the furnace and the middle of the sample occurred. This presents obvious problems with different parts of the sample degrading at different rates perhaps changing the overall products and yields etc. of the process. By taking the temperature profile into account more accurate models were suggested (Yang *et al.*, 2007).

Before larger scale investigations are carried out it is advantageous to have suitable ranges in which to work, i.e. ranges that each specific parameter should be varied in depending on the desired system response. The effects of various parameters, some of which are directly influenced by the limitations mentioned above, have been studied by numerous authors and are presented below.

2.4. Parameters affecting pyrolysis

2.4.1. Temperature

Since pyrolysis is a thermochemical process it would seem obvious that the final process temperature will have an effect on the products of the process. A study conducted by Buah *et al.* (2007) on the pyrolysis of RDF in a fixed bed reactor showed that as the final process temperature was increased from 400 to 700 ºC the char yield decreased while the yield of oils/waxes and gas increased. The calorific value of the product gases increased by 11.1MJ/m^3 with a 300 ºC increase in the final process temperature while the energy density of the char decreased by 9.2 MJ/kg. The relative surface area, ash and fixed carbon of the produced char also increased with increasing temperature. It was noted, however, that these attributes were impacted by the particle size of the feedstock. Increases in the concentration of aromatic compounds in the oil/wax products were found corresponding to higher pyrolysis temperatures.

A study on the pyrolysis of plastic wastes in a semi-batch reactor by Lopez *et al.* (2011) showed the same trends of yields as Buah *et al.* (2007) but, due to the nature of plastics there was extremely little char production and that production was unaffected by the final process temperature. The proximate analysis of the plastics showed no fixed carbon or ash and thus no char formation was expected. The limited char production was attributed to secondary

re-polymerisation reactions in the reactor. Lopez *et al.* (2011) agreed with the postulations of Li *et al.* (1999) that the increase in gas production and decrease in liquid production can be attributed to more cracking of carbon-to-carbon bonds resulting in shorter chain hydrocarbons.

Phan *et al.* (2008) found that at temperatures over 600 ºC the liquid fraction of the product of slow pyrolysis of MSW greatly decreased. This was attributed to thermal and catalytic cracking. The gases obtained in the study were made up mostly of carbon monoxide and dioxide with increasing concentrations of methane and hydrogen with increasing temperatures. It was found that when pyrolysing MSW for the preferred production of char and oils the final pyrolysis temperature should not exceed 500 ºC so that both the physical and energetic yield is maximised.

2.4.2. Heating rate

Garcia *et al.* (1995), Wu *et al.* (1993), Wu *et al.* (1997, I) and Yu *et al.* (2002) all conducted pyrolytic studies on the kinetic behaviour of heterogeneous wastes. All four sets of authors found that the heating rate has an influence on the temperature at which weight loss of the sample occurs and their results depict the same trend. The initial weight loss onset temperature increases with increasing heating rate. The weight loss curves of the sample at the different heating rates keep the same general shape as at the lowest heating rate but the curves are 'shifted' for higher temperature. This shift is depicted in Figure 2.4.1 where W/W_0 is the ratio of weight of the sample at temperature T over the initial weight of the sample (at T_0) and T_{max} is the temperature at which the maximum weight loss rate is observed for each heating rate.

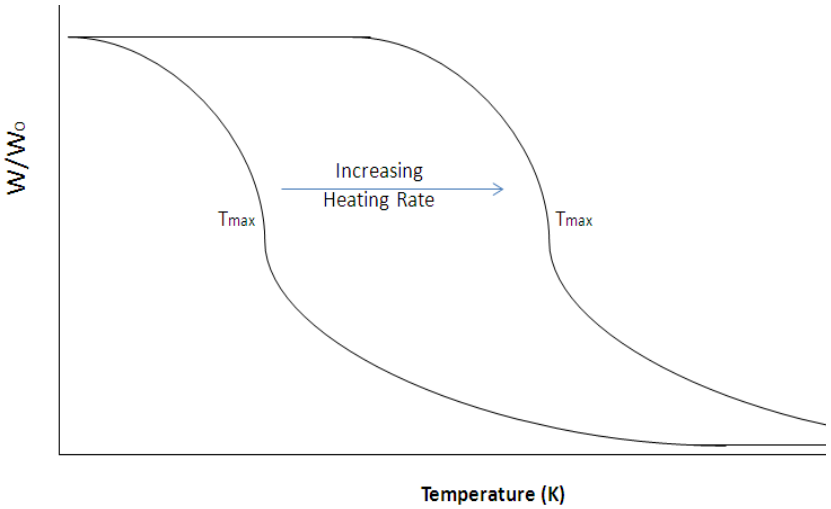

Figure 2.4.1: Depiction of the Shift Phenomenon with Heating Rate (drawn from information in Garcia *et al.* (1995), Wu *et al.* (1993), Wu *et al.* (1997, I) and Yu *et al.* (2002))

Garcia *et al.* (1995) postulate that the shift could be due to a change in process mechanism at different heating rates. It is also stated that the increased changes in T_{max} with heating rate that are observed are as a result of slow heat transfer which causes differences in the actual and nominal temperatures of the system.

Buah *et al.* (2007) found that there was very little impact on the yields of different pyrolysis products due to differences in heating rate between 2 and 10 ºC/min especially with the amount of char at the end of the heating program.

2.4.3. Particle size

Luo *et al.* (2010) performed a study on the effect of particle size on the pyrolysis of MSW. The study dealt with three particle size classes: 0 – 5mm, 5 – 10mm and 10 – 20mm. It was found that the particle size of each component of the MSW had an effect on the yields of char, oil and gas as well as the composition thereof. For materials with high fixed carbon (combustible portion of substance excluding volatile components) and ash contents (e.g. kitchen waste) particle size had more influence than in the product yields for materials with low fixed carbon and ash content (e.g. plastic waste). The gas phase product exhibited a trend of increasing carbon monoxide and hydrogen levels with decreasing particle size while the production of carbon dioxide was reduced. Higher char and tar yields due to incomplete devolatilisation were observed for particles of greater diameter. Buah *et al.* (2007) investigated the effect of particle size on a smaller scale with ranges of 0 – 0.5mm, 0.5 - 1mm and 1 - 3.25mm diameter. The degradation temperature as well as the temperature at which the maximum degradation rate was observed increased with increasing particle size. It was also found that the size of the particles influenced the quality and, to a lesser extent, the yields of the process.

In general, the smaller the particle the better the heat transfer between the particle surface and the surrounding fluid (Luo *et al*, 2010). This is due to the high surface area to volume ratio. This ratio is also dependent on the surface characteristics and overall shape of the particle in question. For pyrolysis, lower heat transfer rates translates into less complete devolatilisation, i.e. less of the original feed is pyrolysed to liquid and gas products leaving more solid char (Luo *et al*, 2010). Thus depending on the desired product distribution between the solid, liquid and gas phases, particle size could be used in conjunction with other parameters to control the output.

2.4.4. Hold time

This is the time that the system is kept at the maximum process temperature before cooling. Depending on the final process temperature and the specific feedstock, the reaction may not have reached completion by the time the heating program is finished. For this reason a hold time is often introduced in order to assure the most complete conversion possible. The optimal hold time is process and feedstock dependent and should be long enough that there is no further appreciable change in the product masses but not so long as to compromise the quality of the products, especially char. This time can be obtained by performing small scale experiments on a TGA system and observing when there is no further weight loss. Lua *et al.* (2004) investigated the effect of hold time on the quality of biochar and reported that char produced at longer hold times was higher in fixed carbon and ash but lower in volatile matter. This shows that longer hold time decreases the calorific quality of the char but can increase the yield of gaseous and liquid products.

2.4.5. Residence time

This is the average time taken for the product gases and volatiles to leave the reaction chamber and has direct implications for all the products' quality (Bridgwater, 1999). The longer the product gas is exposed to the final reaction temperature the more likely it is that it will degrade into secondary products (shorter chains etc.) directly affecting the quality of the product gases and condensed oils (increased water content and decreased calorific values). The quality of the char can also be affected as reactions between the released volatiles and the hot solid residue are more likely to occur the longer the residence time. Residence time also affects the yields of pyrolysis products. The longer the residence time the higher the yield of char and gas but the yield of bio-oil decreases (Scott *et al.*, 1999).

2.5. Kinetics of thermal degradation

The evaluation of chemical kinetics is an important part of engineering a process, especially for reactor design. Accurate kinetics also allow for the prediction of behaviour of a species under untested conditions (Brown *et al.*, 2000). Kinetic methods, and their usefulness and accuracy, have been under much investigation leading to vast literature on the subject. A critical and thorough review on how to perform kinetic computations on thermal analysis data is now available (Vyazovkin, 2011).

Until relatively recently most kinetic computations were based on single temperature or heating rate data. This has been shown to yield widely differing results when predicting the

same original kinetics (Vyazovkin (2006), Maciejewski (2000)). For this reason it is recommended that data obtained by multiple heating rates or at multiple temperatures be used when computing kinetic parameters (Vyazovkin *et al.* 2011).

The study of kinetics of a system or reaction involves calculation of a 'kinetic triplet', activation energy (E_a), pre-exponential factor (A), and a specific reaction model ($f(\alpha)$). The significance of the determined kinetic triplets has two facets; theoretical and practical (Vyazovkin, 2006). The practical level, the prediction of behaviour of a species, has been mentioned before. On a theoretical level, however, the kinetic triplet can be used to describe the actual physical reaction mechanism ($f(\alpha)$), the vibrational frequencies of the species (A) and the energy required by a species before a reaction can begin (E_a).

The kinetic triplet originates from the expansion of the single step parameterisation of a rate of degradation (change in conversion, α) with time, *t* (Equation 2.5.1)

$$\frac{d\alpha}{dt} = k(T)f(\alpha) \qquad 2.5.1$$

k(T) is the rate constant as a function of temperature, *T*, that can be described by the Arrhenius correlation (Equation 2.5.2.) that incorporates the universal gas constant, *R*.

$$k(T) = Aexp\left(-\frac{E_a}{RT}\right) \qquad 2.5.2$$

Expanding this to allow for a specific heating rate, β, one obtains Equation 2.5.3.

$$\beta\frac{d\alpha}{dt} = Aexp\left(-\frac{E_a}{RT}\right)f(\alpha) \qquad 2.5.3$$

The isoconversional principle states that at any specific conversion the reaction rate is only a function of temperature. By combining this premise with Equation 2.5.3 one is left with the Friedman correlation (Equation 2.5.4), the most common differential isoconversional kinetic method (Vyazovkin *et al.* 2011).

$$\ln\left[\beta\frac{d\alpha}{dt}\right] = \ln(Af(\alpha)) - \left(\frac{E_a}{RT}\right) \qquad 2.5.4$$

The value of E_a can be found for each α at a specific linear heating rate as the gradient of the plot $\ln\left[\beta\frac{d\alpha}{dt}\right]$ against 1/T. This can be done without assuming any form of the reaction model

($f(\alpha)$) (i.e. no specific conversion function) and as such the Friedman relationship can be thought of as 'model free'. As the activation energy and pre-exponential factor are independent from specific conversion function and vary with reaction progress such methods are ideal for the examination of actual reaction steps or degradation stages.

If Equation 2.5.3 were integrated and the isoconversional principle applied a general form of an integral isoconversional kinetic method is obtained. An example of such a method is the Ozawa, Flynn and Wall equation which has been shown to give Ea values of poor accuracy due to 'the crude temperature integral approximation' (Vyazovkin *et al.*, 2011).

2.6. Thermal decomposition of the main components of MSW

In general the high calorific fraction of MSW, as considered in this study, is made up of plastics and paper. The most prolific of these are high and low density polyethylene (HD/LDPE), poly(ethylene terephthalate) (PET), glossy paper, office paper and newspaper.

A polymer is a compound made up of chains of repeating units, monomers. Polymers can be classified according to their origin (natural, synthetic etc.) or, perhaps more usefully, according to their physical characteristics. Polymers able to undergo vast amounts of reversible stretching and reformation at room temperature, such as rubbers, are known as elastomers. The term plastic defines a class of polymer that is only partially deformable at room temperature (PET and HD/LDPE) and can be further divided into thermoplastics and thermosets while fibres, such as cellulosic materials (present in all three papers), have high tensile strength. Thus it is important to gain an understanding of the basic thermal decomposition mechanisms for polymeric materials in general.

Thermal breakage of bonds within polymer molecules occurs when the polymer is subjected to temperatures above the minimum decomposition temperature i.e. there is sufficient energy present to overcome the bond enthalpies within the molecule (Gao, 2010). When this happens the polymer is cracked into smaller chains. There are four main types of polymer degradation mechanisms: chain scission, cross linking, side chain stripping and side chain cyclisation (Pielichowski *et al*., 2005).

Although the degradation of polymers is complicated involving numerous reactions in parallel and series they can be grouped into four stages: Initiation, propagation, branching and termination reactions. Branching reactions are of little importance for general polymer degradation and so this mechanism is not considered here (Pielichowski *et al*., 2005).

2.6.1 Initiation reactions

Chain scission can be broken down further into random chain cracking and end chain cracking. When a polymer chain has the same bond strengths throughout the main chain there is an equal chance for any of the C-C bonds to break. This results in a haphazard cracking producing monomers and oligomers. When a polymer chain is cracked such that a single monomer unit is produced leavincg behind the rest of the polymer chain it is said to have undergone end chain cracking. Both random and end chain cracking are types of initiation reaction and the products of these reactions are both radicals that partake in the propagation and termination reactions (Beyler *et al.*, 2002). Homolysis is the breakage of covalent bonds such that the electron pair is equally shared between the two new radicals of random length. This can occur during both end and random chain cracking.

$$P_n \rightarrow R_r + R_{n-r}$$ Random Chain Scission Reaction

$$P_n \rightarrow R_{n-e} + R_e$$ End Chain Scission

Where: P_n is a polymer of n monomer units
R_r is a radical with r monomer units
R_e is a single monomer radical

2.6.2 Propagation reactions

Propagation reactions involve the radicals formed during the initiation stage(s). These reactions can occur either by hydrogen chain transfer or by basic depolymerisation (unzipping). These reaction mechanisms result in the formation of a new radical and polymer combination.

A: Intra and Intermolecular Hydrogen Transfer

Intramolecular hydrogen transfer involves moving of a hydrogen atom either within a radical chain itself from some site on the chain to the radical site. The hydrogen atom can be from any position in the chain although it is usually up to four sites away. This can be more depending on the organisation of the chain in space.

The second type of hydrogen transfer reaction, intermolecular hydrogen transfer, occurs between two distinct polymer chains. A hydrogen atom from a polymer moves to the radical site of another. The polymer then becomes radical with the specific radical site usually formed mid-chain and not on the chain end. This resultant radical breaks up into an unsaturated polymer and a radical (Beyler *et al.*, 2002).

$$R_n \rightarrow R_{n-m} + P_m \qquad \text{Intramolecular H transfer}$$

$$P_m + R_n \rightarrow P_n + P_{m-j} + R_j \qquad \text{Intermolecular H transfer}$$

Where: P_m is a polymer of length m
R_n is a radical of length n

B: Depolymerisation/Unzipping

During this type of propagation reaction no hydrogen transfer occurs. The radical polymer chain merely breaks up into an unsaturated monomer and a radical polymer (Beyler *et al.*, 2002).

$$R_n \rightarrow R_{n-1} + P_1 \qquad \text{Unzipping Reaction}$$

Where: P_1 is a monomer unit
R_n is a radical of length n

The type of propagation reaction that is most likely to occur can be predicted by looking at the architecture of the polymer in question. This is only a guideline and only useful for polymers with a pure carbon backbone, like polyethylene (Section 2.7.1) (Gao, 2010).

Depending on the types of additions to the carbon backbone a polymer will either undergo hydrogen transfer or unzipping reactions (Pielichowski *et al.*, 2005). Polyethylene, for example, has a carbon backbone with hydrogen atoms. Depending on the type of PE, there may also be branches of similar, shorter hydrocarbons emanating from the main chain. The larger the additions to the main chain the greater the barrier to hydrogen transfer (Gao, 2010). Chains with large side chains or side groups such as poly(tetrafluoroethane) will be more likely to undergo end chain scission giving a high monomer yield. Chains with medium sized additions, such as PE and PET (Sections 2.7.1 and 2.7.2), will undergo either end chain or random scission or a combination while chains with small additions, like polyethylene are most likely to undergo random scission and in some cases stripping and cross linking.

2.6.3 Termination reactions

Termination of degradation can occur when two radicals join to form one polymer chain. This is called recombination and is the reverse of random chain scission. The second type of termination reaction, disproportionation, again involves two radicals. One radical donates a hydrogen atom to another leaving the donor as an unsaturated polymer and the acceptor as a saturated polymer (Beyler *et al.*, 2002).

$$R_n + R_m \rightarrow P_{n+m} \qquad \text{Recombination}$$

$$R_n + R_m \rightarrow P_n + P_m \qquad \text{Disproportionation}$$

Where: P_m is a polymer of length m
R_n is a radical of length n

It is important to note that often when producing polymers industrially certain additives are used to enhance/change the product for the specific desired end use. These additives, or fillers, are impurities in the polymer chains and can change the behaviour of degradation. It is for this reason that the physical and chemical properties of the common components in the RDF are described below.

2.7. Physical and chemical properties of MSW components

2.7.1. High & low density polyethylene (HD/LDPE)

Polyethylene (PE) is the polymer of the ethene homopolymer with ethane as the repeating unit (shown in Figure 2.7.1).

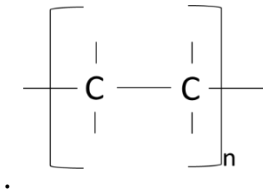

Figure 2.7.1: Repeating unit of PE

PE is a thermoplastic and is found extensively, in different forms, in municipal solid waste (Ceamanos *et al.*, 2002) and is the most widely used plastic today. Thermoplastics, as a group, all exhibit similar physical properties and are composed of long molecular chains Thermoplastics are solid due to the presence of intermolecular forces but these forces also allow for flexibility. Plastics from this family become pliable above a specific temperature, the glass transition temperature, allowing for reforming and, upon cooling to ambient temperature, the new shape is held (Beyler *et al.*, 2002). This change is reversible upon reheating unlike for thermoset plastics where a deformation above the glass transition temperature cannot be undone. Depending on the nature of the molecular chains and intermolecular forces, polyethylene takes on one of three main forms depicted in Figure 2.7.2 below (Gao, 2010).

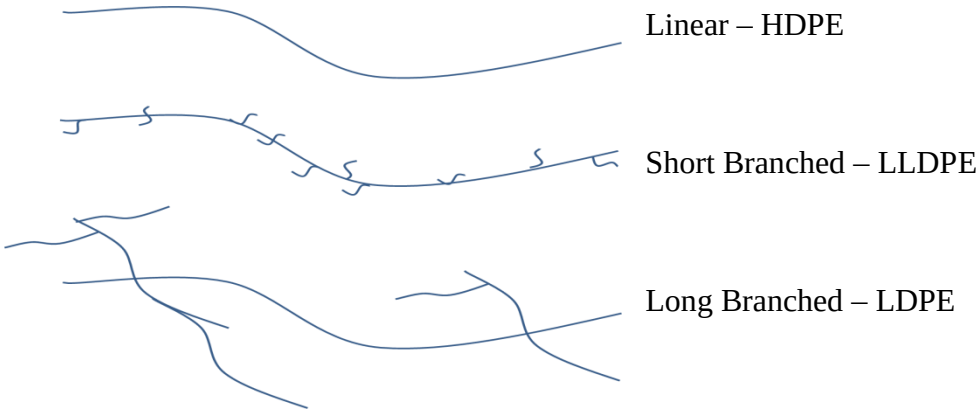

Figure 2.7.2: Chemical Structure of HD/LDPE

Both LD and HDPE have good resistance to chemicals (are not attacked by strong acids/bases) and impact strength i.e. they deform when struck but degrade when exposed to UV light. LDPE is well suited for use as packaging film as well as laminating, shrink wrapping and disposable plastic bags. It can also be used for light-duty containers and chemically resistant linings. HDPE is used more for container production (milk bottles etc) but can be used for heavy-duty shrink wrapping, reusable plastic bags and piping. HDPE has a density of 0.94 g/cm^3 or greater while LDPE can have a density anywhere between 0.91 and 0.94g/cm^3 (Gao, 2010). HDPE has very few or no branches allowing for strong intermolecular forces hence its increased density and strength (Gao, 2010). The degree of crystallinity of the two polyethylene species is also different; 95 and 60% for HD and LDPE respectively (Beyler *et al.*, 2002). Compounds that are less crystalline have a less well defined fusion temperature often degrading over a range as can be seen in Table 2.7.1 (Beyler *et al.*, 2002).

2.7.2. Poly(ethylene terephthalate) (PET)

Like HD and LDPD, PET is a thermoplastic and a polyester (see the repeating unit in Figure 2.7.3). PET is used extensively for beverage bottles as well as food containers. PET fibres are also used to make ‘polar’ fleece and other synthetic textiles. PET exists with densities ranging between 1.3 and 1.5 g/cm^3 depending on how crystalline in nature the sample is (IFA, 2013). PET has a range of rigidity depending on the structure and is a good barrier to gas, alcohol and solvents. These properties, together with the fact that PET has excellent weather durability, means PET has a wide range of industrial applications (e.g. automotive mouldings etc.). PET is usually very crystalline and as such has a specific fusion temperature, unlike PE, available in Table 2.7.1 (Beyler *et al*, 2002).

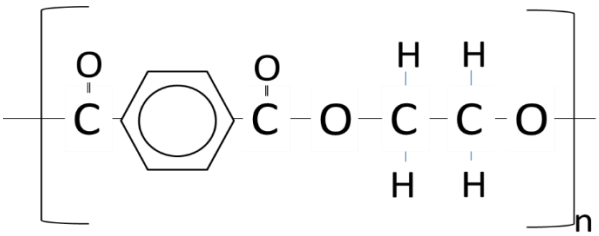

Figure 2.7.3: Repeating Unit of PET

2.7.3. Paper

Although paper comes in many different forms all with different properties depending on the application, the main constituent of all paper is cellulose fibres (Rha *et al.*, 1994). Cellulose is found abundantly in biomass (Lin *et al.*, 2009) as it is the main component in plant cell walls and is a polysaccharide consisting of chains of glucose monomers. The specific monomer that makes up cellulose is D-glucose, a stereoisomer of the glucose molecule. Both glucose and D-glucose have the same molecular formula ($C_6H_{12}O_6$) and the atoms making up the molecules are joined in the same sequence but the orientation of the atoms in space and with relation to each other within the molecule differs. The chemical structure is shown in Figure 2.7.4. below:

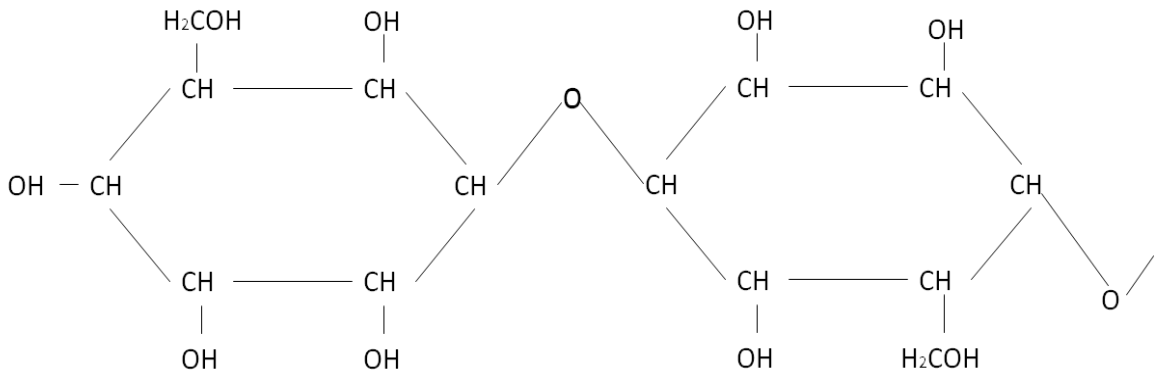

Figure 2.7.4: Chemical Structure of D-Glucose Monomer

All kinds of paper are produced from cellulosic pulp. This pulp can be made either mechanically, chemically or by a combination of both, from a variety of plant materials (Bajpai, 2011). The raw pulp must undergo 'stock preparation' before paper can be produced, it is at this point that fillers and other chemical additives are introduced to the pulp depending on the paper's end use (Biermann, 1996 I). Two broad categories of additive are used: control and functional additives. While they help to improve the paper making process, control additives do not affect the final paper product and are not considered here.

Paper texture, brightness, fluorescence, degree of light refraction (opacity), colour, sizing (reduction of water permeability) and many other properties that make one paper more suited to a particular application than another are controlled by functional additives (Biermann, 1996 I). Fillers, clay, Titanium dioxide, dyes, brighteners and fluorescent brightening agents as well as sizing additives are all different functional additives. These additives will clearly have an impact on the chemical properties of different types of paper thus the three different paper components of the RDF used in this study are mentioned below with a description of common additives to each type.

A: Newspaper

Newspaper is an example of a slack sized paper (as opposed to hard sized) i.e. it has a low resistance to water penetration. Sizing can be performed on the surface (by coating the paper with starch or some other material) or internally which is the more common way today (Biermann, 1996 I). Internal sizing is further broken down to rosin and alkaline sizing. Rosin sizing required the addition of rosin and alum ($Al_2(SO_4)_3$) to the pulp this does however reduce the produced paper's structural strength. Alkaline sizing is done by the addition of alkyl ketene dimer (AKD) or alkyl succinic anhydride (ASA) together with Alum (Biermann, 1996 I) increasing the hydrophobic nature of the paper in certain instances.

Newspapers are made from low brightness, matte paper. They have a high lignin content making them cheaper to produce (as pulp made without removing the lignin produces a much higher yield) and degrade more readily than other stronger papers containing less or no lignin (Biermann, 1996 I). Basic dyes, made from cationic organic substances, are used for the pigmentation of newsprint paper. These types of dyes do not have an affinity for bleached pulp but are attracted to lignin.

B: Office Paper (Writing Paper) and Glossy Paper

Both office (writing) paper and glossy paper are hard sized (as described previously). They are of a much higher grade than newsprint and are required to be very smooth and bright. Smoothness creates a good writing and printing surface and is achieved by using small particle sized fillers (pigments). The fillers must also have a low water solubility, high retention on the paper and a chemical inertness. Common fillers include ground calcium carbonate and clay (kaolin) which are cheap in comparison with titanium dioxide, a filler used of only very high quality papers. Fillers do impact negatively on the inherent strength

of the material and as such are not used in applications where strength of the product is of utmost importance (Biermann, 1996 I).

One of the main differences between the different grades of paper is the degree of gloss. Newspaper is entirely dull where as magazines have a high gloss finish. The degree of gloss is determined, to a large extent, by the addition of a coating, usually clay (kaolin). Ultrafine (<2µm) particles of clay are applied to the paper during calendering (rolling) of the paper for a high gloss finish and large particles are used when a matte or dull finish is desired (Biermann (1996 II), Biermann (1996 III)).

All of these additives, with the exception of some organic dyes, will increase the ash content of the paper. The additives will also affect the moisture content of the paper with office and glossy paper being able to absorb less moisture than slack sized newsprint (Biermann, 1996 I).

In addition to the properties and characteristics mentioned above, the chemical composition and other physical properties will greatly influence each of the six components' kinetic and degradation behaviour. Tables 2.7.1 and 2.7.2 summarise values for these properties as presented in numerous literature sources.

Table 2.7.1: General Comparison of Properties of RDF Components

Component	Calorific Value	Melting Point	Glass Transition Temp	Thermal Conductivity
	$MJ.kg^{-1}$	(°C)		$W.m^{-1}.K^{-1}$
Glossy Paper	15.09[g]	-	-	0.05
Office Paper	11 – 15.7[c,e,g,h]	-	-	0.05
Newspaper	17 – 21[c,g,i]	-	-	0.05
HDPE	43 – 44[a,d,f,j]	130 – 135[k]	-125[k]	0.48
LDPE	28 – 46[a,d,f,j]	109 – 125[k]	-25[k]	0.33
PET	21.85 – 24[a,f,b]	265[k]	70[k]	0.15

a. Berton Technologies (2000)
b. Martin-Gullon *et al.* (2000)
c. Phan *et al.* (2007)
d. Puncochan *et al.* (2012)
e. Strezov *et al.* (2009)
f. Themelis *et al.* (2011)
g. Ucuncu (unknown)
h. Wu *et al.* (1997)
i. Wu *et al.* (2003)
j. Zevenhoven *et al.* (1997)
k. Beyler *et al.* (2002)

The calorific values given are in fact the energy densities of the raw materials. As mentioned previously, the energy density of a substance is one of the main factors in the evaluation of a potential fuel. The raw calorific value also gives an indication of how successful and/or

beneficial any form of treatment carried out on the fuel by giving a baseline value for comparison purposes i.e. a calorific balance between the feed and products. The elemental and proximate analyses of the compounds are also indicators of the quality of the feedstock and could help to indicate the types of products that could be expected.

The thermal conductivity of the substances plays a role in kinetics and thermal degradation, especially in larger scale applications and is discussed in Chapters 5 and 6. The melting point and glass transition temperatures provide useful information (when changes are expected and what observed changes can be attributed to) when examining the degradation pathways of plastics.

Table 2.7.2: Comparison of literature Proximate[1] and Ultimate Analyses[2]

	C (%)	H (%)	N (%)	S (%)	O (%)	Moisture Content (%)	Volatile Matter (%)	Fixed Carbon (%)	Ash (%)
Newspaper	**36.0 – 44.1**	**5 – 7.14**	**0 – 3.66**	**0**	**40.72 – 53.15**	1.77^{g} – 7.9^{d}	79.4^{b} – 88.5^{e}	10.5^{e}- 14.1^{b}	0.6^{d} – 8.7^{g}
*	3,4,6-8,14,15	3,4,6-8,14,15	3,4,6-8,14	4,6,7	3,4,6-8,14,15				
Glossy Paper	**35.5 – 64.2**	**3.39 – 7.14**	**0 – 1.49**	**0 – 0.52**	**30.4 – 53.15**	6.60^{d}	67.3^{e} – 81.9^{d}	4.7^{e} – 10.3^{d}	1.2^{d} – 28^{e}
*	3,4,6-8,10,15	3,4,6-8,10,15	3,4,6-8,10	6-8,10	3,4,6-8,10,15				
Office Paper	**30.5 – 41.7**	**4.6 – 7.14**	**0 – 1.84**	**0 – 1.5**	**37.7 – 53.15**	0.9^{f}	73.6^{e}	6.2^{e}	20.2^{e} – 27.7^{f}
*	2-4,6-8,15	2-4,6-8,15	2-4,6-8	2-4,6-8	2-4,6-8,15				
HDPE	**83.3 – 86.1**	**11.3 – 14.2**	**0 – 0.9**	**0 – 0.3**	**0 – 2.21**	0.16^{h} - 0.3^{b}	99.3^{b} – 100^{e}	$0^{a,e,i}$ – 0.2^{f}	0^{e} – $0.6^{a,h}$
*	1,4-6,9,12,16	1,4-6,9,12,16	1,4-6,9,16	1,4-6,9,12	4-6,9,12,16				
LDPE	**83.3 – 86.35**	**12.15 – 13.51**	**0 – 0.08**	**0 – 0.2**	**0 – 2.21**	0.1^{h} – 0.3^{d}	97.6^{d} – 100^{e}	$0^{a,d,e,i}$	0^{e} – 2.1^{d}
*	1,4-6,9,12	1,4-6,9,12	1,4-6	1,4-6,12	4-6,9				
PET	**62.5**	**4.2**	**0**	**0**	**33.3**	0.13^{c} – 0.40^{b}	85.4^{b} – 93.4^{c}	6.4^{c} – 14.2^{b}	0^{b} – 0.08^{c}
*	11	11	11	11	11				

*Relevant References

1. Aboulkas *et al.* (2008)
2. Chang *et al.* (1997)
3. Cozzani *et al.* (1995, I)
4. Grammelis *et al.* (2009)
5. Ibrahim *et al.* (1996)
6. Islam *et al.* (2004)
7. Islam *et al.* (2005)
8. Li *et al.* (2005)
9. Luo *et al.* (2009)
10. Modh *et al.* (2012)
11. Pohorely *et al.* (2006)
12. Wu *et al.* (1993)
13. Wu *et al.* (1997)
14. Wu *et al.* (2003)
15. Yang *et al.* (2007)
16. Zevenhoven *et al.* (2006)

a. Aboulkas *et al.* (2008)
b. Heikkinen *et al.*(2003)
c. Pohorely *et al.*(2006)
d. Sorum *et al.*(2001, I)
e. Sorum *et al.*(2001, II)
f. Wu *et al.*(1997)
g. Wu *et al.*(2003)
h. Zevenhoven *et al.*(1997)
i. Zhou *et al.*(2006)

1 – Proximate Analysis provides the moisture, volatiles, fixed carbon and ash contents of a substance on a weight basis.

2 – Ultimate Analysis provides the elemental composition of a substance on a weight basis

2.8. Conclusion

For many environmental, energy security and financial reasons, waste is a very attractive feedstock for fuel and energy production applications. Pyrolysis can be used as a waste treatment technique at any stage in an integrated waste management regime. Even though conventional pyrolysis is quite robust and can handle some variations in composition in order to guarantee the quality and an accurate prediction of potential yields of the fuel product the composition and amounts of the potential feed must be known. For this reason any waste stream being considered for a waste-to-energy application, such as the waste from Stellenbosch Municipality, must undergo a full physical characterisation.

The suitability of the potential feedstock(s) as well as the optimum range of operating parameters need to be assessed before large scale pyrolytic experimentation can be carried out. Performing this screening on a small scale is both quicker, does not require specially designed equipment and could prove cheaper than larger scale options. A thermogravimetric analyser (TGA) is one such tool. Since TGA requires only small sample sizes and the operating conditions can be altered so easily, they are also used extensively to gauge the effect of a parameter (e.g. heating rate, final temperature etc.) on thermal degradation. Although there are limitations to using a TGA to predict/model actual processes many authors like Berrueco *et al.* (2005) and Lopez *et al.* (2011) have used preliminary TGA runs to better define the process conditions that should be set in larger scale experiments. Berrueco *et al.* (2005) determined the minimum pyrolysis temperature required for complete conversion of waste tyres. In addition to screening, TG analysis has been used by many different researchers working with waste (Cozzani *et al.* (1994), Grammelis *et al.* (2009), Kawaguchi *et al.* (2002), Lin *et al.* (1999), Sorum *et al.* (2001), Wu *et al.* (1993), Wu *et al.* (1997. I), Yu *et al.* (2002), Zhou *et al.* (2006)) to calculate specific kinetic data of samples like activation energies and rate constants and used to model the thermal degradation of samples under different conditions.

Reaction kinetics are key to the design of a reactor in which the reaction is to take place on a large scale, however normally one product or product quality is desired over another. TG analysis alone cannot give the individual yields of gas and liquid from a process only the combined yield (total weight loss). The condensables in the product gases must be captured and weighed and an overall mass balance performed in order to quantify the individual yields of the gas and liquid products. The sample size used in a TGA is in the order of milligrams

and as such and product gases produced will be limited in volume thus, overall, it would be extremely difficult, if possible at all, to get accurate data for yields. There are, however, options for online off-gas analysis such as online mass spectrometry that could be used to determine the product composition, however it is possible that these products will have different properties than those produced on a larger scale merely due to the small sample size (Yang *et al.* (2007)).

Although Wu *et al.* (1997, II) postulate that their kinetic model is directly transferable to the design of larger scale reactors. Little work has been done on the application of kinetic models and to larger scale applications and it is unclear how the results of online product gas analysis will compare with oils and gases produced at a gram scale. For this reason further work needs to be done comparing the results of milligram scale analysis to laboratory scale experimentation.

Outlined below are the objectives of this study.

2.9. Study objectives

This study aims to determine the composition of the municipal solid waste (MSW) in the Stellenbosch Municipal area and, from this, determine the potential composition of a refuse derived fuel (RDF) for use in thermal waste to energy applications.

Kinetic parameters describing the degradation of these components will be found using multi heating rate TGA data and differential isoconversional methods. This, together with online analysis of pyrolytic degradation volatiles will allow for the postulation of kinetic schemes.

The effects of heating rate and residence time on the degradation product yields and quality will be investigated on a laboratory scale pyrolysis plant for high density polyethylene and glossy paper. These results will be compared with milligram scale experimentation results in order to determine the scalability effect on the yields and degradation products. This study will determine to what extent milligram scale pyrolytic experimentation (TGA) can predict larger (gram) scale pyrolytic behaviour.

Chapter 3: Materials and Methods

3.1. Materials

Physical characterisation of MSW was done on a large scale in conjunction with the Waste Management Department of Stellenbosch Municipality. The 12 municipal areas, consisting of approximately 4400 households (numbers of households and population densities available in Appendix A), within the bounds of Stellenbosch Municipality considered in this study (see map in Appendix A) have their MSW collected on specific days of the week. The municipality collects both the general refuse and source separated recycling on the same day. The recyclables and general MSW are placed on the pavement outside the households in clear bags and black bags, respectively. In order to get a representative sample from each area, over the course of a week, every day prior to the municipality's usual MSW and recyclable pick up, one black bag and one clear bag were collected in a separate truck from every tenth house along the route. Thus, over the course of the week, a total of 880 bags were collected; 440 black and 440 clear bags.

Kayamandi also forms part of the municipality (see map in Appendix A) and is a mix of low cost government houses and informal dwellings. The formal houses in this area have access to the municipality supplied black bins, while the informal houses do not and place their rubbish mainly in shopping bags and other receptacles on the pavement. This makes collection by the municipality very difficult as their MSW collection trucks are designed for emptying bins and not accepting loose bags. Enkanini is an entirely informal, very poor area set on a steep hillside adjacent to Kayamandi. The waste in this area is dumped by residents in 7 different sites, mostly not in any bags or containers at all, where the municipality collects it once a week. During the characterisation study no recycling was found in either of these areas. For this reason it was decided that the data collected from these areas were unreliable and that a different sampling technique needs to be devised before future characterisation attempts in these areas and, as such, is not considered in this study.

The collected waste was then transported to a vacant warehouse where the bags were separated by area. Each bag was weighed unopened and then separated into seven broad categories namely: plastic films, dense plastics, paper, glass, metal, organics (food and garden waste) and other. Once the entire bag was sorted, each bucket was weighed giving an indication of possible losses due to fines etc. as well as of the actual weight composition of each bag. This is in line with the classical MSW sorting technique outlined by Brunner *et al.* (1986).

The results of the characterisation (outlined in Chapter 4) gave an indication of the most prolific components as well as their relative ratios within the waste. It was found that the waste suitable for a thermochemical waste-to-energy application (dry, high calorific value waste) was made up mainly of high and low density polyethylene (HD/LDPE), poly(ethylene terephthalate) (PET), glossy paper, office paper and newspaper.

Mixed samples of the three different waste papers were collected from the Kraaifontein Integrated Waste Management Facility in the Western Cape of South Africa. Samples of waste HDPE, LDPE and PET waste were supplied by Nampak Tissue from their in-house recycling streams. As the materials were collected from waste streams, all of the samples collected were made up of materials from different origins and products spanning a broad spectrum of manufacturers/suppliers giving an accurate representation of the possible composition of waste in the Western Cape. 5 kg of each separate component was coned and quartered from 20kg representative samples from the sources and stored under ambient conditions before processing.

3.1.1. Preparation of materials

To avoid any organic contamination, the plastic samples (HDPE, LDPE and PET) were washed with soap and warm water before being allowed to dry completely under ambient conditions. Samples of each of the six components (HDPE, LDPE, PET, glossy paper, office paper and newspaper) were cut by hand into particles of roughly 50 × 50 mm before being fed into a Retsch SM 100 cutting mill. Each material was separately passed through a series of decreasing sieve sizes from 10 mm to 2 mm on the last pass. Although there were loses of the components at every milling step at least 1 kg of all the samples was present at completion. 100g of each component was poured into a graduated measuring cylinder and left to settle for 5 min whereafter the level of the sample was read giving the non-compressed and un-vibrated bulk density. The components were then stored separately in individual airtight plastic bags under ambient conditions.

3.2. Analyses

3.2.1. Proximate analysis

The determination of the moisture content and amounts of volatile matter, fixed carbon and ash for the feedstocks was carried out by proximate analysis in accordance with the American Standard Testing Method (ASTM) E 1131. This was carried out in a Mettler Toledo STARe Thermogravimetric Analyser. Each sample was loaded into a 70 µL alumina crubible and

heated in an inert (99.999% nitrogen gas - Afrox Baseline 5.0) atmosphere at a heating rate of 50˚C/min from 30˚C to 110˚C after which an isothermal region was maintained until the weight loss stabilised. Thereafter the heating rate was increased to 100˚C/min until the samples reached 900˚C at which a second isothermal region was maintained for 5 min. Finally the 80mL/min of nitrogen purge gas (99.999% Afrox Baseline 5.0) was exchanged for the same amount of oxygen (99.998% Afrox Baseline 4.8) gas for a further 5 min to allow for complete combustion and determination of the ash content.

3.2.2. Elemental analysis

The amounts of elemental carbon, hydrogen, nitrogen and sulphur present in raw components as well as the liquid and solid products of the laboratory scale pyrolysis were determined by elemental analysis. A known mass (between 1 and 3mg) of each sample was placed into the combustion chamber of A LECO TruSpec Micro Elemental Analyser (the limits of detection of carbon and nitrogen are 0.002wt% and 0.02wt% respectively) and the off gases analysed by highly selective individual infrared and thermal conductivity detectors. This information together with chemical standards used for calibration allowed for a mass based quantitative analysis of C, H, N and S. The oxygen was calculated by difference.

The standards used for the char products were AR-2781 (Alpha Resources Inc., USA), BBOT and Atropine (both EuroVector). The standards used in analysis of the oil products were EDTA (502-092), sulphurmethazine (502-209), acetanilide (501-053), benzoic acid (502-184) (all LECO standards), BBOT (EuroVector), and AR-100 Residual Oil (Alpha Resources Inc., USA).

3.2.3. Calorific value

The calorific values of the glossy, office and newspaper were determined experimentally by combustion in an Eco Cal2K bomb calorimeter while those of the HDPE, LDPE and PET were determined on a Baird and Tatlock A136 Bomb Calorimeter (due to the potentially corrosive nature of the plastic samples). The heat of combustion is determined by temperature difference in both bombs once individual bomb and set up correction factors have been accounted for.

Calorific values for liquid and wax pyrolysis products are determined from the results of the elemental analyses as per Equation 3.2.1, the Channiwala *et al.* (2002) correlation (in which C, H, S, O and N refer to the weight percent of each element in the substance) while those of the pyrolytic chars are determined by the Parikh *et al.* (2005) correlation (in which FC and VM

refer to the fixed carbon and volatile matter contents of the substance) using the results from the proximate analyses, Equation 3.2.2. Experimental determination of these values was not possible due to the corrosive nature of the combustion products and their subsequent damage of the calorimetry equipment.

$$\textbf{HHV}\ (\text{MJ/kg}) = 0.3491\textbf{C} + 1.1783\textbf{H} + 0.1005\textbf{S} - 0.1024\textbf{O} - 0.0151\textbf{N} - 0.0211\textbf{Ash} \quad \textbf{3.2.1}$$

Where: $0 < C \leq 92.25\%$
$0.43 \leq H \leq 25.15\%$
$0 \leq O \leq 50\%$
$0 \leq N \leq 5.6\%$
$0 \leq S \leq 94.08\%$
$0 \leq Ash \leq 71.4\%$

$$\textbf{HHV}\ (\text{MJ/kg}) = 0.3536\ \textbf{FC} + 0.1559\ \textbf{VM} - 0.0078\ \textbf{Ash} \quad \textbf{3.2.2}$$

Where: $1 < FC < 91.5\%$
$0.92 < VM < 90.6\%$
$0.12 < Ash < 77.7\%$

The Channiwala *et al.* (2002) correlation is not suitable for materials where there is a very high ash content or extremely strong C-H bonds, as is the case with plastics and rubber but has been indicated for use with gaseous and liquid fuels. Parikh *et al.* (2005) indicated the use of their correlation for any solid or biomass material.

3.2.4. Liquid product composition

A qualitative description of the pyrolytic liquid composition was determined by Gas Chromatography - Mass Spectrometry (GC-MS) on an Agilent 7890A/5975C GC-MSD fitted with a 60m x 250µm x 0.25µm Zebron ZB-1701 GC column (Phenomenex).

The liquid samples were dissolved in Chromasolv 99.9% acetone (Sigma Aldrich) and ≥98.5% methyl ester docosanoic acid (Sigma Aldrich) added as an internal standard. 1µL of the sample was injected and the system kept at 45ºC for 10min then heated at 7 ºC/min to 260ºC and held for 14min. The gas chromatograph separates the different components by differences in their specific retention times, where after a mass spectrometer, set to range between 20 and 500Da and set at 70eV, ionises the components and captures the specific mass-to-charge ratio (m/z) fingerprint. These fingerprints are then compared with the National Institute of Standards and Technology's (NIST) database (NIST Mass Spectral Search Program) and three potential components presented with a quality of fit at each specific retention time.

The water content of the produced oils was determined by Karl-Fischer titration in accordance with ASTM D 1744. The analysis was performed with between 0.02 and 0.2mg of oil on a Metrohm 701 KF Titrino using Hydranal Composite 5 (Sigma Aldrich - Fluka Analytical, 34805 1L R) as the titrant.

3.3. Methods

3.3.1. Determination of thermal parameters, kinetic rates and major degradation products

The kinetic rates of the thermal degradation of all six samples were determined by duplicate analysis of individual, non-isothermal milligram scale pyrolytic runs at four different heating rates (10, 20, 30 and 50ºC/min). These were performed in a thermogravimetric analyser (TGA), specifically a Mettler Toledo TGA/DSC 1 Thermogravimetric Analyser (STARe System). Preliminary screening runs were carried out in duplicate on a Shimadzu TGA 50 in order to find the basic operating ranges needed allowing for efficient experimentation with the more accurate TGA/DSC 1 in which measurements of the sample weight were recorded every 0.7 seconds giving a very precise picture of the degradation. Both machines consist of a microbalance inside a well-insulated furnace that is purged with either reactive gas (for combustive or other reactive conditions) or, as was the case in this study, inert gas (nitrogen/argon) for pyrolytic conditions. Both thermogravimetric analysers were heated from 25 to 900°C. The Shimadzu TGA 50 and Mettler Toledo TGA/DSC 1 had nitrogen and argon (both 99.999% Afrox Baseline 5.0) flow rates of 20 and 50 ml/min respectively. 70µL alumina crucibles containing between 5 and 20mg of sample were used in the TGA/DSC 1 and TGA 50. After the runs the crucibles were thoroughly cleaned to avoid cross contamination between runs. This was done by soaking in 0.1M hydrochloric acid (KIMIX Chemicals & Laboratory Supplies) for 3 hours followed by slowly heating from room temperature in a furnace to 800°C and baking for 1 hour.

The systems were linked to a computer that logged the weight loss data for interpretation using software specific to each machine; TA60 and STARe-Evaluation Software for the Shimadzu and Mettler Toledo systems respectively, where the data could be manipulated and interpreted. The resulting weight loss (TGA) and rate of weight loss (DTG) with temperature data obtained from the multi-heating rate runs on the TGA/DSC 1 were imported into an Advanced Thermal Kinetics Software (AKTS) program. Baselines for integration were defined and the data interpreted under differential isoconversional, model free methods (As described in Section

2.5). These methods, specifically the Friedman method used in this study, are based on the Arrhenius correlation (Equation 2.5.2, Chapter 2). The natural logarithm of Equation 2.5.2 and incorporation of a specific heating rate term, β, yields:

$$\ln\left[\beta\frac{d\alpha}{dt}\right] = \ln(Af(\alpha)) - \left(\frac{E_a}{RT}\right)$$

A plot of $\ln\left[\beta\frac{d\alpha}{dt}\right]$ (ln(reaction rate), in 1/s) against $\frac{1}{T}$ (in 1/K) for values obtained for different heating rates at the same conversion (α) results in lines the slopes of which are equal to specific $\frac{E_a}{R}$ values (Vyazovkin *et al.*, 2011). It is thus possible to determine the dependence of Ea (kJ/mol) and ln(A*f*(α)) (1/s) with α (Figure 3.3.1). In this way the specific rates of reaction, k, and activation energies, E_a, for the degradation of all six compounds were obtained. The resulting data are presented in Chapter 5.

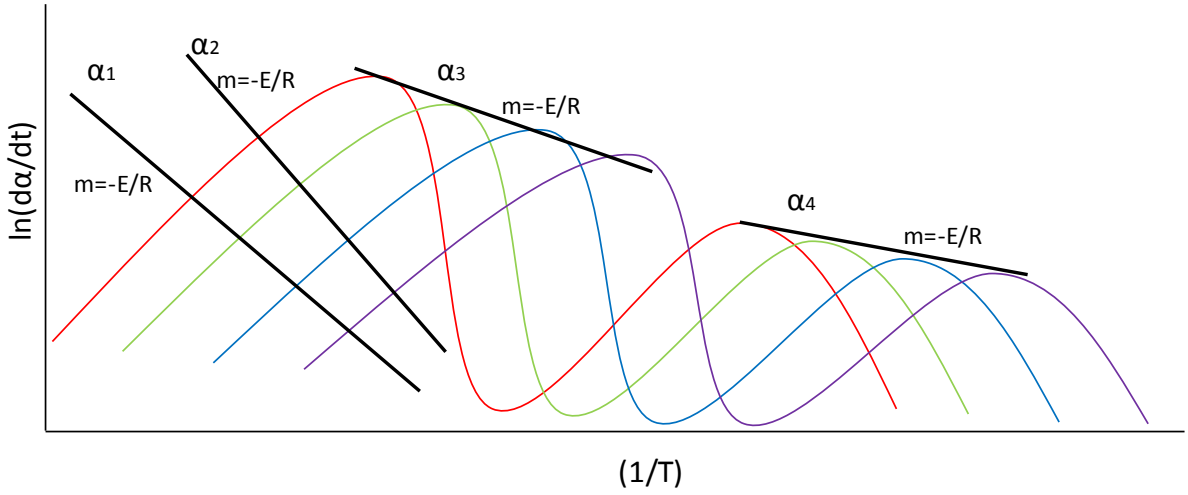

Figure 3.3.1: Friedman Plot for Determination of Kinetic Parameters (from information acquired from Vyazovkin *et al.*, 2011)

The degradation products from the 20 °C/min TGA runs were analysed by way of online mass spectrometry (MS). A small but representative portion of the off gas from the TG analyser was diverted to a Pfeiffer Vacuum Thermostar GSD320 Gas Analysis System mass spectrometer through a well-insulated 5m x 150µm fused silica capillary (SGE Analytical Science, Australia) heated to 200 °C. The sample gas is then bombarded with electrons (electron source/'gun') with a set energy of 70eV (6750kJ/mol) ionising the sample, knocking out an electron from the outermost orbital producing mainly cationic fragments. These cations are separated by way of a quadrupole (four rods in which a magnetic field is induced, 2 positive and 2 negative poles) and reach the Faraday ion detector where ions are quantified following their m/z ratios (Figure

3.3.2). The number of ions detected is related to the intensity of the current measured (in nano-amperes), thus a plot of relative intensity vs time can be produced showing graphically what species is released at each time interval.

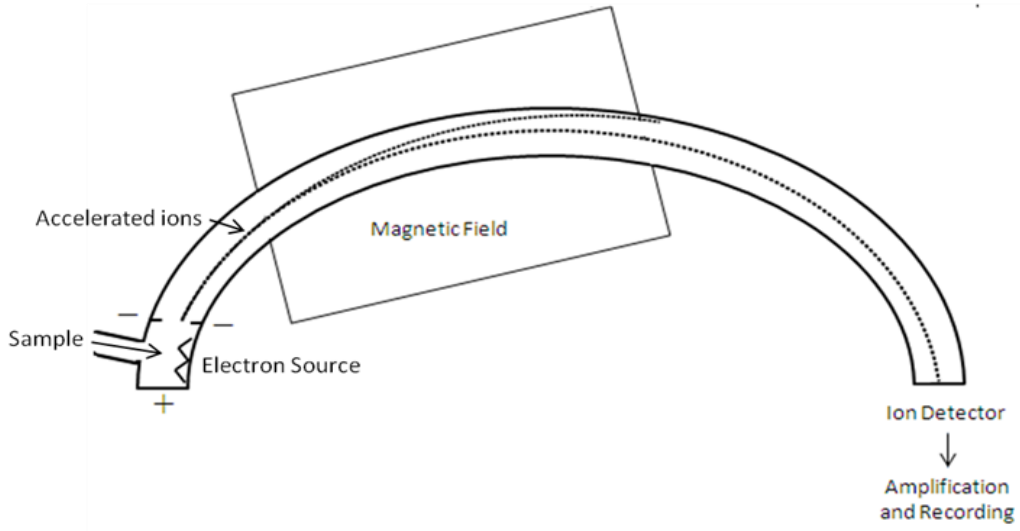

Figure 3.3.2: Schematic Representation of a Mass Spectrometer (adapted from RCS 2014)

Pyrolysis processes, by nature, are very complex, this coupled with the impurities and contaminants found in waste materials makes prediction of behaviour difficult. This also means that deciding which ions to track during degradation is a challenge as degradation schemes obtained in literature values will not necessarily account for the differences in composition. To overcome this problem the MS was used to screen for ions emitted by the samples over the entire m/z range. These scans, found in Appendix D, were compared with literature and the most important molecular masses chosen for tracking during degradation. These ion currents (Table D1, Appendix D) were plotted as a function of time and used to draw an experimental degradation pathway for each component. The signals were normalised with respect to sample size and to the carrier gas ion current (m/z = 40). This was done in order to make the ion currents comparable across different stages and samples and account for changes in the pressure of the system due to blockage of the capillary by large compounds. The area under each of the common ion peaks was obtained and can be used to compare the amount of a specific m/z ion evolved during the degradation of one compound to the amount of that ion evolved during the degradation of the other samples. This allows for the evaluation of each sample and its potential benefits for energy production over another. It is also important to note that argon was used as the purge gas for the TGA and TGA-MS runs as it was desired to track fragments relating to carbon monoxide and dioxide which have the same m/z as nitrogen (m/z=28) thus separation and normalisation of the results would have been impossible.

In order to better describe the milligram scale degradation products a stainless steel thermal desorber (Universal Mix: C3-AAXX-5266) was used for active sampling of the TGA off gases (as per method developed by Nsaful (2013, unpublished work)). This was done by way of a low flow ACTI-VOC vacuum sampling pump (Markes International Ltd, UK) set to match the flow of purge gas from the system. The thermal desorption tube (Markes International Ltd, UK) was filled with three consecutive sorbents, namely Tenax TA, Carbograph 1TD and Carboxen 1003. After the run the desorption tube was attached to a Unity 2 thermal desorber (Markes International Ltd, UK) set to 300ºC and the desorbed volatiles transferred through a line heated to 200ºC to the Agilent 7890A/5975C GC-MSD gas chromatographer under conditions as described in Section 3.2.4.

3.3.2. Laboratory scale vacuum and slow pyrolysis

Both the vacuum and slow laboratory scale pyrolytic runs were carried out in the same horizontal fixed bed reactor (Figure 3.3.3). The reactor consists of a 1m quartz glass tube with an external diameter of 60mm that was sealed with two flanged end caps. The reactor tube was surrounded by a well-insulated furnace consisting of six electrical heating elements arranged such that the heat is evenly distributed around the reactor tube in which approximately 40g of sample in a quartz glass sample plate was placed. The reactor exit pipe was heated to 160ºC to minimise the condensation of any product gases before the condenser train. Five condensers, connected by thick walled rubber tubing, were used for the capture and condensation of released volatiles. The temperatures of the furnace and sample were measured by the two thermocouples inside the quartz reactor tube and the data logged. The temperature profiles for both thermocouples were plotted (see example in Appendix E) in order to gauge the heat transfer limitations between the furnace and sample.

The condensers were kept at progressively colder temperatures; the first at atmospheric temperature, condensers 2 and 3, submerged in water ice, at 4 ºC and the final two at -78 ºC, the temperature of the surrounding dry ice.

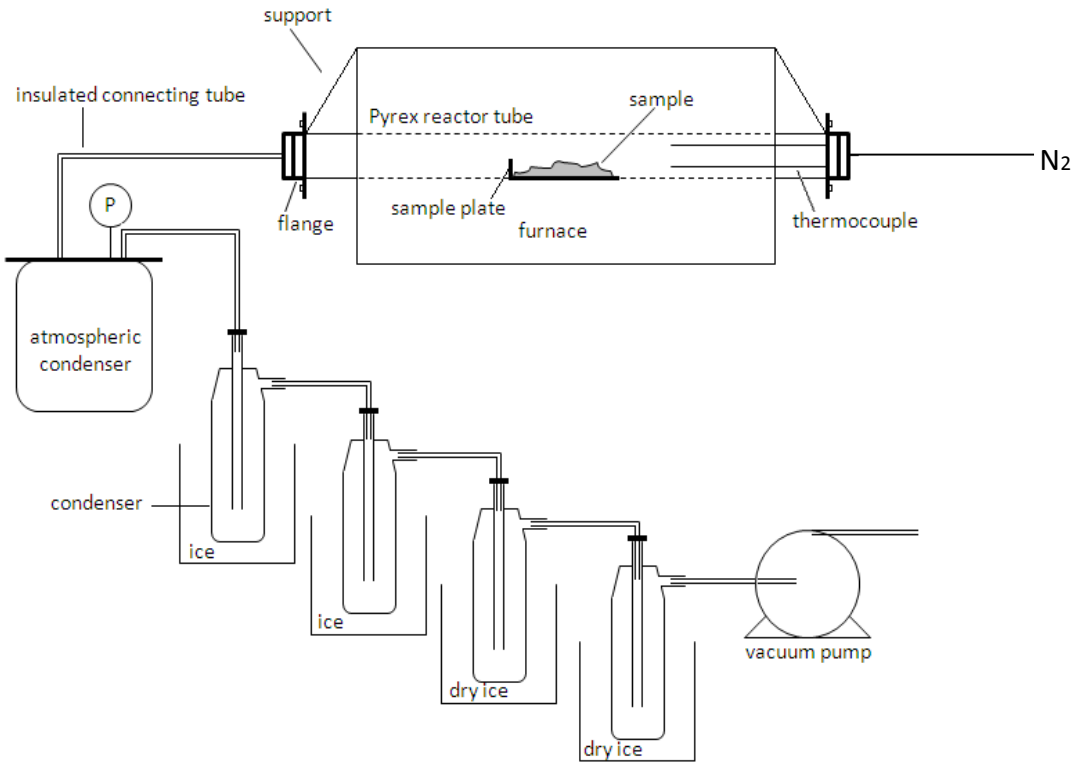

Figure 3.3.3: Schematic of the Laboratory Set-up for Slow and Vacuum Pyrolysis

Glossy paper and HDPE were used as feedstocks and heated from ambient temperature to 550ºC at rates of 10 and 20ºC/min at which point the system was held at maximum temperature for 30min to ensure complete pyrolytic conversion. In the case of slow pyrolysis, nitrogen (Afrox Technical 99.5% purity) was used as a purge gas at a flowrate of 70ml/min whereas, for vacuum runs, a two stage InstruVac laboratory vacuum pump was connected to the end of the condenser train and the purge gas inlet sealed. For the vacuum runs the pressure was kept at 8 kPa absolute. In order to prevent combustion of the hot char, once the runs were complete the system was left to cool under the pyrolytic atmosphere for 2 – 3 hours before being disassembled. The oil products were stored in sealed vials to prevent loss of very volatile components by evaporation and kept in a fridge away from light to prevent degradation caused by heat and light. The char was sealed in airtight bags to prevent contamination and/or degradation.

The yields of oil (Y_{oil}) and char (Y_{char}) were calculated by difference in weight of the condensers (m_c) and tubes (m_t) and sample mass (m_i) and char residue (m_f) before and after the runs respectively (Equations 3.3.1 – 3.3.2). The combined yield of gas (Y_{gas}) and any potential losses were calculated by difference (Equation 3.3.3). The production of pyrolytic water ($Y_{pyro.}$

$_{water}$) was calculated as per Equation 3.3.5 taking into account the individual moisture contents ($MC_{c,i}$) where m_{wt} is the total water yield ($Y_{total\ water}$) (Equation 3.3.4).

$$Y_{oil} = \frac{m_c + m_t}{m_i} \times 100 \quad \textbf{3.3.1}$$

$$Y_{char} = \frac{m_f}{m_i} \times 100 \quad \textbf{3.3.2}$$

$$Y_{gas} = 100 - Y_{oil} + Y_{char} \quad \textbf{3.3.3}$$

$$Y_{total\ water} = \frac{\sum(m_{c,i} \times MC_{c,i})}{m_i} \times 100 \quad \textbf{3.3.4}$$

$$Y_{pyro.water} = \frac{m_{wt} - m_{wi}}{m_i} \times 100 \quad \textbf{3.3.5}$$

Yields are presented in Chapter 6 as average weight percentages with standard deviation with respect to the weight of feedstock repeated over all runs.

The residence time of the volatile/gaseous pyrolytic products was calculated by Equation 3.3.6 where V is the reactor tube volume (m^3) and Q is the volumetric gas flow rate in m^3/s. This gives an estimation of the average time the product molecules remain in the reactor.

$$\tau = \frac{V}{Q} \quad \textbf{3.3.6}$$

One of the aims of performing thermogravimetric analysis on the samples was to see if milligram experimentation can be used as a prediction tool for larger scale runs. In order to properly test this, the TGA was run under the same conditions as the laboratory scale plant i.e. 25 to 550ºC at 10 and 20 K/min and held for 30min under nitrogen at 70ml/min. As described earlier, the original TGA runs for kinetic and thermal degradation analysis were performed under argon. The 25 - 550 ºC runs were repeated under argon to check for any differences in behaviour under the different atmospheres (Appendix E). No significant deviation was observed and it can thus be said that the differences in purge gases do not affect the degradation of either species.

The temperature of the furnace was controlled by a negative feedback system and two thermocouples, one in contact with the sample and the other in contact with the inside of the reactor wall. These two temperature profiles were recorded and compared and it was found that the temperature gradient between the reactor tube wall and the sample was small and decreased

with increasing temperature. All runs were repeated and the average yields for both samples are presented in Tables 7.1.1 and 7.2.1. Full mass balances for both the slow and vacuum pyrolytic runs can be found in Appendix D.

Elemental balances were performed for both HDPE and glossy paper under both atmospheric conditions. The average of the elemental composition duplicates was taken and the repeated runs averaged such that there is one elemental composition per stream per heating rate and atmosphere. This was calculated for glossy paper as per Equation 3.3.7 and HDPE as pre Equation 3.3.8, both on a basis of 100g of feed.

$$X_{Gas} = X_{In} - (X_{Aqueous} + X_{Tarry} + X_{Char}) \quad \textbf{3.3.7}$$

$$X_{Gas} = X_{In} - (X_{Reactor} + X_{Cond.1}) \quad \textbf{3.3.8}$$

Where X is the % of an element (C, H, N, S or O) entering the process (100% or X_{in}) in the indicated phase exiting the process. Aqueous and Tarry are the two separate liquid phases formed from glossy paper while Reactor is the combination of the wax left in the reactor tube as well as that collected in the atmospheric temperature condenser from the degradation of HDPE. Cond. 1 is the wax collected in the first 4ºC condenser during the pyrolysis of HDPE.

Chapter 4: Physicochemical Characterisation of MSW

4.1: Physical characterisation of MSW in Stellenbosch

The raw data gathered from the characterisation of the municipal solid waste are presented in Appendix A (note that the vol% is an estimated volume based on the visual level if waste in each known volume container used during the characterisation process). From this data the general waste and recycling compositions for the formal housing areas in the municipality can be compared on an area basis (Figures 4.1.1 and 4.1.2). While some variation between areas exists, it is clear that the vast majority of waste from all areas in the municipality is organic.

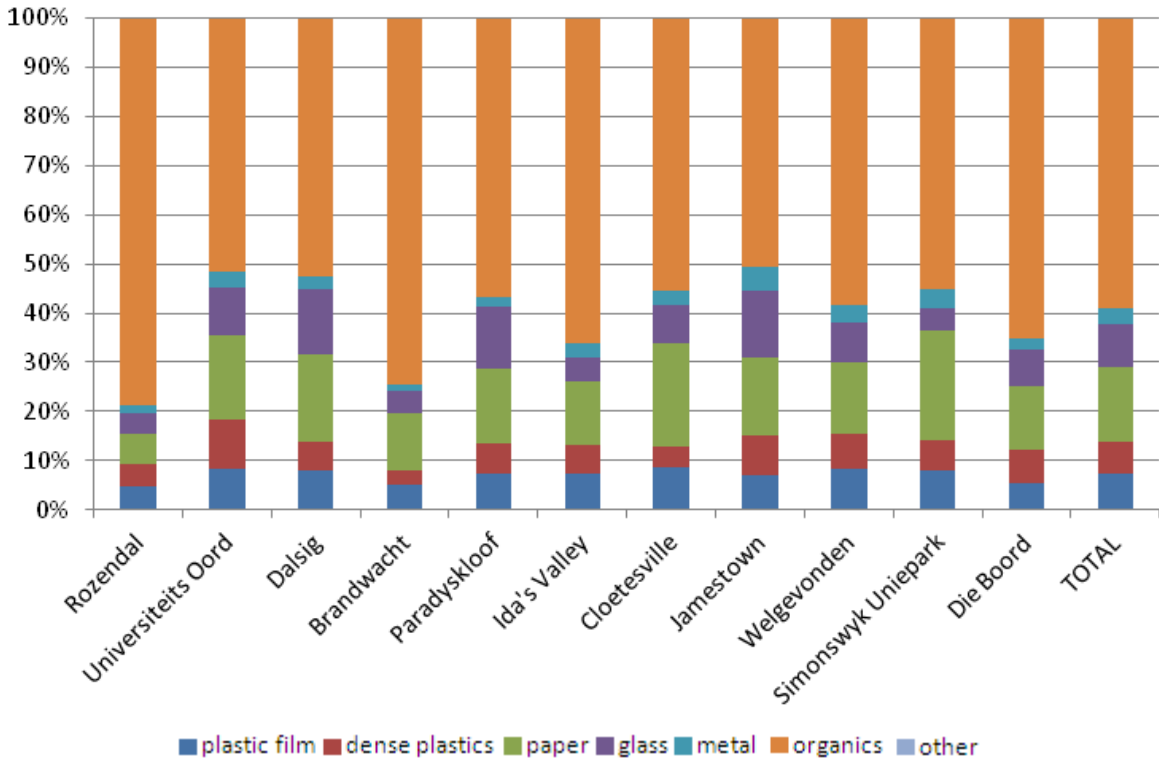

Figure 4.1.1: Composition of the General Refuse from Stellenbosch Municipality

Organics are also present in the recycling streams of all but 1 of the areas sampled (Figure 4.1.2). The presence of an organic fraction contaminates the rest of the recycling making an additional cleaning step in any recycling or sorting process necessary. This cleaning step is costly not only in monetary terms, as there is specialised equipment required, but also in terms of resources used. Cleaning of waste during the recycling process uses large amounts of water and energy and yet more energy is required to dry, agitate and transport the dirty waste. For this reason many municipal recycling facilities, like the one servicing these areas (Kraaifontein Integrated Waste Management Facility), discard all the recyclables that have come in contact with an organic fraction resulting in a large amount of recyclable waste unnecessarily being

landfilled. Public awareness is the key to reducing contamination thereby increasing the recycling rates.

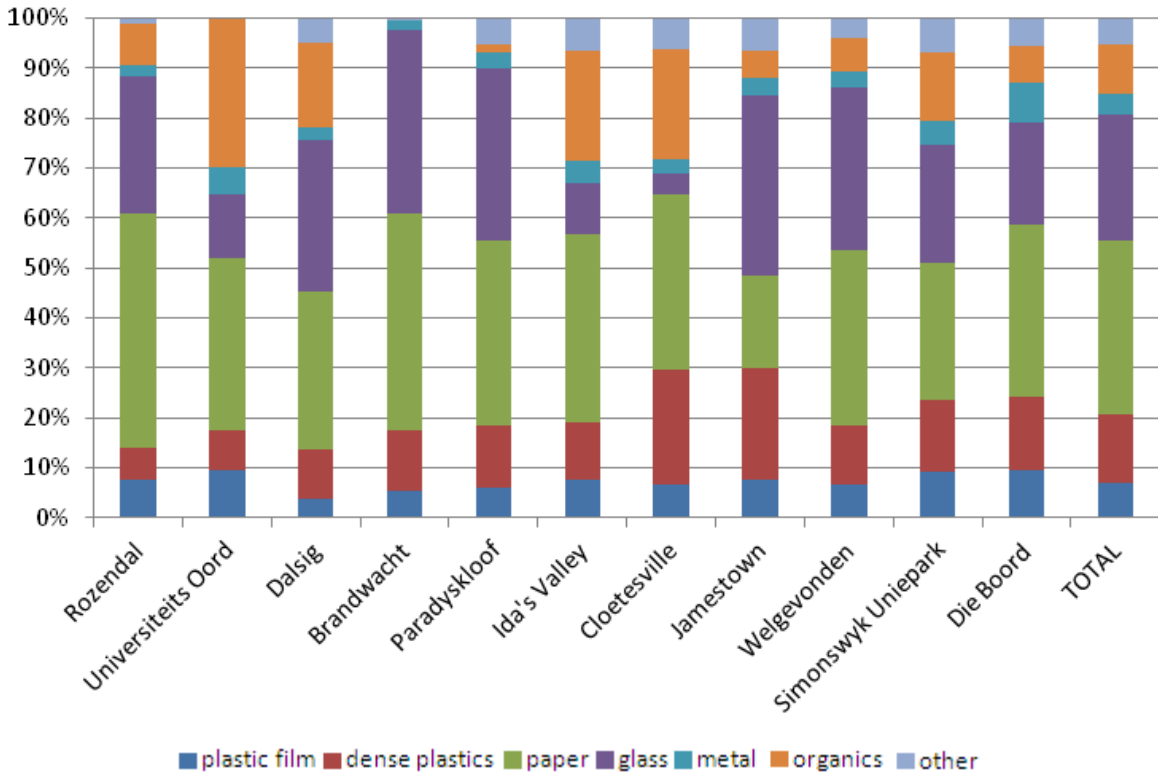

Figure 4.1.2: Composition of the Recycling from Stellenbosch Municipality

Such awareness is generated from exposure to the relevant information and education which differs between income brackets. The solid waste management sector plan for the city of Cape Town (SWMSP (2011/20120)) reports that in general the organics content of MSW from informal/low income areas is high when compared to high income areas where the amount of packaging etc. is a dominant fraction. For this reason, it is interesting to note that the areas with the highest quality recyclables stream (areas with the lowest organics content) are wealthier areas for example Paradyskloof, Brandwacht, Welgevonden and Die Boord while areas like Ida's Valley, Cloetesville and Universiteitsoord which are in a lower income range have more contamination in their recyclables streams. This ties in with global trends for developing countries (Medina (1997), Medina (2004), Sivaknmar *et al.* (2010)).

According to the South African Department of Environmental Affairs (DEA, 2012) approximately 10% of the 108Mt (megatonnes) of waste generated annually in the country is recycled. Table 4.1.1 shows that recycling in the formal areas of Stellenbosch is higher than the approximate national average with 18.48% recycling rate.

Table 4.1.1: Total Waste in Stellenbosch and Ratio of Waste Recycled and Landfilled

	All Waste	Plastic film	Dense Plastics	Paper	Glass	Metal	Organics	Other
Total Waste Sampled (kg)	6486	447	446	1090	680	186	2925	670
Extrapolated Totals (kg)	259424	17892	17822	43589	27201	7432	117007	26810
% Recycled	18.5	18.8	36.0	37.9	44.6	26.1	4.0	9.1
% Landfilled	81.5	81.2	64.0	62.1	55.4	74.0	96.0	90.9

Since approximately 10% of the households in the Stellenbosch area were sampled and only one of the average of four bags left for collection per household the weight of waste that was sampled can be extrapolated to indicate the total waste generated in the 12 sampled areas in a week (Table 4.1.1). This extrapolation is a rough estimate of the amount of waste that could potentially be used as a feedstock for a waste-to-energy application. This can be used as a baseline for any future pre-feasibility studies.

While the main objective of the characterisation was to determine the potential of the waste streams in the Stellenbosch municipality for use as refuse derived fuels it is of interest to examine the data with reference to global and other local trends.

The compositions of waste in several South African areas, both provincial and municipal, have been previously reported (DEA (2012), Fiehn *et al.* (2005), GDACE (2008), Gibb (2008)). However, the differing methods, sampling areas (landfill or source) and sampling times (differing seasons etc.) as well as generally small sample sizes make the data not only to some extent unreliable but also hard to compare from study to study (SPLM (2010), Wise *et al.* (2011)). This said, the results of characterisations performed on residential refuse in the uMgungundlovu District Municipality (UMDM) and the eThekwini Municipality, both KwaZulu Natal, as reported by Trois (2013) are compared with the total waste composition from this study (Table 4.1.2).

Table 4.1.2: Comparison of Waste Composition of UMDM, eThekwini and Stellenbosch

	eThekwini	UMDM	Stellenbosch
	% of Total Waste		
Paper	18	15	17
Plastic	19	9	14
Glass	7	7	10
Metal	5	5	3
Organic	46	34	45
Other	5	30	10

All three municipalities have between a 5 and 10% difference in the values reported for the plastics streams. With the exception of this stream, the waste compositions of the eThekwini and Stellenbosch municipalities do not differ significantly from one another. The values for

UMDM, however, differ from Stellenbosch and eThekwini by 11 and 12% for the organics and 20 and 25% for the 'other' streams respectively. While the UMDM and eThekwini studies were reported by the same author and the same categories were utilised, there is a subjective grey area associated with human error. This would affect what would be sorted as 'other' in borderline cases. For example, some studies classify compound waste, like juice cartons with a plastic lining, as paper some as plastic and in some, as was the case in this study, such waste is classified as 'other'. Although there are governmental designations of general waste categories (DEA, 2012), they are broad and open to interpretation. Thus it is clear that, in order to get reliable, comparable data, explicit definitions of the classifications for each component are required and sampling and sorting guidelines drawn up for use for all future studies. The DEA (2012) presents the composition of waste in South Africa as a mixture of commercial and residential from estimates based on numerous sources (Glass (4%), metals (13%), tyres (1%), non-recyclable MSW (35%), organic waste (13%), construction and demolition waste (20%), paper (8%) and plastic (6%)). The composition of the waste generated in Stellenbosch is comparable to the national approximations and thus can be used to broadly compare South African waste to global data.

The composition of MSW in other countries has been reported in literature. It can be seen from Table 4.1.3 that the high organics content is a problem that is not confined to South Africa and does not seem to be effected by the overall wealth of the countries (i.e. poorer countries such as Poland and India have amounts of organics present in their wastes comparable to the 1st world countries). These are statistics on the total general waste and does not take into account the recyclables stream quality.

Table 4.1.3: Comparison of Composition of MSW from Stellenbosch with Other Countries

Area	Spain[a] (Alicante)	USA[b]	Finland[b]	Norway[b]	Nederlands[b]	USA[c]	India[d] (Maharashtra)	Poland[b]	Stellenbosch[e]
wt% of Total General Refuse Stream									
Paper	38	37	40	33	28	40	6	14	17
Plastics	3	8	5	7	8	3	6	2	14
Wood	3	28	37	15	55	3	10	40	45
Organics	13					28	32		
Glass	4	18	5	7	7	10	-	4	11
Metals	1					9	5		3
Others	10	8	14	38	2	8	36	40	10
Fines	28						5		

a.Garcia *et al.*(1992) b. Sørum (2001) c.Agrawal (1988) d.Namdeo *et al.* (2010) e.This Study

The composition of MSW in Stellenbosch is not remarkably different when compared to the other countries presented and fits in well between the values reported for the poorer countries and the 1st world countries.

As discussed in Chapter 2 one of the main considerations when producing an RDF and when choosing feedstocks for thermal treatment is the energy density of the material being evaluated. The presence of a high oxygen to hydrogen and oxygen to carbon ratios in a substance significantly lowers its energy density and the presence of water greatly increases these ratios. Another factor influencing the energy density is the presence of inert substances. The materials found in the waste with the highest inherent energy density are plastics and dry paper. For this reason the organics (high moisture content), metal and glass (both inert) streams were excluded from the final potential RDF mix. It should be mentioned, however, that there is a large amount of energy that could be recovered from the organics stream if the stream could be better separated and dried in a feasible manner. This avenue could be the topic of future studies.

Although the source separation of the recycling in Stellenbosch is not perfect (Figure 4.1.2), there is a significantly smaller organics fraction present making for relatively easy sorting and less contamination and thus less waste of other calorifically valuable components. This in turn means that the recycling stream would require less treatment and processing, after the removal of the metal and glass fractions, to potentially form a good RDF. As such it was decided that only material collected as recycling would be evaluated in this study.

Removing the organics, metal and glass fractions from the recycling streams results in overall potential RDF mixture obtained from the municipality's total recycling stream. The majority of the potential RDF is paper. During the characterisation it was found that this fraction was mainly made up of newspaper, office and writing paper and glossy paper from magazines and brochures etc. While other paper fractions, such as tissue paper, were present their proportion was small and as a result it was decided that the paper fraction be made up of equal parts of the three main paper components. Similarly, it was decided, in line with the general observations of this study, to represent the plastic film by low density polyethylene (LDPE) and the dense plastic components by a half-half mixture of high density polyethylene (HDPE) and polyethylene terephthalate (PET) (Figure 4.1.3).

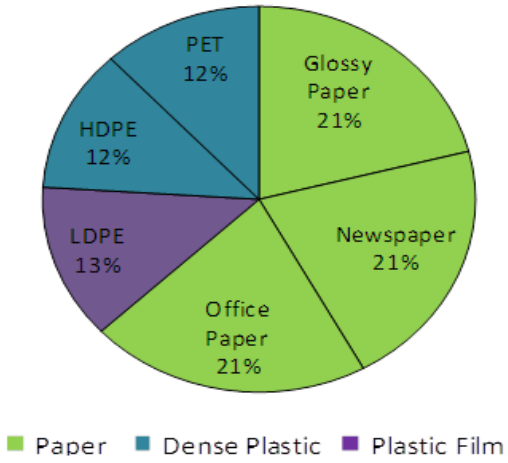

Figure 4.1.3: Final RDF Compositions

4.2. Chemical characterisation of RDF components

The results of the elemental and proximate analyses (moisture content, MC, volatile matter, VM, fixed carbon, FC, and ash) as well as the measured higher heating values (HHV) for all feedstocks are presented in Table 4.2.1 below. Also presented are the values for HHV calculated by the Channiwala *et al.* (2002) and Parikh *et al.* (2005) correlations.

Table 4.2.1: Results from Proximate Analysis, Elemental Analysis and HHV (meas. & calc.)

	Percentage of Total Mass (%)									MJ/kg		
Component	**MC**	**VM**	**FC**	**Ash**	**C**	**H**	**N**	**S**	**O***	**HHV[a]**	**HHV[b]**	**HHV[c]**
Glossy Paper	1.41	69.56	6.60	22.43	31.41	4.31	0.03	0.08	64.17	16.54	8.94	13.19
Office Paper	1.92	77.00	9.76	11.32	35.68	5.45	0.00	0.00	58.87	19.85	12.55	15.67
Newspaper	2.74	78.19	13.21	5.86	42.94	6.17	0.06	0.00	50.83	16.61	16.88	17.29
HDPE	0.21	98.85	0.00	1.03	83.21	14.11	0.00	0.00	2.68	44.90	45.38	15.42
LDPE	0.28	99.72	0.00	0.00	84.47	15.34	0.00	0.00	0.19	44.70	47.54	15.59
PET	0.00	90.54	9.46	0.00	62.65	4.62	0.00	0.00	32.73	22.30	23.93	17.46

a Measured b Channiwala *et al.* (2002) c Parikh *et al.* (2005)

* Oxygen mass percentage found by difference

Comparing the measured HHV's and those predicted using the Channiwala *et al.* (2002) correlation it can be seen that the predictions for the paper components are lower than the measured values (Table 4.2.1). This is due to the extremely high oxygen contents that are out of range for the correlation. Although this correlation is indicated mainly for processed fuels, it predicts the HHV's of the plastic components quite well (within the average absolute error of the formula) as they fall within the ranges of the formula and are similar to fuels in that they are made up of hydrocarbon chains.

Conversely, the Parikh *et al.* (2005) correlation gives a prediction much closer (within 4.3%) to the measured value for the paper samples (within the absolute average error predicted) with the exception of the glossy paper (Table 4.2.1). This could be due to the fillers used in the manufacturing process influencing the combustion of the sample. The Parikh correlation does not predict well for the plastic samples due to the fact that HD and LDPE have higher volatile matter contents while PET has a lower ash content than the allowable range.

The experimental calorific values (Table 4.2.1) are in agreement with those of the literature (24 – 46MJ/kg for plastic and 11 – 21MJ/kg for paper) indicating that plastics and papers wastes could be considered as potential feedstocks for energy production.

Chapter 5: Kinetic and Chemical Aspects of Pyrolytic MSW Degradation

The pyrolytic characteristics of paper (glossy, office and newspaper) and plastic (HDPE, LDPE and PET) were investigated by using a thermogravimetric analyser (Section 5.1) coupled to a mass spectrometer (TGA-MS). The application of this technique led to an in-depth description of pyrolytic degradation steps by determining the kinetic parameters and kinetic rates of degradation (presented in Appendix C) (Section 5.2) and chemical description of volatiles evolved from these degradation stages (Section 5.3).

5.1 Thermal behaviour of feedstocks

5.1.1: Thermal behaviour of paper

In order to examine the degradation characteristics of the paper samples the data sets obtained (TGA and DTG) at the lowest heating rate, 10K/min, are compared (Figures 5.1.1 and 5.1.2). The number of degradation stages is most clearly seen upon examination of the DTG curve (as indicated on Figure 5.1.2). It is evident that the thermal degradation of both glossy paper and office paper occurs in three distinct steps. The second stage exhibits, by far, the greatest weight loss as well as the highest rate of weight loss for the entire degradation. The second greatest weight loss as well as the second greatest rate of weight loss is observed in the third stage of degradation.

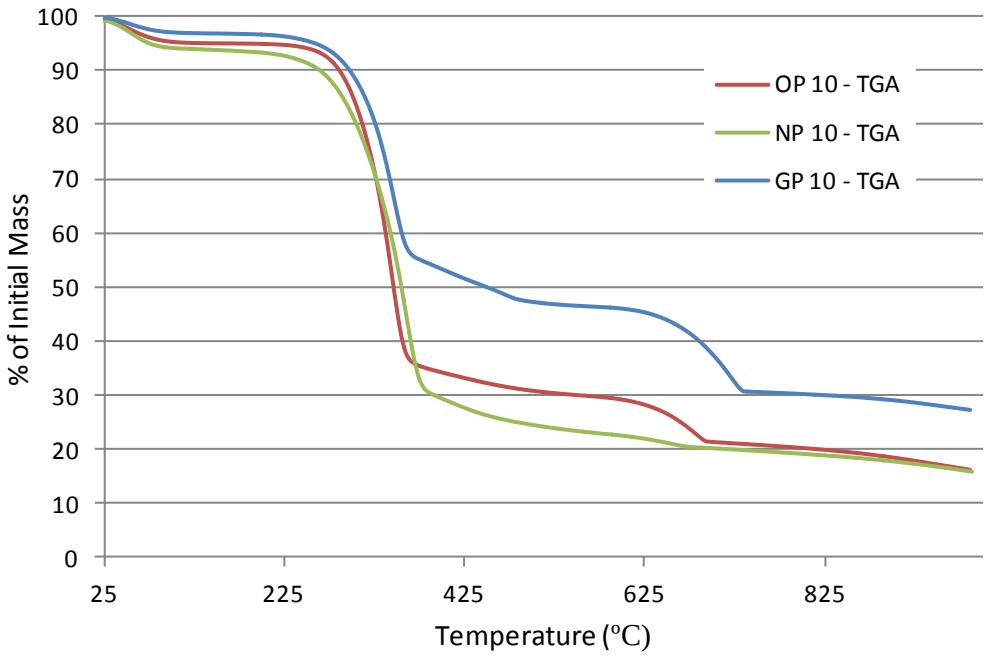

Figure 5.1.1: Weight loss with Temperature Comparison for Paper Samples at 10K/min

(Office paper (OP 10-TGA), Newspaper (NP 10- TGA) and Glossy Paper (GP 10 – TGA)

The TGA curve for newspaper seems to show only two distinct stages of weight loss. There is, however, a small area of inflection of the TGA graph corresponding with an extremely small weight loss step evident in the third set of DTG peaks (Figure 5.1.2). These trends are in line with previous studies on the pyrolytic behaviour of waste papers where the presence of primary (Modh *et al.* (2012)), secondary and tertiary stages were confirmed (Chang *et al.* (1996), Wu *et al.* (1997) and Wu *et al.* (2002)).

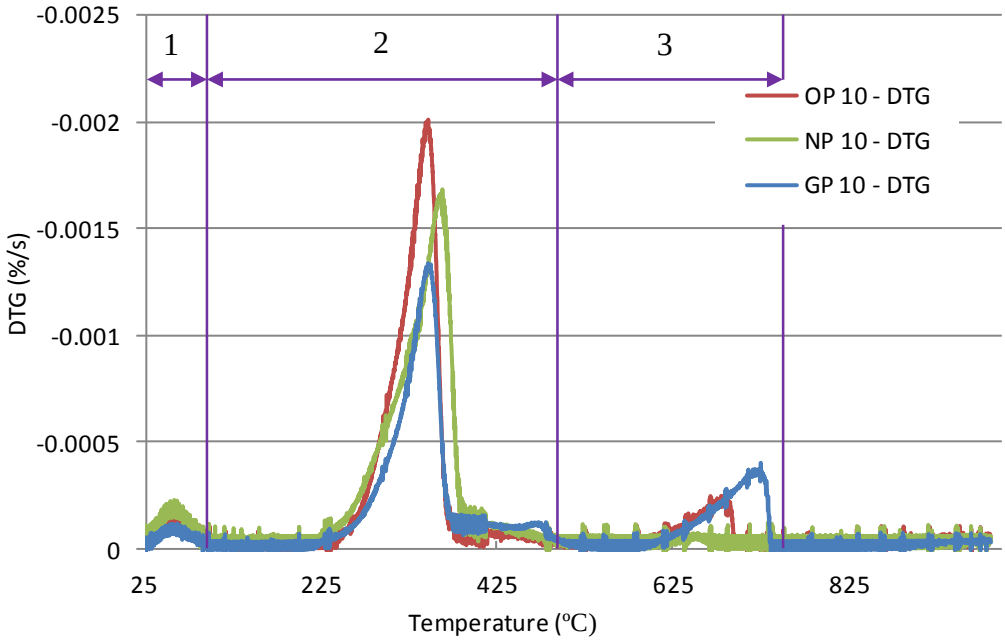

Figure 5.1.2: Rate of Weight loss with Temperature Comparison for Paper Samples at 10K/min
(Office paper (OP 10-DTG), Newspaper (NP 10- DTG) and Glossy Paper (GP 10 – DTG)

Despite this lack of a destinct third stage of degradation, newspaper loses more weight (average total weight loss over all heating rates 82.44%) than the other two paper samples at all heating rates. Table 5.1.1 provides a summary of the degradation stages, onset temperatures, total weight loss and quantification of the maximum rates of degradation for the three paper samples. It can be seen that office paper loses almost as much weight (81.59%) as newspaper, while glossy paper loses an average of 71.82%, over 10% less weight than the other two papers. The onset and offset temperatures for the three samples are very similar, seen most clearly in the DTG curves.

Figure 5.1.2 shows that the rates of weight loss between the paper samples also differ with office paper losing weight at the highest rate and glossy paper at the lowest for the main degradation step (the step associated with the largest weightloss, step 2). This trend in evident at all heating rates (Table 5.1.1) and shows that while the overall degradation characteristics are similar there are differences in the degradation that are specific to each sample. This shows

that glossy paper is the most thermally stable sample while office paper is the most volatile of the three paper samples. Upon examination of the proximate analysis results for the paper (Table 4.2.1) it can be seen that glossy paper contains the least amount of volatile matter (VM), 69.56%, while the VM contents for office and newspaper are very similar (77 and 78.2% respectively). The low VM content of glossy paper could account for the consistently higher thermal stability but the very similar VM contents for office and newspaper do not explain the trend. It is possible that the differences in thermal stability (rates of decomposition) are due to a catalytic effect of ash on the decomposition reaction. Since the majority of paper is cellulose the differences in the elemental compositions are mostly due to the differences in additives, high in oxygen, (clay etc.) which contribute to the ash content Since office paper has almost double the ash content of newspaper as well as 8% more oxygen this would explain this difference.

The weight loss experienced under pyrolytic conditions can be attributed to the thermal decomposition of the sample. This decomposition will include the loss of all the moisture, MC, (1^{st} stage), as temperatures well exceed the boiling point of water, as well as volatile matter present in the sample (2^{nd} and 3^{rd} stage). As the decomposition occurs in an inert atmosphere there should be no loss in the fixed carbon content of the samples. It can be seen (Figure 5.1.1) that all three papers' TGA curves continue a very slight downward trend after the last degradation step. From this one might conclude that none of the papers reach complete pyrolytic conversion (i.e. loss of all MC and VM) which would only be the case if there was absolutely no further weight loss i.e. DTG = 0 %/s. However, by comparing the average total weight losses, mentioned above, with the proximate analyses performed on the raw feedstocks it is possible to gauge the actual extent of devolatilisation by pyrolytic decomposition.

Since paper is mostly cellulose the degradation of paper can be compared with that of pure cellulose however, cellulose exists in many forms. The degree of polymerisation and crystallinity of the polymer as well as any inorganic impurities as well as the source of the cellulose impact the degradation characteristics (Antal *et al.* (1995), Gronli *et al.* (2002)). The differences in the source woods as well as the compounds used as fillers for each of the different types of paper (as per Chapter 2) will further impact the degradation characteristics of papers from one another.

For complete pyrolytic conversion the yield of volatiles, based on the TGA results (Table 5.1.1) would be 70.97% for glossy paper and 78.92 and 80.93% for office and newspaper

respectively. It can be seen that each of the papers lost more weight than is expected at total pyrolytic conversion by 0.84, 3.53 and 0.66% for glossy paper, newspaper and office paper respectively. This can be attributed to the nature of the milled samples and their respective chars and ashes. The ashes and, to a lesser extent, chars of pyrolysed paper have extremely low densities, this coupled with very small particle sizes could lead to the ashes and chars being removed from the crucible due to the flow of nitrogen (70 ml/min) in the TGA furnace. This explanation is supported by the presence of small amounts of ash on the TGA furnace walls after the completion of the runs.

The differences in this excess weight loss by the different papers (Table 5.1.1) can be due to the differences in densities and properties of each paper as this will affect the qualities of the pyrolytic residues. The milled newspaper and office paper are much less dense, 122 and 111g/L, than glossy paper (176g/L). It is probable that the residues would follow the same trend and thus the paper with the lowest density will have the lowest density residues that are the most likely to be removed from the crucible by the flow of purge gas.

Upon inspection of stage 2 for all three paper samples a second shoulder immediately following the unresolved major peak on the DTG curves (Figure 5.1.2) is evident. This is indicative of separate substages or two reaction steps happening in quick succession. These compound steps could be de-convoluted into two definite separate steps occurring partially in parallel, an approach that could prove useful when examining the thermal degradation pathways and kinetic parameters of degradation. This, however, is beyond the scope of this study but could be considered in future studies.

Table 5.1.1: Summary of Weight loss and Weight loss Rates for Paper Components from TGA

Glossy Paper										
Heating Rate (K/min)	Sample Size (mg)	No. of Weight loss Stages	Total Weight loss (%)	Onset Temperature (°C)			Degradation Range (°C)	Max DTG (%/s)		
				Stage 1	Stage 2	Stage 3		Stage 1	Stage 2	Stage 3
10	12.76	3	72.83	26	215	623	26 - 760	-1.22E-04	-1.35E-03	-4.049E-04
20	9.26	3	72.03	26	220	628	26 - 775	-2.88E-04	-3.74E-03	-1.026E-03
30	13.09	3	71.46	26	220	624	26 - 795	-2.55E-04	-3.93E-03	-1.031E-03
50	14.25	3	70.96	26	225	641	26 - 805	-3.86E-04	-6.23E-03	-1.591E-03
Newspaper										
Heating Rate (K/min)	Sample Size (mg)	No. of Weight loss Stages	Total Weight loss (%)	Onset Temperature (°C)			Degradation Range (°C)	Max DTG (%/s)		
				Stage 1	Stage 2	Stage 3		Stage 1	Stage 2	Stage 3
10	8.34	3	84.27	26	212	635	26 - 678	-2.20E-04	-1.70E-03	-5.93E-05
20	5.94	3	80.99	26	218	640	26 - 750	-4.21E-04	-3.98E-03	-1.34E-04
30	7.97	3	82.67	37	224	650	37 - 780	-4.81E-04	-4.73E-03	-1.67E-04
50	8.8	3	81.83	44	238	660	44 - 850	-7.39E-04	-7.61E-03	-2.65E-04
Office Paper										
Heating Rate (K/min)	Sample Size (mg)	No. of Weight loss Stages	Total Weight loss (%)	Onset Temperature (°C)			Degradation Range (°C)	Max DTG (%/s)		
				Stage 1	Stage 2	Stage 3		Stage 1	Stage 2	Stage 3
10	9.76	3	83.92	26	198	608	26 - 710	-1.88E-04	-2.02E-03	-2.73E-04
20	5.49	3	82.07	26	250	624	26 - 722	-5.16E-04	-6.89E-03	-7.59E-04
30	9.66	3	80.35	43	254	640	43 - 737	-3.45E-04	-5.35E-03	-5.87E-04
50	9.15	3	80.03	61	256	653	61 - 750	-5.28E-04	-8.42E-03	-1.04E-03

5.1.2 Thermal behaviour of plastic

Unlike the three paper samples the plastics considered in this study (high and low density polyethylene (HD/LDPE) and poly(ethylene terephthalate) (PET)) decompose in a single step/stage with very little or no weight loss outside of the main weight loss region. This single step behaviour (Figure 5.1.3) and the trends of onset temperature are all in line with previous research on plastic waste TGA experimentation (Ceamanos *et al.* (2002), Cho *et al.* (1998), Jenekhe *et al.* (1983), Martin-Gullion *et al.* (2001), Sasha *et al.* (2005) and Sinfronino *et al.* (2005)).

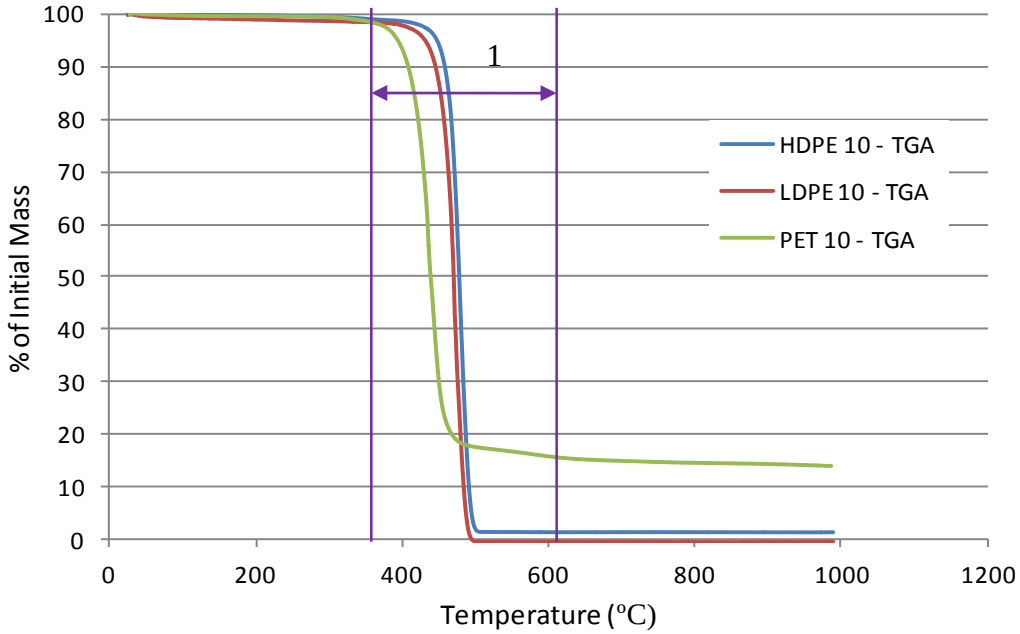

Figure 5.1.3: Weight loss with Temperature Comparison for Plastic Samples at 10K/min

Upon close inspection of the DTG curves for LDPE and PET (Figure 5.1.4) it can be seen that the single step degradation occurs in two sub-steps indicated as single jagged peaks, unlike the phenomenon observed in the second step of the paper degradation where the second peak follows as a continuation of the unresolved main peak. These compound steps could be de-convoluted into two separate steps occurring, for the most part, in parallel and could be useful when determining the kinetics and specific pathway of the thermal degradation of the compounds. It is important to note that the lower the heating rate, the more detail about the degradation process can be observed. This is evident with the secondary peaks for PET that are only observable for the two lower heating rates and are not present at higher heating rates (Appendix B); this is discussed in Section 5.3. While some authors have reported two step reaction mechanisms (from GC-MS and infrared spectroscopy etc.) for PET and PE (Jenekhe *et al.*, 1983), the TGA curves presented are smooth indicating that there is no clear distinction in mass loss between these steps. This could be due to the equipment not capturing data in

infinitesimal ranges of reaction progress thereby missing the small inflections and thus changes in rate, or due to the differences in preparation of the samples.

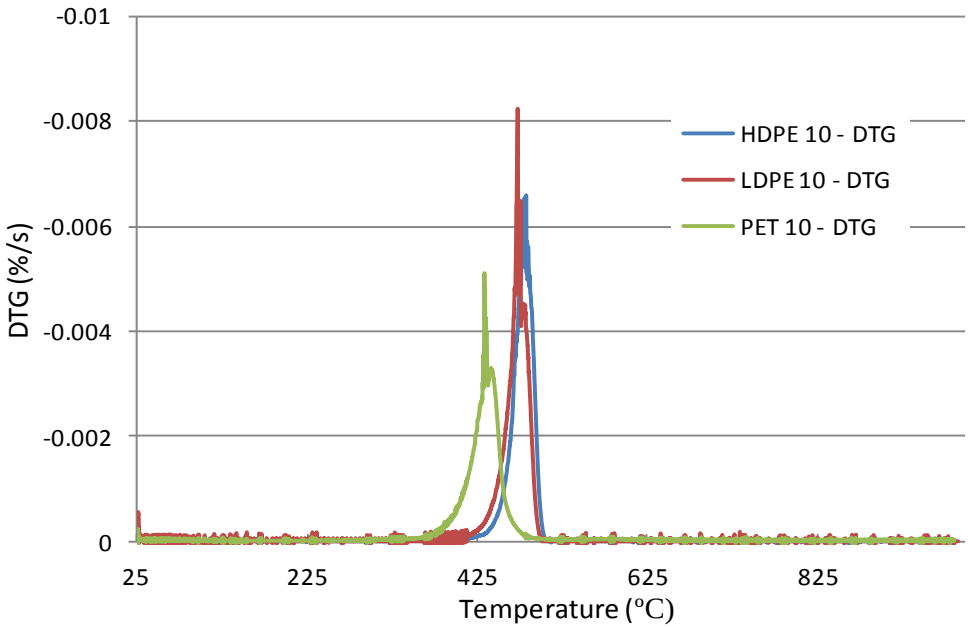

Figure 5.1.4: Rate of Weight Loss with Temperature Comparison for Plastic Samples at 10K/min

The proximate analyses of the plastic samples showed combined moisture and volatiles contents of 99.0, 100.0 and 90.5% for HDPE, LDPE and PET respectively (Table 4.2.1). Comparing these values with the average weight losses of the components (Table 5.1.2) it is evident that both HDPE (0.17%) and, to a greater extent, LDPE (0.70%) lose more weight than is expected at complete pyrolytic conversion. As with the paper, after the completion of the TGA runs on the plastic samples there was ash present on the TGA furnace walls. Vigorous bubbling and spitting was observed at the onset of visible product formation in larger scale pyrolytic experimentation on HDPE (described in Chapter 6). If this were to occur in the TGA some of the sample would leave the crucible and deposit on the furnace walls where it would continue to decompose leaving behind ash. This leads to the probability that the excess mass loss for HDPE was a combination of ash removed from the crucible due to the flow of nitrogen as well as splatter.

The LDPE, however, shows a mass loss of over 100% which is only possible if the actual crucible lost weight. This could be the case if the crucibles were not properly cleaned before the run on the TGA and thus still had trace amounts of previous samples in it or if the sample reacted with the alumina crucible. However, due to the thorough way that the crucibles are cleaned between runs and that this error is seen in all four heating rates and across repeats, the former is unlikely. Some research has been done on the use of alumina loaded catalysts on the

degradation of PE (Aydemir *et al.* 2013). It was found that the alumina catalyst greatly reduced the degradation temperature and that the catalyst itself did not participate in the reaction. Since the degradation of the polyethylene in this study occurred within the normal temperature range it is clear that the crucibles had no catalytic effect and because alumina is used in catalysts for this type of feedstock it can be assumed that the crucibles did not react with the PE.

Another possible explanation is that the nature of the LDPE sample used in the runs was such that it influenced the weighing procedure. The unconventionally shaped (i.e. not spherical or cylindrical) flake like milled LDPE particles (Figure 5.1.5a) have a much larger surface area to weight ratio than the same size HDPE particles (Figure 5.1.5b) (with the milled HD and LDPE having densities of 276 and 124g/L respectively). The greater down force of the purge gas on particles with a large surface area could cause the initial mass recorded to be artificially higher. Once degradation is completed there are no longer any particles to interact with the gas (ash and fixed carbon for LDPE are both zero), hence the negative mass reading. Other authors have not experienced this problem, however it is usual to experiment on virgin pellets rather than previously extruded waste or films (as is the case in this study).

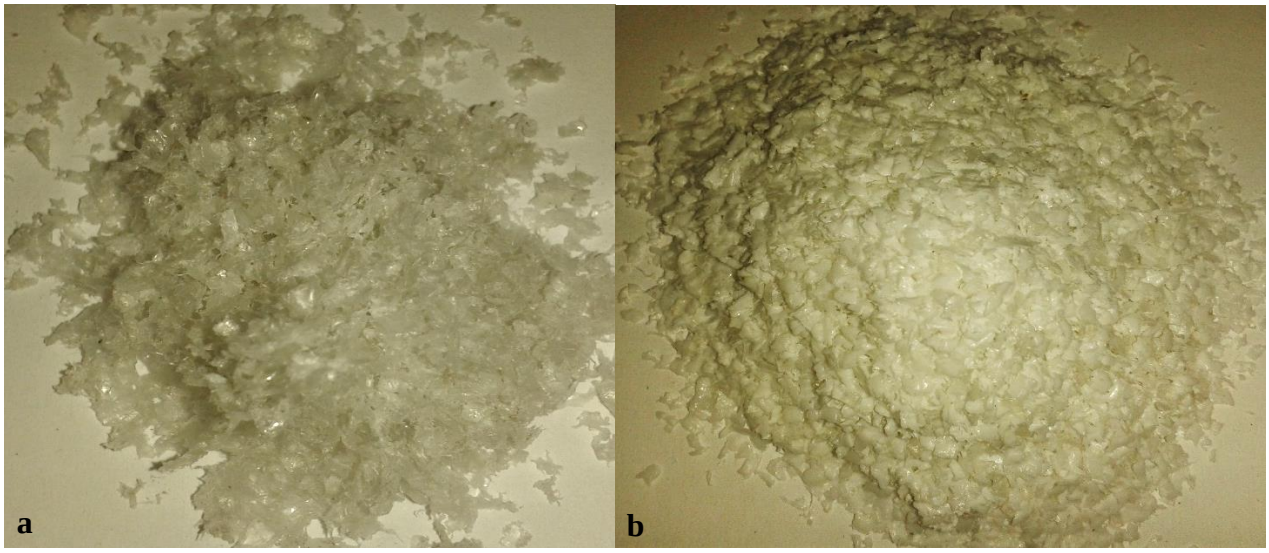

Figure 5.1.5: Physical Appearance of Milled LDPE (a) and HDPE (b)

As with the paper samples, the comparative DTG curve shows that there is a difference in the maximum rates of degradation. LDPE has consistently higher maximum rates of degradation than HDPE and PET, which has the lowest (Table 5.1.2). This trend can be correlated to the VM present in each sample with the highest degradation rates relating to the largest VM content. It is also interesting to note that the trend also correlates with the bulk densities of the samples with low bulk densities relating to high rates of degradation. Although the small scale

of these experiments should minimise the influence of heat and mass transfer limitations on the degradation the effect of bulk density of samples should be considered as a potential parameter affecting pyrolytic decomposition in future studies

The PET samples lost, on average, only 86.72% of their initial mass (Table 5.1.2). Thus 3.93% of the volatiles available in the sample were not released. This, as with the other discrepancies found for the other samples, is most likely due to the nature of the samples themselves. The PET particles are the densest (298g/L) of those considered here. The thermal conductivity (Table 2.7.1) of the PET is 0.15 W/mK, comparing this with the conductivities of HD and LDPE (0.48 and 0.33 W/mK respectively) it is clear that heat transfer will be much more limited for the PET. This coupled with the zero ash content and the inherent particle density, could explain the incomplete conversion. Another possible explanation is that the PET does completely convert but some of the released volatiles are recaptured by the char which could act as activated carbon. PET has a high oxygen concentration which is most likely part of the VM of the sample and would thus be released as CO compounds. This could cause an activation of the fixed carbon during degradation thereby producing an absorbent. Further work should be done on the properties of the residues of PET pyrolysis to see if this is indeed the case.

Table 5.1.2: Summary of Weight loss and Weight loss Rates for Plastic Components from TGA

HDPE						
Heating Rate (K/min)	**Sample Size (mg)**	**No. of Weight loss Stages**	**Total Weight loss (%)**	**Onset Temperature (°C)**	**Degradation Range (°C)**	**Max DTG (%/s)**
10	19.46	1	98.81	415	415 - 500	-6.60E-03
20	18.25	1	98.21	435	435 - 520	-1.31E-02
30	20.02	1	99.53	440	440 - 520	-1.83E-02
50	19.46	1	99.99	456	456 - 538	-2.58E-02
LDPE						
Heating Rate (K/min)	**Sample Size (mg)**	**No. of Weight loss Stages**	**Total Weight loss (%)**	**Onset Temperature (°C)**	**Degradation Range (°C)**	**Max DTG (%/s)**
10	7.99	1	100.38	410	412 - 525	-8.22E-03
20	9.36	1	100.99	414	420 - 535	-1.72E-02
30	8.45	1	100.88	423	425 - 540	-2.09E-02
50	8.85	1	100.54	433	437 - 545	-2.84E-02
PET						
Heating Rate (K/min)	**Sample Size (mg)**	**No. of Weight loss Stages**	**Total Weight loss (%)**	**Onset Temperature (°C)**	**Degradation Range (°C)**	**Max DTG (%/s)**
10	20.9	1	85.9	316	316 - 500	-5.05E-03
20	20.67	1	85.39	366	366 - 511	-1.01E-02
30	21.46	1	86.87	367	367 - 590	-1.42E-02
50	20.51	1	88.31	387	387 - 622	-2.52E-02

5.2 Determination of kinetic parameters and rates

As indicated in Chapter 3, a differential isoconversional method was applied to give a description of the mechanisms for reliable kinetic predictions regarding the degradation of MSW components. The importance of multi heating rate data in obtaining accurate results has been stressed (Section 2.5) thus, a series of TGA runs at different heating rates were performed. The effect of heating rate on degradation is discussed in Section 5.2.1. Section 5.2.2 outlines the variation of activation energy with reaction progress illustrating potential multi-step kinetics, which will be accordingly linked to the volatiles released during pyrolysis (Section 5.3).

5.2.1: Effect of Heating Rate

The effect of heating rate on the degradation of glossy paper can be seen upon the comparative examination of the TGA and DTG curves for all four heating rates (Figures 5.2.1 and 5.2.2). Similar comparative graphs can be found in Appendix B for the other five components.

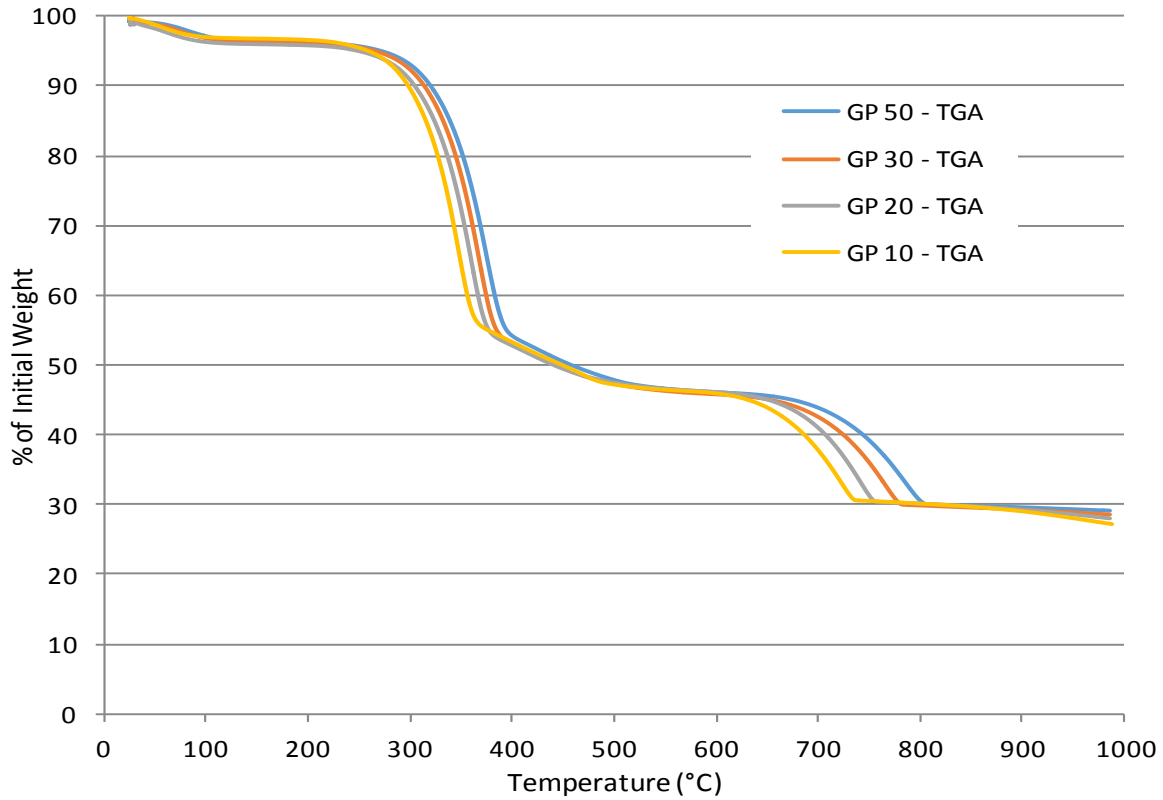

Figure 5.2.1: Comparison of Weight loss of Glossy Paper at Different Heating Rates
(TGA curve for glossy paper at XK/min (GP X - TGA)

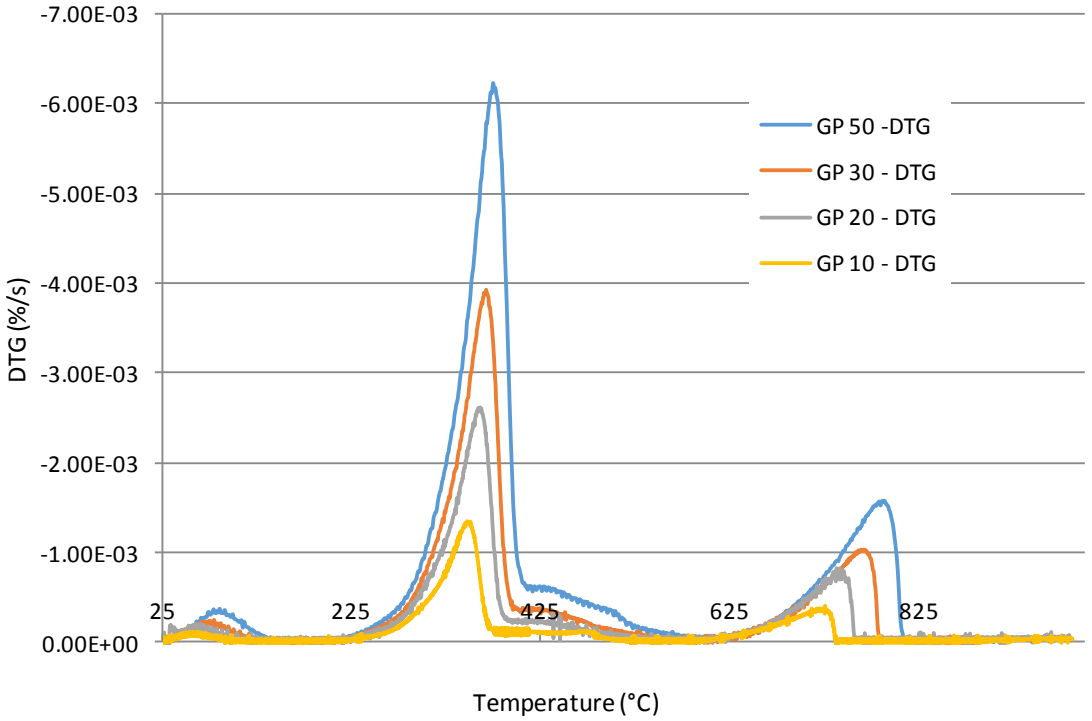

Figure 5.2.2: Comparison of the Rates of Weight loss of Glossy Paper at Different Heating Rates
DTG curve for glossy paper at XK/min (GP X - DTG)

The shift of the curves to higher temperatures with increasing heating rate is apparent in both TGA and DTG graphs (Figures 5.2.1 and 5.2.2). Thus, the onset temperature for each stage of degradation is increased as heating rate is increased. This phenomenon has been observed numerous times by many different authors working with waste and virgin biomass and manufactured papers/plastics (Ceamanos *et al.* (2002), Chang *et al.* (1996), Modh *et al.* (2012), Sinfronino *et al.* (2005) and Wu *et al.* (1997)).

Some authors have attributed the shift in degradation temperature with heating rate, in part, to limitations of the heat transfer within the furnace (Berrueco *et al.* (2005), Lopez *et al.* (2011), Williams *et al.* (1992), Yang *et al.* (2007)). In order to get the most accurate picture of the degradation, the furnace temperature should ideally be changed in accordance with the actual sample temperature and thus accurate measurement of the sample temperature, lacking in many older TGA systems, is needed. Advances in analytical instrumentation have minimised this problem and with new TGA equipment, like that used in this study, the sample and furnace temperatures are almost identical (verified as in example in Appendix B) and as such the effect on the measured degradation is negligible.

Thus the increase in degradation temperature can be attributed to heat transfer limitations between the sample's particles and the inherent thermal conductivity of the sample, i.e. heat transfer limitations within the particle itself thus the well documented effect of particle size on

degradation (Buah *et al.* (2007), Luo *et al.* (2010)). The plastic samples have much higher thermal conductivities than the papers considered in this study. The higher the thermal conductivity of a sample the narrower the degradation temperature range for each stage. This correlation can be clearly seen with the plastic samples and is most clearly illustrated graphically as in Appendix B. Looking at a heating rate of 50K/min the degradation ranges (Table 5.1.2) for HDPE, LDPE and PET are 82, 108 and 235°C and thermal conductivities of 0.48, 0.33 and 0.15W/mK respectively (Table 2.7.1).

All three paper compounds have the same, low thermal conductivity of 0.05W/mK (Table 2.7.1), almost a factor of 10 less than that of HDPE. Thus, when comparing these degradation ranges with those of the plastics, it can be seen that the degradation ranges are much greater for each step than the single step plastic degradation. In addition to the differences between samples, the ranges of degradation of single samples increase with increasing heating rate (Tables 5.1.1 and Table 5.2.2). It can thus be said that the temperature and range of degradation of a paper/plastic compound increases with increasing heating rate for each sample and decreases with thermal conductivity between samples.

From the results of the thermogravimetric analysis carried out in this study (Tables 5.1.1 and 5.1.2) and comparable literature it is clear that an increase in heating rate applied to the pyrolysis of the three plastic samples increases overall weight loss, degradation onset temperatures and degradation ranges as well as the maximum rate of degradation of the samples. Conversely, for the paper samples, an increase in heating rate decreases the overall weight loss, while the other trends are the same as for the plastic samples.

5.2.2: Determination of the kinetic parameters - plastic

A summary of the kinetic parameters, apparent Ea and $\ln(Af(\alpha))$, obtained by the Friedman method is provided in Table 5.2.1. Vyazovkin (2006) states that kinetic parameters found by model free methods are global and are, at any conversion, the sum of the contributions of the different steps to the overall reaction. Thus the kinetic parameters do not represent the production of a single product, but rather encompass all pyrolytic reactions occurring in parallel at that stage. For the plastic samples, where only one degradation step was observed, one global set of kinetic parameters was calculated (Figures 5.2.3 – 5.2.5).

Table 5.2.1: Summary of Global E_a and $Af(\alpha)$ Isoconversional Kinetic Values for Plastics

	Specific α Range R^2 >|0.8|	Average E_a (kJ/mol)	Average ln(Af(α))	$Af(\alpha)$ (1/s)
	Plastics			
HDPE	0.0001 - 0.986	279.20	39.12	9.79E+16
LDPE	0.0001 - 0.957	142.58	17.82	5.49E+07
PET	0.0001 - 0.889	224.66	32.61	1.46E+14

The 'specific conversion (α)' referred to in this section is the reaction progress not the conversion of initial feedstock into products. For example, a specific conversion of 0.1 refers not to a loss in initial mass of 10%, but rather 10% of the total mass lost. The correlation coefficient, R^2, value referred to in Table 5.2.1 is an indication of how well points on the Freidman plots fit a straight line (i.e. degree of linearity). Only data that showed above an 80% linearity (R^2 = |0.8|) were considered showing that the kinetic model is not necessarily reliable for the end of the degradation stages.

Figures 5.2.3 to 5.2.5 show the trends in activation energy for the three plastic components. All three show an increase in E_a with specific conversion; HDPE and PET show more localised increases (especially in the beginning stages) than LDPE which increases steadily throughout conversion. This shows that the more reactive fractions of the feedstocks are released first in the degradation and the less reactive towards the end of degradation. As the less reactive a compound the more energy is required for degradation (higher activation energy).

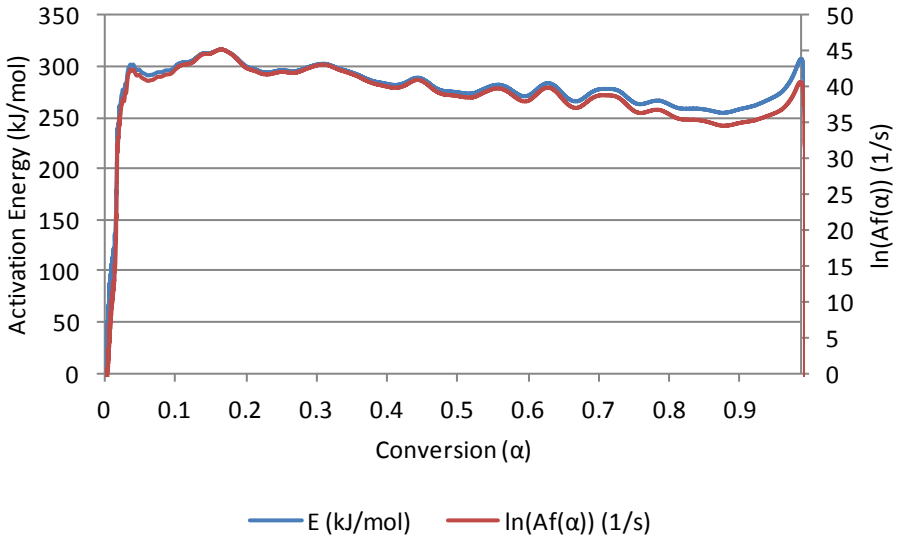

Figure 5.2.3: Activation Energy and ln(Af(α)) Dependence on Specific Conversion for HDPE

HDPE shows a sharp increase in activation energy from 22.13 – 290 kJ/mol from a specific conversion of 0 to 0.03 (Figure 5.2.3). This coincides with the onset of thermal degradation, the 'lag phase' before the rapid devolatilisation apparent as a sharp drop in the TGA plot. The activation energy increases slightly to the maximum, 316.52 kJ/mol, where after the energy

required for the continued degradation of HDPE stabilises to a slight downward trend with minor undulations. The average activation energy for the correlation region is 279.20 kJ/mol. These values are slightly higher (46KJ/mol) than those found by the Friedman method by Wu *et al.* (1993), 233.2kJ/mol. Peterson *et al.* (2001) compared the results of ten authors using thermogravimetry to determine kinetics by different methods. The activation energy found for in that study, 240 kJ/mol, fit within the range found in the literature, 147 – 273 kJ/mol. Sinfronio *et al.* (2005) calculated a series of kinetic parameters using four different methods and reported values of 204.57 – 269.04 kJ/mol. Ceamanos *et al.* (2002) obtained an activation energy of 346.8 kJ/mol using isoconversional methods. This goes to show the great range of reported literature data. It is clear that the method of attaining the kinetics as well as the specifics (density, particle size, virgin/recycled) of the feedstock play a large role in the values obtained for the kinetic parameters. For these reasons, as well as the wide range found between the onset and end of degradation within the good correlation range, it can be said that the values found in this study, while towards the higher side, fit in with the ranges found in literature.

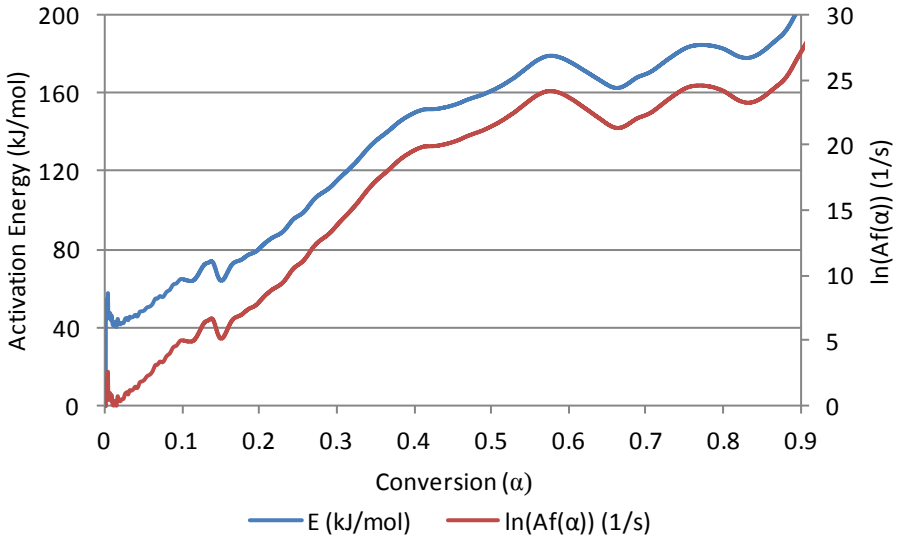

Figure 5.2.4: Activation Energy and ln(Af(α)) Dependence on Specific Conversion for LDPE

In contrast to HDPE, LDPE shows a steady increase in activation energy throughout the specific conversion (Figure 5.2.4). This could be due to the difference in molecular structure of the two feedstocks or the physical differences in surface area to weight ratio. As mentioned previously, HDPE is more crystalline in structure than LDPE and as such has a sharp melting point rather than a range over which it melts (as per Chapter 2). It was also observed during the TGA runs that the range of degradation at each heating rate was up to 40 ºC greater for LDPE than for HDPE. There are also two small peaks visible in the E_a plot (Figure 5.2.4) at α = 0.55 – 0.75. These correspond with the max DTG and the second smaller peak on the DTG plots respectively (Figure 5.1.4). Although these two peaks are not separated in previous

discussion as they occur in such a small temperature range and the effect is not discernable in the MS or DSC (Section 5.2.3) curves this gives credence to the theory that the degradation of LDPE could be considered as two sequential steps of parallel or partially overlapping reactions. Within the region of correlation the activation energy increases from 40.66 – 483.97 kJ/mol with an average of 142.58 kJ/mol. The upper limit of the activation energy was at the very end of the good correlation and as such could be unreliable and should be compared with caution. Sinfronio *et al.* (2005) also worked on LDPE and calculated values of between 126.09 and 275.81 kJ/mol across methods. The average E_a value found in this study fits well within the literature reported limits.

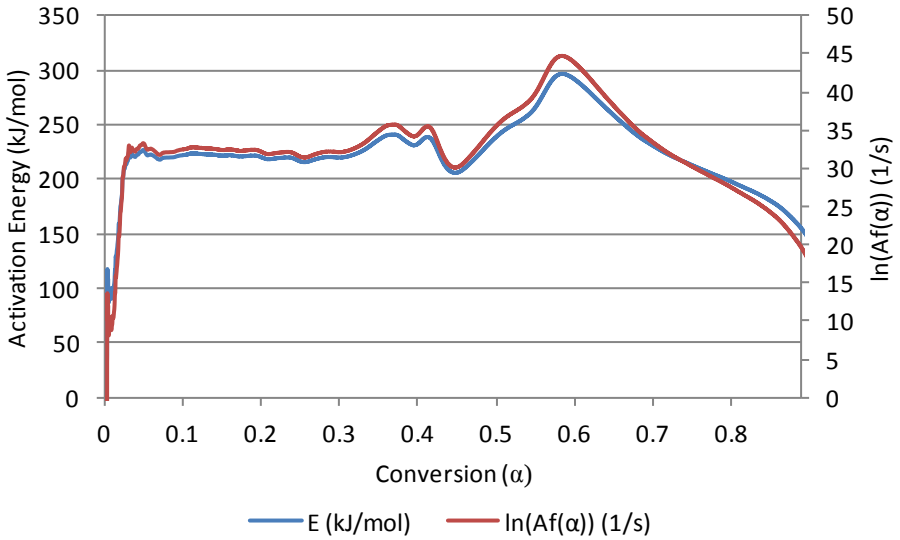

Figure 5.2.5: Activation Energy and ln(Af(α)) Dependence on Specific Conversion for PET

The activation energy required for the degradation of PET increases from 21.07 – 296.73 kJ/mol (an increase of 275.66kJ/mol). This difference as well as the initial trend is very similar to that of HDPE. However, the activation energy curve for PET shows two peaks (Figure 5.2.5), one at α = 0.4 and the other at α = 0.6. As with LDPE, these specific conversions correspond with the maximum rate of degradation and a secondary, smaller peak in the DTG plots (Figure 5.1.4). The secondary peaks for both LDPE and PET are significantly smaller than the main, maximum DTG peak while the associated activation energy is higher (Figure 5.2.6). This implies that the secondary reaction involves the degradation of less reactive components. The secondary peaks are also broader and thus have a larger area implying more mass lost in that region at a lower rate.

Values of activation energy obtained from literature range from 180 to 338.98 kJ/mol (Badia *et al.* (2013), Pilawka *et al.* (2013), Sasha *et al.* (2006), Sasha *et al.* (2005)). The lower end of this range was obtained by kinetic experiments on virgin and slightly processed (milling etc.) PET while the upper end of was obtained from experimentation on waste soft drink bottles.

The activation energies found in this study fit well within the range and the maximum E_a found agrees closely with the Sasha *et al.* (2005) study on waste PET soft drink bottles, the same feedstock used here.

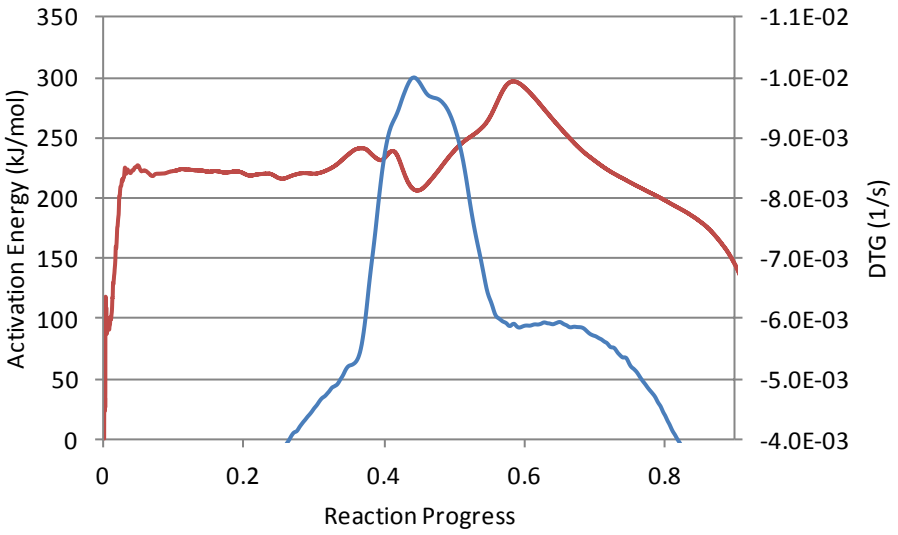

Figure 5.2.6: Reaction Rate and Activation Energy (-) with Specific Conversion for PET (-)

It is often assumed that the activation energy for a reaction should remain constant with conversion. This, however, is only the case for a gas phase reaction (i.e. no reaction medium) that occurs in a single step (Vyazovkin, 2006). Vyazovkin (2006) postulates that the physical parameters associated with solid or liquid reaction media that change with temperature directly affect the energy barrier height (activation energy). Thus, the activation energy will vary as the reaction medium varies (melts/boils etc.) with temperature. Since there are definite physical changes (glass transition, melting etc. (Gao, 2010)) in the plastics during thermal degradation this could explain the changes in trends of activation energies for the plastic samples. Since the plastic samples degrade in one step, the fluctuations and changes in activation energies could also be indicative of different reaction steps as per Vyazovkin (2006) postulations. These could be linked with initiation, propagation and termination reactions in the degradation pathways of the three samples.

5.2.3: Determination of the kinetic parameters - paper

The kinetic calculations for the three paper samples were split into the three main stages of degradation and a set of kinetic parameters calculated for each (Table 5.2.2).

Table 5.2.2: Summary of Global E_a and $Af(\alpha)$ Isoconversional Kinetic Values for Paper

	Specific α Range R^2 >|0.8|	Average E_a (kJ/mol)	Average ln(Af(α))	$Af(\alpha)$ (1/s)
	Glossy Paper			
Step 1	0.0130 - 0.810	52.03	13.13	5.05E+05
Step 2	0.0027 - 0.849	194.32	32.38	1.15E+14
Step 3	0.0012 - 0.997	191.80	17.45	3.79E+07
	Newspaper			
Step 1	0.0088 - 0.850	49.90	12.65	3.12E+05
Step 2	0.0099 - 0.990	186.40	29.86	9.30E+12
Step 3	0.0380 - 0.982	207.56	21.09	1.45E+09
	Office Paper			
Step 1	0.0038 - 0.590	38.560	9.01	8.16E+03
Step 2	0.0011 - 0.996	217.70	36.41	6.52E+15
Step 3	0.0024 - 0.992	231.75	23.68	1.92E+10

The lack of linearity towards the end of each degradation step was particularly prominent in the paper samples' first stages (Appendix C). This is most likely due to variations in each sample' moisture content between the different heating rate runs. The moisture content can vary depending on the length of time the sample is left exposed to ambient conditions before analysis (as seen in the differences in the masses measured initially and those measured as the starting masses during TGA runs (Section 5.1)) This could result from the inherent lack of homogeneity in the samples (as this study deals with waste), as they are waste products, a problem exaggerated due to the small sample sizes. The atmospheric humidity at the time of experimentation is also variable and as such the samples could have absorbed or lost moisture content in the time they were exposed before testing. These are some limitations observed in this study of kinetics obtained by microgram thermogravimetry.

The resultant trends of activation energy with reaction progress for each of these stages for each of the three papers are compared (Figures 5.2.7 – 5.2.9) while the trends for the pre-exponential factor can be found in Appendix C.

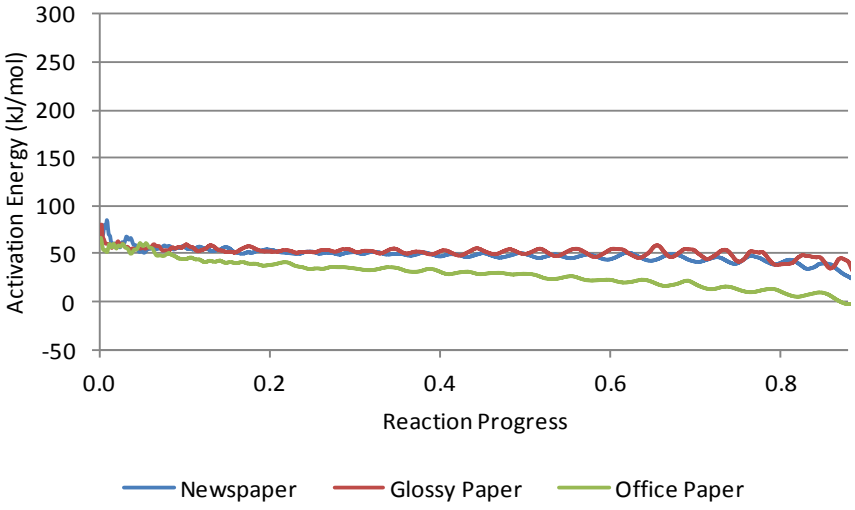

Figure 5.2.7: Activation Energy Dependence on Specific Conversion for all Paper - Step 1

Average activation energies of 52.03, 49.90 and 38.60kJ/mol were found within the acceptable degree of linearity for the first stage of degradation of glossy paper, newspaper and office paper respectively (Table 5.2.2). The heat of vaporisation of water is 40,687kJ/mol and the specific heat capacity 75.31J/molK (Green *et al.*, 2008). Using these values it can be calculated that approximately 46.33kJ/mol of energy is required to increase the water present in the samples from the starting temperature, 25ºC, to 100ºC, the normal boiling point of water, and vaporise them. This value is very close to the average values of activation energy found for the paper samples (Table 5.2.2), especially glossy paper and newspaper for the first stage. This, coupled with the fact that similar conditions are used to determine moisture content by TGA in accordance with ASTM E1131, leads to the probability that this stage of degradation can be related to the release of the water present in the samples. The slightly higher values found for glossy paper and newspaper and the lower average found for office paper can, most likely, be attributed to the differences in the samples' physicality and chemical additives (binders etc.) leading to differences in the absorbance and hygroscopicity (Biermann, 1996 I) i.e. how readily available the water is to be evaporated from the samples.

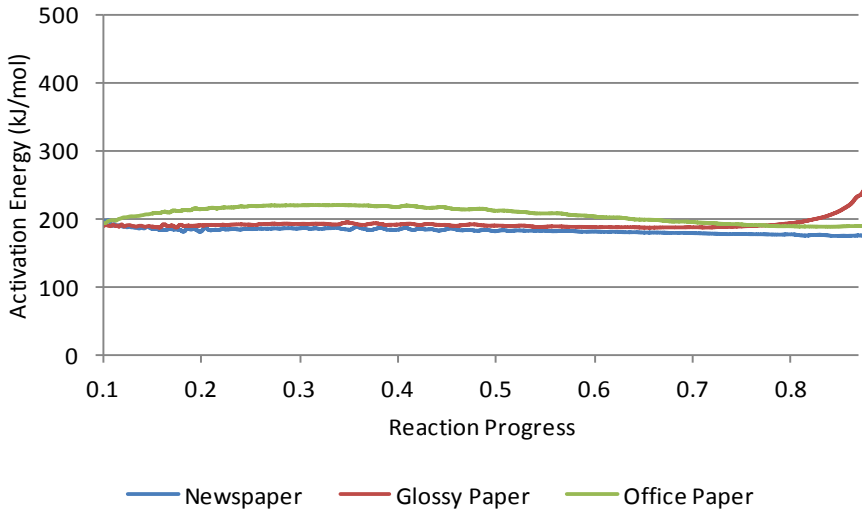

Figure 5.2.8: Activation Energy Dependence on Specific Conversion for all Paper – Step 2

Since cellulose is a main component of paper, it is of interest to compare the kinetic parameters found in this study with those reported for cellulose degradation in literature. Antal *et al.* (1995) conducted an extensive review into the kinetics of cellulose pyrolysis and present values of activation energy found by different authors in many studies.

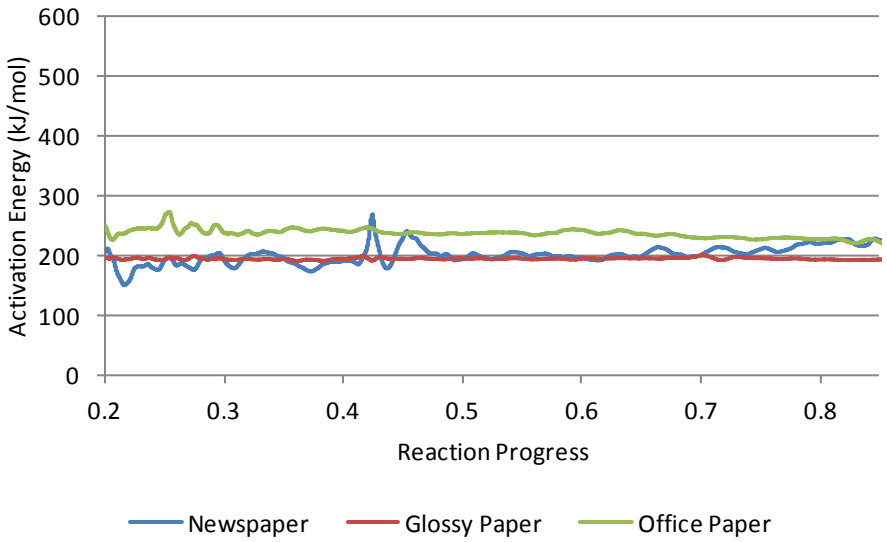

Figure 5.2.9: Activation Energy Dependence on Specific Conversion for all Paper - Step 3

The values reported range from 197 – 239 kJ/mol and include a variety of different cellulose sources and pre-treatments. Lin *et al.* (2009) conducted a kinetic study on micro-crystalline cellulose by thermogravimetry and found an E_a of 198 kJ/mol by two different models. These values are global constants for the entire degradation of dry cellulose and thus relate to the sum of stages 2 and 3 in this study (Figures 5.2.10 – 5.2.12).

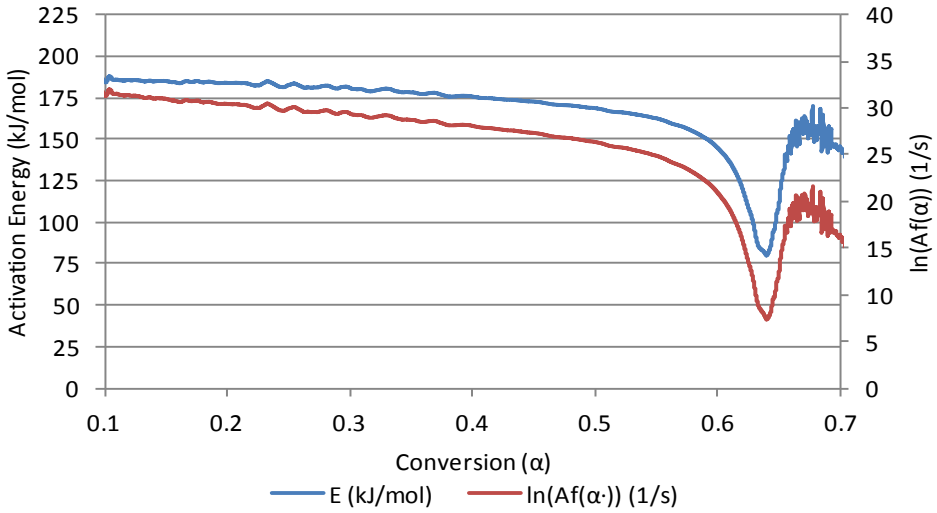

Figure 5.2.10: Activation Energy and ln(Af(α)) Dependence on Conversion for Glossy Paper Overall

Newspaper, glossy paper and office paper have an average E_a of 196.98, 193.06 and 224.72 kJ/mol, respectively (Table 5.2.2) over stages 2 and 3 correlating well with literature values. Modh *et al.* (2012) and Wu *et al.* (1997) conducted studies on waste paper and found the degradation to occur in 2 stages (excl. water desorption). The study conducted by Modh *et al.* (2012) focussed on glossy paper and found E_a values of 173.59 – 192.49 kJ/mol and 184.40 – 187.41 kJ/mol for stages 2 and 3 respectively. Wu *et al.* (1997) worked with glossy, office and tissue paper as well as newspaper and found E_a values of 181.96, 172.34 and 170.25 kJ/mol for stage 2 and 104.58, 170.67 and 117.12 kJ/mol for stage 3 respectively.

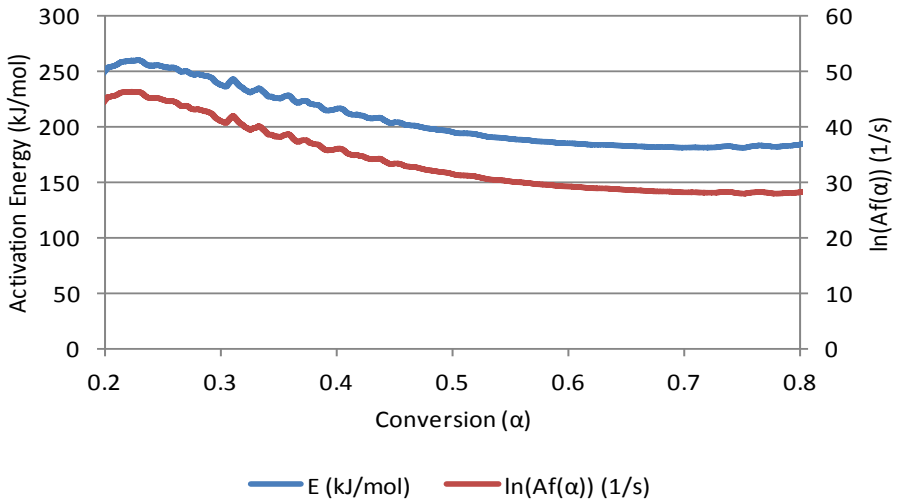

Figure 5.2.11: Activation Energy and ln(Af(α)) Dependence on Conversion for Newspaper Overall

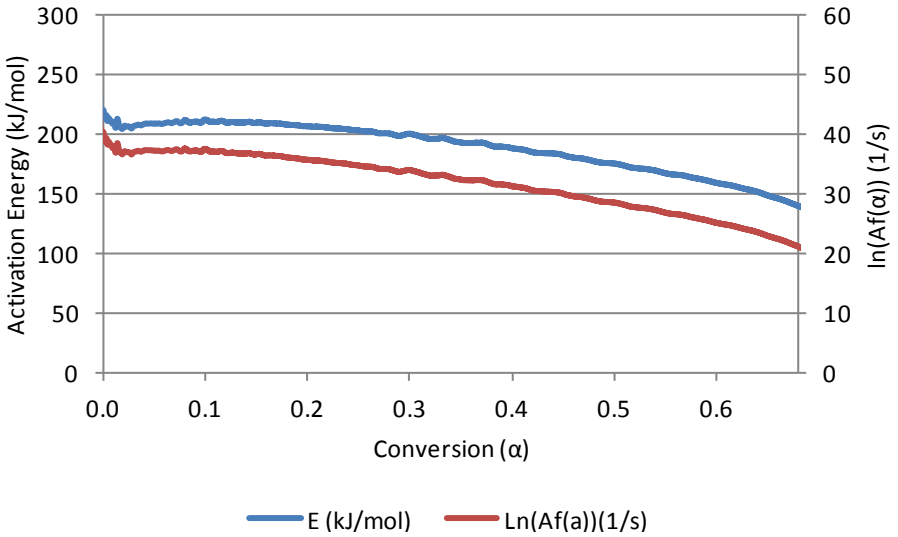

Figure 5.2.12: Activation Energy and ln(Af(α)) Dependence on Conversion for Office Paper Overall

The values for activation energy found by Modh *et al.* (2012) and Wu *et al.* (1997) (as mentioned before) are consistently lower than those found in this study. This difference can be attributed to the variable composition and differences in pre-treatment inherent in waste as well as differences in the way kinetic parameters were calculated.

Comparing the activation energies obtained for stages two and three individually for each paper to their respective overall activation energies (Figures 5.2.10 – 5.2.12) it is clear that some differences exist. The figures of the overall activation energies show only areas of good correlation and thus data relating to the overall contributions of step 1 and most of step three are not reliable. For this reason the overall activation energy plots can only reliably be compared closely to step two since this is the stage where the vast majority of conversion takes place. This could be due to differences in the baselines chosen between the two different types of analyses. While the activation energies are similar especially for glossy and office paper in

the beginning and then for newspaper in the final stages of conversion the trends are different from the step-wise analysis (Figures 5.2.7 – 5.2.12). Where all three paper samples exhibit little change in activation energies in step two the results from the overall analyses show that there is a general declining trend (Figures 5.2.10 – 5.2.12). There is no evidence within the region of correlation of the separate steps known to be taking place for paper degradation, however, upon examination of the full Ea with α trend (outside the correlation regions as per Appendix C) differences can be seen at the conversions corresponding to the different stages. These differences are accompanied with large declines in the correlation and as such the values are unreliable but an indication of some degradation event none the less (Appendix C).

5.3 Identification and comparison of pyrolytic volatiles

As per Chapter 3, volatiles released during degradation of the samples in the TGA were analysed by online mass spectrometry (MS). The ions tracked for each sample were chosen on the strength of preliminary scans as presented in Appendix D. However, although between 15 and 17 individual ions were tracked per sample not all of the signals for the ions that presented in the scans showed activity during the runs.

The applied voltage in the quadrupole varies such that ions within the set Dalton range can be detected. The accuracy of this can be improved by selected ion monitoring (SIM) within the desired range as was the case here. However, there are limitations of detection as not all of the desired ions can be tracked at once leading to the potential for some events to be missed hence the scans with no activity. Optimisation of the tracking process will require much work and is reserved for future studies.

The time period between 0 and 300 seconds in all the MS degradation figures corresponds with settling the actual heating program only starts thereafter. As such any peaks or changes in the ion currents during this time do not relate to the degradation process. Sharp dips in the current curves correspond with a rescan or times when the MS stopped recording and as such are not considered events. The lines represent the ion current of specific m/z ratios as described in the legend.

5.3.1: Volatiles from the degradation of plastic

Figures 5.3.1 to 5.3.3 show only the active mass spectra captured during degradation together with the specific DTG graphs indicating the main degradation steps, onsets at 366, 414 and 435ºC, of PET, HDPE and LDPE respectively.

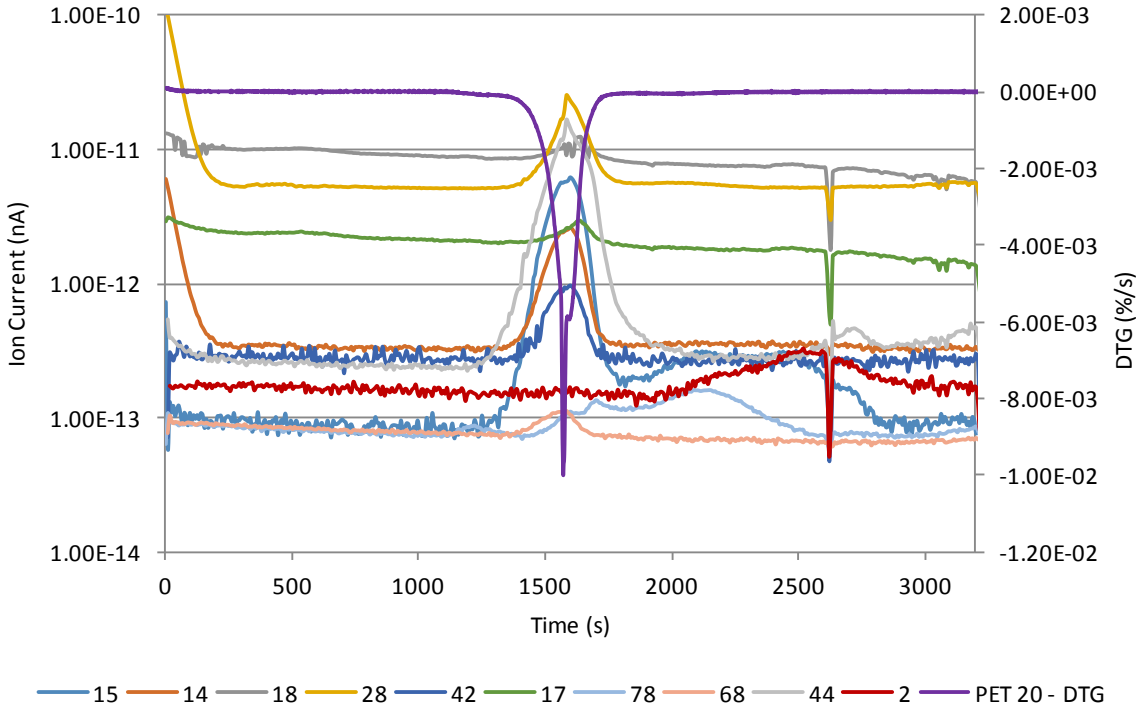

Figure 5.3.1: Mass Spectra and Rate of the Degradation of PET at 20K/min

As discussed previously, the main difference between the two forms of polyethylene in this study is the density due to the degree of linearity of the polymer (Section 2.7.1). As a result, one would expect the degradation for these two compounds to be very similar. This was evident when examining the MS scans performed for the two compounds (Appendix D). Both HDPE and LDPE exhibited groups of peaks around the atomic masses 50, 70 and 80 with HDPE showing a wider range of distinct peaks for the higher molecular mass regions. HDPE also showed groups of peaks around atomic masses 90 and 110. While the vast majority of the peaks in the scans were similar the intensity of the peaks differed most likely to the fact that the more branched a species is the less intense the mass spectral peaks (Van Bramer *et al.*, (1990)). Since only the most intense peaks were chosen the specific ions tracked differ slightly and thus the differences in the active spectra.

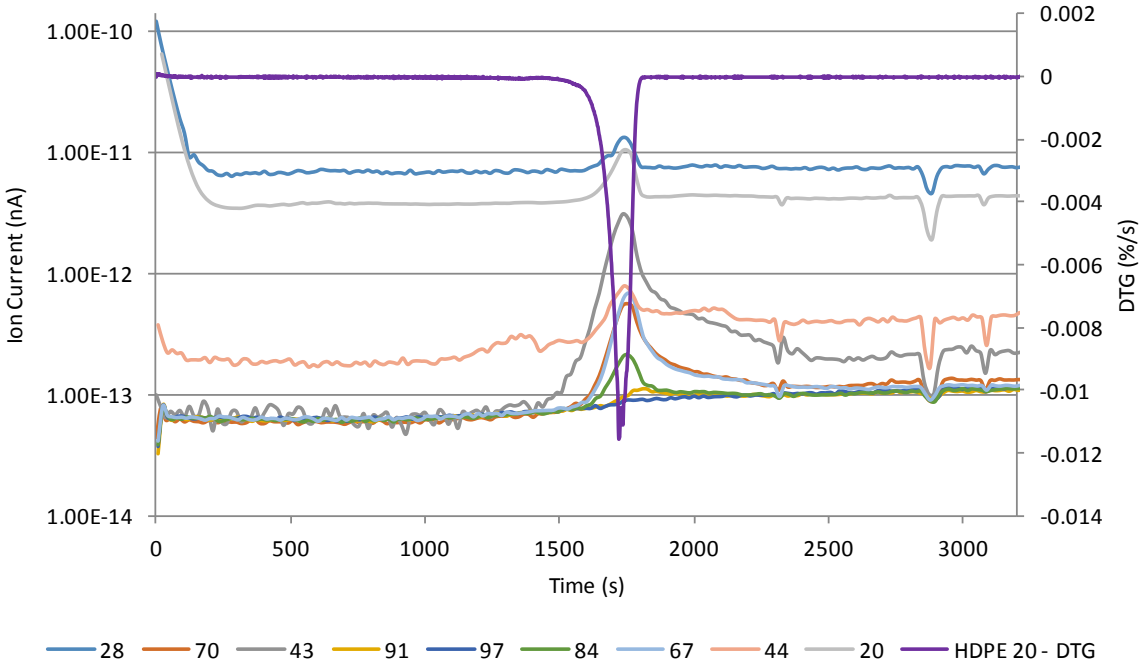

Figure 5.3.2: Mass Spectra and Rate of the Degradation of HDPE at 20K/min

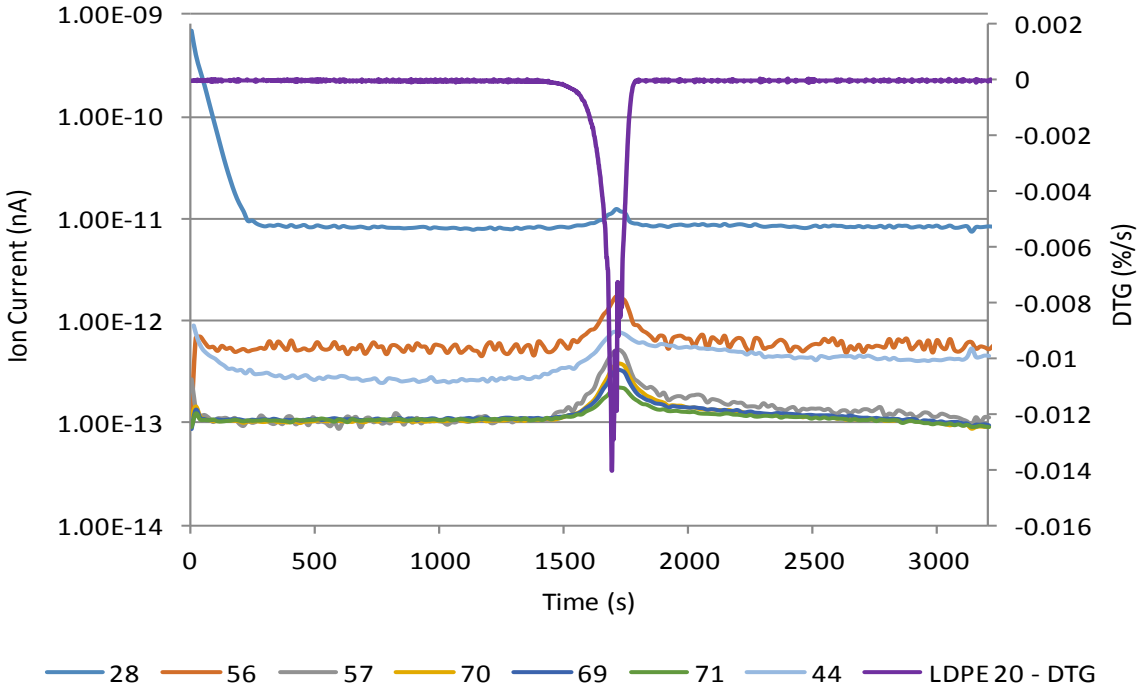

Figure 5.3.3: Mass Spectra and Rate of the Degradation of LDPE at 20K/min

From Figures 5.3.1 – 5.3.3 it is clear that the main degradation steps are coupled with increases in the currents of the majority of the molecular ions. As discussed previously (Section 5.1), the DTG peaks for PET and LDPE are jagged showing evidence of two separate degradations occurring in parallel. This, however, is not observable upon inspection of the formation of

fragment ions during the TGA-MS experiments. As such, the products of the secondary degradation in the main step are not distinguishable from the primary degradation products and so, for discussion purposes, are combined.

A second set of ion fragments indicated by the presence of current peaks between 1800 and 2500 seconds is apparent for PET degradation (Figure 5.3.1). At this point the rate of degradation is constant and extremely low. This shows that while there is very little change in the weight loss at this point there is still some degradation occurring. This must be due, for the most part, to a gas phase reaction involving compounds already volatilised from the original polymer. This distinct secondary degradation is not observable in the degradation of LDPE or HDPE (Figures 5.3.3 and 5.3.2). However, the majority of the ion fragment peaks for HDPE remain unresolved and continue to gradually increase until the end of the TGA run. This implies that small amounts of the molecular ions are steadily being released from the HDPE sample after the main degradation step resulting in little or no weight loss. As there are no distinct peaks these volatiles are not considered indication of a discreet secondary degradation.

From Figures 5.3.1 – 5.3.3 as well as the results of the kinetic evaluations (Section 5.2.2) it is possible to postulate kinetic schemes accompanied with the specific volatiles released. In order to get a more detailed picture of the volatile products of plastic degradation it is necessary to identify the potential molecular ions corresponding to the m/z fragments in Figures 5.3.1 to 5.3.3. Due to the nature of mass spectrometry, identification of the parent compounds of these potential molecular ions can be challenging. For example the fragment 28 could be due to the capture of the CO^+ ions originating with equal intensity from either carbon monoxide or carbon dioxide. It could equally be due to the release of C_2H_4+ ions from any C_xH_y compound. Thus, it is necessary to evaluate all likely possible molecular ions released in order to identify the volatiles from degradation. Figures 5.3.4 to 5.3.6 show the postulated kinetic schemes together with the possible cations detected at each m/z for LDPE, HDPE and PET respectively.

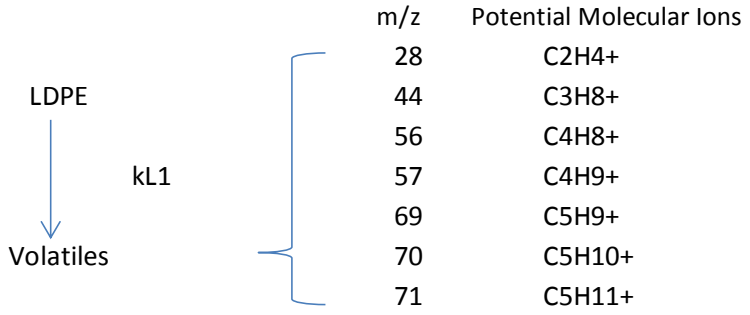

Figure 5.3.4: Proposed Kinetic Scheme for LDPE

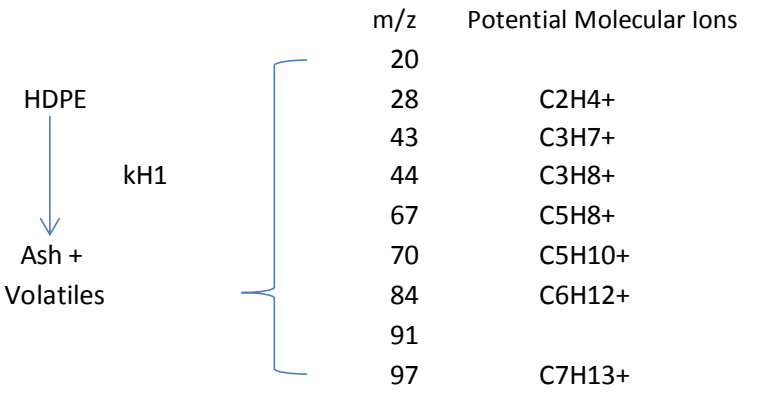

Figure 5.3.5: Proposed Kinetic Scheme for HDPE

The kinetic schemes presented for LD and HDPE correlate with the single step degradation observed in the TGA and DTG graphs and confirmed in the MS results.

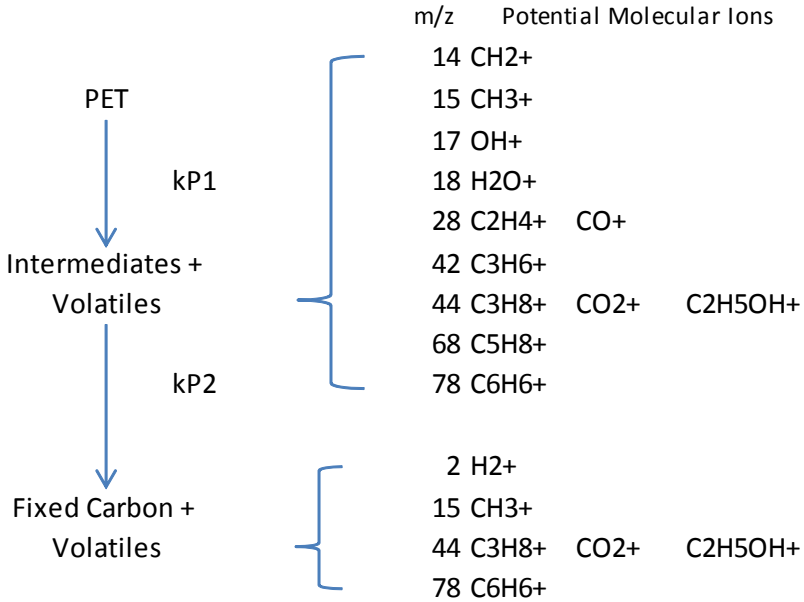

Figure 5.3.6: Proposed Kinetic Scheme for PET

From the TGA-MS results (Section 5.1.2) it is clear that PET has two distinct degradation steps although the second step is not accompanied by a loss in mass. The kinetic parameters found only relate to mass loss and thus the fluctuations in activation energy do not correspond with secondary MS peaks observed in PET or the unresolved peaks observed in HDPE degradation. Thus the rate constants found previously for LDPE and HDPE (kL1 and kH1) can be applied directly to the above kinetic schemes. Only kP1 can be directly correlated with the kinetic parameters found for PET, further experimentation is necessary to determine kP2.

5.3.2: Volatiles from the degradation of paper

Figures 5.3.7 to 5.3.9 show the only the active mass spectra captured during degradation together with the specific DTG graphs indicating the three main degradation steps of glossy paper, newspaper and office paper respectively.

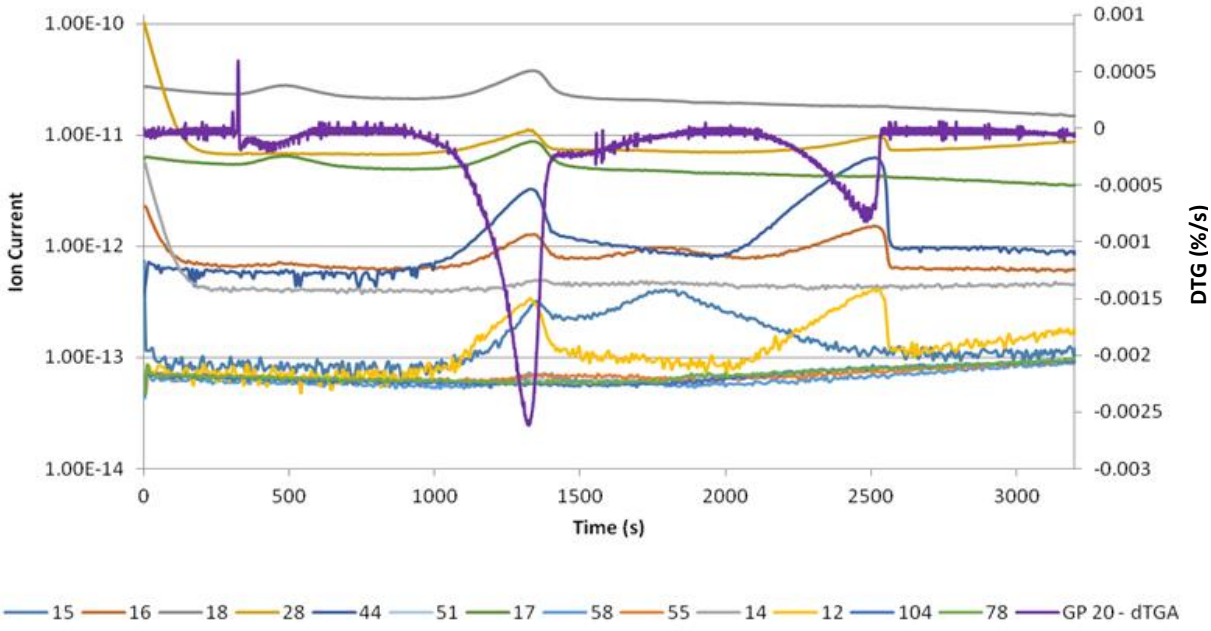

Figure 5.3.7: Online Mass Spectra with Degradation Rate of Glossy Paper

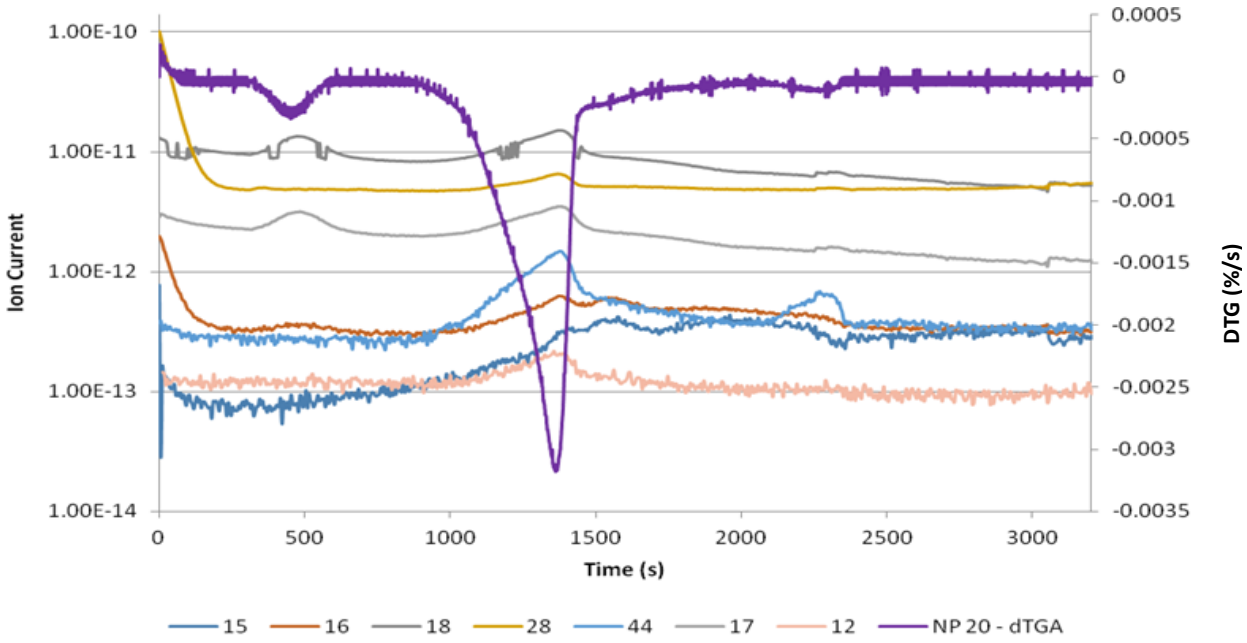

Figure 5.3.8: Online Mass Spectra with Degradation Rate of Newspaper

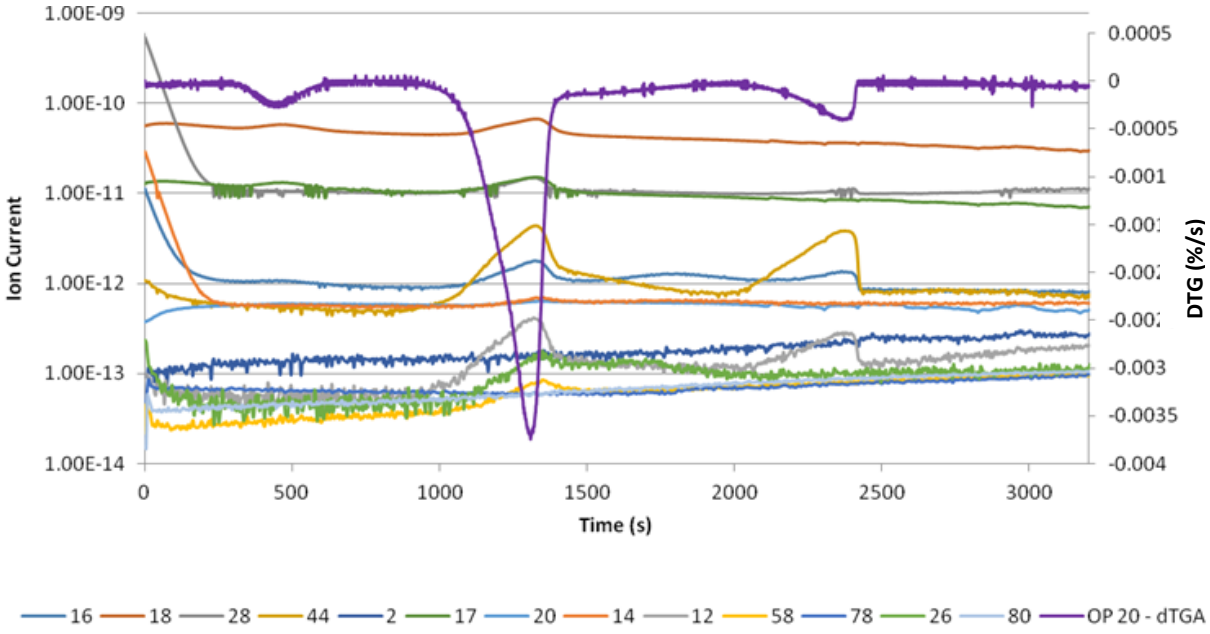

Figure 5.3.9: Online Mass Spectra with Degradation Rate of Office Paper

Peaks in the currents of the tracked ion fragments correlate to DTG events for all three paper samples. The majority of currents peak during the main degradation step, stage 2 for glossy and office paper (Figures 5.3.7 and 5.3.9 respectively) and all currents at stage 2 for newspaper (Figure 5.3.8). In the case of glossy paper, intermediate peaks in m/z 55 and 15 are observed between stages 2 and 3 that do not correspond to any DTG event. Similar peaks in m/z 16 can be seen for office paper while m/z 16 and 15 increase slightly off the tail of unresolved second stage peaks for newspaper. The first of the DTG peaks for all three paper samples is accompanied by increases in the currents of molecular ions 16, 17 and 18.

The DTG peak corresponding to the third degradation stage of office paper (Figure 5.3.9) correlates with peaks at m/z 12, 16, 28 and 58 with m/z 14, 20, 26, 28, 44 and 80 gradually increasing to the end of the run. The same gradual increase can be seen in m/z 55, 58, 78 and 104 with peaks in 12, 16, 28 and 44 for glossy paper stage 3 (Figure 5.3.7). Figure 5.3.8 shows ions with m/z 17, 18 and 44 are the final degradation products of newspaper.

The differences in the mass spectra can, most likely, be attributed to the addition of fillers as well as the differences in molecular structure of the cellulose making up each paper (differing degrees of polymerisation and crystallinity). From the mass spectra as well as the kinetic results presented in Section 5.2.3 a kinetic scheme together with the potential molecular ions possible for every m/z for each of the three papers (glossy paper, newspaper and office paper) can be postulated (Figures 5.3.10 – 5.3.12).

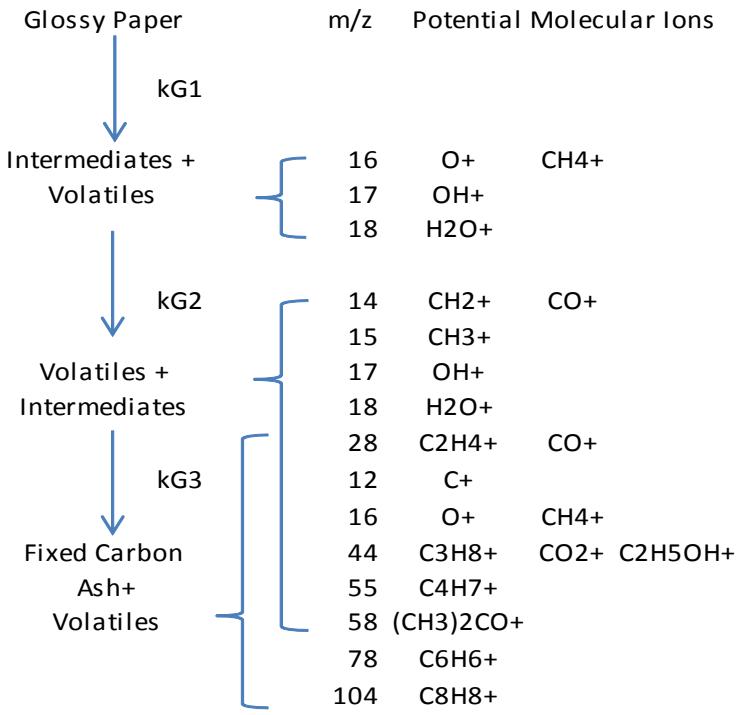

Figure 5.3.10: Proposed Kinetic Scheme for Glossy Paper

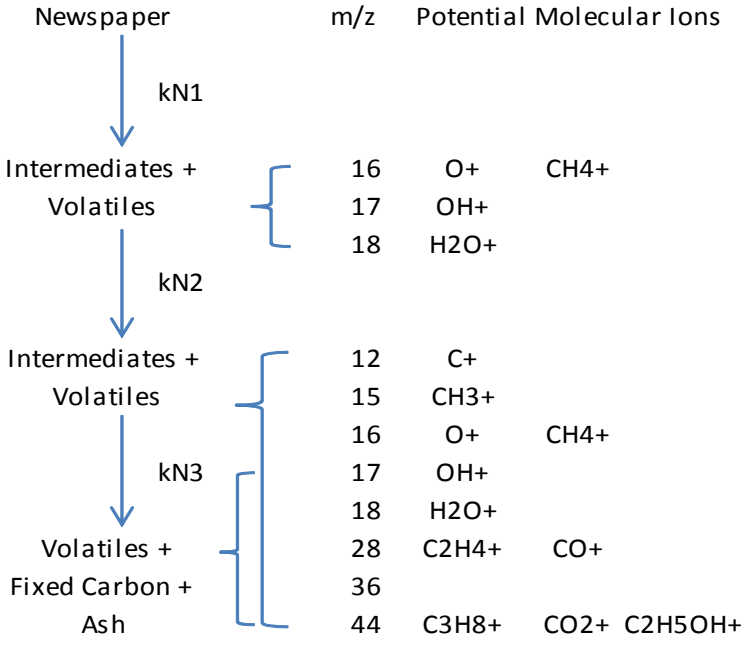

Figure 5.3.11: Proposed Kinetic Scheme for Newspaper

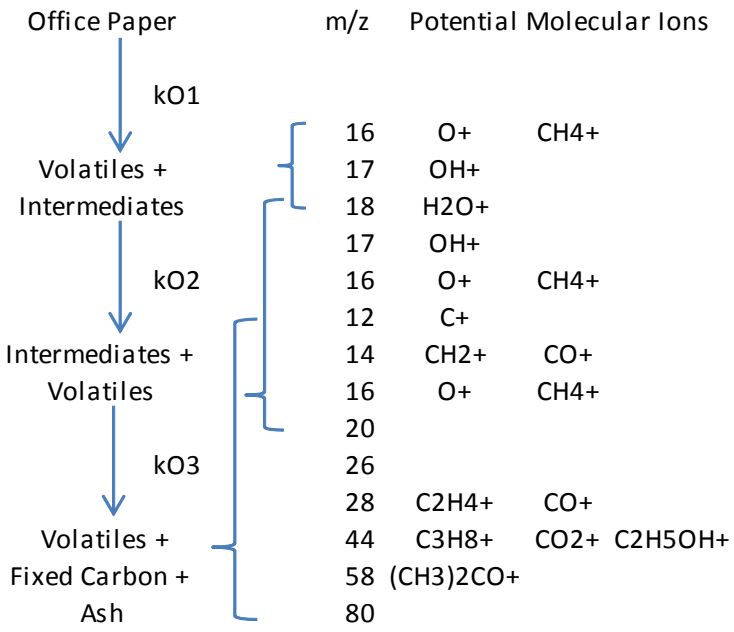

Figure 5.3.12: Proposed Kinetic Scheme for Office Paper

As each of the stages in the kinetic schemes above corresponds directly with a mass loss and thus a change in conversion (α) the kinetic rate constants found previously are directly applicable.

5.3.3: Comparison of volatiles formation

The specific ratio between the intensity of an MS signal and the physical amount of ions detected that produced that signal is called the response factor. This response factor differs between each ion and devices and thus, without calibrating for each individual ion, the use of MS as a quantitative tool is limited (Marsman *et al.*, 2008). Since the response factor of a single device remains constant for a specific ion, independent of the sample, it is possible to compare the relative amount of an ion released by different samples. This can only be done once the curves have been corrected for the initial sample mass as well as the sensitivity of the system by normalising to the m/z curve corresponding to the purge gas.

The DTG and TGA results show that the general trends for the degradation of the three paper samples (Section 5.1.1) are similar especially between office and glossy paper. The same is true of the plastic samples (Section 5.1.2), specifically HDPE and LDPE. More insight into the similarities and differences in the degradation of these components can be gained by comparing the volatiles released.

As discussed, the ions tracked differed between samples depending on the preliminary scans however there are some common ions. Table 5.3.6 shows the relative peak areas (all $x10^{-3}$) of

the ions common amongst the paper samples thus allowing for a comparison of production not only between stages but also between samples. Fragment 15 is common only to glossy paper and newspaper.

Table 5.3.6: Areas (x 10^{-3}) Corrected for Sample Size and Purge Gas of Common MS Peaks for Paper Samples
(from TGA-MS runs to 1000ºC at 20K/min, stdev ≤3X10^{-3})

m/z	Possible Cation	Stage 1			Stage 2			Stage 3		
		GP	OP	NP	GP	OP	NP	GP	OP	NP
12	C^+	-	-	-	2.36	2.69	1.78	3.40	1.65	-
15	CH_3^+	-	-	-	4.69	-	9.52	4.69	-	9.52
16	CH_4^+/O^+	0.33	0.25	1.12	3.73	6.22	6.33	9.62	4.68	
17	OH^+	10.33	16.22	18.75	31.96	47.22	35.47	-	-	-
18	H_2O^+	43.47	54.00	54.07	130.0	200.0	140.0	-	-	-
28	$C_2H_4^+/CO^+$	-	-	-	33.01	37.95	18.97	20.61	-	-
44	CO_2^+	-	-	-	26.14	27.10	21.10	66.97	32.90	6.01

Stage 1 for the paper samples has previously been related to the removal of the inherent moisture content of the samples. All three paper samples release volatiles with ion fragments at m/z 16, 17 and 18 (Figures 5.3.7 – 5.3.12). The known mass spectral fingerprint for water involves the ions 18, 17 and 16 with relative intensities of 100, 23 and 1% respectively (NIST, 2011). Since the temperature range of stage 1 is well below that of the onset of degradation the ion fragment 16 can be related to the O^+ ion from water rather than the CH_4^+ ion from methane or methane fragments from larger hydrocarbon chains (Section 2.7.3 and Figures 5.3.10 – 5.3.12). The measured moisture contents of glossy, office and newspaper are 1.41, 1.92 and 2.74% (Table 4.2.1) while the weighted sum of the three fragments is 45.8, 57.7, and 58.4 respectively (Table 5.3.6). It is clear that while not in the exact ratios the trend between the ion fragment amounts and the moisture contents are the same. It is evident that much more water (fragments 17 and 18 only) was released during the main degradation step, between 3 and 4 times more across the three samples. The release of fragment 16 in this step is probably the sum of the ion fragments from water and methane released whereas the release of fragment 16 in the absence of fragments 17 and 18 in stage three shows that glossy paper releases more than double the amount of methane than office paper.

Newspaper released the least amount of ion fragments 12, 28 and 44 (Table 5.3.6) which are related to the release of carbon monoxide and dioxide (Figures 5.3.8 and 5.3.11). These fragments are released by glossy paper to a slightly lesser extent than office paper but the amounts are comparable (Table 5.3.6). The lack of these low molecular weight gases in the volatiles released from newspaper coupled with its high VM content (Table 4.2.1) leads to the probability that the volatiles released are larger molecules producing longer hydrocarbon

chains. Newspaper also has around half the ash content of office paper and almost a quarter of that of glossy paper (Table 4.2.1). The additional ash could be catalysing the degradation of longer chain volatiles to monomers and the final products of degradation, CO and CO_2 (Section 6.2.2). A known filler in glossy and office papers is $CaCO_3$ (Biermann, 1996 I) which decomposes reversibly to form CaO and CO_2 (Georgieva *et al.*, 2013), another possible explanation for the higher yields of fragments 12, 28 and 44.

The comparison of volatiles released by the three different plastics (Table 5.3.7) is difficult as the ion tracked differed quite substantially. However, it is clear that the production of fragments 28, 44 and 70 is similar for HDPE and LDPE supporting the similar degradation seen in the TGA and DTG results.

Table 5.3.7: Relative Areas of Common MS Peaks for Plastic Samples
(from TGA-MS runs to 1000ºC at 20K/min, stdev $\leq 3X10^{-3}$)

m/z	Possible Cation	HDPE	LDPE	PET
28	$C_2H_4^+/CO^+$	9.09	10.99	83.88
44	$C_3H_8^+/CO_2^+/C_2H_5OH^+$	1.43	2.23	89.66
70	$C_5H_{10}^+$	2.20	1.47	-

There is a substantial difference between the amounts of 28 and 44 ion fragments released between the PE samples and PET (Table 5.3.7). This is most likely due to the high oxygen content present in PET that is lacking in the PE samples (Sections 2.7.1 and 2.7.2). For this reason, the production of CO and CO_2^+ will be much higher for PET while the emission of fragment 28 and 44 is likely mostly due to the $C_2H_4^+$ and $C_3H_8^+$ ions for the PE samples due to their structure (Figures 5.2.4 – 5.3.6). PET also releases a much greater amount of 28 and 44 ion fragments that any of the three papers samples (Tables 5.3.6 and 5.3.7). This shows that the vast majority of the oxygen present in the PET is available for the formation of syngas while that in the paper samples oxygen remains in the solid residue or is used to form OH^+ ions.

5.3.4: Paper-plastic mixtures

Due to the use of HDPE and glossy paper in the gram-scale portion of this study, the behaviour of a 50/50 vol% mixture of glossy paper and HDPE was investigated by TGA-MS. The results of the integration of the MS peaks (Figure 5.3.13) are presented in Table 5.3.8 and are compared with the relative amounts of the fragments released by the pure components. The stages mentioned (Table 5.3.8) relate to the stages observable in the TGA (Figure 5.3.14).

Table 5.3.8: Relative Areas of MS Peaks for GP - HDPE Mixture and Pure Components
(from TGA-MS runs to 1000ºC at 20K/min, stdev ≤3X10^{-3})

m/z	Possible Cation	Degradation Stage 1 Mix	1 GP	2 Mix	2 GP	2 HDPE
14	CH_2^+/CO^+	0.25	-	0.36	0.35	-
15	CH_3^+	0.43	-	3.17	4.69	-
16	CH_4^+/O^+	2.04	0.33	2.65	3.73	-
17	OH^+	18.38	10.33	-	31.96	-
18	H_2O^+	94.47	43.47	-	130.00	-
28	$C_2H_4^+/CO^+$	17.50	-	3.55	33.01	9.09
32	O_2^+	-	-	-	-	-
44	$C_3H_8^+/CO_2^+/C_2H_5OH^+$	8.86	-	-	26.14	1.43
55	$C_4H_7^+$	-	-	5.08	0.07	9.43

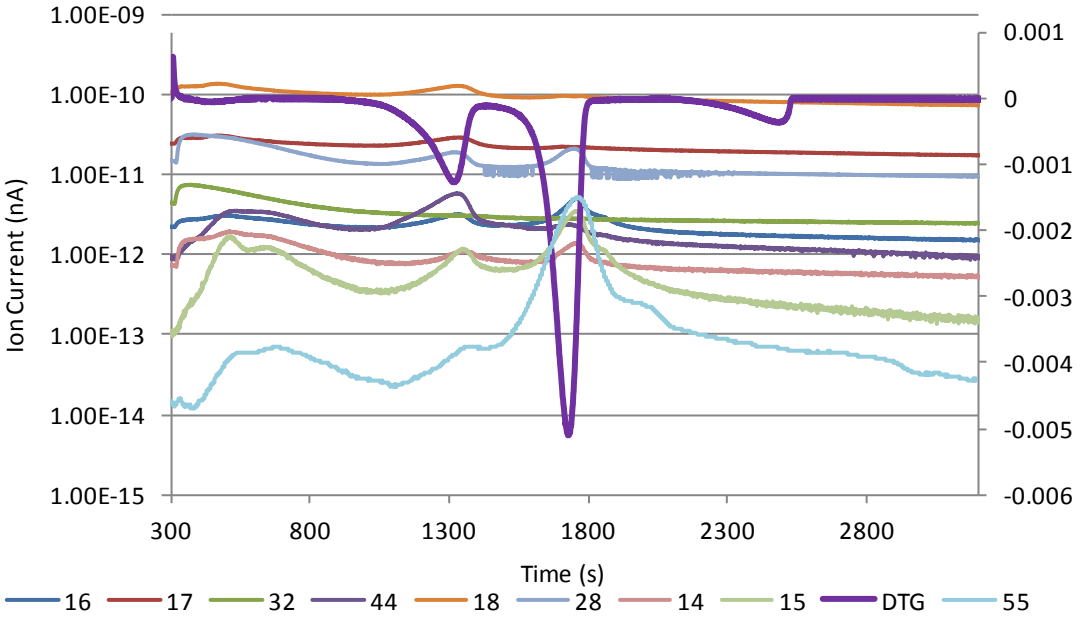

Figure 5.3.13: Online Mass Spectra with Degradation Rate of 50/50vol% GP-HDPE Mixture
(GP - Glossy Paper and HDPE – High Density Polyethylene 50/50vol% Mixture at 20K/min)

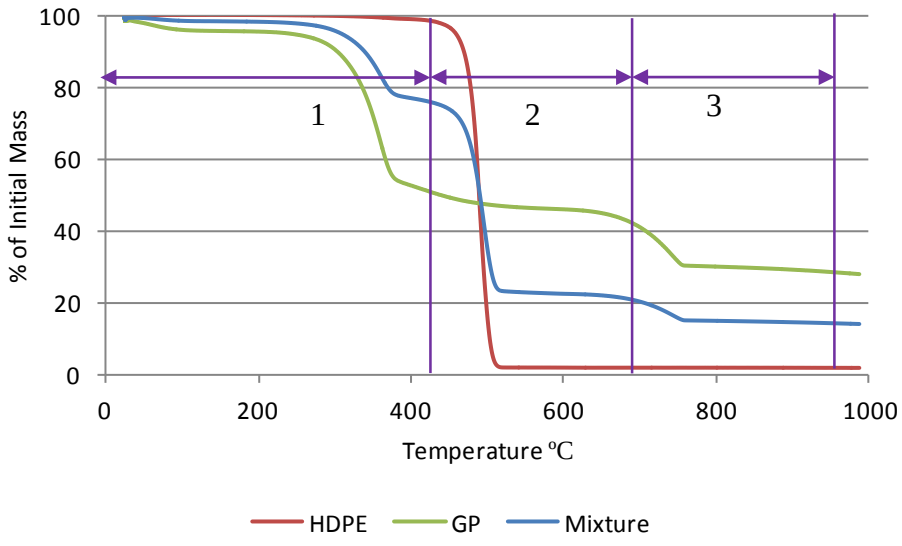

Figure 5.3.14: Weight loss with Temperature of GP-HDPE Mixture and Pure Components at 20K/min
(GP - Glossy Paper and HDPE – High Density Polyethylene 50/50vol% Mixture at 20K/min)

Comparing the TGA results of the pure components with that of the mixture (Figure 5.3.14) it is clear that the mixture degrades in accordance with the stages and ranges of degradation of glossy paper and HDPE. This results in three main weight loss stages relating to stages 2 and 3 for glossy paper degradation and the main degradation step of HDPE in addition to the loss of sample moisture.

During some of the replicates of the TGA-MS runs on the mixture a large drop in the ion current of all fragments at around 2500 seconds was observed. This was caused by the formation of a clot in the capillary tube connecting the TGA and MS. This phenomenon was not present in all of the runs (as is the case in Figure 5.3.13) and thus exact conditions leading to this should be examined if further experimentation is to be done on this mixture in the future. Since the mixture was made up on a volume basis the differences in densities mean that the mixture is 37.1 wt% glossy paper. Figure 5.3.14 shows that the mixture loses less than half of the mass that pure glossy paper loses in stage 1. Since HDPE does not degrade in this temperature range and due to the shape of the degradation profile; it can be assumed that the loss in weight of the mixture during this stage is solely due to the degradation of paper. Taking the mass ratio into account it can be calculated that the glossy paper portion of the mixture loses 67.4% of its initial mass in stage 1, 12% more than pure glossy paper.

This additional loss of weight by the mixture can be related to the much higher relative amounts of m/z 16, 17 and 18 ions released than those of pure glossy paper. The mixture also shows the presence of m/z 14, 15, 28 and 44 in stage 1 (Figure 5.3.13) which are not present in the same stage for glossy paper. Due to the addition of the degradation of HDPE, the mixture loses more weight overall than the pure glossy paper alone. This leads to the possibility of a promotion of glossy paper degradation by the addition of HDPE. However, if the total individual weight losses of glossy paper and HDPE are weighted according to the mass percentage of each in the mixture it can be predicted that, if the weight loss is not synergistic the mixture should lose 88.5% in total. Comparing this with the actual total weight loss of 85.7% it is clear that by mixing the two feedstocks the total conversion is reduced. The results of the integration of the MS peaks at stage 2 (Figure 5.3.13) show that there is an apparent reduction in the degradation of both glossy paper and HDPE; a possible reason for the lower than expected total conversion.

Examination of Figure 5.3.15 shows that the rate of degradation of the mixture is more than halved at each stage in addition to the reduction in overall conversion.

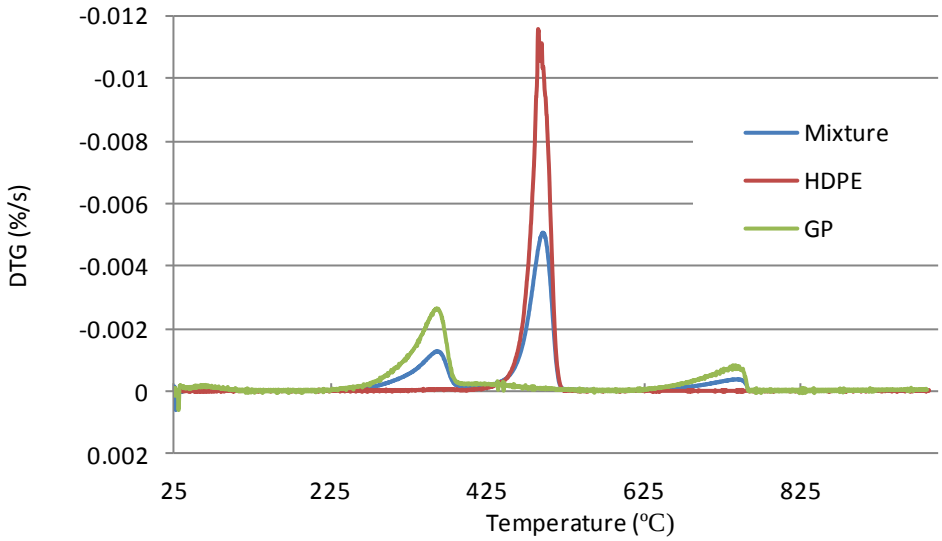

Figure 5.3.15: Comparison of the Rates of Degradation of HDPE, GP and a 50/50vol% Mixture

(GP - Glossy Paper and HDPE – High Density Polyethylene 50/50vol% Mixture at 20K/min)

Thus it can be said that, in this case, there is no synergistic interaction between the glossy paper and HDPE during degradation, however further work is needed to confirm this under different conditions.

Chapter 6: Scalability of MSW Pyrolysis

This chapter aims at integrating results obtained at different scales under different experimental conditions to illustrate the scalability effect on the pyrolysis yields of MSW (Section 6.1 and 6.2). The advantage in combining analytical results for a better description of the degradation is also examined (Section 6.2).

Laboratory scale slow and vacuum pyrolytic runs were performed on one specimen from both the paper and plastic groups in accordance with the methods outlined in Chapter 3. Glossy paper and HDPE were chosen to represent the paper and plastics groups, respectively.

The effect of scalability on the pyrolytic yields was studied between runs under slow pyrolytic conditions on the TGA (milligram scale) and laboratory scale plant (gram scale). In order to ensure maximum comparability, runs were performed on the TGA under the exact heating program used in the plant (25 - 550ºC at 10 and 20K/min with a 30min hold time). This was performed on glossy paper and HDPE and the results of the TGA runs presented in Figures 6.1.1 and 6.1.2. Since the TGA has no condensation capabilities there is no indication of the potential yields of liquid products thus the total volatiles (gas + oil) from the plant are compared to the mass lost during the TGA runs.

6.1: Laboratory scale pyrolysis

6.1.1: Pyrolysis of glossy paper

It was observed that, in runs with glossy paper, the atmospheric temperature condenser as well as the first of the water ice condensers captured a dark, viscous liquid; tarry phase, while the last three condensers captured very light watery liquid; the aqueous phase. There was a certain amount of oil present in the connecting tubes, especially the metal pipe from the reactor tube to the atmospheric temperature condenser and the first of the rubber tubes. This oil was accounted for and forms part of the oil yield for glossy paper. This was the case with both vacuum and slow pyrolytic runs. Table 6.1.1 shows the effects of heating rate and residence time on the pyrolysis of glossy paper as yields calculated as per the methods outlined in Chapter 3.

Table 6.1.1: Yields (%) from the Vacuum and Slow Pyrolysis of Glossy Paper

Glossy Paper	Vacuum		Slow	
	20 K/min	10K/min	20 K/min	10K/min
Oil Y	36.1 ± 1.5	37.4 ± 1.0	24.0 ± 3.3	22.3 ± 0.9
Char Y	35.1 ± 1.5	39.2 ± 0.2	48.3 ± 0.7	48.1 ± 0.5
Gas Y	28.7 ± 3.0	23.4 ± 1.2	27.7 ± 2.6	29.6 ± 0.4
Pyro. Water Y	15.1 ± 0.5	16.0 ± 0.5	13.6 ± 1.4	12.8 ± 1.5

The yields of the three products are comparable to those found by Li *et al.* (2005) while working with mixed waste paper. Phan *et al.* (2008) obtained a maximum liquid yield of 25% from the slow pyrolysis of paper, similar to the yields for slow pyrolysis of glossy paper. However, the yields of char obtained are consistently higher than those quoted in studies performed on a gram scale (Phan *et al.* (2008), Li *et al.* (2005)). These differences can be attributed to the different experimental set ups and conditions used in each study as well as the nature of waste as a feedstock. Thus it can be said that the yields obtained in this study for the slow and vacuum pyrolysis of glossy paper are within the expected ranges. The char produced from glossy paper is similar in appearance to char produced by biomass pyrolysis, was left in the reactor tube as a solid residue.

It can be seen that for vacuum pyrolysis an increase in heating rate increases the gas yield decreasing the oil and, to a greater extent, char yields. There is also slightly less pyrolytic water produced at the higher heating rate. The opposite is true for the slow pyrolysis runs. A higher heating rate promotes the production of oil and, to a lesser extent char, lowering the yield of gas. The residence time of vapours during the vacuum and slow pyrolysis runs differs dramatically; 2 seconds compared to 242 seconds (as per Chapter 3 and calculations by Carrier *et al.* (2011)). This effect can be seen clearly from Table 6.1.1. For biomass, an increased residence time decreases the liquid fraction while increasing the char and gaseous yields as expected due to the increased secondary reactions (Bridgewater *et al.*, 1999).

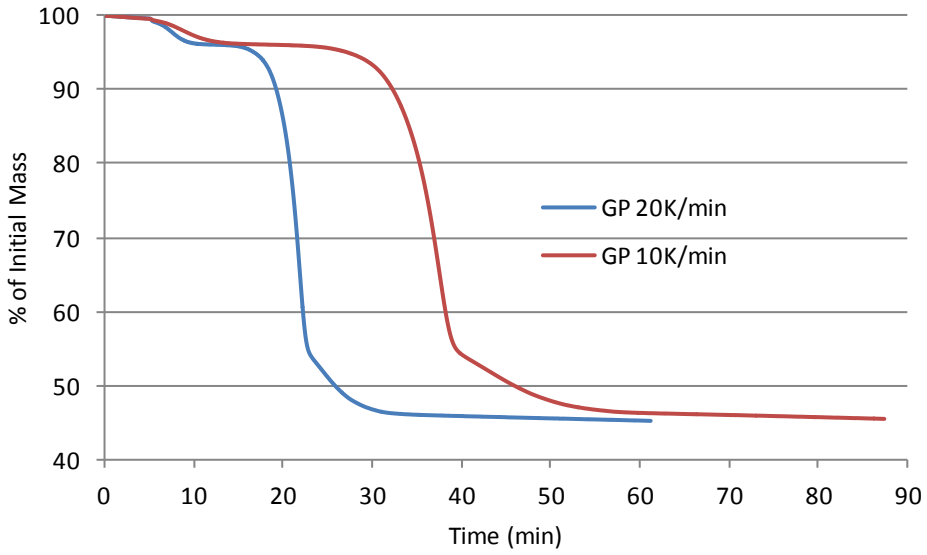

Figure 6.2.1: Results of TGA runs at 10 and 20K/min Under Plant Conditions for Glossy Paper

The yields of char from the TGA runs (Figure 6.1.1) at heating rates of 20 and 10K/min were found to be 45.1 and 45.3% implying a volatiles yield of 54.9 and 54.7%, respectively.

Comparing these yields to those obtained during the plant runs it was observed that 3.2 and 2.8% more volatiles were released in the TGA at 20 and 10K/min, respectively. Thus there was less overall pyrolytic conversion in the plant than TGA but both show the same trend of slightly decreasing weight loss with increasing heating rate.

The difference in yields between the two scales is more pronounced for the higher heating rate. This is an indication of the influence of heat transfer limitations on the conversion of larger samples. The surface area to mass ratio in such a small sample (TGA) will be very high. This high ratio means that the heat transfer between the furnace and the sample and between the sample particles themselves will be fast and heat transfer can be eliminated as a factor impacting on the process. This assumption has been made by authors when experimenting with TG analysis. (Lin *et al.* (1999), Zhou *et al.* (2006)) Lin *et al.* (1999), Wu *et al.* (1997, I) and Zhou *et al.* (2006) all postulated that the use of a very low heating rate limits the influence of heat transfer rates on the outcome of the analysis. Low heating rates were specifically chosen so as to minimise the effect of heat transfer on conversion but it is clear that this did not eliminate the problem. The differences are, however, small when the orders of magnitude difference in the sample sizes are considered.

The proximate analysis results, presented in Section 4.2, show that glossy paper has a combined fixed carbon and ash content of 29.03%, much lower than the 48.25 and 48.10% and the 45.1 and 45.3% char yields from the 20 and 10K/min runs on the plant and TGA respectively. The TGA runs to 1000°C showed a much more substantial weight loss (Table 5.1.1), closer to the expected total conversion (loss of all MC+VM). From this it is clear that, while the heating rate and heat transfer limitations play a role, the largest influence on the conversion of the raw feedstock, and thus the yields, is due to the final process temperature.

Another consequence of secondary reactions and further degradation is the increased water content in the final oil samples (Table 6.1.3) as water is one of the primary products of such reactions. One would expect that the yield of pyrolytic water would be higher for slow than for vacuum conditions which is clearly not the case here. This is because significantly more oil was produced in the vacuum runs. Taking the amount of pyrolytic water produced as a fraction of the total oil produced values of 41.7 and 43.3% and 56.6 and 54.7% were obtained for vacuum and slow pyrolysis at 20 and 10K/min respectively. It can be seen that for both 20 and 10K/min there is greater than 10% more pyrolytic water produced in the slow pyrolytic runs than in the vacuum runs, as expected.

The elemental composition and the results of the proximate analyses and KF titrations are presented in Tables 6.1.2 and 6.1.3 for the chars and oils respectively.

Table 6.1.2: Proximate and Ultimate Analyses (in wt%) and Calculated HHV (MJ/kg) of Char from the Slow and Vacuum Pyrolysis of Glossy Paper as Per Chapter 3

	C	H	N	S	O*	MC	VM	FC	Ash	HHV^ (Parikh)
Slow Pyrolysis										
20 K/min	28.9	0.7	0.2	2.5	67.7	0.0	34.3	17.3	48.4	11.1
10 K/min	32.7	0.9	0.3	2.3	63.9	0.0	31.1	23.1	45.8	12.7
Vacuum Pyrolysis										
20 K/min	24.8	0.5	0.0	1.3	73.3	0.9	26.4	12.8	59.9	8.2
10 K/min	24.1	0.4	0.0	1.3	74.2	0.9	29.6	12.2	57.3	8.5

*obtained by difference; ^Obtained from Proximate Analysis using the Parikh *et al.* (2005) correlation

Table 6.1.2 reveals that for slow pyrolysis the higher heating rate runs produce a seemingly lower quality char. That is, the carbon and hydrogen content is lower and the oxygen content higher; this is seen to a lesser extent with vacuum pyrolysis. There are slight differences in the proximate analysis for both vacuum and slow pyrolysis at 10 and 20K/min. Using the Parikh *et al.* (2005) correlation to calculate the calorific values for the char it was found that the energy density has a standard deviation of only 1.1 and 0.2% for slow and vacuum pyrolysis between heating rates. This shows that the differences in elemental and proximate compositions do not greatly influence the char quality for either vacuum or slow pyrolysis. However there is a clear influence of residence time on the quality with vacuum pyrolysis producing lower quality chars (Table 6.1.2).

Table 6.1.3: Elemental Analysis (% on dry basis) of the Pyrolytic Oils from Glossy Paper

Phase	C	H	N	S	*O	^Water Content	C	H	N	S	*O	^Water Content
	Slow						Vacuum					
20K/min												
Aqueous	65.5	6.9	0.9	5.4	21.3	88.95%	51.6	5.7	1.8	5.0	36.0	81.17%
Tarry	51.5	7.2	0.2	1.4	39.8	58.99%	86.9	4.0	0.9	2.4	5.8	23.38%
10K/min												
Aqueous	63.6	7.5	0.7	4.5	23.7	82.46%	45.4	5.9	1.1	6.2	41.4	79.21%
Tarry	51.2	7.0	0.2	1.3	40.4	46.45%	73.9	3.8	0.6	2.1	19.5	20.86%

*obtained by difference; ^obtained by Karl-Fischer Titration

The higher heating value for the pyrolysis oils was calculated on a dry basis using the results from the elemental analysis by the Channiwala *et al.* (2002) correlation. The values for the aqueous and tarry phases for slow pyrolysis are 29.30 and 22.55 MJ/kg for the 20K/min and 29.01 and 22.09 MJ/kg for the 10K/min runs respectively. The standard deviation of the elemental composition of the oils at different heating rates is less than 1.7% across the board showing that the heating rate has little influence on the energy density and quality of the dry

oil products for slow pyrolysis. Conversely the C and O values for the vacuum runs deviated significantly between heating rates with the 20K/min runs having up to 10% more carbon and thus less oxygen (as it is calculated by difference) than the 10K/min runs. This resulted in values of 19.21 and 28.45MJ/kg and 21.46 and 34.71MJ/kg for the 10 and 20K/min for the vacuum runs respectively. Thus a higher heating rate produces higher quality oils (higher calorific value), an effect most influential at lower residence times. Obviously the water content of the oils would greatly influence the energy density and thus the usefulness of the oils, the ±80% moisture content in the aqueous phase a case in point.

Usually when a bio-oil contains a very high amount of water a phase separation occurs and the water and oil form distinct, easily separated, layers (Boucher *et al.* (2000)). The small sample sizes used in this study, due to equipment limitations, resulted in an extremely small amount of product. This small product amount meant that separation was not feasible and thus the water content was measured on a well-mixed sample. For this reason it is not possible to quantify the extent of separation due to immiscibility that the oils would undergo. The most conservative indication of the products' energy density can be gained by taking the dry HHV and multiplying it by the fraction of dry oil in the whole aqueous/tarry phase. This gives an idea of the actual energy density of the oil as the water content has been taken into account but the hydrogen not contributing to the Channiwala *et al.* (2002) correlation values. These improved values for the aqueous and tarry phases are 5.14 and 12.07 MJ/kg for the 20K/min and 3.21 and 9.06 MJ/kg for the 10K/min slow pyrolysis runs respectively. The actual energy densities of the vacuum pyrolytic oils are 3.99 and 22.5 and 4.04 and 26.4MJ/kg for the aqueous and tarry phases produced at 10 and 20K/min respectively.

For both vacuum and, to a greater extent, slow pyrolysis oils the higher heating rate produced oil with a higher water content implying more degradation occurred. During the residence time the gases in the higher heating rate runs were exposed to a higher temperature than their 10K/min counterparts. This higher temperature caused secondary reactions resulting in more water production (Lappas *et al.* (2002)). This also explains why the difference is more pronounced for the slow runs as the residence time is 162 times longer than in the vacuum runs meaning that the gases in those runs were exposed to significantly higher temperatures.

Generally vacuum pyrolysis produced oils with higher calorific values and lower calorie chars than slow pyrolysis as a result of the limited secondary reactions.

An elemental balance over the whole process was performed for both slow and vacuum pyrolysis at both 10 and 20K/min (Table 6.1.4).

Table 6.1.4: Elemental Balances for Glossy Paper Pyrolytic Runs

% of Element in Glossy Paper Feed								
	20 K/min				10 K/min			
Slow								
	Aqueous	Tarry	Char	Gas + Loss	Aqueous	Tarry	Char	Gas + Loss
C	0.02	8.04	44.32	47.62	3.76	6.49	49.99	39.77
H	22.13	26.60	7.32	43.96	32.07	15.44	10.49	41.99
O	12.28	12.83	50.93	23.96	16.14	7.30	47.90	28.66
Vacuum								
	Aqueous	Tarry	Char	Gas + Loss	Aqueous	Tarry	Char	Gas + Loss
C	4.65	4.80	27.81	62.74	5.10	4.48	30.01	60.40
H	35.57	4.83	4.16	55.44	39.91	4.62	3.45	52.03
O	18.57	1.87	40.18	39.38	20.96	2.15	45.27	31.62

It is clear that the majority of the carbon and hydrogen present in the raw feedstock is transferred to the gas stream. It is likely that a significant amount of the C is being released as CO compounds but due to the high H percentage as well as the low O content it is likely some compounds of calorific value are being produced. For this reason it may be advantageous to capture the gas or use it directly as a fuel for heating the pyrolysis process. A method for the capture and analysis of the off gases should be developed to further this investigation in future studies.

6.1.2: Pyrolysis of HDPE

The pyrolysis of HDPE produced no char and, rather than oil, produced a light yellow, pungent smelling wax. The wax was collected in the metal pipe and atmospheric temperature condenser as well as both the water ice condensers. An aqueous phase was collected in the dry ice condensers for the vacuum runs only. It was observed that when the furnace reached degradation temperature violent spitting and bubbling of the molten plastic resulting in audible and visible vibrations of the suspended reactor tube. Table 6.1.5 shows the effects of heating rate and residence time on the pyrolysis of HDPE as yields calculated as per Chapter 3.

Table 6.1.5: Yields (%) from the Vacuum and Slow Pyrolysis of HDPE

HDPE	Vacuum		Slow	
	20 K/min	10K/min	20 K/min	10K/min
Aqueous Y	4.6 ± 0.2	4.3 ± 1.1	-	-
Wax Y	79.2 ± 4.0	88.6 ± 0.2	81.6 ± 0.4	76.7 ± 0.9
Gas Y	14.0 ± 6.9	8.7 ± 3.3	18.4 ± 0.4	23.3 ± 0.9

The yield of pyrolytic water is omitted due to the fact that so little aqueous phase was collected and was observed in the vacuum runs only. The fraction that was captured split into two distinct

layers giving unreliable results when analysed by Karl Fischer titration. The yields above are in line with those found by Demirbas (2004) and Pinto *et al.* (1999) who worked on a small scale as well as those of Mastral *et al.* (2003) found when working on a fluidised bed set up.

The losses in the form of gas are much higher for slow pyrolysis than for the vacuum runs and more wax is produced in the vacuum runs indicating that the longer residence time (slow pyrolysis) promotes secondary degradation reactions of the primary products. The effect of residence time is more prominent for the runs with HDPE than those with glossy paper. This could be due to the simplicity of the HDPE compound, basic alkane chains with few impurities making decomposition easier than the more complex paper components (cellulose with fillers and other additives). The aqueous phase consists of the most volatile products as they were only condensed at the lowest temperature. The fact that the slow pyrolytic runs did not produce measurable amounts of aqueous phase while ±4 wt% was collected in the vacuum runs is further indication of the increased secondary reactions at longer residence times.

The increase in heating rate decreased wax yield while increasing the aqueous and gas yields for the vacuum runs. Thus the higher the heating rate the more degradation occurs. An increase in heating rate under slow pyrolytic conditions decreases the gas yields and results in an increase in the yield of waxy product. Gao (2010) found a similar phenomenon and attributed the increased gas yields to higher heating rates promoting initial random cracking reactions rapidly producing short chain non-condensables.

It is more difficult to link the TGA to the laboratory scale runs with HDPE than with glossy paper as what is left behind in the reactor after a run is not char but rather a mixture of wax that condensed in the cool end of the reactor tube and ash. As a result it is difficult to say how much ‘char’ was produced. However, the proximate analysis of HDPE shows no fixed carbon and an ash content of 1.03% and, by coupling this with the similarity of the wax in the reactor tube and the wax in the atmospheric condenser, it can be said that the HDPE samples reached 100% conversion. There was also no visible un-reacted feedstock present in the reactor tube or any condensers after the runs. Figure 6.2.2 shows the results from the TGA runs for HDPE.

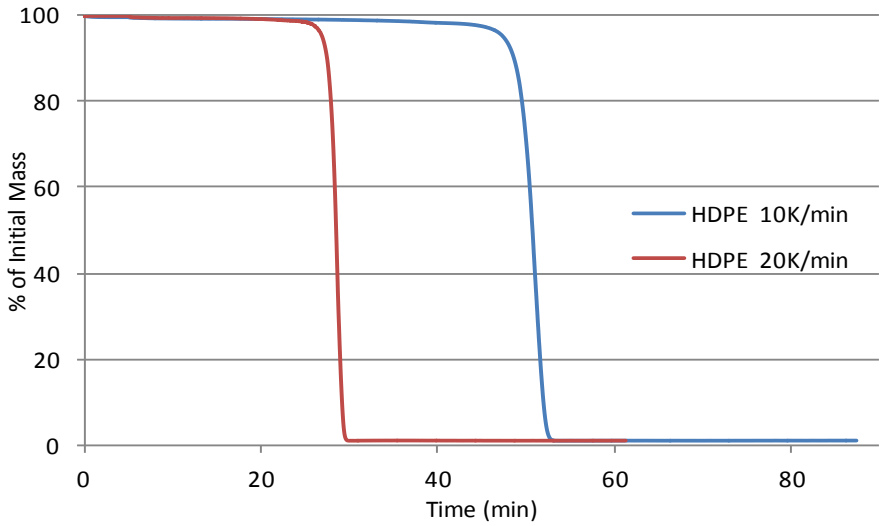

Figure 6.2.2: Results of TGA runs at 10 and 20K/min Under Plant Conditions for HDPE

From Figure 6.2.2 the yields of volatiles and 'char' were calculated to be 98.9 and 1.1% and 99.1 and 0.9% for the 20 and 10K/min runs respectively. Proximate analysis shows HDPE does not have any fixed carbon and only 1.0% ash, very close to the 1.1 and 0.9% residue from the 20 and 10K/min runs. Thus it can be said that there is almost no difference between the two scales and thus TGA runs would be a good indication of plant yields under different conditions for materials with high volatile matter content, high thermal conductivity.

The elemental analysis results for the wax obtained from the runs with HDPE are presented in Table 6.1.6. Proximate analysis was also performed on the wax samples collected from the reactor tube. ASTM E 1131 is indicated for the analysis of plastic and other polymeric materials, however, its effectiveness and accuracy for the analysis of waxes is unknown. When the Parikh *et al.* (2005) correlation was applied to the data obtained the calorific values were extremely low in comparison to the raw HDPE feed and did not correlate with the low oxygen, high carbon and hydrogen elemental results as shown in Table 6.1.6.

Table 6.1.6: Ultimate Analysis (in wt%) and Calculated HHV (MJ/kg) of Wax from the Slow and Vacuum Pyrolysis of HDPE

K /min		C	H	N	S	O*	HHV (Channiwala)
Slow Pyrolysis							
20	Reactor	86.1	13.8	0	0	0.2	46.16
	Condenser 1	84.6	13.9	0	0	1.6	45.67
10	Reactor	85.0	13.5	0	0	1.5	45.42
	Condenser 1	83.6	14.3	0	0	2.1	45.41
Vacuum Pyrolysis							
20	Reactor	83.6	14.3	0	0	2.1	45.82
	Condenser 1	80.5	13.7	0	0	5.2	43.64
10	Reactor	84.7	14.4	0	0	0.9	46.44
	Condenser 1	79.1	13.3	0	0	7.6	42.51

Overall, the wax produced in the slow pyrolysis runs is of a slightly better quality (higher C and HHV) than that produced under vacuum. Both conditions showed less than 1% standard deviation on both the elemental and calorific results between heating rates. The wax collected in the atmospheric condenser and reactor tube ('reactor' in Table 6.1.6) is higher in C and much lower in O than the wax collected in the first 4°C condenser (condenser 1 in Table 6.1.6) resulting in a higher calorific value for the reactor wax. This is much more pronounced in the vacuum runs with differences of 2.18 and 3.93MJ/kg compared with 0.49 and 0.01MJ/kg for the slow runs between the reactor and condenser waxes for 20 and 10K/min respectively.

An elemental balance over the whole process was performed for both slow and vacuum pyrolysis at both 10 and 20K/min (Table 6.1.7).

Table 6.1.7: Elemental Balances for HDPE Pyrolytic Runs

% of Element in HDPE Feed						
	20 K/min			10 K/min		
Slow						
	Reactor	Cond 1	Gas	Reactor	Cond 1	Gas
C	58.8	25.1	16.1	52.2	26.3	21.4
H	55.4	24.4	20.3	49.2	26.5	24.2
O	4.2	14.3	81.5	3.8	20.2	76.1
Vacuum						
	Reactor	Cond 1	Gas	Reactor	Cond 1	Gas
C	56.6	28.7	14.7	67.0	24.2	8.8
H	57.1	28.8	14.1	67.2	24.0	8.8
O	43.2	57.8	0.0	22.1	71.8	6.1

The majority of the H and C present in the original HDPE is present in the product waxes with only between 16 and 25% lost to the gas stream for slow pyrolysis (Table 6.1.7). This is even less for the vacuum runs with between 8.8 and 14.7% lost. 70 and 81.5% more oxygen is lost in the gas stream of the slow pyrolysis runs at 10 and 20K/min than in the vacuum runs (Table 6.1.6). This is evidence of the secondary reactions taking place due to the higher residence time during the slow runs. The oxygen leaving as gas is most likely in the form of CO compounds which have low calorific value but could, potentially be used as an addition to a syngas line. The gas produced from the vacuum runs is likely to be of higher quality but in less volume and could, potentially, be used as a fuel gas for the process. Further work needs to be done on the analysis of these off gases to gauge their potentials. The majority of the oxygen in the vacuum runs is present in the product wax of the first condenser, lowering its calorific value slightly (Table 6.1.6).

6.1.3: Comparison of glossy paper and HDPE pyrolysis

As discussed, the HDPE does not produce any solid comparable to traditional char from biomass, such as is obtained from the pyrolysis of glossy paper. The HDPE wax is a solid oil phase and can thus be compared to the oil yields and quality from glossy paper. Overall an increase in heating rate increases the yield of the oil phase and decreases the gas yield for both glossy paper and HDPE for slow pyrolysis conditions (Tables 6.1.1 and 6.1.5). The opposite is true for both feedstocks under vacuum where there is up to 12% more oil produced than in inert atmosphere (Tables 6.1.1 and 6.1.5). This shows that a low residence time promotes pyrolytic reactions with extensive pyrolytic water production for papers. Under both inert and vacuum conditions glossy paper produces approximately double the amount of gas and half the amount of oil as HDPE.

Generally the pyrolysis of HDPE produces much higher calorific value products than glossy paper with no moisture (Sections 6.1.1 and 6.1.2). However, the pyrolytic oils are solid at room temperature and thus are not necessarily suitable for many applications where liquid fuel is required. In cases like these dry glossy paper pyrolytic oil would be more suitable, however the separation and removal of the moisture from the oil requires much work.

6.2: Scalability effect on the determination of degradation pathways

A thermogravimetric analyser (TGA) alone can only measure weight loss with time and temperature and as such can only provide predictions of quantitative results for the degradation products. When coupled with a mass spectrometer (MS) the quality of the exiting gases can be evaluated (as seen in Section 5.3). The volatiles exiting the TGA are a mixture of condensable and non-condensable products and thus the qualitative information gained from this analysis is a mixture of what would be the liquid and gas phase products from a larger scale batch reactor. In order to gauge the effectiveness of the TGA-MS system at predicting larger scale pyrolysis behaviour it is of interest to investigate the degradation pathways presented in literature for the pyrolysis of HDPE and paper (Sections 6.3.1 and 6.3.2) and compare these to the MS results from this study. Section 6.3.3 illustrates the comparison of TGA-MS and TGA thermal desorption (gas capture) results with GC-MS results from both new and aged bio-oils.

6.2.1: Degradation pathway for polyethylene

As one of the most used plastics in the world, polyethylene and its degradation mechanisms have been investigated by many authors (Bockhorn *et al.* (1999), Peterson *et al.* (2001), Gao

et al. (2003), Poutsma (2003) and Cit *et al.* (2010)). All these authors accept the same basic degradation process but Bockhorn *et al.* (1999) and Poutsma (2003) give a more detailed discription of the possible pathways. Scheme 6.3.1 clearly indicates the possibilities at each point, initiation, propagation and termination for the degradation of polyethylene.

As PE is a basic straight chain hydrocarbon the main products from its degradation are, as would be expected, polymeric alkenes (paraffins) and alkenes (olefins) (Bockhorn *et al.* (1999), Cit *et al.* (2010) Gao *et al.* (2003) and Poutsma (2003)). Peterson *et al.* (2001) postulated that monomer production was low indicating that the unzipping of the PE chain occurs only to a small extent and that the most abundant products are propene and 1-hexene. They proposed that this is due to the geometric favourability of the 1 to 5 radical shift (intra molecular H transfer) due to an intermediate state within the polymer melt, shown in Figure 6.2.1, followed by scission.

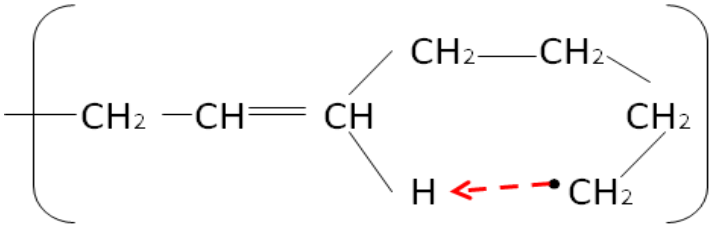

Figure 6.2.1: Intramolecular H transfer in PE (adapted from Peterson *et al.*, 2001)

In degradation Scheme 6.2.1 below:

P is an alkane polymer chain of random length of the form –(CH_2CH_2)- depicted as:

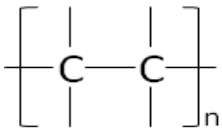

R_r is an alkane radical of random length. r_r is a short version of R_r both with radical sites positioned at the end of the chain of the form –(CH_2CH_2●) depicted as:

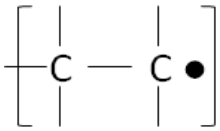

R_r* is an alkane radical of random length with the radical sites sporadically along the length of the chain. Rr^1 is an alkane radical of random length with the radical sites near the end of the chain both of the form –(CH_2CH●CH_2CH_2)- depicted as:

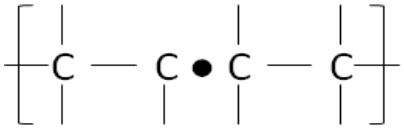

Y* is a polymer side chain radical or other polymer radical caused by scission at a weak bond site such as at a side chain or before a double, C=C, bond.

B is an alkane polymer with long chain branches of the form $–(CH_2CH_2CH(CH_2)-)_2$ depicted as:

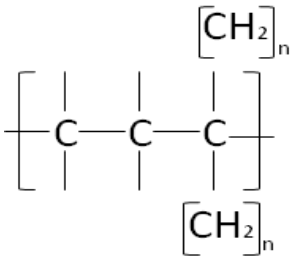

MB is a multi-branched alkane polymer of the form $(-(CH_2)_2CHCH((CH_2)_2-)$ depicted as:

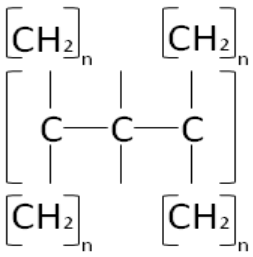

V is a polymer with vinylene functionality of the form $–(CH_2CH=CHCH_2)-$ depicted as:

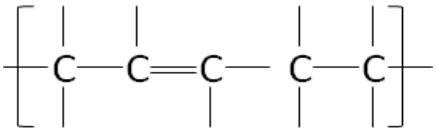

Scheme 6.2.1: Degradation Pathways Possible for Polyethylene*

	Initiation	
I_A	$P \rightarrow R_r + R_r$	*R/E Scission*
I_B	$P \rightarrow R_r + Y^*$	*Weak Link Scission*
	Propagation	
P_{A1}	$R_r \rightarrow R_r + CH_2=CH_2$	*β Scission*
P_{A2}	$R_r + P \rightarrow$ Poly(alkane) $+ R_r^*$	*Intermolecular H Transfer*
P_{A3}	$R_r \rightarrow R_r^1$	*Intramolecular H Transfer*
P_{A4}	$R_r \rightarrow R_r^*$	*Intramolecular H Transfer*
P_{B1}	$R_r^* \rightarrow R_r +$ Poly(alkene)	*Scission*

P_{B2}	$R_r^1 \rightarrow R_r$ + alkene	*Scission*
P_{B3}	$R_r^1 \rightarrow$ Poly(alkene) + r_r	*Scission*
P_{B4}	R_r^1 + P → Poly(alkane) + R_r^*	*Intermolecular H Transfer*
P_{C1}	r_r → alkane	*Intermolecular H Transfer*
P_{C2}	r_r → alkane + alkene	*Intermolecular H Transfer*
	Termination	
T_{A1}	$R_r + R_r \rightarrow P$	*Recombination*
T_{A2}	$R_r + R_r \rightarrow$ Poly(alkane) + Poly(alkene)	*Recombination*
T_{B1}	$R_r + R_r^* \rightarrow B$	*Recombination*
T_{B2}	$R_r + R_r^* \rightarrow$ Poly(alkane) + V	*Recombination*
T_{B3}	$R_r + R_r^* \rightarrow$ Poly(alkene) + P	*Recombination*
T_{C1}	$R_r^* + R_r^* \rightarrow$ MB	*Cross Linkage*
T_{C2}	$R_r^* + R_r^* \rightarrow P + V$	*Recombination*
T_D	$R_{r\,(liquid)} \rightarrow R_{r\,(vapour)}$	*Evaporation*

*(Adapted from Bockhorn *et al.* (1999) and Poutsma (2003))

Gao *et al.* (2003) also postulate that intramolecular hydrogen transfer plays a large role in the degradation pathway and suggest the preferential formation of C_6, C_{10} and C_{14} hydrocarbons in the same manner. It is also noted that the presence of hydrogen in the products is a possibility but would most likely be due to secondary degradation reactions.

Poutsma (2003) noted an increase in the unsaturation of the polymer melt in the early stages of degradation (before the main degradation temperature) showing that initiation can occur before volatile product formation begins or in the absence thereof. It was also observed that ethane, ethylene, propane, propylene, butane and butene were the main products with production of some dienes at higher temperatures, although Bockhorn *et al.* (2010) state that the abundance of such diene molecules is low.

The mass spectra from the most important light molecular products (Appendix D) discussed above were found to have a high correlation when compared to the TGA-MS data found in this study (Table 6.2.1). However, it should be noted that some authors observed the formation of high molecular weight alkenes and alkanes as well as some dienes in a tar (eg eicosane, $C_{20}H_{24}$) during pyrolysis of PE (Cit *et al.* (2010)). Many of these polymeric chains of higher masses are likely to form as per the degradation Scheme 6.2.1 thus Table 6.2.1 is not exhaustive. However, such molecules were not detected in the preliminary scans and thus were either not produced due to the nature of the feedstocks used in this study or were formed and immediately broken down to smaller hydrocarbon chains.

The mass spectra from the degradation of PE show a high rate of production of low molecular weight ion fragments (e.g. m/z 20, 24, 44, 43, 56 and 57) forming during the main degradation step and a low production rate of higher molecular weight ion fragments (e.g. m/z 84, 91 and 97) forming at the end of the heating program, after the main degradation step. Thus, it can be said that the initiation and, to a greater extent, propagation reactions (mainly cracking) occur quickly thereby releasing many short chain hydrocarbon volatiles. The termination reactions (mainly recombination) form longer chain products much more gradually and only after the main degradation step.

From this information it can be said that the degradation pathway found by TGA-MS in this study is in agreement with the degradation mechanisms presented in literature (as presented in scheme 6.2.1). However, the question as to whether these results can accurately predict the behaviour of PE on a larger scale remains. For this, one would need to be able to analyse the products from the plant runs in terms of compounds present. Since the wax produced in this study was a non-polar solid that formed an emulsion instead of dissolving in non-polar solvents, it is not possible to use a GC-MS for this. In future studies a portion of the gases exiting the reactor (i.e. before the condenser train) could be sampled at certain points during the degradation and analysed offline for comparison with the MS data.

Products with five or more carbons in the main chain will be condensable as they will have boiling points above 30ºC and will thus be liquid at room temperature. This gives an indication of what compounds would be present in the wax produced and could be used for comparison with TGA-MS results to further the information on the scalability effect.

Table 6.2.1: MS Spectra Comparison for HDPE and LDPE

Species	MS Matches		Species	MS Matches	
	HDPE	LDPE		HDPE	LDPE
Propane	20	28	Pentane	28	28
	28	44		43	56
	43			44	69
	44				70
Propene	20	28			71
	28		Pent-1-ene	28	28
	43			43	56
Butane	28	28		67	69
	43	44		70	70
	44	56			71
		57	Pent-2-ene	28	28
But-1-ene	28	28		43	44
		56		44	56
		57		67	57
But-2-ene	28	28		70	69
		56			70
		57			71
Hexane	28	28	Heptane	28	28
	43	44		43	44
	44	56		44	56
	70	57		67	57
		69		70	69
		70		84	70
		71			71
Hex-1-ene	28	28	Hept-1-ene	28	28
	43	44		43	44
	44	56		44	56
	67	57		67	57
	70	69		70	69
	84	70		84	70
					71
Hex-2-ene	28	28	Hept-2-ene	28	28
	43	44		43	44
	44	56		44	56
	67	57		67	57
	70	69		70	69
	84	70		84	70
				97	71
Hex-3-ene	28	28	Hept-3-ene	28	28
	43	44		43	44
	44	56		44	56
	67	57		67	57
	70	69		70	69
	84	70		84	70
		71		97	71

6.2.2: Degradation pathway for paper

As discussed previously, most paper has cellulose as a main component. For this reason and due to the fact that the kinetic analysis of the papers compared well to literature on cellulose (Section 5.2.3) the degradation pathways for its thermal degradation are considered here. These pathways are complex, but can be broken down into two main possibilities after desorption of physically bound intermolecular water. The two parallel pathways are depolymerisation and dehydration to anhydrocellulose followed by further decomposition (Beyler *et al.*, 2002).

The depolymerisation reaction occurs by breakage of the glycosidic bonds by a hydroxyl group either inter or intramolecularly, this process is called transglycosylation, a form of unzipping reaction (Beyler *et al.*, 2002, Shafizadeh 1982). This results in the formation of a tarry phase made up of anhydrosugars the most abundant of which is levoglucosan (1, 6 anhydro – β – D-glucopyranose). In addition to the anhydrosugars some char is also formed along with other decomposition gases. The levoglucosan and other anhydrosugars formed in this step further decompose into tars, low molecular weight volatiles and finally carbon monoxide, carbon dioxide and water vapour.

Dehydration occurs by cross-linking of the cellulose chains with the production of water (Beyler *et al.* 2002). This reaction is furthered by the scission of intra-ring bonds leading, finally, to the production of carbon monoxide, carbon dioxide, water vapour and carbonyl and carboxylic acid compounds (Pielchowski *et al.*, 2005).

As discussed previously, the degradation of paper has been shown to occur in three stages (depicted by DTG curves, Section 5.1.1). This, together with the degradation postulations made in literature, allows for some prediction of what products to expect at each stage. From the degradation schemes presented it can be seen that all three paper samples release fragments 16, 17 and 18 in the first stage of the decomposition. As discussed in Section 5.3.3, this relates directly to the MS ionic fingerprint of water and coupled with desorption as outlined in literature, the weight loss in stage 1 can be attributed to the loss of the moisture content from the sample.

Stage 2 is the main degradation step and as such the two main competing pathways for pyrolytic decomposition can be assumed to be occurring here. Finally, stage 3 relates to the breakdown of the more stable components or solid/liquid products of the second stage of degradation (like levoglucosan).

Table 6.2.2 summarises the main products that can be expected at stages 2 and 3 from the degradation schemes presented in literature as well as the pathway that gives rise to them. The mass spectral fragments that are present both in the MS footprint of each of these compounds as well as in the experimental degradation schemes postulated in this study were compared (Table 6.2.3).

Table 6.2.2: Products Expected in the 2nd and 3rd Decomposition Stages of Paper

Expected Stage 2	Origin
Carbon Dioxide Carbon Monoxide Methane Water Vapour	*Degradation Products of Cellulose and Levoglucosan*
Levoglucosan 1,4:3,6 dianhydro-α-D-glucopyranose 1,6 anhydro-β-D-glucofuranose Levoglucosanone	*Transglycosylation*
Acetaldehyde Propanal Glyoxal Acetic Acid Formic Acid	*Degradation Products of Levoglucosan*.

Expected Stage 3	Origin
Carbon Dioxide Carbon Monoxide Methane Water Vapour	*Degradation Products of Cellulose and Levoglucosan.*
Acetaldehyde Propanal Glyoxal Acetic Acid Formic Acid Levoglucosanone	*Degradation Products of Levoglucosan*.
Levoglucosan	*Recombination/Further Cellulose Degradation*.

The mass spectra for the degradation of newspaper and glossy paper show that all of the compounds expected are possible in both stages 2 and 3 (Figures 5.3.7 and 5.3.8). This includes the possibility that the anhydrosugars, expected only in stage two (as per Beyler *et al.* 2002 and Pielchowski *et al.*, 2005), are also produced in stage three. It is postulated that this is due to the breakdown of cellulose that was formed by the recombination of levoglucosan in stage 2. With the exception of this anomaly, the degradations of newspaper and glossy paper seem to conform well to the proposed degradation of cellulose in literature (mentioned above).

The degradation of office paper is similar to that of glossy paper in that the anhydrosugars seem to be produced in the third degradation step (Section 5.3.2); however there are fewer matching spectra for the anhydrosugars in the second stage (Figure 5.3.9 and Table 6.2.3). This seems to indicate that the transglycosylation of the cellulose in office paper is a secondary reaction or that the anhydrosugars are degraded as soon as they are produced leaving only their degradation products behind.

Table 6.2.3: Mass Spectra Comparison for Paper

Species	Structure	MS Matches		
		Glossy Paper	Newspaper	Office Paper
Carbon Dioxide	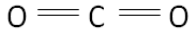	12 16 28 44	12 16 28 44	12 16 28 44
Carbon Monoxide		12 16 28	12 16 28	12 16 28
Water Vapour	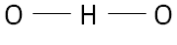	16 17 18	16 17 18	16 17 18
Methane	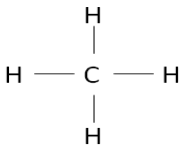	12 14 15 16 17	12 15 16 17	12 14 16
Levoglucosan	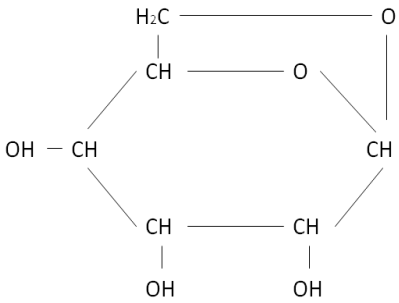	15 44 55	15 44	44
Acetaldehyde	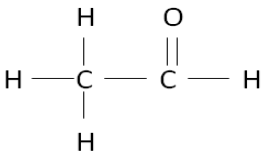	12 14 15 16 28 44	12 15 16 28 44	12 14 16 28 44
2-Propenal	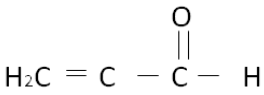	14 16 28 55	16 28 36	14 16 26 28
Glyoxal	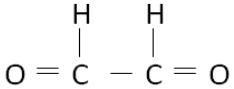	12 14 15 16 28 44 58	12 15 16 28 36 44	12 14 16 20 26 28 44 58
Acetic Acid	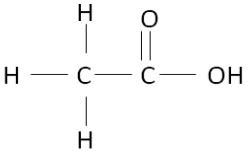	14 15 16 17 18 28 44	15 16 17 18 28 44	14 16 28 44

Formic Acid	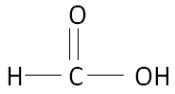	12 16 17 28 44	12 16 17 28 44	12 16 28 44
Levoglucosanone	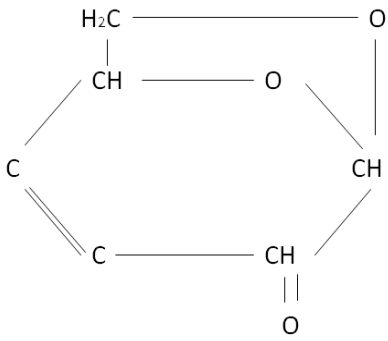	12 14 15 16 17 18 28 44 55 78 104	12 15 16 17 18 28 36 44	12 14 16 26 28 44 80
1,6 anhydro-β-D-glucofuranose	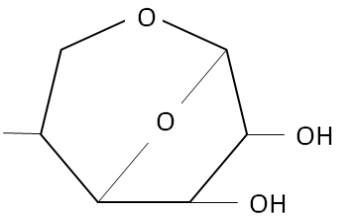	15 28 44 55 58	15 28 44	28 44 58
1,4:3,6 dianhydro-α-D-glucopyranose	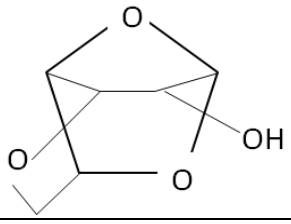	15 44 55 58	15 44	26 44 58

This study has attempted to compare the degradation of the paper components to that of cellulose; however, it is known that there are many additives and fillers present in paper waste (Biermann, 1996 III) that could influence to the degradation and the products thereof. Although the feedstocks used in this study were separated into type (glossy, office and newspaper) the sources were mixed and thus there is no way of knowing exactly what additives to expect. The degradation schemes from literature also do not ensure that the products reported are, in fact, primary degradation products (due to the experimental techniques employed), as one would expect to be released from a TGA and thus captured in the mass spectrometer. It is also evident that there is a definite lack of fragments tracked that compare to some of the main expected compounds (levoglucosan, a case in point).

In order to gain a clearer picture of the complex degradation of paper and to what extent it is comparable to that of cellulose, an analysis of the TGA off gases was performed as per Chapter 3 (TGA/TD-GC-MS). The results (Table 6.3.4) show only the compounds released that have a GC-MS peak area of greater than 0.5% of the total area and a better than 80% match in the

NIST database for retention time and corresponding MS fingerprint. All of the components presented as cellulose degradation products (Table 6.2.3), with the exception of the light molecular weight permanent gases (CO, CO_2 and CH_4), were present in the GC-MS chromatogram (Appendix E). However, the areas of the corresponding peaks were below 0.5% and are thus not presented in Table 6.2.4. This shows that while the degradation of paper is similar to that of cellulose the fillers added do impact the degradation significantly.

From the GC-MS results, five important fragments that were not tracked in the initial TGA-MS runs (m/z 31, 60, 82, 91 and 96) due to their low intensity in the preliminary MS scans were selected and tracked in follow up runs. These correspond to the most intense peaks on the MS fingerprint for 2-methyl furan, hydroxy-acetaldehyde, toluene, ethyl benzene and furfural. The mass spectra are presented in Figure 6.2.2 from which it can be seen that these fragments are released during the second degradation step.

Fragments with an m/z ratio of 60 were also tracked in order to verify the presence of levoglucosan in the degradation products. Although small, there is a peak in the ion current from the m/z 60 molecular fragment. This added to the other common fragments shown in Table 6.2.3 shows that levoglucosan is indeed a degradation product of the glossy paper in this study.

Table 6.2.4: GC-MS Results - Components in Glossy Paper TGA Off-Gas

NIST Library ID	Structure	NIST Library ID	Structure
2-Methyl-Furan	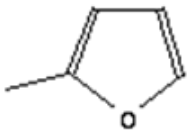	Styrene	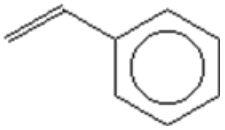
2,3-Butanedione	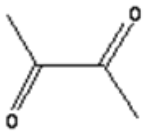	Furfural	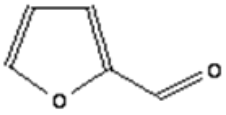
3-Pentanone	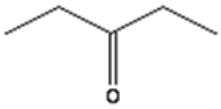	2-Furanmethanol	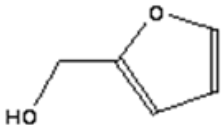
Benzene		α-Methylstyrene	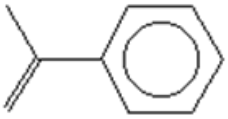
Hydroxy-Acetaldehyde		1,2-Cyclopentanedione	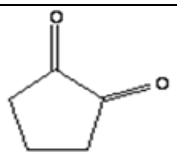
Acetic acid	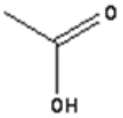	2(5H)-Furanone	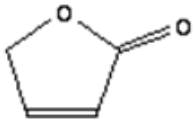
Hydroxy-2-Propanone	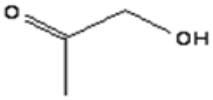	2-hydroxy-3-methyl-2-Cyclopenten-1-one	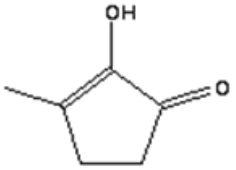
Toluene	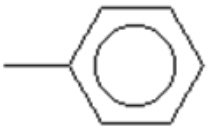	1,4:3,6-Dianhydro-α- D -glucopyranose	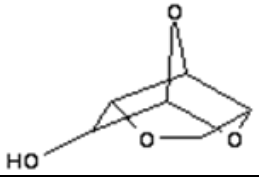
Ethylbenzene	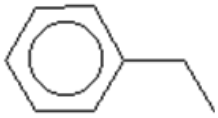	5-Hydroxymethyl dihydrofuran-2-one	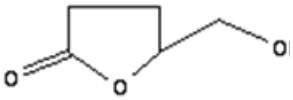
Succindialdehyde	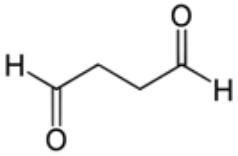	1,6-anhydro 3-β-D-Glucopyranose	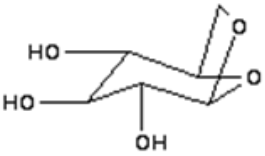
1,1'-(1,3-propanediyl) bis Benzene	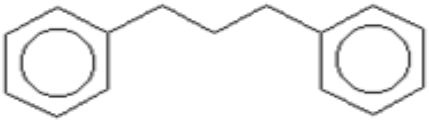		

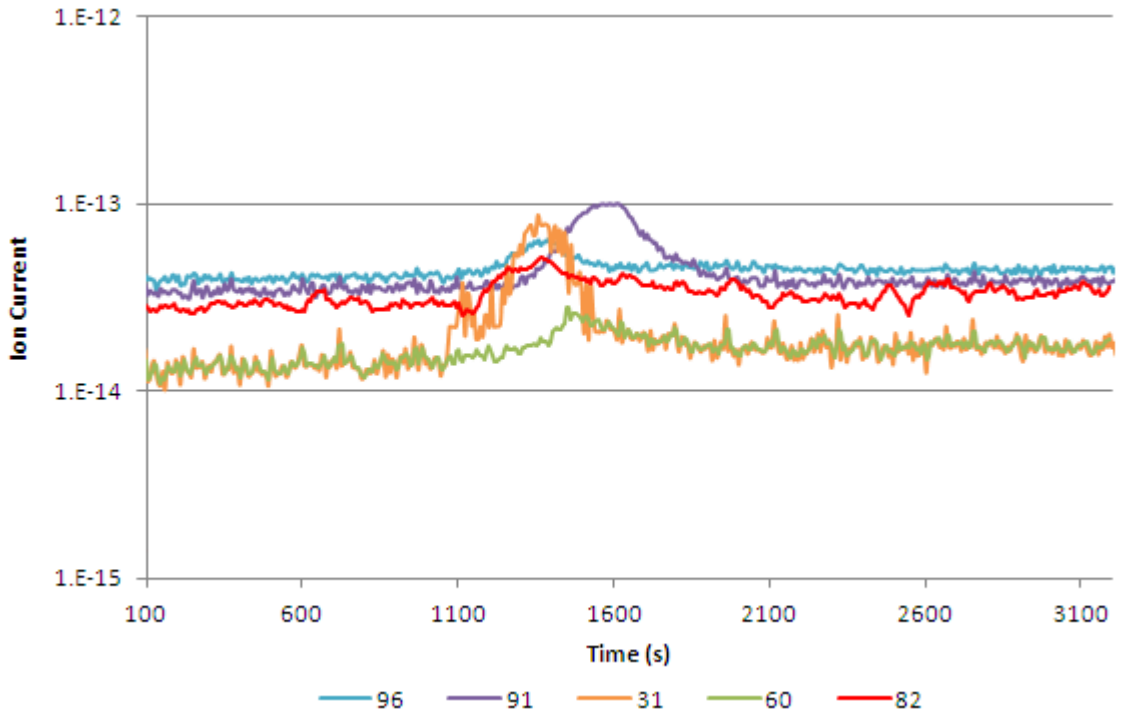

Figure 6.2.2: Online Mass Spectra of New Fragments for Glossy Paper Degradation

Styrene was found to be the most intense (area and peak height wise) compound from the GC-MS results (Appendix E). By examining the mass spectral fingerprint for styrene it is clear that the peak with the highest intensity (100% relative intensity) is that at an m/z of 104 (Appendix E). As can be seen in the degradation scheme for glossy paper (Figure 5.3.7) fragment 104 is released in both the second and third degradation steps. While some of the peak's intensity is doubtless due to contributions from the degradation of other compounds the GC-MS results show that the majority is due to the degradation of styrene.

It is well known that post 1955 synthetic additives have been increasingly used in the manufacture of paper products (Biermann, 1996 III). Polystyrene butadiene and polystyrene maleic anhydride (polystyrene 2,5 - furandione), both shown in Figure 6.2.3, are used as a binding coating and surface sizer respectively (Biermann, 1996 III). These additives are obviously a potential source of styrene, ethyl benzene and toluene. The 2,5-furandione and butadiene could easily react or degrade to form other compounds that are present in the GC-mass spectra 2(5H)- furanone by the removal of one oxygen and 2,3-butanedione by addition of oxygen to the double bond sites).

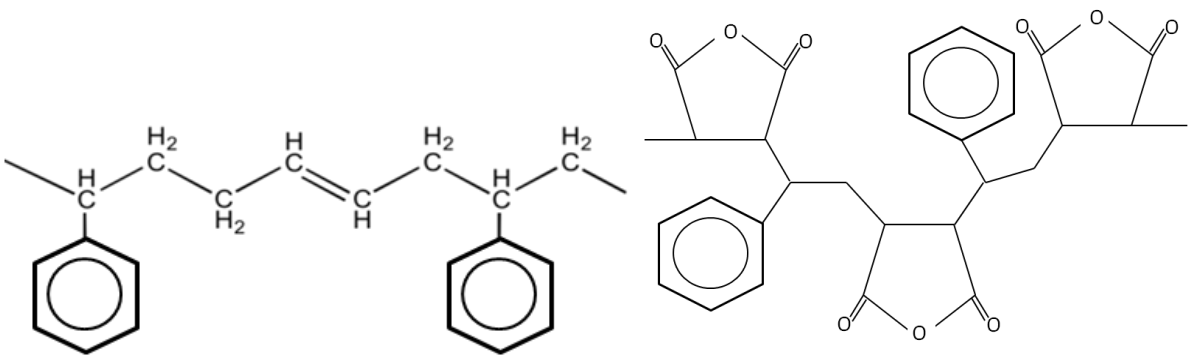

Figure 6.2.3: Structures of Polystyrene Butadiene (left) and Polystyrene Maleic Anhydride (right)

It can thus be said that while the vast majority of paper is cellulose the degradation of cellulose cannot be used to fully describe the degradation of paper due to the presence of additive and fillers and their contribution to the degradation products.

6.2.3: Degradation products of paper pyrolysis at different scales

GC-MS analysis was performed on the tarry phase bio-oil obtained from the slow pyrolysis of glossy paper at 20K/min. To further the scalability investigation for glossy paper these results needed to be comparable to the TGA gas-capture GC-MS results and thus this analysis was performed within 2 days of the runs to ensure minimal aging of the oil. Table 6.2.5 shows the compounds in the bio-oil that had a peak area of over 0.5% of the total peak area and only compounds identified to above an 80% match with other GC-MS fingerprints on the NIST library. All chromatograms and NIST identification lists are available in Appendix E.

As can be seen the bio-oil is made up mainly of ketones, furans and phenols and includes the products of the transglycosylation of cellulose, levoglucosan and 1,4:3,6 dianhydro-α-D-glucopyranose as well as simple carboxylic acids (Table 6.2.5). This is in accordance with the degradation pathways as described by the literature sources consulted in Section 6.2.2. Helt *et al.* (1988) and Phan *et al.* (2008) performed GC-MS analysis on tarry bio-oil obtained from the slow pyrolysis of newspaper and cardboard, respectively and found the composition (in groups e.g. furans etc.) to be similar to that obtained in this study (Appendix E).

Table 6.2.5: GC-MS Glossy Paper Bio-Oil Composition

Hydroxy-Acetaldehyde		Furfural	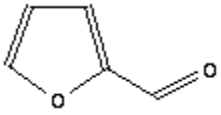
Acetic acid	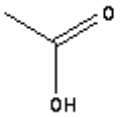	2-Furanmethanol	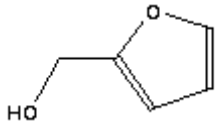
1-Hydroxy-2-Propanone	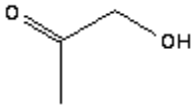	2-Butanone	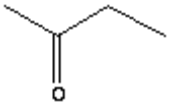
Propanoic acid	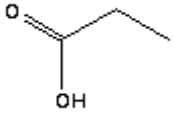	1,2-Cyclopentanedione	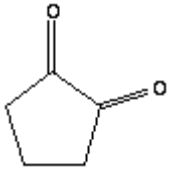
1-Hydroxy-2-Butanone	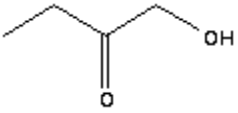	3-Methyl-2-Cyclopenten-1-one	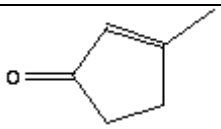
Tetrahydro-2-Furanmethanol	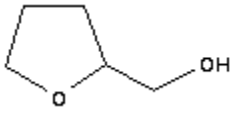	Butyrolactone	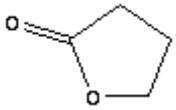
1,4 Butandione	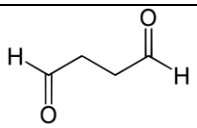	2(5H)-Furanone	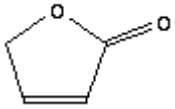
2-Cyclopenten-1-one	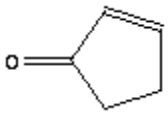	3-Methyl-1,2-Cyclopentanedione	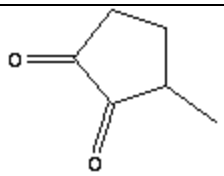
2-Methoxy-Phenol	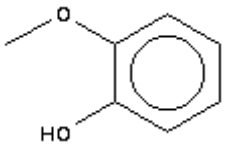	3-Ethyl-2-Hydroxy-2-Cyclopenten-1-one	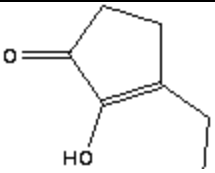
Creosol	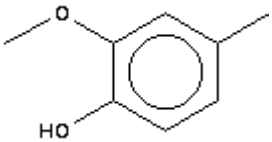	1,6-anhydroβ-D-Glucopyranose	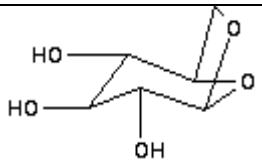
1,4:3,6-Dianhydro-α-d-Glucopyranose	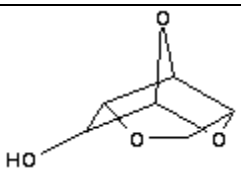	Vanillin	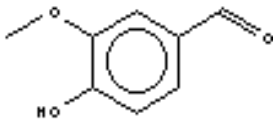

Homovanillic acid 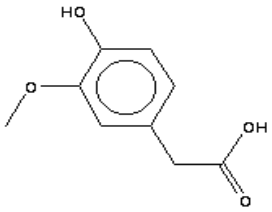	
Old Bio-Oil Only	**New Bio-Oil Only**
Butanoic acid 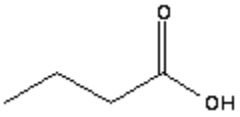	2-Methoxy-4-Vinylphenol 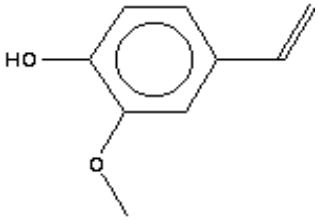
New Bio-Oil Only	
4-Ethyl-2-Methoxy-Phenol 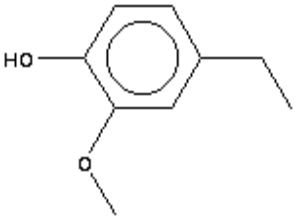	2-Methoxy-4-(1-propenyl)-Phenol 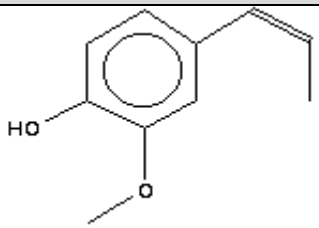

It is well know that bio-oils degrade very quickly and as such their composition can change with time (Czernik *et al.* (1994)). In order to get an idea of the stability of the tarry bio-oil (from pyrolysis of glossy paper) obtained in this study, GC-MS analysis was performed on oil that obtained under the same conditions (25 - 550ºC at 20K/min) as the oil described above four months previously. The oil was kept in sealed vials in a fridge, away from light. It was found that with the exception of the presence of butanoic acid and the absence of the more complex methoxy-phenols (as shown in Table 6.3.5) the oil was extremely similar (as evidenced in Table 6.2.5). One of the main products from the degradation of bio-oil is water due to re-polymerisation reactions, or aldol condensations (Mohan *et al.* 2006), and thus comparing the moisture content of old and new oil can be used, together with the GC-MS results as an indication of extent of degradation. The moisture content had increased by 5 wt% indicating that the oil had degraded little (when the usual highly unstable nature of bio-oils is taken into account) and hence the tarry phase bio-oil from glossy paper can be considered relatively stable.

Comparing these results to those presented in Section 6.2.2, it can be seen that acetaldehyde, acetic acid, 1-hydroxy-2-propanone, 1,2-cyclopentanedione, 2-furanmethanol, 1,6-anhydro-β-D-glucopyranose (levoglucosan), 1,4:3,6-dianhydro-α-D-glucopyranose, fufural, 1,4 butandione (succindialdehyde), 2(5H)-furanone are all present both in the bio-oil (old and new) and were captured as off gas from the TGA.

With regard to the components that differed between the captured gas and oils, the broad functional groups are the same (furans, ketones, aromatics, phenols, small carboxylic acids and transglycosylation products); however there are some differences in the actual molecular makeup of the compounds. Table 6.2.6 shows components found in the bio-oil only and closely related compounds found in the gas capture.

Table 6.2.6: Bio-Oil Compounds and their Gas Capture Counterparts

Bio-Oil Component	Gas Capture Counterpart
Propanoic acid 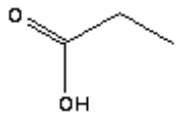	1-hydroxy 2-Propanone - 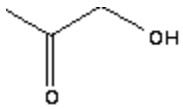
1-Hydroxy-2-butanone 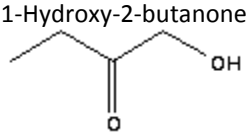	1-hydroxy-2-Propanone 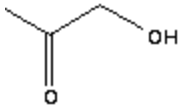
Tetrahydro-2-furanmethonol 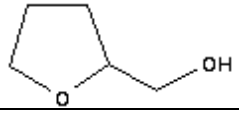	5-Hydroxymethyldihydrofuran-2-one 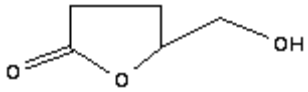
2-butanone 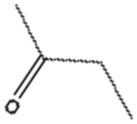	2,3-Butanedione 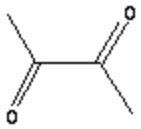
3-methyl 2-cyclopenten-1-one 	2-hydroxy-3-methyl-2- Cyclopenten-1-one 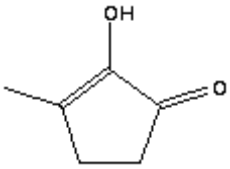
Butyrolactone 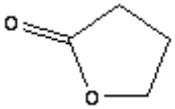	2(5H)-Furanone 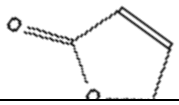
3-methyl 1,2-cyclopentanedione 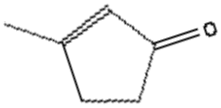	1,2-Cyclopentanedione 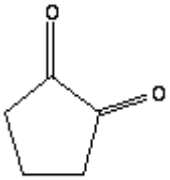

From Table 6.2.6 it can be seen that compounds found exclusively in the bio-oils are closely related to compounds found in the thermal desorber. Due to the differing natures of the capture of the released volatiles in the two cases (condensation for the bio-oil and absorption for the TGA- gas capture set up) differences in the compounds are expected. The bio-oil compounds, for the most part, are simpler molecules than their gas capture counterparts implying that these

differences are due to secondary reactions that occur in the plant due to the high relative residence time and/or degradation of the condensed oil before GC-MS analysis could be carried out.

The bio-oil contains phenols where none were found in the TGA-gas capture GC-MS results (Tables 6.2.4 and 6.2.5). Simple aromatics (benzene, toluene, ethyl benzene, styrene, α-methyl styrene and 1,1'-(1,3-propanediyl) bis-benzene) were found in the captured gas. One would expect that the more complex phenolic compounds (2-methoxy-4-vinylphenol, 4-ethyl-2-methoxy-phenol and 2-methoxy-4-(1-propenyl)-phenol) would be found in the primary degradation (TGA/TD-GC-MS) products like those from the TGA rather than those found in the oil. This could be due to the fact that during the gas capture the thermal desorber is attached to the TGA for the full duration of the run, including the 30 min hold time where it has been observed, in the laboratory scale runs, no further degradation occurs. This means that gases at 550ºC are being drawn into the desorption tube past the adsorbed compounds increasing the effective residence time to the full 30 min. When this is compared to the 5.4 min residence time that the product gases are subjected to in the laboratory scale pyrolysis set up it is clear that simpler or more degraded products should be found in the GC mass spectra for the gas capture. It is also possible that these more complex compounds are result of re-polymerisation degradation reactions in the bio-oil.

The aromatic compounds, as discussed in Section 6.2.2, can be attributed to the presence of paper fillers like polystyrene butadiene and polystyrene maleic anhydride. These fillers degrade at around 500 ºC (Lah *et al.*, 2013) while paper degrades between 200 and 500ºC (Section 5.1.1). Thus the complex aromatic and phenolic products that are released at 500 ºC are amongst the last and will be captured by the sorbent closest to the outside. Hence those products will be exposed to high temperatures for the longest time and will be thermally degraded while protecting the earlier degradation products of the cellulose.

From these results it is clear that while some differences exist the TGA-MS gas capture system can effectively be used to predict the functional groups of volatiles produced on a larger scale.

Chapter 7: Conclusions and Future Work

This study aimed to determine the composition of the municipal solid waste streams from the Stellenbosch Municipality and determine the potential of the waste for use as a refuse derived fuel. Subsequently, the thermal properties and kinetic parameters of degradation of certain components as well as the extent to which milligram scale thermal degradation under pyrolysis conditions could be used to predict gram scale pyrolytic behaviour were investigated.

7.1: Conclusions

- Recycling to landfill ratio of MSW in Stellenbosch is higher than the South African average with higher income areas recycling more than their lower income counterparts and producing a higher quality recyclables stream.

- The overall composition of the waste in the Stellenbosch municipality is comparable to that of uMgungundlovu District Municipality (UMDM) and the eThekwini Municipality in KwaZulu Natal and none is remarkable to global information.

- The recyclables stream, excluding inerts (glass and metal), from the Stellenbosch Municipality has the potential, with some treatment, to be a used as a refuse derived fuel (RDF) or a feedstock to a thermal treatment plant for energy recovery with a composition of approximately two thirds paper and plastic making up the balance.

- The thermal degradation of paper and plastic occur in three distinct stages and one step respectively. Glossy paper is the most thermally stable of the three paper samples while PET is that of the plastic components followed by HDPE, with LDPE being the least thermally stable of all the MSW components.

- A higher heating rate increases weight loss for plastics but decreases the weight loss for paper samples. The degradation temperature, maximum degradation rate and the degradation temperature ranges are increased with increasing heating rate for both the plastic and paper components considered here. The degradation temperature range is also decreased with increasing thermal conductivity.

- The activation energies and pre-exponential factors found for the plastic components were higher than those found for the paper samples in this study. Distinct peaks were observed in the activation energy trends with specific conversion possibly relating to the onset of individual parallel and/or series pyrolytic reactions occurring during the plastics degradation. The values found were comparable to literature and most similar to other studies working with waste.

- The activation energy calculated for the paper samples were found to be fairly constant and similar for all three species during the three individual steps. Calculations based on the integration of the degradation as a whole, including all three steps, showed a declining trend. The results obtained from the overall degradation were found to have a small range of acceptable linearity. As such results obtained in this way could be less reliable than those obtained for individual steps. However, both sets of values were found to be comparable to those in literature for both waste paper and pure cellulose degradation.

- The mass spectra obtained during the degradation of all the samples confirmed the three step degradation scheme for the three paper samples and single step plastic degradation for HD and LDPE the rates of which can be directly related to those calculated by the Friedman method. PET exhibited a secondary degradation step not relating to any measured weight loss thus a two-step kinetic scheme is proposed, however only the first step's rate can be related to that calculated by the Friedman method.

- The relative amounts of the ion fragments released in step 1 of paper degradation matching the MS fingerprint of water correlate with the respective moisture contents of the three paper samples.

- Ion fragments relating to the release of CO^+ and CO_2^+ were released in much greater quantities by PET than HD and LDPE due to the high oxygen content. The same fragments released by the polyethylene samples are more likely to have originated from $C_2H_4^+$ and $C_3H_8^+$ due to the structure of the compounds.

- The glossy paper-HDPE mixture achieved a lower total conversion than the weighted sum of the individual components' conversions under the same conditions. The overall rate (DTG) was also lower for the mixture than for the individual components. This leads to the probability that under these conditions there is no synergistic interaction between the two species. However, it is possible that HDPE catalyses the degradation of glossy paper as more weight was lost and relatively more ions released during the stages where it is expected only glossy paper degrades.

- Increasing heating rate increases the yield of the oil phase and decreases the gas yield for both glossy paper and HDPE under inert conditions; the opposite is true for both feedstocks under vacuum. This shows that a low residence time promotes pyrolytic reactions. Under both inert and vacuum conditions glossy paper produces approximately double the amount of gas and half the amount of oil as HDPE.

- For vacuum pyrolysis of glossy paper an increase in heating rate increases the gas yield decreasing the oil and, to a greater extent, char yields there is also slightly less pyrolytic water produced. The opposite is true for the slow pyrolysis runs. A lower residence time decreases the production of pyrolytic water while increasing the overall yield of the liquid fraction and decreasing the char and gaseous yields.

- For glossy paper, heating rate has little effect on the quality of the products for slow pyrolysis or on the char from vacuum pyrolysis, however a higher heating rate produces higher calorific value dry oils under vacuum. The increased water production at higher heating rates means that the wet oils produced at 20K/min have a lower actual calorific value than their lower heating rate counterparts. Similarly, heating rate was found to have little influence on the quality of wax produced from HDPE but that produced by slow pyrolysis is of slightly better quality than that produced under vacuum.

- The majority of the carbon and hydrogen present in the raw glossy paper was lost as a gas under both atmospheres at gram (laboratory plant) scale, whereas the majority of the carbon and hydrogen and thus calorific value in the raw HDPE was maintained in the wax product. HDPE produces a higher calorific value product free from moisture than glossy paper under the conditions tested.

- By comparing pyrolysis at milligram and gram scales (Chapter 6) it was found that while the heating rate and heat transfer limitations play a role, the largest influence on the conversion of the raw feedstock, and thus the yields, is due to the final process temperature. However TGA experimentation can give a good indication of laboratory scale pyrolytic plant behaviour (yields) at low heating rates; the accuracy of which is improved with increasing thermal conductivity of the feedstock.

- The degradation pathway found for polyethylene by TGA-MS in this study is in agreement with literature, however the degradation of glossy paper cannot be fully described by the degradation of cellulose as initially postulated due to the presence of fillers such as polystyrene butadiene and maleic anhydride, detected by large styrene peaks in the online gas capture (TGA-TD/GC-MS).

- There is little difference in the composition found by GC-MS between the new and four month old oil stored away from light and well below room temperature. It can be concluded that the tarry phase oil obtained from the slow pyrolysis of glossy paper is relatively stable.

- The GC-MS results of the pyrolytic oils and those from the online thermal desorption exhibited the same broad functional groups with slight differences in the exact molecular makeup of the compounds due to differences in the capture and analysis. Thus an online TGA-gas capture (TGA-TD/GC-MS) can be used to effectively predict the functional groups present at larger scales.

7.2: Future work and recommendations

- Further investigation into the removal of sample from the crucibles during TGA runs is recommended with the use of sealed (lidded) crucibles for comparison in order to better understand the effect of particle shapes and mass-to-surface ratios on the TGA weighing technique.

- The tracking of specific ions during TGA-MS runs needs to be optimised for different feedstocks in order to ensure that no events are missed resulting in a more accurate and better understanding of the degradation occurring.

- Further work is required in order to fully understand the complex degradation of waste PET as well as to determine the rate of the second step during degradation.

- More common ions should be tracked on future TGA-MS runs making the comparison of the volatiles released easier.

- Further experimentation at different heating rates should be performed on the HDPE-GP mixture allowing for a comparison of the kinetics relating to the individual pure compounds and mixtures. This will give a clearer indication of any potential synergy not observed in this study. In addition, investigation into the formation of plugs in the capillary tube connecting the TGA to the MS should be carried out before more information is gathered on the degradation of plastic-paper mixtures.

- If future work is to be done on the pyrolysis of plastics the current experimental set up should be modified such that the volatilised HDPE cannot run along the reactor tube out of the hot zone where it condenses. The tubes connecting the condensers should also be heated to avoid any blockages caused by wax build up.

- More pyrolysis runs should be done at different heating rates at the gram scale for comparison with the TGA runs to further validate the use of TGA as a prediction tool for larger scale yields. Greater caution must be exercised when predicting for materials with low VM and low thermal conductivities. In addition, it would be interesting to investigate a potential correlation between sample size and conversion in future studies.

- More investigation into a suitable solvent for HDPE pyrolytic wax is needed such that it can be subjected to GC-MS as well as a system developed for the sampling of off gases both for comparison with the TGA-MS results providing more information as to the scalability.

- Great caution needs to be exercised when choosing ions to track on a TGA-MS. If only low molecular weight fragments are tracked, as was the case in this study, it is a very difficult task to identify the specific parent molecule due to the complicated fragmentation patterns and the numerous molecules that can fragment giving rise to an ion of specific m/z ratio.

- Due to the nature of mass spectrometry its use as a tool for the identification of released volatiles is very limited. It should be used rather as a way of validating the presence or absence of a suspected product and can be used to investigate the effects of different process conditions on the production of specific products.

References

Aboulkas, A., El harfi, K., Nadifiyine, M., El bouadili, A. (2008). Investigation on pyrolysis of Moroccan oil shale/plastic mixtures by thermogravimetric analysis. *Fuel 89*, p. 1000 – 1006

Agrawal, R. (1988). A rapid technique for the characterization and proximate analysis of refuse derived fuel and its implications for thermal conversion. *Waste Management and Research, Vol. 6, p.* 271-280

Alter, H. (1978) Development of specifications for recycled products. *Conservation & Recycling. Vol. 2.* P. 71-84.

Antal, M., Varhegyi, G. (1995) Cellulose pyrolysis kinetics: the current state of knowledge. *Industrial Engineering Chemical Research. Vol. 34*. p. 703 – 717.

Arena, U. (2012). Process and technological aspects of municipal solid waste gasification: a review. *Waste Management. Vol. 32.* p. 625 – 639.

ASTM Annual Book of ASTM Standards, Vol. 1994, Section 5, American Society of Testing Materials, Philadelphia, 1993, pp. D3172–D3189

ASTM (i) International – Standards Worldwide (2007). Proximate Analysis. *Paper ID: MNL11271M, Committee/Subcommittee: D05.21, DOI: 10.1520/MNL11271M*. Accessed online 4th May 2012. [Available] www.astm.org/digital_library/mnl/pages/mnl11271m.html

ASTM International (ii) – Standards Worldwide (2007). Ultimate Analysis. *Paper ID: MNL11272M, Committee/Subcommittee: D05.21, DOI: 10.1520/MNL11272M.* Accessed online 4th May 2012. [Available] www.astm.org/ digital_library/mnl/pages/mnl11272m.html.

Aydemir, B., Sezgi, N. A. (2013). Alumina and tungstophosphoric acid loaded mesopourous catalysts for the polyethylene degradation reaction. *Industrial and Engineering Chemical Research. Special Issue: NASCRE 3.*

Badia, J., Martinez-Felipe, A., Santonja-Blasco, L., Ribes-Greus, A. (2013). Thermal and thermo-oxidative stability of reprocessed poly(ethylene terephthalate). *Journal of Analytical and Applied Pyrolysis*. *Vol. 99.* p.191 – 202.

Bajpai, P (2011). *Biotechnology for Pulp and Paper Processing.* Springer; 2012 edition. p. 7 – 13.

Belgiorno, V., De Feo, G., Della Rocca, C., Napoli, R. M. A. (2002). Energy from gasification of solid wastes. *Waste Management. Vol. 23*. p. 1 – 15.

Berrueco, C., Esperanza, E., Mastral, F., Ceamanos, J., Garcia-Bacaicoa, P. (2005). Pyrolysis of waste tyres in an atmospheric static-batch reactor: Analysis of the gases obtained. *Journal of Analytical and Applied Pyrolysis 74.* p 245 – 253.

Berton Technologies (2000). Incineration of PVC and other products in MSW: Assessment of additional costs for various wastes with comparison to PVC in domestic Waste Incineration. *Intended for ECVM (European Council of Vinyl Manufacturers).*

Beyler, C. L., Hirschler, M., M. (2002). Thermal Decomposition of Polymers. In: DiNenno, P. ed. SFPE Handbook of Fire Protection Engineering 3rd Edition. NFPA 2002. p. 110.

Biermann C. J. (1996 I). *Stock Preparation and Additives for Papermaking.* Handbook of Pulping and Papermaking. Academic, San Diego, p. 190

Biermann C. J. (1996 II). *Papermaking Chemistry.* Handbook of Pulping and Papermaking. Academic, San Diego, p. 439

Biermann C. J. (1996 III). *Paper Manufacture.* Handbook of Pulping and Papermaking. Academic, San Diego, p. 209

Bockhorn, H., Hornung, A., Schawaller, D. (1999). Kinetic study on the thermal degradation of polypropylene and polyethylene. *Journal of Analytical and Applied Pyrolysis. Vol. 48.* p. 93 – 109

Boucher, M., Chaala, A., Pakdel, H., Roy, C. (2000). Bio-oils obtained by vacuum pyrolysis of softwood bark as a liquid fuel for gas turbines. Part II: Satbility and ageing of bio-oil and its blends with methanol and a pyrolytic aqueous phase. *Biomass and Bioenergy. Vol. 19.* p. 351-361.

Bridgwater, A. V. (2003). Renewable fuels and chemicals by thermal processing of biomass. *Chemical Engineering Journal. Vol 91.* p. 87 – 102.

Bridgwater A. V. (1999). Principles and practice of biomass fast pyrolysis processes for liquids. *Journal of Analytical and Applied Pyrolysis. Vol.51.* p.3-22

Brown, M. E., Maciejewski, M., Vyazovkin, S., Nomen, R., Sempere, J., Burnham, A., Opfermann, J., Strey, R., Anderson, H. L., Kemmler, A., Keuleers, R., Janssens, J., Desseyn, H. O., Chao-Rui Li, Tang, T. B., Roduit, B., Malek, J., Mitsuhashi, T. (2000). Computational aspects of kinetic analysis Part A: The ICTAC kinetics project-data, methods and results. *Thermochemica Acta. Vol. 355*. p. 125 – 143.

Brunner, P, Ernst, W. (1986) Alternative methods for the analysis of municipal solid waste. *Waste Management and Research. Vol. 4.* p. 147 – 160.

Buah, W. K., Cunliffe, A. M., Williams, P. T. (2007). Characterisation of products from the pyrolysis of municipal solid waste. *Process Safety and Environmental Protection. Vol. 85.* p. 450 – 457.

Carrier, M., Hugo, T., Gorgens, J., Knoetze, H. (2011). Comparison of slow and vacuum pyrolysis of sugar cane bagasse. *Journal of Analytical and Applied Pyrolysis. Vol. 90.* p. 18-26.

Ceamanos. J., Mastral, J., Millera, A., Aldea, M. (2002) Kinetics of pyrolysis of high density polyethylene – comparison of isothermal and dynamic experiments. *Journal of Analytical and Applied pyrolysis. Vol. 62.* p. 93 – 110.

Channiwala, S. A., Parikh, P. P., (2002). A unified correlation for estimating HHV of solid, liquid and gaseous fuels. *Fuel Vol. 81.* p. 1051 – 1063

Chang, C., Wu, C., Hwang, J., Lin, J., Yang, W., Shih, S., Chen, L., Chang, F. (1996). Pyrolysis kinetics of uncoated writing paper of MSW. *Journal of Environmental Engineering. Vol. 122 (4).* p 298.

Chen, T. H.; Chynoweth, P.; Biljetina, R. (1990) Anaerobic digestion of municipal solid waste in a nonmixed solids concentrating digestor. *Applied Biochemistry and Biotechnology, volume 24-25, number 1,* p. 533-544.

Cho, Y., Shim, M., Kim, S. (1998). Thermal degradation kinetics of PE by the Kissinger equation. *Materials Chemistry and Physics. Vol. 52.* p.94-97.

Cit, I., Smag, A., Yumak, T., Ucar, S., Misirhoglu, Z., Canel, M. (2010). Comparative pyrolysis of polyolefins (PP and LDPE) and PET. *Polymer Bulletin Vol. 64.* p. 817 – 834.

Cozzani, V., Petarca, L., Tognotti, L. (1995). Devolitization and pyrolysis of refuse derived fuels: characterization and kinetic modelling by a thermogravimetric and calorimetric approach. *Fuel, Vol 76 Issue 6,* p. 903-912.

Cozzani, V., Nicolella, C., Petarca, L., Rovatti, M., Tognotti, L. (1995, I). A fundamental study on conventional pyrolysis of a refuse derived fuel. *Industrial Chemical Research. Vol 34.* p 2006 – 2020.

Cozzani, V., Petarca, L., Tognotti, L. (1995, II). Devolatilisation and pyrolysis of refuse derived fues: Characterisation and kinetic modelling by thermogravimetric and calorimetric approach. *Fuel 74 – 6.* p 903 – 912.

Czernik, S., Johnson, D., Black, S. (1994). Stability of wood fast pyrolysis oil. *Biomass and Bioenergy. Vol. 7.* p. 187-192.

Dalai, A. K., Batta, N., Eswaramoorthi, I., Schoenau, G. J. (2009). Gasification of refuse derived fuel in a fixed bed reactor for syngas production. *Waste Management. Vol. 29.* p. 252 – 258.

DEA (2012). National Waste Information Baseline Report. Department of Environmental Affairs, Pretoria, South Africa.

Demirbas, A. (2009). Biorefineries: Current activities and future developments. *Energy Conversion and Management Vol. 50.* p. 2782 – 2801.

Demirbas, A. (2004). Pyrolysis of municipal plastic wastes for recovery of gasoline-range hydrocarbons. *Journal of Analytical and Applied Pyrolysis Vol. 72.* p. 97 – 102.

Diaz, L.F.; Savage, G.M.; Eggereth, L.L. (2005) Production of Refuse Derived Fuels (*Solid Waste Management Volume* 1 UNEP p. 295 - 392)

EPA (2011). Overview of Greenhouse Gases – Methane. United States Environmental Protection Agency. Accessed online [November 2013]: http://epa.gov/climatechange/ghgemissions /gases/ch4.html.

EPA (2011, I). Global Greenhouse Gas Emissions Data. United States Environmental Protection Agency. Accessed online [November 2013]: http://www.epa.gov/climatechange/ghgemissions /global.html

Fiehn, H and Ball, J. (2005). Background research paper: Waste. South Africa Environment Outlook. National State of the Environment Project. Department of Environmental Affairs and Tourism: Pretoria

Gao, Z., Amansaki, I., Nakada, M. (2003) A thermogravimetric study on thermal degradation of polyethylene. *Journal of Analytical an Applied Pyrolysis. Vol. 67.* p. 1 – 9.

Gao, F. (2010). Pyrolysis of Waste Plastics into Fuels. Doctor of Philosophy in Chemical Engineering. University of Canterbury, UK.

Garcia, A. N., Font, R., Marcilla, A. (1992). Kinetic studies of the primary pyrolysis of municipal solid waste in a Pyroprobe 1000. *Journal of Analytical and Applied Pyrolysis. Vol. 23,* p. 99-119.

Garcia, A., N., Marcilla, A., Font, R. (1995). Thermogravimetric kinetic study of the pyrolysis of municipal solid waste. *Thermochemica Acta Vol. 254,* p. 277-304.

Garg, A.; Smith, R.; Hill, D.; Simms, N.; Pollard, S. (2007). Wastes as Co-Fuels: The Policy Framework for Solid Recovered Fuel (SRF) in Europe, with UK Implications. *Environmental Science & Technology. Vol 41,* p. 4868-4874.

GDACE (2008) Gauteng Waste Minimisation Plan: Status Quo Report V3. Gauteng Department of Agriculture, Conservation and Environment, 2008

Gendebien, A.; Leavens, A.; Blackmore, K.; Godley, A.; Lewin, K.; Whiting, K.J.; Davi, R.; Giegrich, J.; Fehrenbach, H.; Gromke, U.; del Bufalo, N.; Hogg, D. (2003) *Refuse Derived Fuel, Current Practise and Perspectives: Final Report* European Commission – Directorate General Environment.

Georgieva, V., Vlaev, L., Gyurova, K. (2013). Non-isothermal degradation kinetics of $CaCo_3$ from different sources. *Journal of Chemistry. Vol. 2013.*

Gibb (2008). A study on waste categorisation for solid waste services in the City of Cape Town.

Grammelis, P., Basinas, P., Malliopoulou, A., Sakellaropoulos, G. (2009). Pyrolysis kinetics and combustion characteristics of waste recovered fuels. *Fuel Vol. 88,* p. 195-205.

Green, D., Perry, D. (2008). Perry's Chemical Engineering Handbook, 8th Edition. Mc Graw Hill, New York, USA.

Gronli, M. G., Varhegyi, G., Di Blasi, C. (2002). Thermogravimetric analysis and devolatilisation kinetics of wood. *Industrial and Engineering Chemistry Research Vol. 41*. p.4201-4208.

Helt, E. J., Agrawal, R. K. (1988). Liquids from Municipal Solid Waste. In Soltes, J., Milne, T. A. ed. 1988: Pyrolysis oils from Biomass. American Chemical Society.

Hernandez-Atonal, F.D.; Ryu, C.; Sharifi, V.N.; Swithenbank, J. (2007). Combustion of refuse-derived fuel in a fluidised bed. *Chemical Engineering Science Vol 62* p. 627 – 635.

Hopewell, J., Dvorak, R., Kosior, E. (2009). Plastics recycling: challenges and opportunities. *Philosophical Transactiomsof the Royal Society, B. Vol. 364.* p. 2115 – 2126.

Ibrahim, M., Hopkins, E., Seehra, M. (1996). Thermal and catalytic degradation of commingled plastics. *Fuel Processing Technology. Vol. 49.* p 65 – 73.

IFA (2013). Polyethylene terephthalate. *Institut für Arbeitsschutz der Deutschen Gesetzlichen Unfallversicherung* (Institute for Occupational Safety and Health of the German Social Accident Insurance). Available Online: http://gestis-en.itrust.de/nxt/gateway. dll/gestis_en/530566.xml?f=templates$fn=default.htm$3.0

Islam, M. N., Islam, M. N., Beg, M. R. A. (2004). The fuel properties of pyrolysis liquid derived from urban solid wastes in Bangladesh. *Bioresource Technology Vol. 92.* p 181 – 186.

Islam, M. N., Islam, M. N., Beg, M. R. A., Islam, M. R. (2005). Pyrolytic oil from fixed bed pyrolysis of municipal solid waste and its characterisation. *Renewable Energy Vol. 30.* p 413 – 420.

Jenekhe, S. A., Lin, J. W. (1983). Kinetics of thermal degradation of polyethylene terephthalate. *Thermochemica Acta. Vol. 61*. p. 287 – 299.

Kawaguchi, K., Miyakoshi, K., Momonoi, K. (2002). Studies on the pyrolysis behaviour of gasification and melting systems for municipal solid waste. *Journal of Material Cycles and Waste Management Vol. 4* p. 102-110

Knox, A. (2005). An overview of incineration and EFW technology as applied to the management of municipal solid waste (MSW).University of Ontario. Prepared for: ONEIA Energy Subcommittee.

Kumar, S., Gaikwad, S., Shekdar, A., Kshirsagar, P., Singh, R. Estimation method for national emission from solid waste landfills. *Atmospheric Environment. Vol. 38.* p. 3481-3487.

Lah, B., Klinar, D., Likozar, B. (2013). Pyrolysis of natural, butadiene, styrene–butadiene rubber and tyre components: Modelling kinetics and transport phenomena at different heating rates and formulations. *Chemical Engineering Science. Vol. 87.* p. 1 – 13.

Lappas, A., Samolada, M., Iatridis, D., Voutetakis, S., Vasalos, I. (2002). Biomass pyrolysis in a circulating fluid bed reactor for the production of fuels and chemicals. *Fuel. Vol.81.* p. 2087 – 2095.

Lee, V. K. C., Kwok, K. C. M., Cheung, W. H., McKay, G. (2007) Operation of a municipal solid waste co-combustion pilot plant. *Asia-Pacific Journal of Chemical Engineering Vol. 2.* p. 631 – 639.

Li, L., Zhang, H., Zhuang, X. (2005). Pyrolysis of Waste Paper: Characterisation and composition of pyrolysis oil. *Energy Sources. Vol. 27.* p. 867-873.

Li, A., Li, X., Li, S., Ren, Y., Chi, Y., Yan, J. (1999). Pyrolysis of solid waste in a rotary kiln – Influence of final pyrolysis temperature on the pyrolysis products. *Journal of Analytical and Applied Pyrolysis 50*. p 149 – 162.

Lin, K., Wang, H., Liu, S., Chang, N., Huang, Y., Wang, H. (1999) Pyrolysis kinetics of Refuse Derived Fuel. *Fuel Processing Technology Vol. 60*, p. 103-110.

Lin, Y., Cho, J., Tompsett, G., Wesrmoreland, P., Huber, G. (2009) Kinetics and mechanism of cellulose pyrolysis. *Journal of Physical Chemistry C. Vol. 113*. p. 20097 – 20107.

Lopez, A., de Marco, I., Caballero, B. M., Laresgoiti, Adrados, A. (2011). Influence of time and temperature on pyrolysis of plastic wastes in a semi-batch reactor. *Chemical Engineering Journal 173.* p 62 – 71.

Lua, A.C., Yang, T. (2004). Effects of vacuum pyrolysis conditions on the characteristics of activated carbons derived from pistachio-nut shells. *Journal of Colloid and Interface Science*. *Vol.* 276. p.364-372

Luo, S., Xiao, B., Zhiquan, H., Liu, S. (2010). Effect of particle size on pyrolysis of single component municipal solid waste in fixed bed reactor. *International Journal of Hydrogen Energy. Vol. 35.* p. 93 – 97.

Madina, M (1997). The effect of income on municipal solid waste generation rates for countries of varying levels of economic development: a model. *Journal of Solid Waste Technology and Management Vol. 24.* 149–155.

Madina, M (2004). Medina, M., 2004. Scavenger cooperatives in Asia and Latin America. Global Development Network. <http://www.gdnet.org/pdf/medina.pdf> .

Malkow, T. (2003). Novel and innovative pyrolysis and gasification technologies for energy efficient and environmentally sound MSW disposal. *Waste Management. Vol. 24.* p. 53 – 79.

Martin-Gullon, I., Esperanza, M., Font, R. (2001). Kinetic model for the pyrolysis and combustion of poly (ethylene terephthalate) (PET). *Journal of analytical and applied pyrolysis. Vol. 58 – 59.* p 635 – 650.

Marsman, J. H., Wildschut, J., Evers, P., de Koning, H. J. (2008). Identification and classification of components in flash pyrolysis oil hydrodeoxygenated oils by two-dimensional gas chromatography and time-of-flight mass spectrometry. *Journal of Chromatography A, 1188.* p. 17-25.

Mastral, F. J., Esperanza, E., Berrueco, C., Juste, M., Ceamanos, J. (2003). Fluidized bed thermal degradation products of HDPE in an inert atmosophere and in air-nitrogen mixtures. *Journal of Analytical and Applied Pyrolysis. Vol. 70.* p. 1 – 17.

Miskolczi, N., Buyong, F., Angyal, A., Bartha, L. (2010). Two stage catalytic pyrolysis of refuse derived fuel: Production of biofuel via syncrude. *Bioresource Technology Vol. 101.* p. 8881 – 8890.

Modh, J., Namjoshi, S., Channiwala, S. (2012). Kinetics and pyrolysis of glossy waste paper. *International Journal of Engineering Research and Applications. Vol. 2, Issue 2.* p 1067 – 1074.

Mohan, D., Pittman, C.U., Steele, P. H. (2006). Pyrolysis of Wood/Biomass for Bio-oil: A Critical review. *Energy & Fuels. Vol.* 20 p.848-889

Namdeo, S., Pondhe, G. M. (2010). Characterisation and composition of Municipal Solid Waste (MSW) generated in Sangamner City,District Ahmednagar, Maharashtra, India. *Environmental Monitoring and Assessment. Vol 170.* p:1–5

Nicoletti, R.; Ham, L.; Knight, N.; Naylor, L. (2010) Biodrying biosolids using an agitated bin composting system. In: *Proceedings of 15th European Biosolids and Organic Resources Conference*. Leeds, UK: Aqua Enviro Technology Transfer.

NIST (2011). Water. *National Institute for Science and Technology*. Accessed Online: http://webbook.nist.gov/cgi/cbook.cgi?Name=water&Units=SI.

Parikh, J., Channiwala, S. A., Ghosal, G. K. (2005). A correlation for calculating HHV from proximate analysis of solid fuels. *Fuel Vol. 84.* p. 487 – 494

Peterson, J., Vyazovkin, S., Wight, C. (2001). Kinetics of the thermal degradation of polystyrene, polyethylene and poly(propylene). *Macromolecular Chemistry and Physics. Vol. 202.* p. 775 – 784.

Petts, J. (1994) Incineration as a Waste Management Option. In: R. E. Hester and R. M. Harrison eds. (1994). Waste Incineration and the Environment. Royal Society of Chemistry. P. 1 – 25

Phan, A. N., Ryu, C., Sharifi, V. N., Swithenbank, J. (2008). Characterisation of slow pyrolysis products from segregated wastes for energy production. *Journal of Analytical and Applied Pyrolysis. Vol 81.* p. 65 – 71.

Pielichowski, K., Njuguna, J. (2005). Thermal Degradation of Polymeric Materials. Rapra Technology Limited, Shawbury, Shrewsbury, Shropshire, UK.

Pinto, F., Costa, P., Gulyurtlu, I., Cabrita, I. (1999). Pyrolysis of plastic wastes 1: effect of plastic waste composition on product yield. *Journal of Analytical and Applied Pyrolysis Vol. 51*. p. 39 – 55.

Pohorely, M., Vosecky, M., Hejdova, P., Puncochar, M., Skoblja, S., Staf, M., Vosta, J., Koitsky, B., Svoboda, K. (2006) *Fuel 85*, p. 2458 – 2468

Rha, C., Timonen, M. (1994). Paper Composition and Methods Therefor. US Patent: 5,354,424. 11th October 1994.

RSC (2014). Mass Spectrometry. *Modern Chemical Techniques – Royal Society of Chemistry.* [Available online]: http://www.rsc.org/learn-chemistry/resource/res00001304/mass-spectrometry.

Sasha, B., Ghoshal, A. (2005). Thermal degradation of poly(ethylene terephthalate) from waste soft drinks bottles. *Chemical Engineering Journal. Vol. 111*. p. 39 – 43.

Sasha, B., Maiti, A., Ghoshal, A. (2006). Model free method for isothermal and non-isothermal decomposition kinetics analysis of PET sample. *Thermochemica Acta. Vol. 444.* p. 46 – 52.

Scott, D. S., Majerski, P., Piskorz, J., Radlein, D. (1999). A second look at fast pyrolysis of biomass – the RTI process. *Journal of analytical and Applied Pyrolysis. Vol. 51.* p. 23 37.

Sinfronio, F., Santos, J., Pereira, L., Souza, A., Conceicao, M., Fernandes, V., Fonseca, V. (2005). Kinetic of thermal degradation of low-density and high-density polyethylene by non-isothermal thermogravimetry. *Journal of Thermal Analysis and Calorimetry. Vol. 79.* p. 393 – 399.

Singh, R. P., Tyagi, V. V., Allen, T., Hakimi Ibrahim, M., Kothari R. (2011) An overview for exploring the possibilities of energy generation from municipal solid waste (MSW) in Indian Scenario. *Renewable and Sustainable Energy Reviews Vol. 15*. 4797 – 4808

Shafizadeh, F. (1982) Introduction to pyrolysis of biomass. *Journal of Analytical and Applied Biomass. Vol. 3.* p. 285 – 305.

Sivaknmar, K., Sugirtharan, M. (2010). Impact of family income and size on per capita solid waste generation: a case study in Manmunai North Divisional Secretariat Division of Batticaloa. *Journal of Science of the University of Kelaniya Sri Lanka. Vol 5.* p. 13 – 23.

Sørum, L. (2001). *Technical report: Characterisation of MSW for Combustion Systems*. SINTEF Energy Research 2001. Accessed online 4th May 2012. [Avalible] http://www.energy.sintef.no

Sørum, L., Grønli, M., G. Hustad, J., E. (2001, I). Pyrolysis characteristics and kinetics of municipal solid wastes. *Fuel Vol. 80*, p. 1217-1227.

Sørum, L., Oyvind, S., Glarborg, P., Jensen, A., Dam-Johansen, K. (2001, II). Formation of NO from combustion of volatiles from municipal solid wastes. *Combustion and Flame 124/1-2.*

Soyez, K.; Plickert,S. (2002) Mechanical-Biological Pre-Treatment of Waste: State of the Art and Potentials of Biotechnology *Acta Biotechnologica Vol 22, Issue 3-4*, p 271–284.

Speight, J. (2011). The Biofuels Handbook. Royal Society of Chemistry, 2011.

SPLM. (2010). Sol Plaatjie Local Municipality Integrated Waste Management Plan. Sol Plaatjie Local Municipality, 2010.

Stegmann, R. (2005). Mechanical and biological pre-treatment of municipal solid waste. In: *Proceedings of the Tenth International Waste Management and Landfill Symposium.* Italy, St. Margherita di Pula, Cagliari: CISA, Environmental Sanitary Engineering Centre.

Strezov, V., Evans, T. (2009). Thermal processing of paper sludge and characterisation of its pyrolysis products. *Waste Management Vol. 29.* p 1644 – 1648.

SWMSP (2011/2012). The solid waste management sector plan for the city of Cape Town (incorporating integrated waste management plan). Department of Solid Waste Management Western Cape. Available Online: http://www.capetown.gov.za/en/IDP/Statutory%20plans%202011%20%202012/AnnexureJ_Draft_Solid_Waste_Sector_Plan_2_2011_2012.pdf

Tammemagi, H. (1999). The Waste Crisis: Landfills, Incinerators, and the Search for a Sustainable Future: Landfills, Incinerators, and the Search for a Sustainable Future. Oxford University Press, 22 Nov 1999.

Themelis, N., Castaldi, M., Bhatti, J., Arsova, L. (2011). Energy and economic value of non-recycled plastics (NRP) and municipal solid wastes (MSW) that are currently landfilled in the fifty states. *EEC Study of non-recycled plastics-August 2011.*

Thitame, S., Pondhe, G, Meshram, D. (2010). Characterisation and composition of municipal solid waste (MSW) generated in Sangamner City District Ahmednagar, Maharashtra, India. *Environmental Monitoring and Assessment. Vol. 170.* p. 1 – 5.

Troschinetz, A. M., Mihelcic, J. R. (2008). Sustainable recycling of municipal solid waste in developing countries. *Journal of Waste Management Vol. 29*, p. 915-923.

Trois, C. (2013). Status and future of waste to energy in South Africa. In: Waste to Energy in South Africa Workshop. Cape Town 2013.

Ucuncu, A. (Unknown). Energy recovery from waste mixed paper. Final report to Sunshares. Department of Civil and Environmental Engineering, Duke University, Durham, North Carolina.\

UNEP (2005). *Solid Waste Management Volume 1, Part II: Processing and Treatment.* . United Nations Environmental Programme, 2005. Available online: http://www.unep.org/ietc/InformationResources/Publications/SolidWasteManagementPublication/tabid/79356/Default.aspx

UNEP (2009). *Converting Waste Plastics into a Resource: Compendium of Technologies.* United Nations Environmental Programme, Division of Technology, Industry and Economics, International Environmental Technology Centre. Osaka/Shiga, Japan

Van Bramer, S. E., Johnston, M., V. (1990). 10.5eV Photoionization mass spectrometry of aliphatic compounds. *Journal of the American Society for Mass Spectrometry. Vol 1.* p.419-426.

Visvanathan, C., Trankler, J., Chiemchaisri, C. (2005). Mechanical-biological pretreatment of municipal solid waste in Asia. *From the Proceedings of the International Symposium on MBT, 23-25 November 2005, Hanover, Germany.*

Vyazovki, S., Burnham, A., Criado, J., Perez-Maqueda, L., Popescu, C., Sbirrazzuoli, N. (2011). ICTAC Kinetics Committee recommendations for performing kinetic computations on thermal analysis data. *Thermochimica Acta. Vol 520.* p. 1-19.

Vyazovkin, S. (2006). Model Free Kinetics. *Journal of Thermal Analysis and Calorimetry, Vol. 83.* p. 45–51.

Wang, Z., Huang, H., Li, H., Wu, C., Chen, Y. (2002). Pyrolysis and combustion of refuse derived fuels in a spouting-moving bed reactor. *Energy and Fuels. Vol. 16.* p. 136 – 142.

Wevers, M., De Fré, Rymen, T., Geuzens, P. (1992). Reduction of dioxin formation from municipal solid waste incinerator by wet gas scrubbing. *Chemosphere. Vol. 25, 7-10*. p. 1435 – 1439.

Williams, P. T., Besler, S. (1992). The pyrolysis of rice husks in a thermogravimetric analyser and static batch reactor. *Fuel 72.* p 151-159.

Williams, E. A., Williams, P. T. (1997). Analysis products derived from the fast pyrolysis of plastic waste. *Journal of Analytical and Applied Pyrolysis. Vols. 40 – 41*. p. 347 – 363.

Wise, CC., Emery, RC, Coetzee, JA. (2011). Composition of waste landfilled at metropolitan landfills and the impact of the new draft waste regulations. In: Proceedings of the Landfill 2011 Seminar, "Waste Management Facilities – The New Order". Durban, South Africa. (2011).

Wu, C., Hor, J., Shih, S., Chen, L., Chang, F. (1993). On the thermal treatment of plastic mixtures of MSW: Pyrolysis kinetics. *Waste Management. Vol. 13.* p. 221 – 235.

Wu, C., Chang, C., Lin, J., Hwang, J. (1997, I). Thermal treatment of coated printing and writing paper in MSW: Pyrolysis kinetics. *Fuel 76/12.* p. 1151 - 1157

Wu, C., Chang, C., Lin, J. (1997, II). Pyrolysis kinetics of paper mixtures in municipal solid waste. *Journal of Chemical Technology and Bioechnology 68.* p 65 – 74.

Wu, C., Chang, C., Tseng, C., Lin, J. (2003). Pyrolysis product distribution of waste newspaper in MSW. *Journal of Analytical and Applied Pyrolysis 67,* p. 41 – 53.

Yang, Y., Phan, A., Ryu, C., Sharif, V., Swithenbank, J. (2007). Mathematical modelling of slow pyrolysis of segregated solid wastes in a packed bed pyrolyser. *Fuel Vol. 86.* p 169 – 180.

Yu, Y., Kim, S., Lee, J., Lee, K. (2002). Kinetic studies of dehydration, pyrolysis and combustion f paper sludge. *Energy. Vol 27.* p. 457 – 469.

Zevenhoven, R., Karlsson, M., Hupa, M., Frankenhaeuser, M. (1997). Combustion and gasification properties of plastic particles. *Journal of the Air and Waste Management Association 47:8,* p. 861 – 870.

Zhang, X., Wang, T., Ma, L., Chang, J. (2007). Vacuum pyrolysis of waste tires with basic additives. *Waste Management. Vol. 28.* p. 2301 – 2310.

Zhou, L., Wang, Y., Huang, Q., Cai, J. (2006). Thermogravimetric characteristics and kinetics of plastic and biomass blends co-pyrolysis. *Fuel Processing Technology 87,* p. 963 – 969.

Appendices

Table A1: Raw Characterisation data of recycling

Appendix A: Characterisation of MSW in Stellenbosch Municipality

Clear Bag	Unopened mass (kg)	Plastic film		Dense Plastics		Paper		Glass		Metal		Organics		Other		
		Mass	vol%	Mass	vol%	Mass	vol%	Mass	vol%	Mass	vol%	Mass	vol%	Mass	vol%	
1	4.46	0.16	10	0	0	3.86	100	0.46	10	0	0	0	0	0	0	Rozendal
2	7.56	0	0	0.72	100	4.03	100	2.1	10	0.1	5	0	0	0.02	5	
3	5.92	0.74	20	0.14	10	2.62	100	3.06	50	0	0	0	0	0	0	
4	1.16	0.24	50	0.38	50	0	0	0	0	0.06	5	0	0	0.02	5	
5	0.9	0.48	80	0.2	50	0.1	20	0	0	0.12	5	0	0	0	0	
6	2.72	0.46	50	0.22	100	0.88	50	0.38	5	0.12	5	0	0	0.04	5	
7	0.52	0.24	20	0.08	50	0.12	20	0	0	0.12	5	0	0	0	0	
8	4.62	0.16	90	0.34	40	0.98	100	1.98	50	0	0	0	0	0	0	
9	3.38	0.58	100	0.14	60	3.04	60	0.5	5	0.16	5	0	0	0	0	
10	4.8	0.18	80	0.1	20	4.34	100	0	0	0.02	5	0	0	0.02	0	
11	2.96	0.7	100	0.58	100	0.44	90	0.76	10	0.4	0	0	0	0	0	
12	2.2	0.46	100	0.46	40	0.34	80	0.42	10	0.22	20	0	0	0.1	10	
13	1.02	0.06	50	0.12	10	0.22	40	0.5	10	0	0	0	0	0	0	
14	2.05	0.28	100	0.2	20	0.72	100	0	0	0	0	0	0	0	0	
15	1.14	0.2	100	0.24	30	0.24	70	0	0	0	0	0	0	0.32	30	
16	2.9	0.34	100	0.02	70	1.76	100	0	0	0	0	0	0	0.08	10	
17	4.6	0.04	80	0.14	30	3.66	100	0.48	10	0.12	10	0	0	0	0	
18	3.52	0.04	70	0.2	50	0.62	100	2.5	40	0	0	0	0	0	0	
19	2.78	0.1	80	0.5	80	1.62	90	0.46	10	0	0	0	0	0	0	
20	0.92	0.08	80	0.32	60	0.16	20	0	0	0.3	10	0	0	0.16	40	
21	10.12	0	0	0.14	40	5.4	100	4.1	80	0	0	0.22	5	0.16	15	
22	8.02	0.26	50	0	0	5.2	100	2.42	20	0	0	0.1	5	0	0	
23	7.24	0.24	50	0.2	5	0.84	100	0	0	0.14	1	5.4	80	0	0	
24	2.9	0.32	100	0.24	10	0.24	30	1.5	20	0.1	5	0.5	5	0	0	
25	4.16	0.32	12	0.2	10	0.4	50	3	50	0	0	0	0	0	0	
26	1.36	0	0	0	0	0	0	0	0		0	1.36	100	0	0	
27	1.90	0.20	95	0.42	100	0.42	50	0.52	10	0.22	15	0.00	0	0.00	0	Universiteits Oord
28	1.62	0.30	40	0.06	20	0.66	100	0.38	5	0.06	5	0.00	0	0.00	0	
29	1.20	0.10	30	0.00	0	1.08	100	0.00	0	0.00	0	0.00	0	0.00	0	
30	1.66	0.00	0	0.00	0	0.00	0	0.00	0	0.00	0	1.66	100	0.00	0	
31	0.86	0.06	5	0.08	10	0.22	40	0.00	0	0.10	10	0.40	50	0.00	0	
32	5.72	0.34	100	0.9	100	2.72	90	1.14	20	0.28	10	0	0	0.16	10	Dalsig
33	6.06	0.06	20	0.22	20	1.14	60	4.54	90	0.06	10	0	0	0.02	10	
34	3.5	0.06	10	0.52	100	0.92	60	1.98	30	0	0	0	0	0	0	
35	2.72	0.14	60	0.14	30	1.46	100	0.96	20	0.02	10	0.04	10	0.02	10	

Table A1: Raw Characterisation data of recycling

36	1.84	0.1	80	0.2		1.34	100	0	0	0.14	10	0	0	0.04	10	
37	2.16	0.08	50	0.3	50	0.54	60	0.86	20	0.24	10	0	0	0	0	
38	3.08	0.08	50	0.36	60	0.6	80	1.7	30	0	0	0	0	0.36	20	
39	4.18	0.08	20	0.58	100	0.14	30	3.2	60	0.02	10	0	0	0	0	
40	5.56	0.18	30	0.24	20	1.26	100	3.9	80	0	0	0	0	0	0	
41	7.3	0.24	80	2.74	55	1.08	140	2.94	50	0.1	10	0.08	10	0	0	
42	3.56	0.46	60	0.66	100	1.58	100	0.56	5	0.12	5	0	0	0.04	10	
43	3.64	0.36	100	0.36	30	0.92	100	1.66	30	0.08	10	0	0	0.3	40	
44	6.26	0.26	100	0.36	100	2.64	100	2.34	50	0.48	50	0	0	0	0	
45	5.7	0.14	80	0.66	100	1.28	100	3.08	70	0.52	30	0	0	0	0	
46	2.9	0.14	60	0.6	100	1.3	100	0.9	20	0.48	50	0	0	0.2	50	
47	3.16	0	0	0.2	30	1	60	1.94	30	0.04	10	0	0	0	0	
48	8.06	0.3	80	0.2	20	6.18	150	0	0	0.04	1	0	0	1.3	15	
49	4.6	0.1	80	0.98	100	0.76	50	2.76	50	0	0	0	0	0.2	10	
50	3	0.08	20	0.12	10	0	0	0	0	0	0	0	0	2.86	100	
51	2.86	0.1	80	0	0	2.76	50	0	0	0	0	0	0	0	0	
52	3.86	0.04	10	0	0	0	0	0	0	0	0	3.78	100	0	0	
53	1.16	0.04	10	0.01	10	0.96	100	0	0	0	0	0	0	0.16	20	
54	13.64	0	0	0	0	0	0	0	0	0	0	13.64	100	0	0	
55	0.88	0.18	40	0.18	20	0.36	30	0.18	0	0	0	0	0	0	0	
56	1.8	0.08	10	0.2	40	1.42	10	0	0	0	0	0.12	5	0	0	
57	2.38	0.18	80	0.36	90	1.9	100	0	0	0	0	0	0	0	0	
58	6.62	0.08	70	0.46	60	3.88	100	1.82	30	0.2	5	0	0	0.14	5	Brandwacht
59	1.88	0.24	100	0.1	20	1.38	100	0.16	5	0	0	0	0	0	0	
60	5.72	0.06	100	0.4	80	2.62	100	2.42	50	0.18	5	0	0	0	0	
61	1.02	0.36	100	0.34	70	0.26	60	0	0	0.06	5	0	0	0	0	
62	2.48	0.34	100	0.93	100	1.06	100	0.06	5	0	0	0	0	0	0	
63	6.86	0.18	100	0.5	100	1.44	100	4.62	100	0	0	0	0	0	0	
64	0.38	0.04	10	0.28	40	0.04	5	0	0	0	0	0	0	0	0	
65	0.9	0.1	70	0.46	70	0.24	30	0	0	0	0	0.08	5	0	0	Paradyskloof
66	0.36	0.06	20	0.12	50	0.16	50	0	0	0	0	0	0	0	0	
67	0.82	0.04	10	0.46	50	0.12	20	0	0	0	0	0	0	0.16	50	
68	1.14	0.14	80	0.26	50	0.08	10	0	0	0.14	10	0	0	0.56	30	
69	2.58	0.46	100	0.66	100	1.38	100	0	0	0.1	5	0	0	0.02	5	
70	5.6	0.56	100	0.22	20	3.3	100	1.1	20	0.08	5	0	0	0.3	10	
71	3.94	0.16	70	0.6	70	0.38	100	1.38	40	0.08	5	0	0	1.4	50	
72	4.5	0.04	20	0.14	10	0.64	100	3.52	80	0.08	5	0	0	0.08	5	
73	5.6	0.24	5	0.76	100	0.22	50	4.13	80	0.16	10	0	0	0	0	
74	5.48	0.04	5	0.36	50	4.58	100	0.52	10	0	0	0	0	0	0	
75	8.46	0.14	50	0.46	90	0.94	90	6.86	100	0.04	5	0	0	0.06	5	

Table A1: Raw Characterisation data of recycling

76	3.64	0	0	0	0	0	0	3.64	80	0	0	0	0	0	0
77	5.24	0.2	100	0.2	10	4.22	100	0	0	0.6	20	0	0	0.04	5
78	0.88	0.12	60	0.24	60	0.5	100	0	0	0	0	0	0	0	0
79	4.04	0.14	100	0	0	1.3	100	2.6	50	0	0	0	0	0	0
80	3.08	0.2	80	0.16	30	1.14	100	1.3	20	0.2	10	0	0	0.1	5
81	1.62	0.1	70	0.14	10	1.16	100	0	0	0	0	0	0	0.2	20
82	4.64	0.32	100	0.56	80	2.52	100	1.18	20	0.1	10	0	0	0	0
83	2.36	0.24	80	0.54	80	0.8	100	0.46	10	0.1	5	0	0	0.2	5
84	2.34	0.1	60	0	0	0.96	80	0	0	0.1	5	0	0	1.18	100
85	1.42	0.1	60	0.36	80	0.08	10	0.74	10	0.06	5	0	0	0.1	10
86	1.82	0.96	50	0	0	0.04	5	0	0	0	0	0.86	100	0	0
87	1.52	0	0	0	0	0	0	1.52	50	0	0	0	0	0	0
88	3.36	0.1	50	0	0	2.06	100	1.08	20	0.04	5	0	0	0	0
89	6.92	0	0	0.12	20	6.86	100	0	0	0	0	0	0	0.06	5
90	3.7	0.02	5	0.32	70	0.46	100	2.94	60	0	0	0	0	0	0
91	5.62	0.22	70	0.56	100	0.8	60	2.28	30	0.1	5	0	0	1.7	20
92	6.74	0.24	100	0.44	50	4.48	100	1.52	20	0	0	0	0	0.18	5
93	7.22	0.12	80	0.86	30	1.18	100	3.28	80	0.06	10	1.7	30	0	0
94	3.16	0.14	80	0.52	40	1.46	80	0.6	10	0.46	40	0	0	0	0
95	1.64	0	0	0	0	1.64	100	0	0	0	0	0	0	0	0
96	1.84	0.08	40	0.14	20	0.66	100	0.6	15	0.32	15	0	0	0.06	5
97	3.78	0.14	80	0.68	100	1	100	1.2	10	0.12	5	0	0	1.36	10
98	9.98	0.2	90	0.94	100	2.88	70	5.86	100	0.06	5	0	0	0	0
99	4	0.36	100	0.44	80	0.98	100	2.2	30	0	0	0	0	0	0
100	4.64	0	0	0.1	10	1.86	100	2.62	60	0	0	0	0	0	0
101	2.08	0.28	100	0.34	40	0.52	100	0.48	5	0.04	5	0	0	0.4	5
102	0.92	0	0	0.4	40	0.52	100	0	0	0	0	0	0	0	0
103	5.56	0.32	100	0.1	20	1	90	0.72	10	0.06	5	0	0	3.24	100
104	2.72	0.3	100	0.68	100	0.78	100	0.68	10	0.28	20	0	0	0.04	5
105	1.64	0.08	20	0.3	40	1.28	90	0	0	0	0	0	0	0	0
106	1.52	0.22	100	0.36	40	0.74	100	0	0	0.24	20	0	0	0	0
107	1.58	0.34	100	0.52	70	0.76	100	0	0	0.06	5	0	0	0.04	5
108	3.34	0.1	60	0.22	40	0.34	90	2.52	50	0.14	10	0	0	0	0
109	2.06	0.16	50	0.54	100	0.54	100	0.42	10	0.1	10	0	0	0.26	20
110	1.9	0.24	80	0.72	100	0.3	30	0.44	10	0.02	10	0	0	0.14	10
111	2.5	0.14	80	0.54	80	1.08	100	0.5	10	0.18	10	0	0	0	0
112	1.62	0.36	100	0.24	20	0.64	100	0	0	0.02	10	0	0	0.26	30
113	5.92	0.06	50	0	0	1.04	100	4.62	90	0	0	0	0	0.02	10
114	1.82	0.2	100	0.22	40	0.96	90	0.22	5	0.22	10	0	0	0	0
115	1.14	0.02	10	0	0	1.12	100	0	0	0	0	0	0	0	0
116	1.02	0.42	100	0.1	5	0.04	5	0	0	0	0	0.42	10	0	0

Table A1: Raw Characterisation data of recycling

117	0.92	0.2	100	0.24	100	0.2	30	0	0	0	0	0	0	0.26	50	
118	1.1	0.12	60	0.62	100	0.06	10	0.12	5	0	0	0	0	0.14	10	
119	7.38	0.42	80	0.92	100	1.08	90	4.84	90	0.06	5	0	0	0.05	5	
120	1.1	0.32	100	0.38	80	0.32	80	0	0	0.1	5	0	0	0	0	
121	1.92	0.14	70	0.18	40	1.08	90	0.38	5	0	0	0	0	0.08	5	
122	2.52	0.18	50	0.16	20	0.66	60	0	0	0.16	10	1.1	10	0.12	5	
123	4.58	0.12	35	0.04	10	0.8	100	3.12	70	0.22	25	0	0	0	0	
124	2.18	1.1	100	0.16	50	0.46	100	0.38	50	0	10	0	0	0	0	
125	3	0.18	100	0.36	100	1.98	100	0.52	30	0.04	10	0	0	0	0	
126	3.04	0.36	100	0.24	70	0.6	100	1.54	100	0.18	15	0	0	0.16	10	
127	2.32	0.18	80	0.36	80	0.32	100	1.06	90	0.3	20	0	0	0.2	15	
128	4.78	0.34	100	0.46	80	3.22	100	0.2	10	0.02	10	0	0	0.44	30	
129	2.76	0.24	50	0.6	80	1.22	100	0.08	10	0.34	40	0	0	0.16	40	
130	3.54	0.02	10	0.78	100	2.02	100	0.24	10	0.24	30	0	0	0.06	10	
131	4	0.28	100	1	100	2.66	100	0	0	0.06	10	0	0	0	0	
132	3.12	0.08	100	0.66	100	1.46	100	0.46	40	0.22	10	0.14	10	0.02	10	
133	1.68	0.08	100	0.54	100	0.98	100	0	0	0.02	10	0	0	0	0	
134	1.88	0.08	100	0.3	100	0.48	100	0.9	20	0	0	0	0	0.04	10	
135	3.2	0.06	50	1.36	100	1.22	100	0.32	10	0.1	10	0	0	0.04	30	
136	1.82	0	0	1.16	100	0.28	80	0	0	0.28	10	0	0	0.04	30	
137	5.72	0.12	100	0.32	80	4.02	100	0.74	10	0.42	30	0	0	0.04		
138	0.9	0.1	20	0.3	30	0.22	30	0.28	10	0	10	0	0	0	0	
139	3.86	0.14	30	0.68	100	1.28	100	1.48	30	0.18	0	0	0	0.08	10	
140	2.78	0.14	80	0.68	100	2	100	0	0	0	0	0	0	0	0	
141	2.12	0.12	100	0.56	100	1.12	100	0	0	0	0	0.1	10	0.02	10	
142	3.4	0.12	80	0.36	30	0.48	100	2.28	50	0.16	10	0	0	0	0	
143	3.88	0.4	100	0.24	30	1.92	100	1	10	0.18	5	0	0	0	0	
144	5.8	0.26	50	0.66	100	1.08	100	2.86	30	0.32	20	0	0	0	0	
145	3.68	0.26	50	0.44	30	1.96	100	0.74	5	0.22	10	0	0	0	0	
146	6.06	0.22	100	1.46	100	0.64	100	3.56	50	0.14	10	0	0	0	0	
147	1.86	0.1	80	0.58	100	0.26	80	0.6	10	0.12	10	0	0	0.2	10	Ida's Valley
148	6.62	0.76	100	0.72	100	0.68	80	1.24	10	0.18	5	2.52	500	0.44	5	
149	5.46	0.06	50	0.28	70	0	0	5.12	90	0	0	0	0	0	0	
150	1.4	0.08	50	0.24	30	0.92	100	0	0	0	0	0	0	0.14	20	
151	1.66	0.24	70	0.42	80	0.44	80	0	0	0.2	5	0	0	0.32	40	
152	1.64	0	0	0.3	40	0.5	80	0.5	20	0.18	5	0	0	0.08	10	
153	12.55	0.04	30	0	0	12.46	100	0	0	0	0	0	0	0	0	
154	6.22	0.04	5	0.4	100	5.78	100	0	0	0	0	0	0	0	0	
155	1.48	0.32	50	0.12	80	0.44	70	0	0	0.28	10	0	0	0.28	60	
156	2.04	0.12	80	0.4	90	1.06	90	0	0	0	0	0	0	0.42	80	

Table A1: Raw Characterisation data of recycling

157	4.96	0.04	10	0.16	10	4.16	100	0.4	5	0.2	5	0	0	0	0	
158	0.52	0.14	80	0.3	40	0.04	10	0	0	0	0	0.02	5	0	0	
159	3.92	0.74	80	0.1	5	0.62	90	0	0	0.32	10	2.1	50	0	0	
160	0.66	0.46	100	0	0	0.2	30	0	0	0	0	0	0	0	0	
161	1.94	0.08	50	0.1	5	0.54	100	0	0	0.24	10	0.98	20	0	0	
162	2.12	0.2	70	0.52	90	1.44	100	0	0	0	0	0.04	10	0	0	
163	3.42	0.1	30	0.62	100	0.24	20	0.38	10	1.08	100	0.68	40	0.42	30	
164	3	0.18	90	0.28	20	1.18	100	0.46	10	0.18	30	0.32	10	0.12	10	
165	2.56	0.08	10	0.74	100	0.36	90	0.82	30	0.34	20	0	0	0.22	50	
166	1.44	0.24	40	0.4	100	0.52	90	0	0	0.2	20	0	0	0.18	30	
167	0.96	0	0	0.26	60	0.42	100	0	0	0.04	10	0	0	0.16	40	
168	0.62	0.08	40	0.38	100	0.14	40	0	0	0	0	0	0	0	0	
169	2.52	0.1	20	0.92	100	0.56	90	0	0	0.32	30	0.16	10	0.44	50	
170	1.1	0.1	40	0.12	30	0.84	100	0	0	0	0	0	0	0.06	10	
171	0.68	0	0	0.68	100	0	0	0	0	0	0	0	0	0	0	
172	1.38	0.24	60	0.14	20	0.78	100	0	0	0	0	0	0	0.24	20	
173	5.88	2.94	100	0.01	10	2.12	50	0.1	10	0	0	0	0	0.64	20	
174	1.58	0.12	30	0.32	80	0.28	50	0	0	0.62	20	0	0	0.14	10	
175	6.72	0.4	100	0.58	110	0.36	40	0	0	0.06	10	3.2	30	1.44	75	
176	0.68	0	0	0.68	100	0	0	0	0	0	0	0		0	0	
177	3.08	0.08	90	0.72	110	1.06	100	0.76	10	0.12	10	0.1	10	0.04	10	
178	2.82	0.2	100	0.3	60	1.52	120	0.72	10	0.08	10	0	0	0.02	10	
179	2.42	0.2	90	0.12	70	1.08	100	0.52	10	0.22	10	0.08	10	0.16	10	
180	1.76	0.08	10	0.44	100	0.06	10	0.56	10	0.06	10	0.5	10	0.02	10	
181	1.44	0.12	90	0.22	70	0.9	90	0	0	0.12	10	0	0	0.06	10	
182	3.48	0.06	10	0.6	100	2.64	120	0	0	0.18	10	0	0	0	0	
183	0.92	0.1	80	0.34	70	0.3	40	0	0	0.08	10	0.02	10	0.04	10	
184	2.44	0.1	10	0.42	60	0.76	20	0	0	0	0	0	0	0	0	
185	15.84	0	0	0	0	0	0	0	0	0	0	15.84	100	0	0	
186	2.26	0.14	100	0	0	0.3	80	0	0	0	0	0.18	10	1.6	40	
187	7.44	0.52	90	0.68	90	1.32	80	0.3	10	0	0	4.3	80	0.2	40	Cloetesville
188	8	0.18	90	2.4	70	3.5	100	0	0	0.62	10	0	0	1.22	80	
189	1.88	0.42	100	0.4	80	0.84	100	0.2	10	0.02	10	0	0	0	0	
190	5.52	0	0	0	0	5.52	100	0	0	0	0	0	0	0	0	
191	2.18	0.38	90	0.66	100	0.82	90	0	0	0.22	10	0	0	0.14	20	
192	0.9	0.12	90	0.08	10	0.18	10	0	0	0	0	0.54	10	0	0	
193	1.94	0.24	40	0.74	60	0.12	10	0	0	0.26	30	0	0	0.52	100	
194	1.32	0.04	60	0.2	40	0.9	90	0	0	0.08	20	0	0	0	0	
195	1.14	0.06	30	0.26	50	0.56	80	0	0	0.01	10	0	0	0.2	50	
196	2.6	0.16	50	1.96	100	0	0	0	0	0.06	10	0	0	0.26	10	

Table A1: Raw Characterisation data of recycling

197	1.58	0	0	1.58	100	0	0	0	0	0	0	0	0	0	0	
198	2.58	0	0	0.14	20	2.06	100	0.3	10	0	0	0	0	0	0	
199	0.68	0	0	0.68	100	0	0	0	0	0	0	0	0	0	0	
200	3.1	0.06	20	0.72	100	1.48	100	0.78	10	0	0	0	0	0.06	10	
201	2.4	0.54	100	0.38	80	1.36	100	0	0	0.06	10	0	0	0.01	10	
202	0.58	0	0	0.48	100	0.1	10	0	0	0	0	0	0	0	0	
203	1.38	0	0	1.38	100	0	0	0	0	0	0	0	0	0	0	
204	1.62	0.3	100	0.36	80	0.74	100	0	0	0.14	10	0.04	10	0.1	10	
205	3.18	0.28	100	0.28	30	0	0	0.54	20	0.04	10	1.3	30	0	0	
206	2.58	0.22	70	0.26	50	0.9	100	0	0	0	0	1.1	10	0	0	
207	2.08	0.22	100	0.14	50	0.58	100	0.06	10	0	0	1	30	0.14	40	
208	1.28	0.14	60	0.5	100	0.7	100	0	0	0	0	0	0	0	0	
209	4.62	0	0	0	0	0	0	0	0	0	0	4.56	100	0.04	10	
210	0.68	0.06	10	0.64	100	0	0	0	0	0	0	0	0	0	0	
211	1.28	0.06	10	0.5	100	0.1	50	0.32	10	0.2	10	0	0	0.12	10	
212	1.66	0.54	100	0.24	50	0.8	100	0	0	0.02	10	0	0	0.08	10	
213	4	0	0	0	0	0	0	0	0	0	0	4	100	0	0	
214	1.6	0.22	100	0.5	70	0.3	10	0	0	0.08	10	0.54	10	0	0	
215	2.64	0.08	100	1.64	300	0.3	100	0	0	0.28	10	0	0	0.36	10	
216	1.52	0.06	50	0.28	100	0.4	100	0.76	10	0	0	0	0	0	0	
217	2.98	0.18	60	0.12	30	0.42	80	0	0	0.08	10	0.66	10	1.54	50	
218	1.72	0.1	100	0.46	120	0.8	100	0	0	0.26	20	0	0	0.04	10	
219	4.5	0.18	50	0.3	150	4.02	200	0	0	0	0	0	0	0	0	
220	2.32	0.08	50	0.5	100	0.54	100	1.18	20	0	0	0	0	0.04	5	Jamestown
221	0.76	0.06	20	0.7	100	0	0	0	0	0	0	0	0	0	0	
222	2.12	0.06	30	0.78	100	0.78	100	0.5	10	0	0	0	0	0	0	
223	1.02	0.12	80	0.16	30	0.68	20	0	0	0.06	5	0	0	0	0	
224	1.46	0.14	50	0.52	100	0.66	100	0	0	0.12	10	0	0	0	0	
225	1.2	0.06	20	0.58	100	0.1	10	0.4	5	0	0	0	0	0.04	5	
226	8.6	0.06	10	0.48	100	0.04	10	8.04	100	0	0	0	0	0	0	
227	3.34	1.54	100	0.86	100	0	0	0.02	10	0.44	10	0.04	10	0.18	40	
228	5.34	0.08	80	0.35	50	0.64	100	4.04	80	0.18	5	0	0	0.05	5	
229	1.7	0.12	50	0.5	80	0.46	80	0.26	5	0	0	0	0	0.26	80	
230	3.78	0.24	100	0.57	80	1.17	50	1.2	10	0.35	10	0.1	5	0.1	5	
231	1.06	0.2	5	0.08	5	0.46	70	0.1	5	0.12	5	0	0	0.08	5	
232	2.06	0.22	80	1.258	180	0.62	90	0	0	0.06	10	0	0	0	0	
233	1.48	0.02	5	0.82	50	0.28	50	0	0	0.22	10	0	0	0.18	10	
234	2.66	0.04	10	0.5	100	0.5	100	0	0	0.12	5	0	0	1.42	50	
235	4.02	0.56	100	0.94	50	0	0	0.26	10	0.14	10	0	0	1.66	50	
236	2.34	0.26	100	0.82	100	0.86	100	0.12	5	0.02	5	0	0	0.42	50	

Table A1: Raw Characterisation data of recycling

237	1.72	0.06	5	0.76	50	0	0	0.9	20	0	0	0	0	0.04	5	
238	1.44	0.04	10	0.18	50	0.46	80	0.4	10	0.32	30	0	0	0.14	30	
239	1.52	0.4	20	0.96	100	0.16	30	0	0	0	0	0	0	0	0	
240	1.78	0.1	80	0.6	100	0.28	80	0.6	30	0.04	10	0.12	10	0	0	
241	5.8	0.02	10	1.02	100	0.26	80	4.48	80	0	0	0	0	0	0	
242	2.4	0.14	50	0	0	0.3	60	0	0	0.04	10	1.78	50	0.01	10	
243	3.22	0.04	30	0.16	40	0.2	30	2.68	50	0.01	10	0	0	0	0	
244	2.32	0.36	90	0.6	70	0.6	80	0.14	10	0	0	0.64	10	0.08	10	
245	1.94	0.12	90	0.86	100	0.56	80	0	0	0	0	0.36	20	0.01	10	
246	2.5	0.04	10	0.2	20	2.22	100	0	0	0	0	0.01	10	0	0	
247	2.06	0.22	60	0.2	30	0.4	70	0.4	20	0.14	10	0.88	40	0	0	
248	2.52	0.18	20	0.26	50	1.96	100	0.1	5	0	0	0	0	0	0	Welgevonden
249	4.58	0.12	100	0.54	100	3.18	100	0.64	20	0	0	0	0	0.04	5	
250	4.64	0.22	100	0.3	50	0.88	100	2.4	50	0.02	5	0	0	0.9	5	
251	4.22	0.24	100	0.54	100	0.5	50	2.58	30	0.28	5	0	0	0	0	
252	1.88	0.06	20	0.24	50	1.3	100	0	0	0	0	0	0	0.26	50	
253	3.1	0.14	50	0.3	40	0.04	10	2.56	10	0.1	5	0	0	0.18	10	
254	3.74	0.24	20	0.24	20	1.6	20	1.3	20	0.08	5	0	0	0.12	5	
255	3.3	0.32	50	0.48	100	0.42	40	1.82	50	0.3	10	0	0	0	0	
256	0.94	0.28	50	0.04	5	0.3	100	0	0	0.22	10	0	0	0.06	5	
257	3.48	0.08	40	0.64	100	0.84	100	1.6	30	0.26	30	0	0	0.02	5	
258	1.32	0.1	100	0.22	50	0.98	100	0	0	0	0	0	0	0	0	
259	1.7	0.08	100	0.28	10	0.72	100	0.5	10	0.06	5	0	0	0	0	
260	4.02	0	0	0	0	0	0	0	0	0	0	4.02	100	0	0	
261	5.24	0.12	100	0.64	100	0.58	100	3.62	100	0.2	10	0	0	0.08	5	
262	0.76	0.08	20	0.38	50	0.24	50	0	0	0	0	0	0	0.04	5	
263	5.02	0.36	40	0.52	100	1.72	100	2.32	50	0	0	0	0	0.04	5	
264	1.42	0.22	100	0.54	100	0.34	50	0	0	0.22	20	0	0	0.08	5	
265	1.64	0.12	20	0.34	20	1.16	100	0	0	0.04	5	0	0	0.08	5	
266	1.24	0.1	20	0.44	50	0.66	100	0	0	0	0	0	0	0.1	5	
267	1.64	0.28	100	0.26	20	0.84	100	0	0	0.04	5	0	0	0.18	10	
268	2.1	0.1	100	0.12	10	0.6	50	1.3	20	0	0	0	0	0	0	
269	1.74	0.2	100	0.84	100	0.08	10	0.54	10	0.1	10	0	0	0	0	
270	2.6	0.1	30	0.46	100	0.32	100	1.62	10	0.12	10	0	0	0	0	
271	4.48	0.26	40	0.56	20	0.82	80	0	0	0.16	10	1.34	40	1.38	100	
272	2.62	0.18	60	0.42	90	1.98	100	0	0	0	0	0	0	0.1	10	
273	3.5	0.1	40	0	0	3.22	100	0	0	0	0	0	0	0.14	20	
274	1.38	0.08	30	0.94	100	0.3	70	0	0	0	0	0	0	0.12	20	
275	3.32	0	0	0.08	10	2.42	100	0.84	10	0	0	0	0	0	0	
276	3.7	0.3	100	0.08	10	0.6	10	3.06	60	0.08	5	0	0	0.1	10	

Table A1: Raw Characterisation data of recycling

277	1.88	0.48	100	0.32	40	0.82	80	0	0	0.26	10	0	0	0.02	5	
278	2.12	0.1	100	0.3	50	0.84	100	0.74	10	0.08	5	0	0	0	0	
279	3.18	0.06	15	0.42	60	2.28	100	0.26	5	0.12	5	0	0	0.12	10	
280	1.08	0.18	100	0.12	20	0.18	50	0.6	10	0.04	5	0	0	0.02	5	
281	3.4	0.08	15	0.2	30	1.04	100	2.04	15	0	0	0	0	0.1	10	
282	3.56	0.06	40	0.36	100	0.14	10	2.82	40	0.22	10	0	0	0	0	
283	6.22	0.28	100	0	0	3.42	100	2.38	30	0	0	0	0	0.04	10	
284	5.06	1.24	100	0.44	40	1.06	95	0.04	5	0.32	10	2.04	30	0	0	
285	2.36	0.08	80	0.78	150	0.8	100	0.2	10	0.12	10	0.02	10	0.44	100	Simonswyk - Uniepark
286	0.32	0	0	0.2	40	0.08	20	0	0	0.04	10	0	0	0	0	
287	1	0.4	150	0.08	10	0.4	80	0	0	0.12	10	0	0	0.04	10	
288	1.6	0.12	80	0.44	80	0.26	40	0	0	0.64	30	0	0	0.08	10	
289	3.58	0	0	0	0	0	0	3.58	100	0	0	0	0	0	0	
290	1.2	0.12	100	0.24	80	0.32	100	0.46	10	0	0	0	0	0	0	
291	5.42	0	0	0	0	0	0	0	0	0	0	5.42	100	0	0	
292	1.42	0.14	90	0.1	10	0.56	100	0.2	10	0	0	0.52	10	0	0	
293	1.6	0.12	40	0.28	80	0.92	100	0.2	5	0	0	0	0	0	0	
294	1.94	0.2	100	0.76	100	0.86	100	0.08	5	0	0	0	0	0.02	5	
295	0.8	0.3	100	0.5	100	0	0	0	0	0	0	0	0	0	0	
296	1.3	0.1	50	0.4	60	0.2	30	0	0	0.3	10	0	0	0.3	10	
297	3.3	0.34	100	0.26	20	1.3	100	0.14	5	0.28	10	0.52	10	0.24	10	
298	2.86	0.48	100	0.6	100	1.02	100	0.6	10	0.16	5	0	0	0	0	
299	2.64	0.22	80	0.3	70	1.5	100	0	0	0.24	5	0	0	0.36	30	
300	3.42	0.06	30	0.76	50	0.24	40	2.32	30	0.04	5	0	0	0	0	
301	3.84	0.44	100	0.64	100	0.78	80	1.5	20	0.08	5	0	0	0.34	30	
302	4.58	0.34	100	0.36	50	0.74	50	0.8	20	0.04	5	2.28	50	0	0	
303	8.42	0.8	20	0.36	100	0.68	50	7.12	100	0.02	5	0	0	0.1	5	
304	3.62	0.3	100	0.12	10	2.38	100	0.86	20	0	0	0	0	0	0	
305	2.94	0.38	100	0.42	50	0.94	100	0.92	50	0.08	5	0	0	0.28	20	
306	1.12	0.16	10	0.44	100	0.14	10	0.2	5	0.08	5	0	0	0.12	5	
307	2.78	0.2	100	0.58	100	1.4	100	0.46	20	0.1	5	0	0	0.08	5	
308	3.26	0.22	50	0.64	50	1.42	100	0.74	10	0.14	20	0	0	0.06	5	
309	0.82	0.1	5	0.26	40	0.5	100	0	0	0	0	0	0	0	0	
310	0.92	0	0	0.92	200	0	0	0	0	0	0	0	0	0	0	
311	1.26	0.18	100	0.14	30	0.4	90	0.26	10	0.36	30	0	0	0.04	10	
312	4.86	0.32	100	0.66	60	1.22	100	1.42	10	0.26	20	0	0	1	80	
313	4.08	0.46	100	0.18	10	0.23	60	0	0	0.22	10	0.5	10	2.46	80	
314	2.64	0.66	110	0.32	80	1.1	110	0	0	0.46	10	0	0	0	0	
315	2.04	0.34	100	0.1	10	0.62	80	0.72	10	0.18	10	0	0	0.02	10	

Table A1: Raw Characterisation data of recycling

316	2.9	0.04	20	0.4	90	1.36	110	0.8	10	0.14	10	0	0	0.1	60	
317	1.4	0.12	100	0.38	80	0.26	70	0.4	10	0.2	10	0	0	0	0	
318	5.18	0.34	100	0.44	60	0.44	100	0.38	10	0.34	10	2.64	30	0.28	10	
319	1.38	0.08	90	0.08	10	0.16	40	0	0	0.18	10	0.78	10	0.04	10	
320	5.98	0.26	95	0.5	100	4.86	100	0.18	10	0.1	10	0	0	0.4	10	
321	2.7	0.18	95	0.02	10	0.34	20	0	0	0	0	1.84	20	0.3	20	
322	1.7	0.84	110	0.44	50	0.16	60	0	0	0.08	10	0	0	0	0	
323	1.52	0.12	60	0.9	110	0.32	50	0	0	0.04	10	0	0	0.02	10	
324	1.74	0.1	100	0.38	40	1.12	200	0	0	0.18	15	0	0	0	0	Die Boord
325	1.7	0.26	80	0.24	20	0.8	100	0.16	5	0.02	5	0	0	0.32	50	
326	1.26	0.06	10	0.36	80	0.54	80	0	0	0.02	5	0	0	0.22	5	
327	1.34	0.38	100	0.24	40	0.48	80	0	0	0.1	5	0	0	0.18	5	
328	1.3	0.18	10	0.54	60	0.46	80	0	0	0.04	5	0	0	0.06	20	
329	2.16	0.14	90	0.72	100	0.3	50	0.82	20	0.02	5	0	0	0.14	50	
330	3.22	0.14	50	0.48	80	0.58	100	1.8	30	0	0	0	0	0.28	50	
331	2.48	0.52	100	0.22	30	1.6	100	0.08	5	0	0	0	0	0	0	
332	1.52	0.16	50	0.88	100	0.44	80	0	0	0.06	5	0	0	0	0	
333	2.44	2.44	500	0	0	0	0	0	0	0	0	0	0	0	0	
334	2.44	0.42	100	0.5	80	0.56	100	0.48	10	0.14	10	0.16	40	0.26	10	
335	2.88	0.16	80	0	0	2.56	100	0	0	0.16	5	0	0	0	0	
336	2.68	0.24	80	0.22	10	0.58	100	1	10	0.18	5	0	0	0.36	50	
337	1.02	0.22	50	0.34	80	0.38	80	0	0	0.02	5	0	0	0.02	5	
338	3.2	0.12	5	0.38	80	1.68	100	0	0	0.16	5	0	0	0.78	5	
339	1.32	0.12	50	0.9	100	0.34	80	0.2	5	0.02	5	0	0	0.1	10	
340	3.92	0.7	60	0.36	50	0.74	100	0	0	0.18	10	2.12	50	0.24	30	
341	2.98	0.52	100	0.46	50	0.62	80	0	0	0.28	5	0.92	50	0.1	5	
342	6.98	0.08	10	0.48	100	2.48	40	4	50	0	0	0	0	0	0	
343	2.02	0.08	10	0.74	100	0.56	80	0.44	10	0.32	30	0	0	0	0	
344	2.3	0.3	50	0.6	100	1.04	100	0.26	10	0.08	10	0	0	0.08	10	
345	4.14	0.14	90	0.56	150	2.7	100	0.64	10	0.1	10	0.04	10	0	0	
346	2.42	0.18	100	0.64	100	0.9	100	0.48	10	0.2	30	0	0	0.06	10	
347	1.86	0.24	100	0.34	50	1.1	100	0	0	0.12	5	0	0	0.1	10	
348	4.48	0.2	100	0.58	100	3.3	100	0	0	0.42	30	0	0	0	0	
349	8.44	0.4	100	0.24	30	4.44	100	2.42	40	0.58	20	0	0	0.38	40	
350	0.66	0.08	80	0.34	50	0.28	30	0	0	0	0	0	0	0	0	
351	1.4	0.08	80	0.12	10	0.58	90	0	0	0	0	0.4	50	0.2	20	
352	2.54	0.04	5	0.26	30	0	0	2.04	50	0.2	5	0	0	0	0	
353	1.18	0.24	30	0.42	20	0.36	20	0.08	5	0.1	5	0.08	5			
354	0.78	0.1	50	0.12	20	0.44	50	0	0	0.06	5	0	0	0.08	5	
355	2.62	0.28	80	0.4	80	0.86	80	0.96	10	0	0	0	0	0.04	5	

Table A1: Raw Characterisation data of recycling

356	1.62	0.1	80	0.44	80	0.52	70	0.32	5	0.24	10	0	0	0	0
357	2.22	0.24	100	0.32	40	0.6	100	0.96	10	0	0	0.02	5	0.04	5
358	2.5	0.38	60	0.18	20	0.78	60	1.06	10	0	0	0	0	0.08	5
359	2.26	0.18	90	0.56	80	0.46	80	0.74	5	0.26	10	0	0	0.06	5
360	2.36	0.52	70	0.12	2	0.56	80	0.14	5	0.18	10	0	0	0.88	100
361	1.88	0.22	100	0.52	80	0.46	80	0.48	5	0	0	0	0	0.06	5
362	3.08	0.2	100	0.5	80	1.08	100	0.82	10	0.1	5	0	0	0.12	10
363	3.82	0.16	80	0.34	10	0.16	50	1.66	10	1.38	100	0	0	0.12	10
364	1.8	0.2	100	0.5	90	0.34	50	0.54	10	0.14	5	0	0	0.08	5
365	2.24	0.16	80	0.3	50	0.48	100	1.12	10	0	0	0	0	0.16	5
366	3.06	0.2	100	0.32	50	0.62	80	1.54	10	0.08	5	0	0	0.3	50
367	3.38	0.16	80	0.44	80	2.04	100	0	0	0	0	0	0	0.7	10
368	9.42	0.54	90	0.34	30	3.12	100	3.78	50	0	0	0	0	1.5	20
369	1.2	0.2	100	0.14	5	0.5	80	0	0	0.06	5	0	0	0.3	5
370	2.96	0.2	80	0.64	70	0.34	80	1.48	10	0.24	10	0	0	0.04	5
371	1.36	0.14	80	0.3	10	0.22	50	0.18	5	0.3	20	0	0	0.14	5
372	1.64	0.04	10	0.2	20	0.82	50	0.4	10	0.14	5	0	0	0	0
373	0.8	0.12	50	0.3	50	0.36	50	0	0	0	0	0	0	0	0
374	4.7	0.34	100	0.4	60	1.48	100	0.7	10	0.24	10	1.5	40	0	0
375	1.74	0.3	100	0.6	90	0.34	80	0.22	5	0.18	10	0	0	0.04	5
376	8.32	0.16	90	0.14	20	0.28	40	0.56	20	6.92	100	0.02	10	0.04	10
377	2.96	0.26	100	0.46	100	1.5	150	0.5	10	0.01	10	0	0	0.18	20
378	2.04	0.1	20	0.22	80	0.26	80	1.48	20	0.02	10	0	0	0.06	10
379	2.54	0.28	100	0.3	30	0.88	100	0.6	20	0.34	10	0	0	0.22	40
380	3.36	0.16	80	0.14	20	2.64	100	0	0	0.1	10	0	0	0.26	10
381	3.28	0.28	100	0.04	10	3.02	100	0	0	0	0	0	0	0	0
382	1.64	0.1	80	0.36	90	0.54	80	0.56	10	0.1	10	0	0	0	0
383	3.42	0.16	100	0.46	30	1.2	100	1.2	20	0.12	10	0	0	0.32	30
384	2.72	0.36	90	0.28	40	0.66	100	1.24	20	0.1	10	0	0	0.06	10
385	1.32	0.1	80	0.22	40	0.76	100	0.2	10	0.06	10	0	0	0	0
386	2.12	0.12	90	0.38	80	0.52	60	0.98	20	0.08	10	0	0	0.06	10
387	2.78	0.22	100	0.5	90	0.74	100	0	0	0.22	10	0.54	20	0.36	50
388	0.82	0.14	80	0.22	30	0.12	20	0.14	10	0.12	20	0	0	0.04	10
389	1.28	0	0	0.38	80	0.56	90	0.28	10	0	0	0	0	0.02	10
390	2.9	0.12	80	0.34	60	2.02	100	0.34	10	0.04	10	0	0	0.1	10
391	1.1	0.03	20	0.14	20	0.94	100	0	0	0	0	0	0	0	0
392	1.2	0.2	100	0.1	20	0.84	100	0	0	0.04	10	0	0	0.06	10
393	0.8	0.02	20	0.29	30	0.44	100	0	0	0	0	0	0	0	0
394	1.62	0.22	100	0.2	50	0.62	80	0.5	10	0.02	10	0.2	10	0	0
395	0.9	0.06	70	0.18	40	0.36	70	0	0	0.06	10	0	0	0.22	30
396	1.2	0.26	90	0.28	30	0.16	20	0.44	10	0	0	0	0	0.12	10

Table A1: Raw Characterisation data of recycling

397	2.86	0.72	100	0.87	70	0.28	40	0.4	10	0.02	10	0.66	10	0	0
398	1.58	0.22	100	0.12	10	0.9	90	0.22	10	0.04	10	0	0	0	0
399	0.58	0.06	60	0.18	40	0.26	80	0	0	0.02	10	0	0	0	0
400	0.78	0.3	100	0.2	40	0.2	50	0	0	0	0	0	0	0.02	10
401	1.26	0.16	75	0.26	40	0.32	80	0	0	0.2	10	0.02	10	0.2	10
402	3.24	0.34	100	0.5	100	0.36	20	0	0	0.1	10	1.86	45	0.02	10
403	2.14	0.08	30	1.16	100	0.52	90	0.2	10	0	0	0	0	0.1	10
404	7.46	0.36	100	0.26	30	0.18	20	0	0	0.04	10	6.24	90	0.32	10
				160.2		413.1		303.2							
Total	1198.56	84.21		7		9		9		48.40		117.11		61.29	
Average	2.97	0.21		0.40		1.02		0.75		0.12		0.29		0.15	

Table A2: Raw Characterisation data of general waste

Black Bag	Unopened mass (kg)	Plastic film		Dense Plastics		Paper		Glass		Metal		Organics		Other		
		Mass	vol%	Mass	vol%	Mass	vol%	Mass	vol%	Mass	vol%	Mass	vol%	Mass	vol%	
1	2.6	0.12	50	0.56	100	0.18	10	0.46	10	0.14	10	1.14	60	0.04	10	Rozendal
2	4.46	0.22	60	0.6	80	0.42	50	0	0	0	0	3.1	50	0.06	10	
3	2.44	0.2	100	0.18	50	0.42	100	0.44	10	0.36	20	0.9	10	0.14	10	
4	6.1	0	0	0	0	0	0	0	0	0	0	6.1	100	0	0	
5	7.02	0	0	0	0	0	0	0	0	0	0	7.02	100	0	0	
6	7.06	0.32	100	0.74	80	0.74	100	0.34	10	0.14	10	4.6	80	0.26	10	
7	3.32	0	0	0	0	0	0	0	0	0	0	3.32	100	0	0	
8	1.8	0.44	100	0.02	10	0.28	50	0	0	0.02	10	0.54	10	0.62	20	
9	4.01	0.5	100	0.32	30	0.4	80	0	0	0.12	10	2.6	30	0.04	10	
10	1.96	0.3	100	0.26	30	0.34	80	0	0	0.34	10	0.76	10	0	0	
11	7.2	0	0	0	0	0	0	0	0	0	0	7.2	100	0	0	
12	8.18	0	0	0	0	0	0	0	0	0	0	8.18	100	0	0	
13	2.42	0.3	100	0.28	40	0.72	60	1	15	0.08	5	0	0	0	0	
14	5.14	0.86	50	0.08	10	0.32	10	0.12	10	0	0	3.64	100	0	0	
15	3.38	0	0	0.14	40	0.82	50	0	0	0	0	0	0	2.4	50	
16	4.96	0	0	0	0	0	0	0	0	0	0	2.36	50	2.58	100	
17	18.8	0	0	0	0	0	0	0	0	0	0	18.8	100	0	0	
18	6.3	0.22	80	0.56	40	0.52	50	0.88	25	0.02	1	4.06	90	0	0	
19	4.06	0	0	0	0	0	0	0	0	0	0	4.06	100	0	0	
20	2.54	0.48	100	0.72	90	0.24	35	0.8	5	0.12	5	0	0	0.32	10	
21	6.2	0.8	100	0.44	15	0.66	80	0.578	5	0.24	10	2.66	40	0.7	80	
22	5.36	0.3	100	0.54	50	2.3	100	0.54	10	0.3	15	0	0	1.24	35	Uniepark
23	8.38	0	0	0	0	8.38	100	0	0	0	0	0	0	0	0	
24	4.26	0.06	10	0.28	50	1.5	100	0.32	5	0	0	1.78	0	0.22	30	
25	7.74	0	0	0	0	0	0	0	0	0	0	7.74	100	0	0	
26	0.78	0.22	40	0.24	30	0.14	0	0	0	0	0	0	0	0	0	
27	2.24	0.74	100	0	0	0	0	1.34	5	0.05	5	0	0	0	0	
28	2.98	0.24	100	0.76	100	0.92	100	0.7	10	0.06	10	0	0	0.1	30	
29	0.96	0	0	0.28	60	0.1	10	0.4	10	0.18	10	0	0	0	0	
30	1.6	0.16	80	1	100	0.04	10	0	0	0	0	0	0	0.3	40	
31	5.74	0.5	100	0.24	60	0.34	80	4.32	80	0.06	10	0	0	0.04	10	
32	0.34	0.03	20	0	0	0.24	70	0	0	0	0	0	0	0.04	10	
33	2.3	0.42	100	0.1	0	0.54	50	0	0	0	0	0	0	1.2	5	
34	5.16	0.28	40	0.3	40	0	0	2.08	40	0.06	5	2.4	40	0	0	
35	4.32	0	0	0	0	0	0	0	0	0	0	4.32	100	0	0	
36	2.64	0.08	80	0.02	10	0.54	90	0.1	10	0.06	10	1.66	50	0	0	
37	2.56	0.24	100	0.38	100	0.68	100	0.74	5	0.02	5	0.38	5	0	0	

Table A2: Raw Characterisation data of general waste

38	6.86	0.44	100	0.16	30	1.12	50	0.78	10	0.28	10	3.78	80	0.04	10	
39	4.56	0.7	100	0.82	80	0.4	30	0	0	0.06	10	2.32	30	0.2	20	
40	3.44	0.34	100	0.16	30	0.62	90	0.74	10	0.16	20	1.28	40	0.1	10	
41	4.78	0.32	90	1.04	80	1.18	100	0.00	0	0.20	10	1.40	20	0.38	10	Universiteits Oord
42	2.96	1.20	40	0.10	30	0.40	60	0.38	10	0.08	10	0.26	10	0.34	10	
43	3.74	0.46	100	0.26	30	2.70	100	0.00	0	0.00	0	0.00	0	0.22	10	
44	3.74	0.38	100	0.00	0	0.58	70	0.00	0	0.32	10	2.20	30	0.16	10	
45	2.12	0.48	90	0.12	20	0.48	90	0.00	0	0.06	10	0.94	30	0.12	10	
46	5.24	0.18	70	0.32	50	0.28	40	0.78	10	0.12	10	2.70	50	1.14	10	
47	1.74	0.54	100	0.58	100	0.62	70	0.00	0	0.00	0	0.00	0	0.00	0	
48	1.46	0.04	50	0.16	50	0.06	20	0.00	0	0.12	10	0.38	10	0.12	10	
49	1.92	0.12	80	0.14	10	0.56	100	0.00	0	0.08	10	0.94	10	0.02	10	
50	2.92	0.36	100	0.00	0	0.38	80	0.40	10	0.01	10	1.26	30	0.42	20	
51	3.86	0.00	0	0.00	0	0.00	0	0.00	0	0.00	0	3.86	150	0.00	0	
52	4.48	0.00	0	0.00	0	0.00	0	0.00	0	0.00	0	4.48	150	0.00	0	
53	4.66	0.34	100	0.20	30	0.58	90	0.24	10	0.58	40	2.54	50	0.84	10	
54	2.20	0.22	100	0.14	20	0.24	40	0.14	10	0.30	20	0.80	20	0.30	20	
55	4.34	0.04	70	0.24	50	4.00	100	0.00	0	0.00	0	0.00	0	0.00	0	
56	1.68	0.06	10	0.14	30	0.30	50	0.72	10	0.22	20	0.28	20	0.00	0	
57	5.92	0.36	100	0.18	20	0.68	100	0.00	0	0.26	20	4.42	100	0.16	10	
58	9.22	0.30	100	2.28	80	0.34	40	2.58	40	0.14	10	2.96	50	0.54	30	
59	1.62	0.02	10	0.04	10	0.84	90	0.00	0	0.02	10	0.14	10	0.10	10	
60	4.20	0.42	90	0.30	30	0.24	40	1.10	10	0.30	10	1.74	30	0.22	20	
61	1.92	0.20	90	0.06	10	0.16	20	0.00	0	0.16	10	1.20	20	0.00	0	
62	5.00	0.16	60	0.64	100	1.08	100	1.12	10	0.32	10	1.64	50	0.04	10	
63	4.02	0.00	0	0.00	0	0.00	0	0.00	0	0.00	0	4.02	100	0.00	0	
64	2.64	0.36	90	0.92	100	0.56	70	0.00	0	0.26	10	0.68	10	0.10	10	
65	2.56	0.30	80	0.20	50	0.22	20	0.00	0	0.00	0	1.30	40	0.06	10	
66	7.40	0.96	80	2.38	150	0.50	50	0.78	10	0.14	10	2.12	50	0.64	40	
67	3.16	0.00	0	0.06	5	0.98	100	0.24	5	0.00	0	1.88	50	0.00	0	
68	4.14	0.22	40	0.20	5	0.22	50	2.00	30	0.00	0	1.54	60	0.00	0	
69	4.53	0.00	0	0.08	40	0.00	0	0.00	0	0.00	0	4.00	100	0.00	0	
70	4.22	0.38	100	0.20	30	0.32	50	0.76	10	0.06	5	2.38	50	0.00	0	
71	1.12	0.10	80	0.16	10	0.58	100	0.00	0	0.07	10	0.06	10	0.04	10	
72	4.90	0.00	0	0.00	0	0.00	0	0.00	0	0.00	0	4.90	100	0.00	0	
73	8.40	1.06	100	0.90	100	1.06	100	0.00	0	0.12	10	4.56	80	0.56	80	
74	1.78	0.22	100	0.80	80	0.22	30	0.00	0	0.00	0	1.00	20	0.00	0	
75	4.20	0.50	100	0.12	30	0.90	50	1.26	30	0.20	20	1.20	10	0.00	0	
76	2.56	0.14	100	0.08	10	0.36	80	0.00	0	0.00	0	2.14	30	0.00	0	
77	2.52	0.18	90	0.52	80	0.76	100	0	0	0.58	20	0.1	10	0.3	60	Dalsig

Table A2: Raw Characterisation data of general waste

78	3.08	0.66	100	0.08	10	0.76	90	0.18	10	0	0	1.24	20	0.12	10	
79	4.04	0.4	90	0.28	40	0.44	70	0.84	10	0	0	2.08	40	0.16	20	
80	4.78	0.28	60	0.26	50	0.72	100	0	0	0	0	2.04	50	1.36	30	
81	5.84	0.4	100	0.46	60	0.14	30	0	0	0	0	1.02	20	3.76	80	
82	5.12	0.46	100	0	0	0.363	50	1.02	10	0.14	10	2.36	60	0.6	30	
83	4.04	0.3	70	0.46	70	1.8	100	0.4	10	0.3	10	0.78	20	0	0	
84	4.06	0.3	90	0.04	10	1.76	100	0	0	0	0	1.92	90	0	0	
85	3.74	0.36	70	0.16	10	0.56	100	0	0	0.06	10	2.48	50	0	0	
86	5.5	0.04	30	0.2	50	0.16	30	1.48	40	0.06	10	2.54	60	0.86	50	
87	1.8	0.02	5	0.1	20	0.04	10	0.36	10	0.12	10	0.52	20	0.42	20	
88	3.8	0.16	90	0.08	1	0.16	5	0.18	1	0.02	1	0.76	2	2.5	50	
89	3.98	0.32	80	0.38	40	0.24	20	0.84	5	0.04	1	1.78	10	0.42	40	
90	11.22	0	0	0	0	0	0	0	0	0	0	11.2	400	0.02	10	
91	2.78	0.5	100	0.05	1	0.14	2	0	0	0	0	1.18	10	0.92	10	
92	5.38	0.3	100	0.54	40	1.42	85	0	0	0	0	2.66	30	0.38	20	
93	3.36	0.32	95	0.16	5	0.3	50	0	0	0.14	2	2.16	40	0.12	2	
94	3.82	0.28	100	0.1	30	0.66	60	0	0	0.3	30	2.46	130	0.1	2	
95	3.6	0.34	100	0.52	50	0.74	100	0.74	10	0.02	10	1.08	20	0.22	10	
96	1.26	0.1	30	0.04	10	0.66	80	0	0	0.02	10	0.54	30	0.06	10	
97	5.2	1.04	100	0	0	0.28	30	0	0	0.01	10	4.44	50	0.1	10	
98	4.1	0.38	80	0.02	10	0.82	80	0.12	10	0.02	10	2.6	70	0	10	
99	1.88	0.02	10	0	0	0	0	0	0	0	0	1.82	100	0	0	
100	4.92	0.1	70	0.01	10	0.6	100	0	0	0.01	10	2.6	60	1.46	23	
101	6.94	0.44	100	0.02	10	1.46	100	0	0	0.01	10	4.86	100	0.01	10	
102	4.02	0.5	100	0.24	30	0.62	50	0.62	10	0.16	10	1.88	30	0.08	10	
103	2.74	0.08	50	0.16	30	0.22	50	0.7	10	0.18	10	1.32	50	0.14	10	
104	2.78	0.28	80	0.16	30	0.46	40	0	0	0.14	10	1.74	50	0.06	10	
105	5.24	0.12	40	0.26	50	1.38	100	3.5	80	0.08	10	0	0	0.18	30	
106	5.3	0.13	80	0.26	50	1.36	100	3.28	80	0.08	10	0	0	0.18	50	
107	3.66	0.3	80	0.24	80	1.06	100	1.46	40	0.34	40	0	0	0	0	
108	3.76	0.14	90	0.92	75	0.8	90	0.54	25	0.12	20	0	0	1.04	20	
109	5.04	0.44	100	0.72	90	0.7	100	0.2	30	0.2	30	2.24	80	0.06	5	
110	0.78	0.04	20	0.08	10	0.04	10	0	0	0.1	10	0.42	30	0.16	10	Brandwacht
111	6.62	0.3	90	0.34	60	0.68	100	0	0	0.01	10	5.16	100	0	0	
112	1.98	0.24	90	0.1	20	0.6	100	0	0	0	0	0.84	20	0.02	10	
113	4.5	0.54	100	0.14	20	0.54	50	0	0	0.14	10	2.2	50	0.96	30	
114	2.32	0.24	100	0.04	10	1.46	100	0	0	0.04	10	0.54	30	0.1	10	
115	12.9	0	0	0	0	0	0	0	0	0	0	12.9	100	0	0	
116	8.6	0	0	0	0	0	0	0	0	0	0	8.6	100	0	0	
117	2.24	0.22	90	0.3	10	0.42	80	0.12	1	0.06	1	1.14	10	0.1	1	

Table A2: Raw Characterisation data of general waste

118	5.32	0.63	100	0.36	75	1.42	100	1.84	10	0.16	5	1.18	10	0.08	1	
119	5.62	0.28	100	0.16	20	1.06	80	0	0	0.12	10	3.84	80	0.16	10	Paradyskloof
120	4.28	0.56	100	0.76	50	1.22	90	0.48	10	0	0	1.12	20	0.1	10	
121	3.14	0.4	70	0.02	10	0.6	80	0.36	10	0.06	10	1.28	30	0.38	20	
122	7.38	0	0	0	0	0	0	0	0	0	0	7.38	100	0	0	
123	3.98	0.16	80	0.48	60	0.28	100	1.2	10	0.1	10	1.68	40	0.06	10	
124	2.26	0.32	90	0.34	70	0.32	40	0.16	10	0.02	10	1.08	20	0.06	10	
125	4.42	0.24	70	0.12	30	1.46	100	0	0	0	0	2.56	50	0.04	10	
126	5.64	0.22	80	0.34	40	0.28	80	4.12	70	0.16	20	0.54	10	0.02	10	
127	7.24	0.28	80	2.86	100	0.66	70	0.84	30	0.06	10	2.38	50	0.06	10	
128	2.16	0.16	80	0.56	60	0.18	30	0.56	10	0	0	0.56	20	0	0	
129	1.46	0.38	100	0.08	10	0.14	20	0	0	0.14	10	0.66	10	0.12	20	
130	5.62	0.48	100	0.58	70	1.58	100	1.36	10	0.08	5	1.32	20	0.06	10	
131	2.04	0.14	90	0.66	70	0.32	80	0.4	10	0.06	10	0.32	20	0.06	10	
132	3.32	0.28	80	0.12	10	0.98	90	0.22	10	0.04	10	1.6	30	0.08	20	
133	4.72	0	0	0	0	0	0	0	0	0	0	4.72	100	0	0	
134	5.16	0.14	100	0.24	40	1.02	100	0.22	10	0.12	10	1.68	30	2.02	40	
135	0.96	0.1	60	0	0	0.16	20	0	0	0	0	0.38	10	0.26	10	
136	3.3	0.12	90	0.14	30	0.54	60	0.2	10	0.08	10	1.82	40	0.44	30	
137	1.64	0.88	90	0.14	20	0.22	50	0	0	0	0	0.7	10	0.1	10	
138	8.14	0.99	100	0.14	20	0.2	20	0.58	10	0.06	10	6.14	100	0.04	10	
139	2.6	0.28	100	0.06	10	0.12	10	0	0	0	0	2.06	50			
140	4.24	0.28	80	0	0	0.06	10	0	0	0	0	3.86	40	0	0	
141	5.44	0.2	100	0.06	10	1.2	100	0	0	0.02	10	3.72	80	0.02	10	
142	6.72	0.5	100	0.28	30	0.58	80	0	0	0.24	10	5.02	100	0.1	10	
143	4.18	0.16	100	0.12	10	1.2	100	0	0	0.02	10	2.68	100	0.06	10	
144	2.74	0.28	100	0.08	10	0.44	40	0	0	0.12	10	1.74	50	0.12	10	
145	7.92	0.22	40	0	0	0	0	0	0	0	0	7.72	100	0	0	
146	5.82	0.32	90	0.72	100	0.62	50	0.74	10	0.18	20	2.66	50	0.52	20	
147	2.34	0.16	80	0.16	10	0	0	0.5	10	0	0	1.12	30	0	0	
148	1.72	0.18	80	0.26	30	0.44	70	0	0	0	0	0.6	60	0.16	10	
149	8.78	0	0	0	0	0	0	0	0	0	0	8.78	100	0	0	
150	1.02	0.04	20	0.06	10	0.34	20	0	0	0.12	10	0.32	20	0.04	10	
151	2.66	0.12	80	0.34	10	0.42	80	0	0	0.08	10	0.84	30	0.9	10	
152	2.46	0	0	0	0	2.46	100	0	0	0	0	0	0	0	0	
153	2.44	0.04	10	0.14	10	0.36	20	0	0	0.02	10	1.08	50	0.54	20	
154	3.02	0.02	10	0	0	0.1	10	2.84	60	0	0	0.04	20	0	0	
155	7.28	0.5	100	0.48	80	0.7	100	1.5	20	0.24	20	3.66	70	0.22	10	
156	4.74	0.3	40	0.06	10	0.94	50	0.18	10	0.12	10	3.12	60	0	0	
157	0.4	0.04	10	0	0	0.37	100	0	0	0	0	0	0	0.02	40	

Table A2: Raw Characterisation data of general waste

158	1.96	0.01	10	0	0	0.02	10	0	0	0.02	10	1.9	70	0	0	
159	1.92	0.26	95	0.18	30	0.36	60	0	0	0.12	2	1.7	30	0	0	
160	4.36	0.32	100	0.42	50	1.78	100	0.82	5	0	0	0.02	1	0.46	40	
161	1.78	0.1	90	0.1	30	0.58	55	0.86	5	0	0	0	0	0.1	1	
162	2.72	0.42	100	0.3	50	0.62	50	0.24	1	0.2	5	1	10	0.06	1	
163	1.24	0	0	0	0	0	0	0	0	0	0	1.24	100	0	0	
164	3.48	0.1	60	0.34	50	0.6	80	1.6	20	0	0	0.84	2	0.02	1	
165	13.52	1.18	100	0.12	2	1.4	60	0.82	5	0.22	5	9.88	98	0.18	1	
166	2.82	0.22	100	0.12	50	0.68	50	0	0	0.66	20	0.36	10	0.52	35	
167	5.84	0.22	100	0.08	5	1.16	85	0.1	1	0.42	20	3.66	50	0	0	
168	4.92	0.2	100	0.32	45	1.14	100	0.8	5	0.14	5	1.78	30	0.28	30	
169	6.44	0.22	80	0.24	90	1.14	100	0.74	5	0.02	2	2.1	40	0.06	2	
170	3.56	0.38	100	0.26	50	0.98	100	0.46	2	0.22	5	1.1	20	0.18	5	
171	5.06	0.2	90	0.28	50	0.02	1	4.48	70	0.14	1	0	0	0	0	
172	1.84	0.14	90	0	0	0.64	70		0	0	0	1.1	40	0	0	
173	1.2	0.64	100	0.04	1	0.16	30	0	0	0.06	2	0.3	5	0	0	
174	2.82	0.22	100	0.18	10	0.6	85	0	0	0.08	5	1	10	0.88	60	
175	6.44	1.22	100	0.12	5	0.42	50	0.6	5	0.02	5	4.04	50	0	0	
176	6.84	0.4	90	0.4	10	0.72	60	0.7	10	0.24	5	3.86	80	0.54	10	
177	4.44	0.42	100	0.02	5	0.38	30	0	0	0	0	3.62	100	0	0	
178	4.4	0.66	100	0.36	30	0.34	50	0.6	20	0.06	5	2.36	60	0	0	
179	2.56	1.68	100	0	0	0.14	100	0	0	0	0	0.46	20	0.2	10	Ida's Valley
180	3.74	0.32	100	0.2	10	0.68	100	0	0	0.32	15	2.14	40	0.08	5	
181	3.52	0.14	100	0.08	5	0.32	100	0.46	5	0.22	10	1.24	20	1	30	
182	2.88	0.7	100	1.48	100	0.08	10	0	0	0	0	0.06	10	0	0	
183	1.06	0	0	0.06	5	0	0	0	0	0	0	0.94	50	0.02	10	
184	2.58	0.08	30	0.2	30	0.04	10	0.22	10	0.2	10	1.74	50	0.04	10	
185	5.94	0	0	0	0	0	0	0	0	0	0	5.94	100	0	0	
186	2.54	0.26	100	0.48	90	0.26	50	0.06	10	0.28	10	0.78	50	0.58	10	
187	2.08	0.8	100	0.18	10	0.12	10	0	0	0.1	10	0.88	10	0	0	
188	7.14	0.32	100	0.6	50	1.62	60	0	0	0.18	10	4.36	80	0	0	
189	4.54	0	0	0	0	0	0	0	0	0	0	4.54	100	0	0	
190	1.56	0.08	100	0.08	5	0.28	80	0.6	20	0.1	20	0.32	10	0	0	
191	5.08	0.26	100	0.64	60	1.14	100	0.34	10	0.12	10	2.38	40	0.42	40	
192	7.72	0.54	100	0.48	60	0.7	50	0	0	0.22	10	5.78	90	0	0	
193	7.84	0.6	100	0.22	60	1.08	95	0.1	10	0.14	10	3.56	70	2.14	50	
194	2.24	0.2	80	0.58	70	0.28	30	0	0	0.1	10	0.92	20	0.08	10	
195	2.02	0.2	90	0.32	60	0.86	100	0	0	0.14	10	0.42	10	0.04	10	
196	7.84	0.52	90	0.54	90	0.78	90	0	0	0.3	10	3.18	90	2.84	60	
197	2.62	0.16	40	0.12	10	0.48	60	0	0	0.1	10	1.46	30	0.34	20	

Table A2: Raw Characterisation data of general waste

198	6.02	0.22	80	0.2	20	0.4	90	0	0	0.32	10	1.04	20	3.88	90	
199	5.28	0.38	100	0.56	90	0.32	30	2.28	40	0.06	10	1.4	30	0.4	80	
200	6.76	0.68	100	0.26	60	0.48	50	1.6	50	0	0	3.68	60	0	0	
201	2.38	0.08	30	0.16	20	0.32	60	0.24	10	0.18	10	1.3	40	0.04	10	
202	5.06	0.06	20	0	0	0.22	20	0	0	0.12	10	2.2	80	2.44	30	
203	3.76	0.06	40	0.14	20	3.54	100	0	0	0	0	0	0	0	0	
204	5.26	0	0	0	0	0	0	0	0	0	0	5.26	100	0	0	
205	5.36	0.88	100	0.12	10	0.8	60	0	0	0.24	10	2.58	20	0.64	40	
206	4.3	0.16	90	0.08	10	0.4	60	0	0	0.16	10	3.46	60	0.04	10	
207	6.44	0.26	90	0.1	10	0.46	60	0	0	0	0	5.34	40	0.26	10	
208	2.38	0.42	90	0	0	0.2	30	0	0	0.14	10	1.64	20	0	0	
209	2	0.34	80	0.1	20	0.56	100	0.28	10	0.1	10	0.56	20	0.06	10	
210	6.96	0.36	100	0.46	80	0.64	100	1.12	20	0.56	30	3.84	100	0.08	20	
211	9.26	0	0	0	0	0	0	0	0	0	0	9.26	100	0	0	
212	4.7	0	0	0	0	0	0	0	0	0	0	4.7	100	0	0	
213	11.3	0	0	0	0	0	0	0	0	0	0	11.3	100	0	0	
214	6.88	0.44	100	0.7	30	1.62	95	0.7	10	0.18	20	3.06	50	0.28	40	
215	9.82	0.38	100	1.28	100	0.68	100	0	0	0	0	3.48	90	4.02	90	
216	4.34	0.66	100	0.4	80	0.64	100	0	0	0.2	10	2.44	90	0	0	
217	6.78	0.14	90	0.88	100	3.24	100	0.5	10	0.3	10	0.78	20	0.96	80	
218	19.26	0	0	0	0	0	0	0	0	0	0	19.26	100	0	0	
219	6.24	1.1	100	0.66	100	0.72	100	0.36	10	0.12	10	3.12	70	0.08	10	
220	6.72	0.6	100	0.16	10	0.72	90	0	0	0.26	20	4.22	80	0.78	30	
221	3.68	0.16	80	0.18	30	0.36	50	0.52	10	0.12	10	2.26	30	0.04	10	
222	4.34	1.46	100	0	0	1.82	100	0	0	0.36	10	0	0	0.66	10	
223	2.62	0.5	100	0.14	10	0.96	100	0.44	10	0.12	10	0.44	50	0	0	
224	7.68	0.5	100	0.5	30	0.52	20	1.58	20	0.26	20	4.26	100	0	0	
225	7.36	0	0	0	0	0	0	0	0	0	0	7.36	100	0	0	
226	1.64	0.06	70	0	0	0.82	80	0	0	0	0	0.68	30	0.02	10	
227	2.16	0	0	0.4	10	0.1	20	0	0	0.28	30	1.36	100	0	0	
228	6.78	0.94	100	0.38	50	0.86	70	2.04	20	0.08	5	2.08	10	0.4	50	Cloetesville
229	6.36	0.68	100	0.22	30	1.22	90	0	0	0.14	10	3.56	90	0.48	40	
230	10.64	0.9	80	0.44	50	1.44	80	4.6	80	0.3	10	1.58	20	1.67	50	
231	5.54	0.6	100	0.34	10	2.16	100	0.14	5	0	0	1.1	30	1.18	70	
232	3.56	0.2	100	0.54	40	0.44	70	0	0	0.18	10	2.22	70	0	0	
233	11.08	0.62	100	0	0	1.14	90	0	0	0.12	5	4.18	50	5.04	90	
234	1.84	0.1	40	0.04	5	0	0	0.26	5	0.1	5	1.18	20	0.12	10	
235	2.16	0.4	90	0.1	5	0.16	10	0	0	0.14	5	1.32	20	0	0	
236	6.82	0.16	80	0.04	5	0.22	60	0	0	0.18	5	5.74	80	0.38	10	
237	2.08	0.4	90	0	0	0.3	20	0	0	0	0	1.3	20	0.08	5	

Table A2: Raw Characterisation data of general waste

238	2.73	0.44	100	0.2	10	0.32	80	0	0	0.14	5	1.62	30	0	0
239	4.86	0.26	100	0.16	60	1.12	80	0.4	10	0.16	10	2.92	100	0	0
240	5.04	1.32	100	0.36	80	0.88	100	0	0	0.08	10	1.5	30	0.92	30
241	7.14	1.1	100	0.26	20	1.1	100	1.06	200	0.24	20	2.86	80	0.6	20
242	3.08	0.58	100	0.54	70	1.36	80	0.46	10	0.18	10	0	0	0	0
243	3.34	0.36	80	0	0	0.48	50	0	0	0	0	1.28	30	1.14	10
244	5.66	0.32	100	0.08	10	0.86	90	2.12	30	0.12	10	1.76	20	0.52	10
245	1.86	0.18	100	0.02	5	1.64	100	0	0	0	0	0	0	0.06	5
246	2.96	0.14	80	0.06	10	0.5	100	0.22	10	0.72	30	0.46	30	0.94	90
247	4.88	0.42	90	0.36	90	0.68	100	0	0	0.52	20	2.78	30	0.24	20
248	4.7	1.04	100	0.24	30	0.56	80	0	0	0.44	20	2.22	40	0.04	10
249	3.86	0.22	80	0.16	40	1.92	100	0	0	0.04	10	1.4	30	0.24	10
250	6.14	0.16	20	0.18	10	0.44	20	0	0	0	0	1.94	40	3.42	80
251	9.52	0.08	20	0	0	0.04	10	0	0	0	0	9.44	100	0	0
252	2.86	0.3	100	0.3	40	0.1	20	0.8	20	0.08	10	1.36	70	0.06	10
253	3.9	0.48	100	0.64	40	1.08	90	0.36	10	0.06	10	0	0	0.9	10
254	5.64	0.2	80	0.22	25	0.58	80	0	0	0.08	10	3.62	40	1.04	30
255	0.8	0.8	100	0	0	0	0	0	0	0	0	0	0	0	0
256	4.62	0.34	100	0.08	10	0.12	20	2.18	20	0.08	10	1.3	10	0.5	5
257	5.78	0.14	40	0.44	80	1.02	90	0	0	0	0	3.92	70	0.22	5
258	6	0.32	100	0.06	10	4.42	100	0	0	0	0	1.78	75	0.06	5
259	1.48	0.14	80	0.04	10	0.06	20	0	0	0.02	5	1.16	60	0	0
260	1.18	0.01	20	0.4	50	0.16	20	0	0	0	0	0.58	50	0	0
261	4.3	0.18	40	0.1	10	0.28	40	0	0	0.54	10	2.04	5	1.08	50
262	3.04	0.56	100	0.02	5	0.7	80	0	0	0.06	5	1.58	30	0.02	5
263	4.06	0.22	80	0.08	5	1.3	100	0	0	0.28	10	1.82	50	0.44	40
264	7.32	0.46	100	0.12	15	1.28	100	0	0	0.16	5	0.96	20	4.36	100
265	10.66	0.8	100	0.06	5	1.8	80	0.14	5	0.26	10	7.86	110	0.6	20
266	1.94	0.28	80	0.02	100	0.44	80	0.12	10	0.18	20	0.86	30	0.04	10
267	12.54	0.12	10	0.94	100	8.76	100	0.1	10	0.08	10	2.42	50	0.1	10
268	3.92	0.12	40	0	0	0.36	40	0	0	0.01	10	3.18	100	0.2	20
269	2.18	0.28	80	0.06	10	0.38	50	0.14	10	0	0	1.3	40	0	0
270	12.44	0	0	0	0	0	0	0	0	0	0	12.44	100	0	0
271	1.94	0.2	80	0.08	10	0.32	50	0	0	0.06	10	1.02	50	0.24	10
272	11.2	0.92	100	0.16	30	1.44	100	0.2	10	0.1	10	8.18	100	0.2	20
273	4.74	0.18	80	0.1	10	2.14	70	0.8	20	0.4	30	0.78	20	0.38	10
274	2.48	0.18	90	0.58	20	0.72	90	0	0	0.06	10	0.82	20	0.08	30
275	4.52	0.56	100	0.12	10	0.86	90	0.24	10	0.06	10	2	40	0.5	50
276	15.2	0.16	90	0.18	20	0.3	30	0.46	10	0	0	14.04	100		
277	4.92	0.62	100	0.26	100	0.72	100	0.06	10	0.3	20	2.2	50	0.66	80
278	3.68	0.24	70	0.2	40	0.86	100	1.34	10	0.1	10	0.86	10	0.06	10

Table A2: Raw Characterisation data of general waste

279	5.54	0.22	100	0.22	50	0.42	80	0.44	10	0.06	10	0.8	20	3.36	80	
280	2.68	0.2	100	0.48	100	0.6	100	0.62	20	0.1	20	0.66	20	0	0	Jamestown
281	6.02	0.12	80	0.28	40	1.64	100	0	0	0.1	5	3.72	80	0.1	5	
282	3.62	0.16	100	0.44	80	0.72	100	0.1	5	0.06	5	2.06	80	0.02	20	
283	1.86	0.2	50	0.4	70	0.14	30	0	0	0.38	20	0.52	20	0.16	30	
284	3.34	0.28	80	0.58	100	0.98	100	1.42	70	0	0	0.06	5	0.08	10	
285	4.74	0.3	100	0.24	20	0.46	80	1	30	0	0	2.6	10	0.04	5	
286	0.7	0.2	100	0.06	10	0.22	50	0	0	0.08	10	0	0	0.2	40	
287	2.66	0.16	70	0.12	10	0.96	100	0	0	0.08	10	1.38	40	0.06	10	
288	9.38	0.4	80	0.28	15	0.5	80	0	0	0.42	10	2.88	100	4.94	80	
289	9.46	0.24	40	0.18	10	2.56	100	4	60	0.08	10	0.62	10	1.82	40	
290	9.28	0.5	50	0	0	1.86	80	0	0	0.04	10	2.18	40	4.74	90	
291	5.46	0.44	100	0.7	30	1.32	80	0.14	10	0.38	10	1.92	30	0.22	10	
292	14.46	0.34	100	0.04	10	0.72	90	0.32	10	0.1	10	8.72	100	4.2	80	
293	10.1	0.2	30	0.26	30	1.68	50	0.8	20	0.06	10	4.16	100	2.88	60	
294	5.42	0.36	100	0.4	50	0.86	100	0.38	10	0.38	30	2.72	70	0.44	50	
295	4.14	0.1	40	0.56	30	0.04	10	1.2	30	0.12	10	1.96	50	0	0	
296	2.34	0.08	40	0.12	10	0.4	50	0.3	5	0.04	5	1.3	50	0.1	5	
297	2.88	0.12	80	0.52	100	0.26	40	0.12	5	0.08	20	1.46	30	0.28	20	
298	2.44	0.14	100	0.6	100	0.88	100	0.8	10	0	0	0	0	0	0	
299	3.4	0.34	80	0.74	20	0.36	30	0.32	10	0	0	1.32	20	0.18	10	
300	4.1	0.26	100	0.2	50	0.7	100	0	0	0.22	10	2.76	20	0.02	10	
301	1.58	0.14	90	0.02	10	0.76	100	0	0	0.26	20	0.46	10	0	0	
302	3.1	0.22	80	0.22	10	0.64	80	0	0	0.08	10	0.5	10	1.04	20	
303	4.7	0.5	100	0.28	50	1.16	100	0.56	10	0.32	20	1.96	30	0	0	
304	4.28	0.58	100	0.46	100	0.5	100	0.64	10	0.26	10	1.9	40	0.12	20	
305	6.12	0.84	100	0.22	20	0.66	100	0	0	0.12	30	3.74	50	0.46	30	
306	5.42	0.32	100	0.6	100	0.5	70	0.86	10	0.08	10	3.1	80	0.08	10	
307	6.34	0.58	100	0.42	40	0.74	100	0	0	0.08	10	2.56	25	1.8	25	
308	4.72	0.1	10	0.04	10	0.64	50	0.04	5	0.04	5	3.86	100	0.06	5	
309	6.66	0.02	10	0.2	10	0.38	40	0.36	5	0.58	50	5.1	100	0	0	
310	1.84	0.06	10	0.52	90	0.32	50	0.12	5	0.4	40	0	0	0.44	20	
311	3.46	0.1	10	0.48	50	0	0	0.68	10	0.06	5	2.32	40	0.04	5	
312	3.88	1.48	100	0.2	10	0	0	0	0	0.06	5	1.72	30	0.18	5	
313	2.36	0.08	20	0.08	5	0.64	90	0	0	0.24	10	1.18	100	0.1	5	
314	5.02	0.1	10	0.34	50	1.2	100	2.18	30	0.48	30	0.72	10	0	0	
315	4.26	0.54	100	0.3	30	0.44	50	0.26	5	0	0	2.62	100	0.1	5	
316	4.2	0.42	50	0.1	10	0.04	10	0	0	0.06	5	3.68	100	0.1	5	
317	5.54	0.46	50	0.15	30	0.8	90	3.04	50	0.12	10	0	0	0.97	5	
318	5.62	0.1	5	0.08	5	0.22	10	0.46	5	0.26	10	0.46	20	4.12	100	

Table A2: Raw Characterisation data of general waste

319	2.64	0.18	20	0.24	10	0.32	10	0	0	0.5	20	1.3	100	0.12	5	
320	5.84	0.06	10	0.62	40	0.14	10	1.08	20	0.36	20	3.46	100	0	0	
321	6.94	0.28	50	0.92	60	0.42	100	1.32	10	0	0	1.98	50	1.42	40	
322	2.64	0.06	10	0	0	0	0	0.46	5	0.3	10	1.5	50	0.12	10	
323	4.58	0.22	20	0.28	5	0.04	5	0.52	5	1.85	100	1.12	40	0.4	5	
324	5.16	0.3	50	0.12	10	0.4	5	0	0	0.02	5	4.26	100	0	0	
325	3.08	0.32	50	0.72	40	0.38	100	0.74	10	0.08	5	0.76	10	0.02	5	
326	3.9	0.34	100	0.72	90	0.54	100	0.16	10	0.38	20	1.26	20	0.56	40	Welgevonden
327	3.74	0.82	100	0.4	40	0.88	80	0	0	0	0	1.54	30	0	0	
328	2.84	0.4	100	0.3	10	1.02	90	0	0	0.3	10	0.76	10	0	0	
329	5.36	0.26	80	0.42	40	0.42	90	0	0	0.14	20	3.92	100	0.26	30	
330	3.26	0.3	90	0	0	0.24	20	0.46	10	0.06	10	2.18	20	0	0	
331	2.88	0.22	50	0.36	30	0.7	80	0.42	10	0.1	20	1.1	30	0.08	10	
332	7.26	0.7	90	0.52	40	1.62	100	0.34	10	0.12	10	3.26	40	0.62	20	
333	1.56	0.06	20	0.1	10	0.12	20	0	0	0.1	10	1.3	20	0	0	
334	7.78	0.36	80	0.24	30	0.82	20	1.92	30	0.64	15	3	50	0.94	20	
335	5.2	0.52	100	0.4	30	0.44	80	0	0	0.36	20	3.02	30	0.42	10	
336	5.7	0.94	100	0.7	90	0.8	100	1.7	20	0.36	10	0.82	20	0.54	20	
337	2.42	0.14	50	0.08	5	0.04	5	0	0	0	0	1.78	40	0.36	5	
338	1.94	0.14	50	0.1	10	0.14	30	0	0	0	0	0.78	30	0.72	5	
339	1.64	0.24	80	0	0	0.18	20	0	0	0.02	5	0.98	20	0.16	20	
340	1.66	0.04	40	0.14	5	0.42	80	0	0	0.06	5	0.86	40	0.14	5	
341	5	0.34	80	0.56	60	0.18	20	0.4	10	0.1	5	2.58	30	0.8	20	
342	3.9	0.32	80	0.24	40	0.34	20	0.74	10	0.38	10	1.66	20	0.16	10	
343	3.14	0.26	100	0.06	5	0.38	30	0	0	0	0	2.32	90	0.1	10	
344	7.26	0.1	50	0.74	80	0.96	100	0	0	0	0	4.36	100	1.12	30	
345	5.1	0.32	100	1.4	100	1.48	100	0.32	20	0.16	20	1.44	30	0.08	10	
346	4.74	0.3	80	0.2	30	2.46	100	0	0	0	0	1.68	60	0.16	10	
347	8.86	0.32	90	0.16	40	0.68	50	1.16	20	0.3	20	2.64	50	4.24	100	
348	2.88	0.44	100	0.62	50	0.68	100	0	0	0.14	20	0.5	20	0.06	10	
349	1.62	0.14	60	0.16	20	0.28	40	0	0	0	0	0.74	50	0.36	20	
350	7.38	0.5	100	0.26	30	0.58	80	2.18	40	0.3	20	3.38	80	0.2	30	
351	3.54	0.28	100	0.06	10	0.52	50	1.38	30	0.06	10	1.18	50	0.1	20	
352	3.86	0.24	100	0.12	20	0.66	80	0.42	20	0.1	10	1.12	40	1.26	60	
353	4.12	0.12	20	0.06	10	0.34	40	0	0	0.02	10	1.22	40	2.38	60	
354	3.1	0.22	80	0.52	80	0.64	80	0	0	0.12	10	1.6	60	0	0	
355	5.24	0.18	50	0.06	10	0.22	20	0	0	0.16	10	4.62	100	0.04	10	
356	0.5	0.28	60	0	0	0.14	20	0	0	0	0	0.12	10	0	0	
357	2.68	0.36	100	0.04	10	0.42	90	1.4	15	0	0	0.56	40	0	0	
358	2.1	0.1	40	0.06	10	0.4	40	0	0	0.24	10	1.26	20	0.12	10	

Table A2: Raw Characterisation data of general waste

359	1.16	0.3	90	0.1	10	0.46	80	0	0	0.06	10	0	0	0.3	10	
360	2.42	0.52	40	0	0	0.1	20	0	0	0.48	10	1.08	40	0.28	10	
361	9.1	0.14	10	0	0	0.72	40	0	0	0.04	10	3.44	70	4.54	70	
362	2.38	0.04	10	0.12	10	0.9	100	0	0	0	0	1.28	90	0.08	10	
363	3.7	0.84	100	0	0	0.12	10	0	0	0.3	10	2.48	60	0.12	10	
364	6.88	0.56	100	0.14	10	0.36	50	0.62	10	0.08	10	0	0	5.24	40	
365	2.72	0.04	50	0.16	50	1.38	100	0	0	0	0	0.72	40	0.3	40	
366	2.12	0.08	100	0.38	100	0.64	100	0.26	5	0.1	10	0.6	30	0	0	
367	11.58	0	0	0	0	0	0	0	0	0	0	11.58	100	0	0	
368	1.71	0.04	50	0.1	20	0.24	50	0	0	0.08	20	1.14	20	0	0	
369	2.7	1.78	100	0.16	20	0.52	30	0	0	0.1	10	0	0	0.02	5	
370	1.3	0.06	10	0	0	0.1	50	0	0	0	0	1.1	100	0.08	5	
371	1.52	0.08	10	0.1	20	0.5	60	0.24	5	0.02	5	0.5	20	0	0	
372	1.68	0.2	80	0.08	20	0.52	100	0	0	0.29	20	0.44	20	0	0	
373	2.14	0.2	10	0.38	50	0	0	1.22	60	0.32	20	0	0	0.02	5	
374	0.42	0.12	10	0.1	50	0.1	10	0	0	0.04	5	0	0	0.02	5	
375	19.8	0	0	0	0	0	0	0	0	0	0	19.8	100	0	0	
376	3.4	0.18	100	0.5	10	0.46	60	0	0	0	0	1.62	50	0.82	30	
377	4.38	0.36	100	0.68	100	0.38	70	0	0	0.08	5	2.82	50	0.1	10	
378	1.88	0	0	0	0	0	0	0	0	0	0	1.28	100	0.66	20	
379	4.7	0.12	90	0.22	20	0.86	90	0.3	10	0	0	1.98	30	1.34	50	Simonswyk - Uniepark
380	1.06	0.16	90	0.06	10	0.46	80	0	0	0	0	0.42	20	0	0	
381	1.52	0.06	20	0.18	30	0.46	100	0	0	0.14	10	0.72	30	0.04	10	
382	3.48	0.14	90	0	0	0.6	90	0	0	0	0	2.6	80	0.12	10	
383	0.72	0.06	30	0.02	10	0.16	30	0	0	0.03	0	0.38	50	0.05	10	
384	1.62	0.16	90	0	0	0.34	30	0	0	0	0	1.04	30	0	0	
385	5.44	0.92	100	0.4	50	0.92	100	0	0	0.42	30	2.5	50	0	0	
386	4.74	0.8	100	0.7	30	0.46	50	0.28	5	0.28	10	0.88	10	1.42	60	
387	5.28	0.18	80	0.28	30	3.62	100	0	0	0.04	5	1.14	40	0	0	
388	2.4	0.42	80	0.36	30	0.9	60	0	0	0.1	5	0.58	60	0.04	5	
389	5.64	0.04	5	0.05	5	0.04	5	0.46	5	0	0	4.98	50	0	0	
390	3.46	0.1	80	0.6	50	0.32	10	0	0	0	0	2.24	40	0.2	10	
391	2.5	0.1	30	0.22	20	0.9	100	0	0	0	0	0.98	50	0.32	50	
392	6.8	0.4	100	0.08	10	1.72	100	0	0	0.18	20	4.16	90	0.2	10	
393	7.96	0.62	100	0.12	10	0.7	90	0	0	0.36	30	1.76	30	4.46	90	
394	3.22	0.2	100	0.16	10	1.42	100	0	0	0.06	5	0.64	10	0.78	20	
395	1.08	0.1	10	0.02	5	0.32	50	0	0	0.06	10	0.34	40	0.26	10	
396	2.24	0.28	30	0.04	5	0.18	10	0.14	5	0.04	10	1.42	10	0.12	10	
397	2.76	0.16	100	0.4	90	1.52	100	0	0	0.58	20	0	0	0.04	10	
398	1.6	0.12	90	0.08	10	0.94	100	0	0	0	0	0	0	0.42	10	

Table A2: Raw Characterisation data of general waste

399	3.74	0	0	0	0	0	0	0	0	0	0	3.74	300	0	0	
400	5.46	0.46	100	0.34	90	0.22	10	0.96	10	0.14	10	3	25	0.36	20	
401	3.84	0.18	60	0.22	20	0.76	90	0.34	5	0.02	3	1.74	20	0.5	5	
402	3.18	0.2	80	0.1	10	0.4	80	0.78	10	0.64	20	0.94	15	0.08	5	
403	4.08	0.3	80	0.14	10	0.72	80	0.7	10	0.08	5	2.24	40	0	0	
404	4.3	0.24	80	0.22	30	0.3	40	0	0	0.1	5	2.52	60	0.98	70	
405	5.56	0.1	80	0.16	10	0.16	10	0	0	0.08	3	1.68	30	3.38	70	
406	2.4	0.1	50	0.06	5	0.16	20	0	0	0.12	10	1.62	20	0.36	5	
407	4.38	0.32	100	0.32	40	0.42	30	0.24	5	0.06	5	3.02	100	0	0	
408	2.08	0.14	85	0.26	40	0.52	50	0	0	0.02	10	1.12	50	0	0	Die Boord
409	3.72	0.18	70	0.2	40	0.34	60	0	0	0	0	2.34	80	0.52	40	
410	1	0.1	90	0.02	10	0.34	50	0	0	0	0	0.48	10	0.02	10	
411	4	0.4	100	0.34	80	0.54	100	0.32	10	0.16	10	2.04	30	0.08	10	
412	2.74	0.08	40	0.24	20	0.42	95	1.54	10	0.02	10	0.3	10	0.14	10	
413	1.28	0.1	90	0.12	50	0.06	10	0.34	10	0.04	10	0.5	10	0.08	10	
414	2.7	0.16	90	0.18	70	0.84	100	0	0	0.1	10	1.4	30	0	0	
415	5.22	0	0	0	0	0	0	0	0	0	0	5.22	300	0	0	
416	3.46	0.42	100	1.06	120	0.76	80	0.16	10	0.04	10	0.92	10	0.06	10	
417	7.68	0	0	0	0	0	0	0	0	0	0	7.68	300	0	0	
418	3.28	0.14	80	0.1	10	0.36	70	0	0	0.16	10	2.44	75	0.04	10	
419	6.04	0	0	0	0	0.04	10	0	0	0	0	6	300	0	0	
420	2.44	0.22	100	0.34	75	0.64	70	0	0	0.06	10	1.06	10	0.08	10	
421	2.36	0.18	80	0.02	10	0.36	70	0	0	0	0	1.62	20	0.14	10	
422	1.68	0.24	70	0.04	10	0.1	10	0	0	0	0	1.24	10	0	0	
423	1.58	0.4	90	0.48	80	0.28	75	0	0	0.04	10	0.2	10	0.12	10	
424	2.12	0.18	90	0.66	100	0.68	90	0	0	0.06	5	0.32	10	0.16	50	
425	6.84	0.28	100	0.28	70	0.76	100	4.14	70	0.14	5	1	50	0.04	5	
426	3.58	0.36	80	0.12	10	0.88	100	0.62	10	0.12	10	1.06	30	0.4	40	
427	3.56	0	0	0.16	50	0.26	50	0	0	0.06	5	2.8	80	0.26	5	
428	3.86	0.18	80	1.28	100	1	100	0	0	0.4	10	0.58	10	0.34	30	
429	3.28	0.24	100	0.14	10	1.04	100	0.32	5	0.16	10	1.38	30	0	0	
430	13.36	0	0	0	0	0	0	0	0	0	0	13.36	500	0	0	
431	6.42	0.28	70	0.08	5	0.86	80	0.36	5	0.06	5	4.72	70	0	0	
432	1.9	0.16	50	0.2	10	0.22	30	0	0	0.06	5	1.18	30	0.08	5	
433	2.42	0.2	80	0.04	10	0.3	60	0.24	5	0.4	50	1.16	20	0.04	5	
434	2.92	0.16	50	0.12	10	0.24	50	0.14	5	0	0	0.82	20	1.34	10	
435	3.12	0.5	80	0.28	10	0.32	50	0.18	5	0.06	10	1.58	30	0.02	5	
436	3.44	0	0	0	0	0	0	0	0	0	0	3.44	200	0	0	
437	2.16	0.18	50	0	0	0.16	10	0	0	0	0	1.7	40	0	0	
438	4.62	0.56	100	0.38	50	0.68	100	0.06	5	0.18	5	1.84	50	0.56	30	

Table A2: Raw Characterisation data of general waste

439	5.52	0	0	1.7	50	0.88	50	0	0	0	0	1.88	100	0.56	30	
440	4.14	0.36	100	0.14	10	1	80	0	0	0.16	30	2.18	80	0	0	
441	5.78	0.22	100	0.08	10	0.24	15	0	0	0	0	4.3	80	0.96	100	
442	4.8	0.34	100	0.36	50	0.62	20	0	0	0.86	50	2.48	90	0.22	20	
443	1.9	0.28	100	0.24	20	1	80	0.24	10	0	0	0.2	10	0	0	
444	4.78	0	0	0	0	0	0	0	0	0	0	4.78	100	0	0	
445	4	0.22	50	0.08	5	0.24	30	0	0	0.02	5	1.48	100	2.02	50	
446	5	0.4	80	0.32	40	0.26	50	0.82	5	0.08	5	2.98	80	0.1	5	
447	6.68	0.08	5	0.26	30	0.46	60	2.97	60	0	0	1.98	30	0	0	
448	7.64	0	0	0	0	0	0	0	0	0	0	7.64	100	0	0	
449	4.22	0.08	20	0	0	0	0	0	0	0	0	4.12	90	0	0	
450	2.96	0	0	0	0	0	0	0	0	0	0	2.96	100	0	0	
451	0.66	0.1	20	0.4	80	0.18	30	0	0	0	0	0	0	0	0	
452	0.64	0	0	0	0	0	0	0	0	0	0	0	0	0.64	100	
453	1.36	0.01	10	0.01	10	0.01	10	0	0	0	0	1.28	90	0	0	
454	2	0.02	10	0.18	30	0	0	0	0	0	0	0.5	30	1.32	80	
455	1.66	0.26	90	0.12	20	0.54	40	0.72	20	0	0	0	0	0	0	
456	4.76	0.4	100	0.2	10	0.5	80	0.46	10	0.14	30	2.98	100	0.06	20	
457	2.94	0.06	50	0.02	10	0.5	20	0	0	0	0	1.98	80	0.28	20	
458	2.66	0.44	100	0.38	70	0.88	100	0.28	5	0.22	10	0	0	0.5	100	
459	3.32	0.26	100	0.42	90	0.54	50	0	0	0.28	15	1.84	60	0	0	
460	5.92	0.14	50	0.28	10	2.36	100	0	0	0.02	5	0.62	20	2.44	100	
461	6.18	0.76	50	0	0	0.5	50	0.08	5	0	0	1.3	20	3.42	20	Enkeneni
462	10.92	0.64	80	0.32	20	0.44	20	0	0	0.34	50	5.65	100	3.5	100	
463	6.42	1.84	100	0.72	50	0.26	50	0	0	0.42	20	2.22	50	0.5	20	
464	6.96	0.4	20	0.08	20	1.3	20	0.22	10	0.14	10	3.74	50	1.02	10	
465	7.82	0.34	10	0.22	10	0.78	10	0	0	0.06	0.5	5.3	100	1.2	20	
466	9.56	0.66	100	0.06	5	0.74	20	0	0	0	0	7.12	100	1.08	20	
467	6.4	0	0	0	0	0	0	0	0	0	0	6.4	100	0	0	
468	4.18	0.38	10	0.2	30	0.44	20	0	0	0.1	20	0.64	20	2.42	80	
469	9.76	0.24	5	0.36	10	0.16	10	0	0	0.22	20	8.26	100	0	0	
470	9.5	0.64	100	0.2	10	0.7	80	0.28	10	0.34	10	2.92	30	4.4	100	
471	8.02	0.3	20	0.34	30	0.68	20	0.46	10	0.48	10	5.7	50	0	0	
472	8.78	0.82	100	0.22	15	1.22	20	0.18	5	0.1	5	2.3	20	4.04	80	
473	15.4	0.68	80	0.16	5	0.06	5	0.22	5	0	0	12.9	100	1.44	20	
474	15.16	0.26	5	0.16	5	0.08	5	0	0	0	0	14.66	100	0	0	
475	15.36	0	0	0	0	0	0	0	0	0	0	15.36	100	0	0	
476	9.34	0.14	20	0.3	70	0.2	10	0	0	0.1	10	0.38	10	8.18	120	
477	1.98	0.4	100	0.18	10	1.12	100	0	0	0	0	0.18	10	0	0	
478	7.64	0.84	90	0.14	10	0.66	75	0.14	10	0.5	10	4.24	50	1.02	20	

Table A2: Raw Characterisation data of general waste

479	6.42	0.74	100	0.68	80	0.88	20	0.12	10	0.12	10	2.14	30	1.62	80
480	9.64	0.8	50	0.06	10	0	0	0.08	10	0	0	8.02	200	0.64	10
481	3.74	0.62	90	0.42	70	0.3	70	0.58	10	0.42	10	0.96	10	0	0
482	1.4	0.14	100	0.1	10	0.24	10	0.18	10	0	0	0.18	10	0.52	10
483	2.18	0.6	100	0.14	10	1.12	100	0	0	0	0	0.18	10	0.1	10
484	13.16	1.62	100	0.52	60	1.06	50	0.52	10	0.1	10	8.14	100	1.1	50
485	11.26	1.94	100	0.32	50	0.68	75	0.14	10	0.18	10	8.38	100	0.86	20
486	12.6	0.54	100	0.08	10	0.24	30	0.24	10	0.4	10	1.32	20	8.28	120
487	8.8	0.16	20	0.4	50	1.88	50	0	0	0.66	5	2	50	3.66	70
488	5.32	0.78	100	0.7	70	0.44	50	0.64	5	0.3	5	1.02	10	1.4	20
489	9.32	0.34	100	0.5	100	0.44	40	1.06	10	0.24	5	5.54	100	1.14	50
490	6.38	0.32	80	0.14	30	2.08	90	0	0	0.3	5	1.66	20	1.84	50
491	3.58	0.22	50	0.58	100	0.48	60	0	0	0.16	5	1.82	30	0.22	10
492	6.1	0.98	100	0.24	20	0.64	60	0	0	0.38	10	2.7	40	1.1	70
493	12.84	0.34	80	0.36	20	0.1	5	2.94	40	0	0	8.66	80	0.42	10
494	6.54	0.54	80	0.62	70	1.04	40	0.76	5	0.54	10	2.16	30	0.74	20
495	10.68	0	0	0	0	0	0	0	0	0	0	0	0	10.68	100
496	10	0.76	100	0.3	50	0.7	40	0.36	5	0.3	10	4.78	40	2.66	50
497	6.66	0.16	50	0.48	50	0.34	10	0.3	10	0.06	10	5	100	0.28	20
498	10.82	0.16	5	0.24	10	0.34	10	0	0	0	0	7.4	100	2.66	60
499	9.2	0.44	80	0.3	40	0.96	90	1.06	20	0.54	50	4.92	100	0.86	20
500	13.46	0.28	30	0.34	20	0.54	20	0.66	10	0.42	30	6.06	100	5.02	100
501	11.56	0.82	100	0.92	90	0.76	40	0.62	10	0.92	20	5.26	100	2.02	90
502	9.56	1.72	100	0.16	5	2.18	100	0.64	2	0.26	5	3.8	100	0.84	10
503	10.16	0.96	100	0.32	20	0.94	10	0.32	5	0.32	10	4.1	40	3.24	90
504	5.66	0.64	100	0.4	20	0.6	90	0.68	5	0.66	20	2.44	50	0.36	10
505	11.7	1.7	100	0.34	20	2.06	100	0	0	0	0	5.72	60	1.82	20
506	9.32	1.22	100	0.36	40	0.62	60	0.92	5	0	0	6	90	0.12	5
507	9.98	1.94	100	0.04	2	0.42	20	0.04	50	0.22	5	4.94	60	2.42	30
508	8.6	0.72	100	1.66	100	0	0	0	0	0.22	5	6.04	100	0	0
509	11.54	1.36	100	0.42	80	1.18	90	0	0	0.1	2	7.6	90	0.96	20
510	11.26	2.68	100	0.5	20	2	100	0.42	2	0	0	5.28	90	0.22	5
511	14.3	1.06	100	0.38	30	1.62	100	0	0	0.32	5	6.92	90	3.6	80
512	4.72	0.2	80	0.1	20	0.62	50	0.06	10	0.22	10	3.36	100	0	0
513	9.3	0	0	0	0	0	0	0	0	0	0	9.3	100	0	0
514	9.46	0.74	90	0.5	30	0.24	20	0	0	0	0	4.2	90	3.78	50
515	15.52	0.02	10	0.24	40	0.16	30	0	0	0.02	10	14.38	400	0	0
516	4.52	0.5	100	0.1	5	0.54	70	0.14	5	0	0	2.06	90	0.98	
517	7.4	0.96	100	0.36	20	0.64	80	0.24	25	0.3	20	4.38	100	0.52	
518	5.98	0.18	30	0.6	50	0.44	60	0	0	0.28	25	4.5	100	0	
519	6.4	0.18	30	0.56	50	0.26	40	0	0	0	0	5.08	100	0.32	

Table A2: Raw Characterisation data of general waste

	520	1.86	0.08	5	0.12	10	1.36	100	0	0	0	0	0	0	0	
	521	7.52	0.08	5	2.4	100	0.12	10	0.52	50	2.16	100	1.18	100	0.54	
	522	11.56	0.82	100	0.24	25	0.14	10	0.38	40	0.4	30	9.58	100	0	
	523	4	0.34	90	0.32	70	0.32	20	0.46	10	0.62	10	1.12	20	0.62	10
	524	2.26	0.26	90	0	0	0.14	40	0	0	0.34	10	0.32	10	1.24	10
	525	5.56	0.62	100	0.3	60	1.24	100	0.44	10	0.24	10	1.88	30	0.88	50
	526	5.16	0.26	100	0.24	60	1.7	100	0.46	10	0.08	10	2.42	40	0	0
	527	2.56	0.22	80	0.08	40	0.1	10	0	0	0.12	10	1.7	20	0.86	20
	528	4.2	0.28	80	0.14	10	0.2	30	2.48	30	0	0	1.12	10	0	0
	529	6.7	3.8	100	0	0	1.86	100	0	0	0	0	0.86	5	0.22	5
	530	6.82	0.84	100	0.46	80	1.54	100	0.44	5	0.2	5	3.36	50	0.08	5
	531	6.6	0.64	100	0.58	80	0.78	100	0.28	5	0.12	5	3.18	30	1.06	10
	532	5.38	0.68	100	0.32	30	0.84	100	0.42	5	0.22	5	2.88	50	0	0
	533	5.16	0.32	50	0.06	10	0.4	5	0	0	0	0	4.48	50	0	0
	534	11.78	0.58	80	0.4	60	1.38	100	0	0	0.02	5	4.7	90	4.66	80
	535	1.5	0.52	100	0	0	0.96	100	0	0	0	0	0	0	0	0
	536	6.6	0.64	100	0.44	40	0.8	100	0.98	5	0.08	5	2.44	30	0.98	20
	537	2.88	0.42	100	0.2	40	0.28	20	0	0	0	0	1.8	20	0.14	10
	538	8.28	0.1	40	0.12	40	1.06	60	6.06	70	0.26	10	0	0	0.6	20
	539	5.06	0.36	60	0.32	20	0.06	5	0	0	0.08	5	3.56	60	0.54	10
	540	13.26	0.12	40	0.32	30	0.3	20	0	0	0	0	10.46	100	1.74	80
	541	8.7	1.48	80	0.54	80	1.24	50	0	0	0.1	5	3.46	100	1.92	50
	542	9.42	0.26	80	0.12	10	0.78	80	0.04	5	0.06	5	4.06	100	4.06	80
	543	2.42	0.3	80	0.22	50	0.26	50	0	0	0.08	5	0.98	50	0.44	50
	544	9.58	0.7	100	0.16	30	1.14	50	0	0	0.12	5	4.66	100	2.74	100
	545	2.82	0.56	100	0.28	10	0.22	20	0.18	5	0	0	1.12	50	0	0
	546	6.24	0	0	0	0	0	0	0.02	5	0	0	4.64	100	1.36	20
	547	13.84	0.34	50	0.48	40	0.3	40	0.38	5	0.14	5	11	100	0.5	30
	548	3.22	0.14	10	0	0	0.34	50	0	0	0.02	5	2.58	100	0	0
	549	3.56	0.1	20	0.12	20	0.14	20	0	0	0.24	20	1.1	30	1.96	40
	550	6.76	0.54	100	0.34	80	0.68	50	0.1	10	0	0	4.64	100	0.42	10
	551	4.4	0.48	100	1.06	90	0.36	40	0.74	10	0.04	10	1.1	40	0.64	10
	552	11.2	0.38	80	0.66	50	0.34	30	0	0	0	0	7	100	2.86	90
	553	2.78	0.8	40	0.7	10	0.88	20	0	0	0	0	2.4	20	0.72	10
	554	4.82	0.52	100	0.72	100	0.24	50	0.36	10	0.08	10	2.26	30	0	0
Total		2740.28	190.35		147.49		348.70		195.29		70.33		1452.67		320.10	
Average		4.95	0.34		0.27		0.63		0.35		0.13		2.62		0.58	

Kayamandi

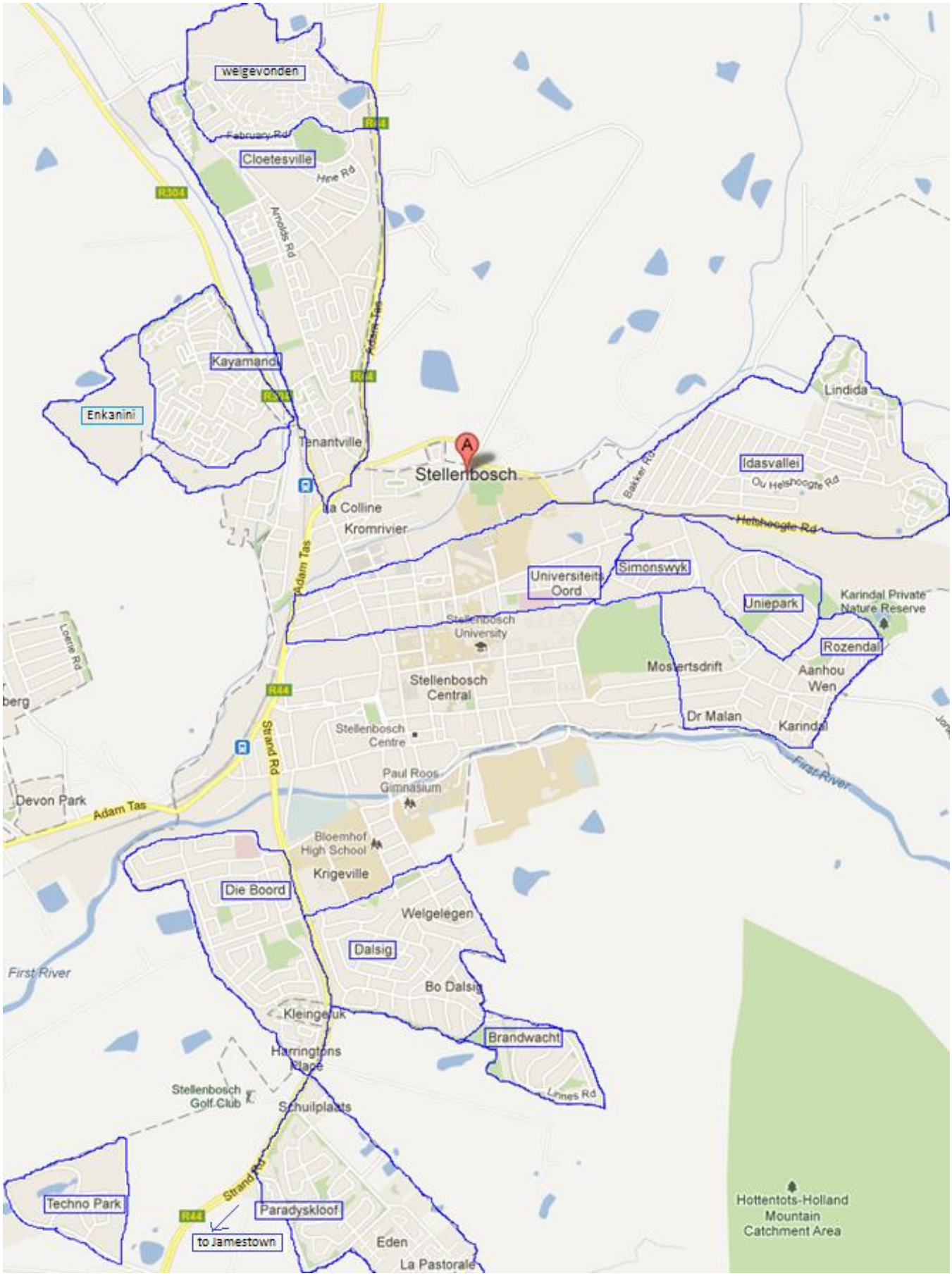

Figure A1: Map of Areas in Stellenbosch Municipality

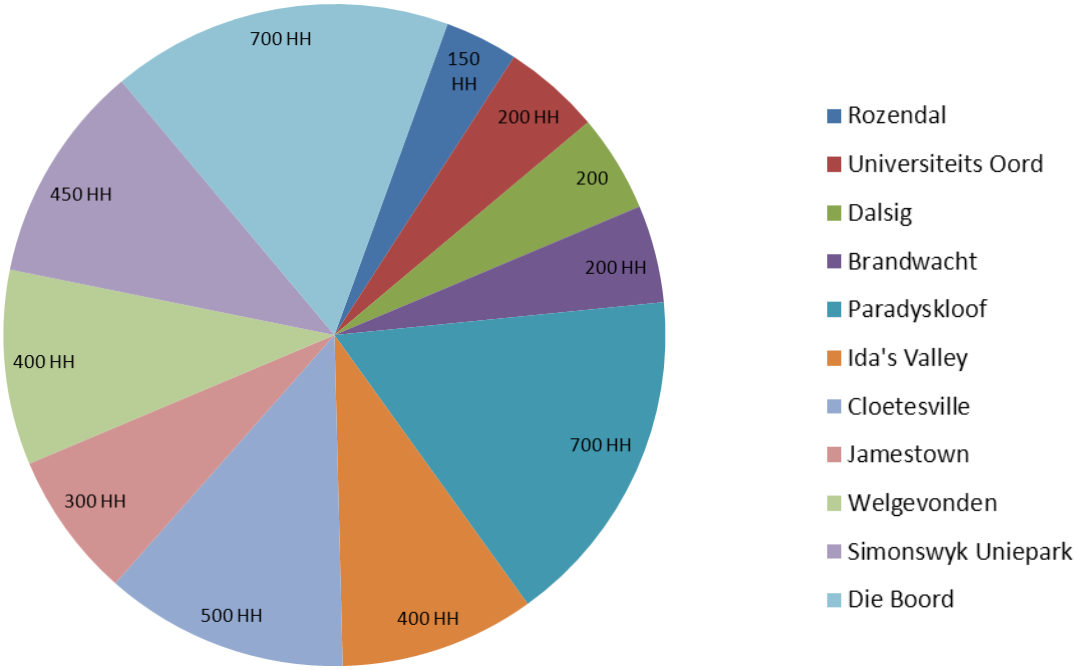

Figure A2: Household per Area Distribution

It is important when comparing the compositions of the waste per area as well as the volumes of waste to have an idea of the number of households in each area sampled; this is depicted in Figure A2. The population density per area is also given in Table A3.

Table A3: Population Density per Area

Area	No. of HH	Area (km^2)	Population Density (HH/km^2)
Rozendal	150	0.802	187
Universiteits Oord	200	1.065	188
Dalsig	200	0.826	242
Brandwacht	200	0.199	1005
Paradyskloof	700	1.026	682
Ida's Valley	400	1.284	312
Cloetesville	500	2.017	248
Jamestown	300	0.601	499
Welgevonden	400	0.75	533
Simonswyk/Uniepark	450	0.642	701
Die Boord	700	0.868	806

Appendix B: Comparison of TGA and DTG at different HR

B1: Paper TGA and DTG comparisons

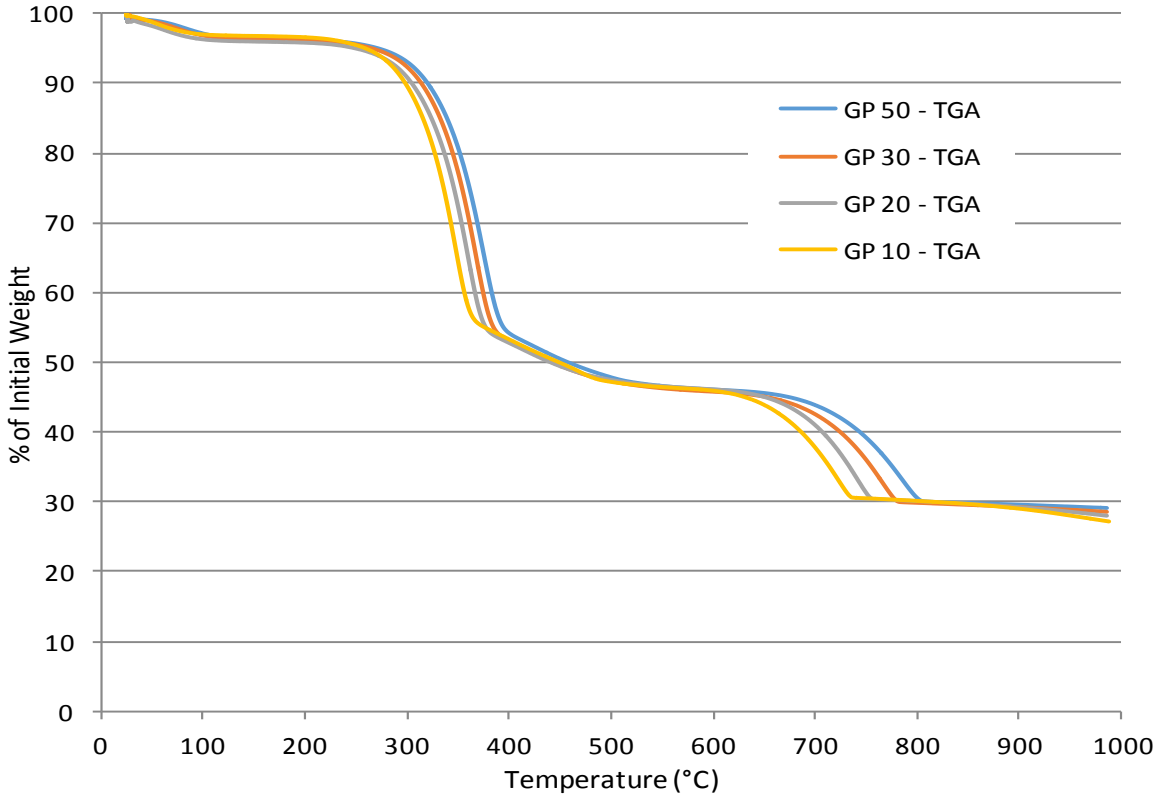

Figure B.1.1: Comparison of Weight loss of Glossy Paper at Different Heating Rates

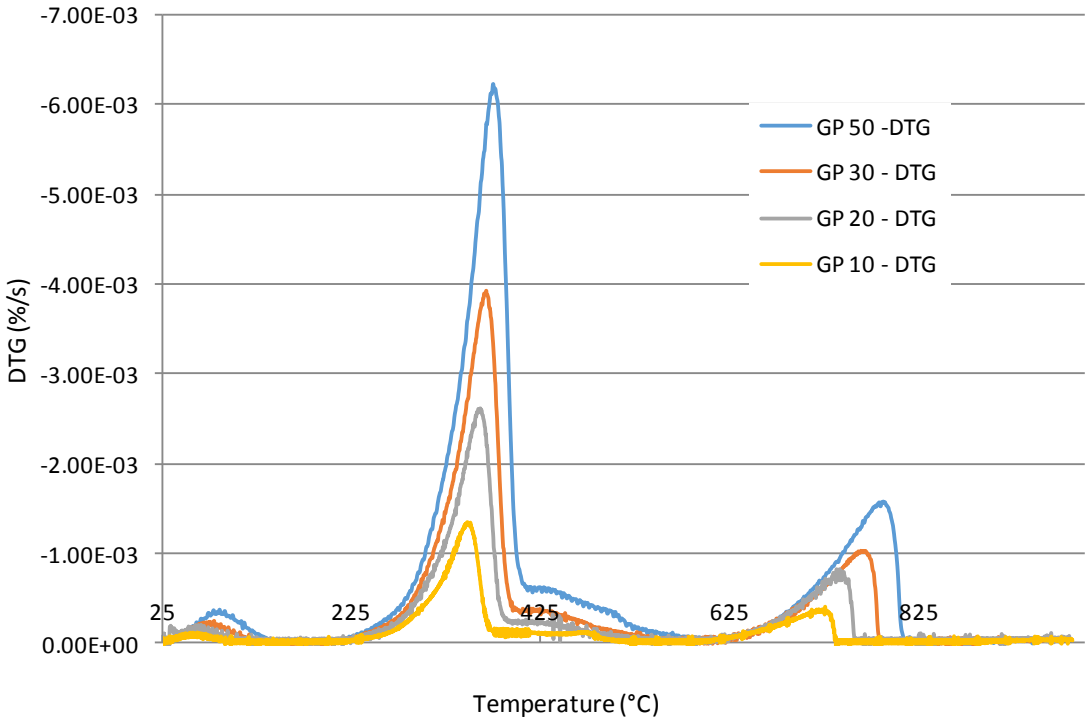

Figure B.1.2: Comparison of the Rates of Weight loss of Glossy Paper at Different Heating Rates

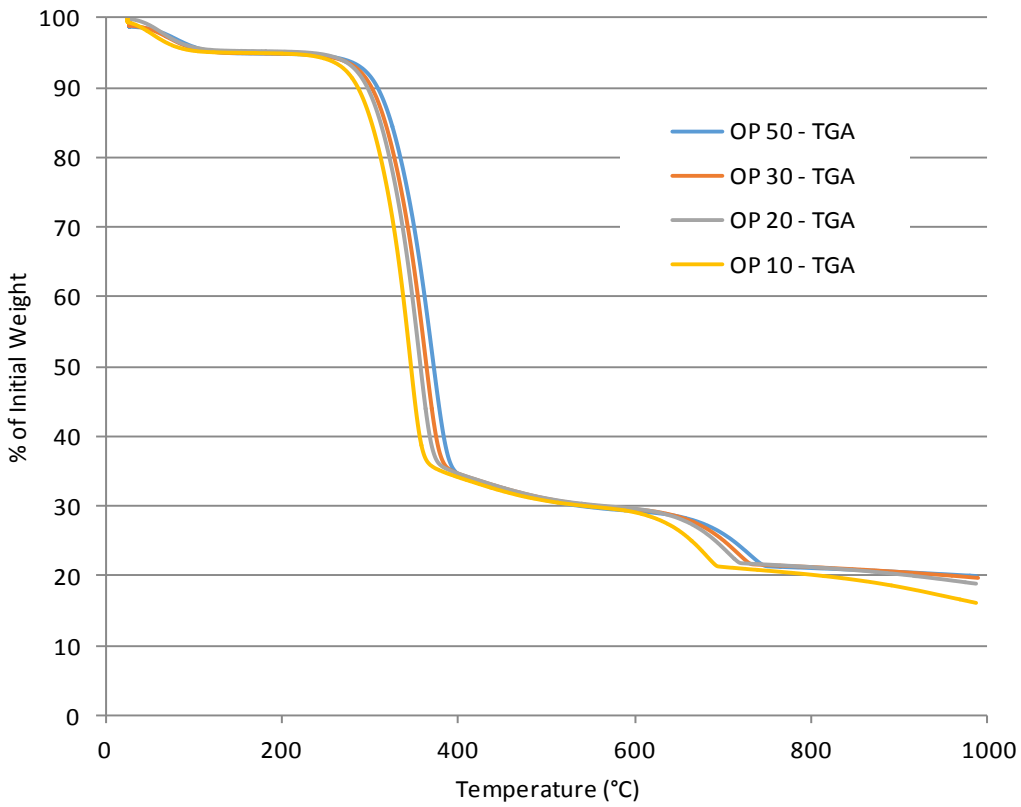

Figure B.1.3: Comparison Weight loss of Office Paper at Different Heating Rates

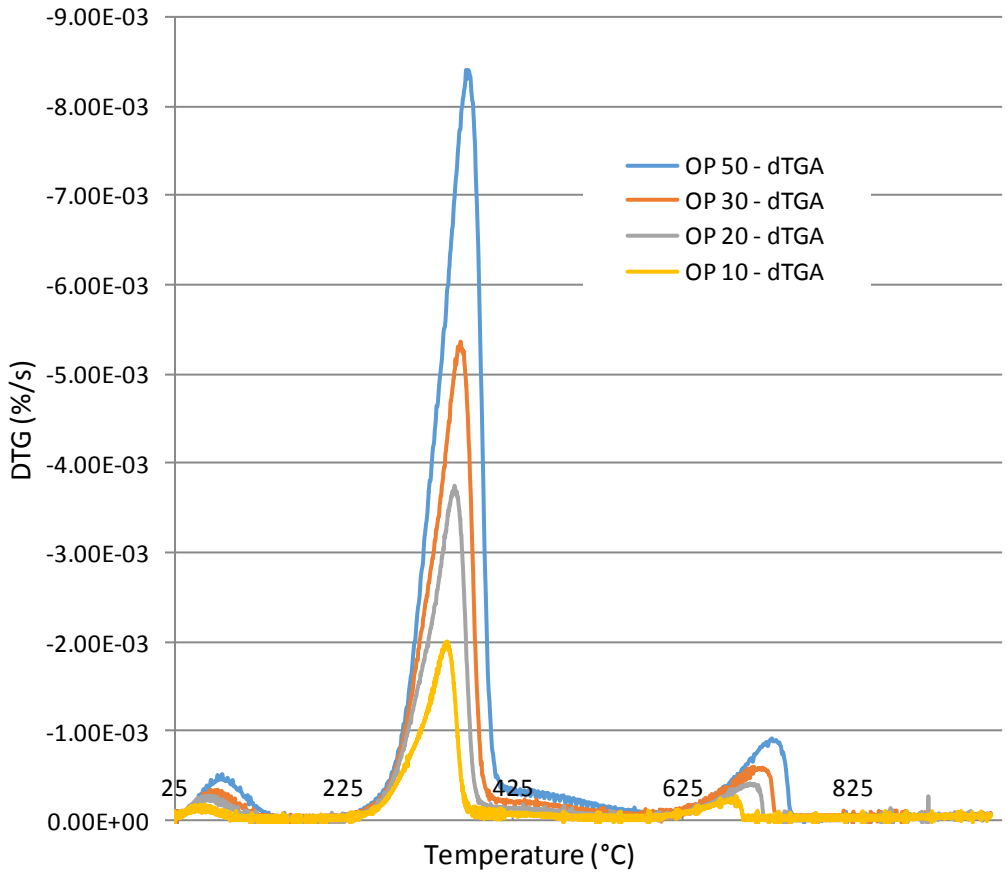

Figure B.1.4: Comparison of the Rates of Weight loss of Office Paper at Different Heating Rates

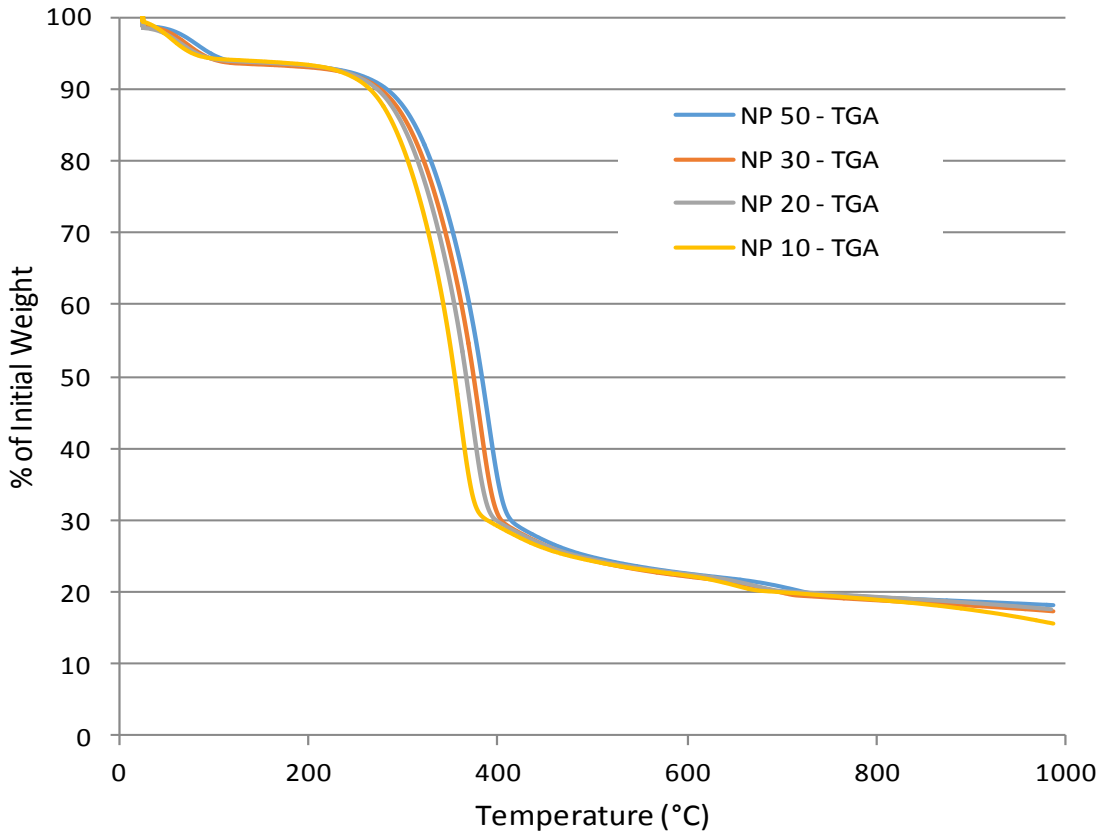

Figure B.1.5: Comparison of Weight loss of Newspaper at Different Heating Rates

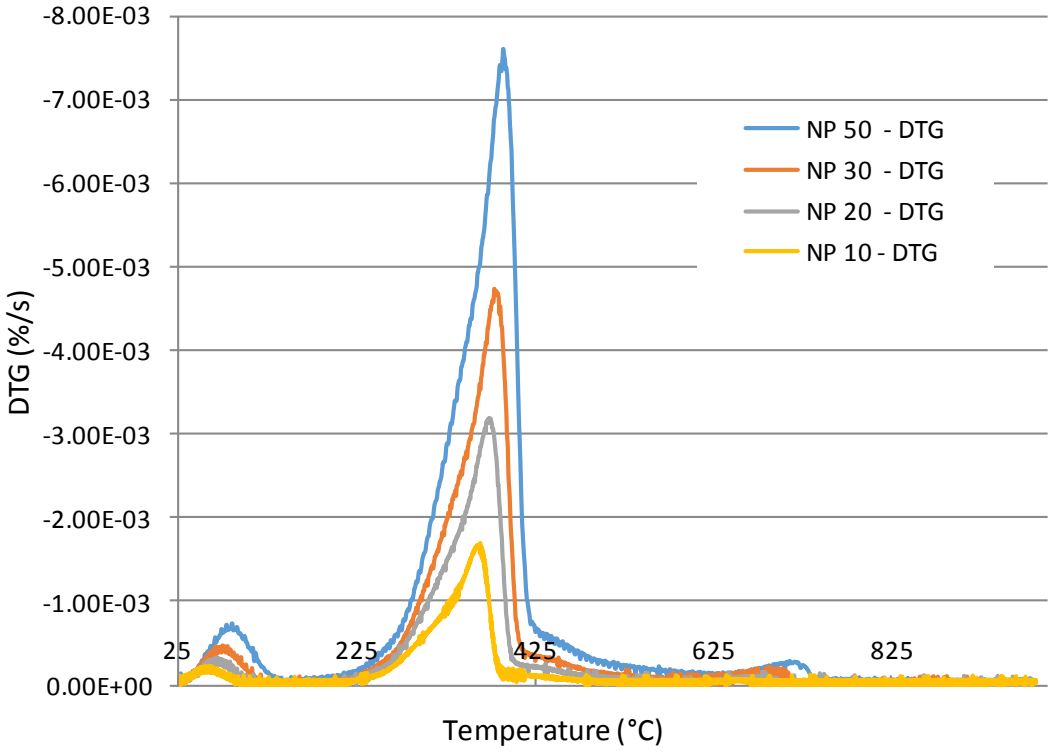

Figure B.1.6: Comparison of the Rates of Weight loss of Newspaper at Different Heating Rates

B2: Plastic TGA and DTG Comparisons

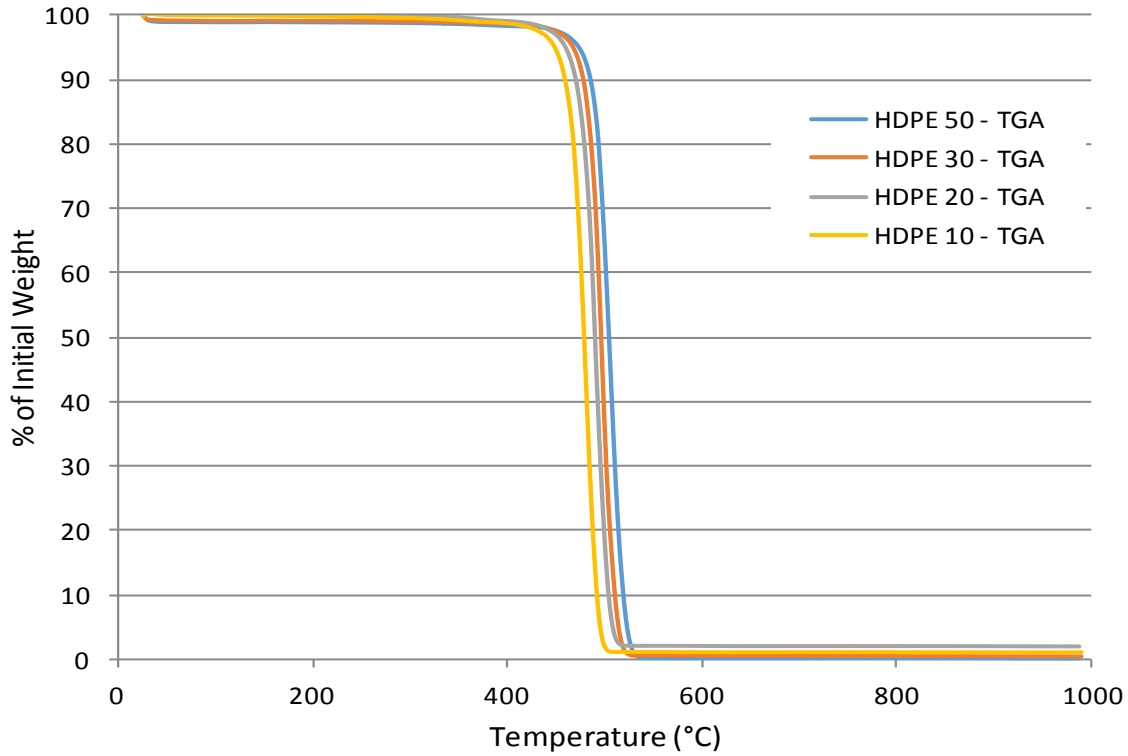

Figure B.2.1: Comparison of Weight loss of HDPE at Different Heating Rates

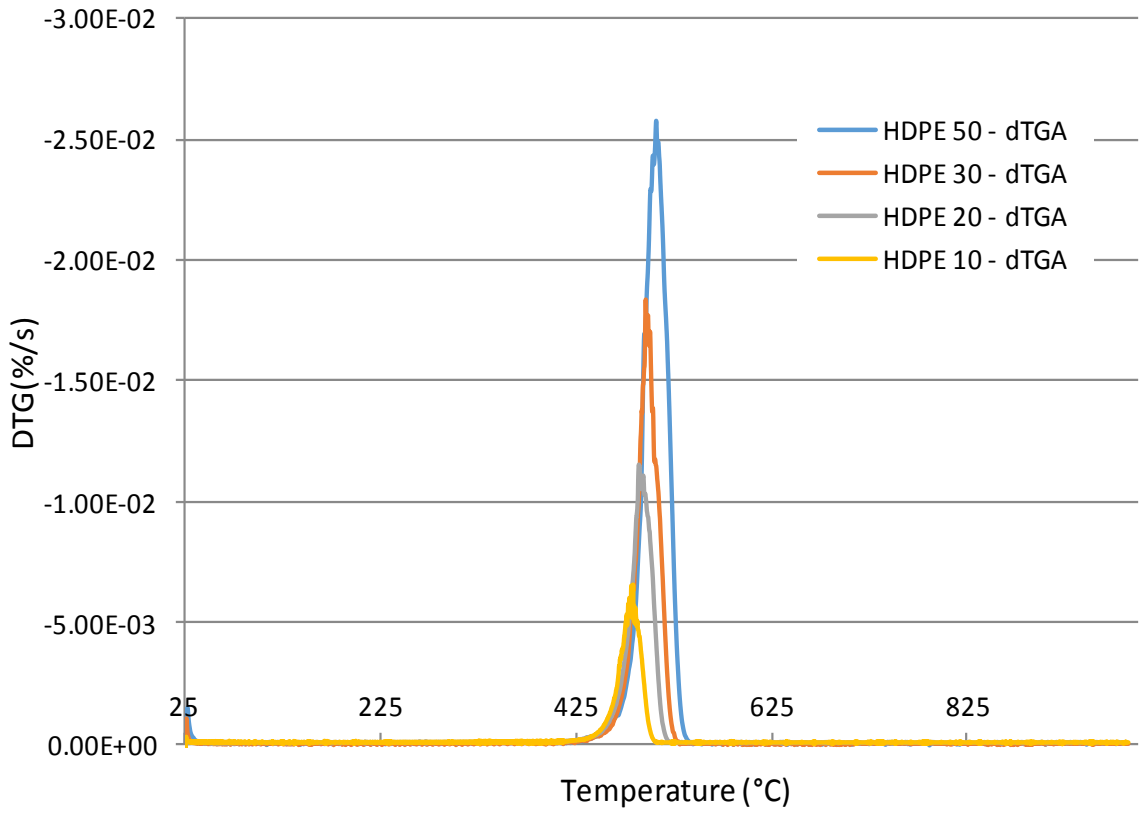

Figure B.2.2: Comparison of the Rates Weight loss of HDPE at Different Heating Rates

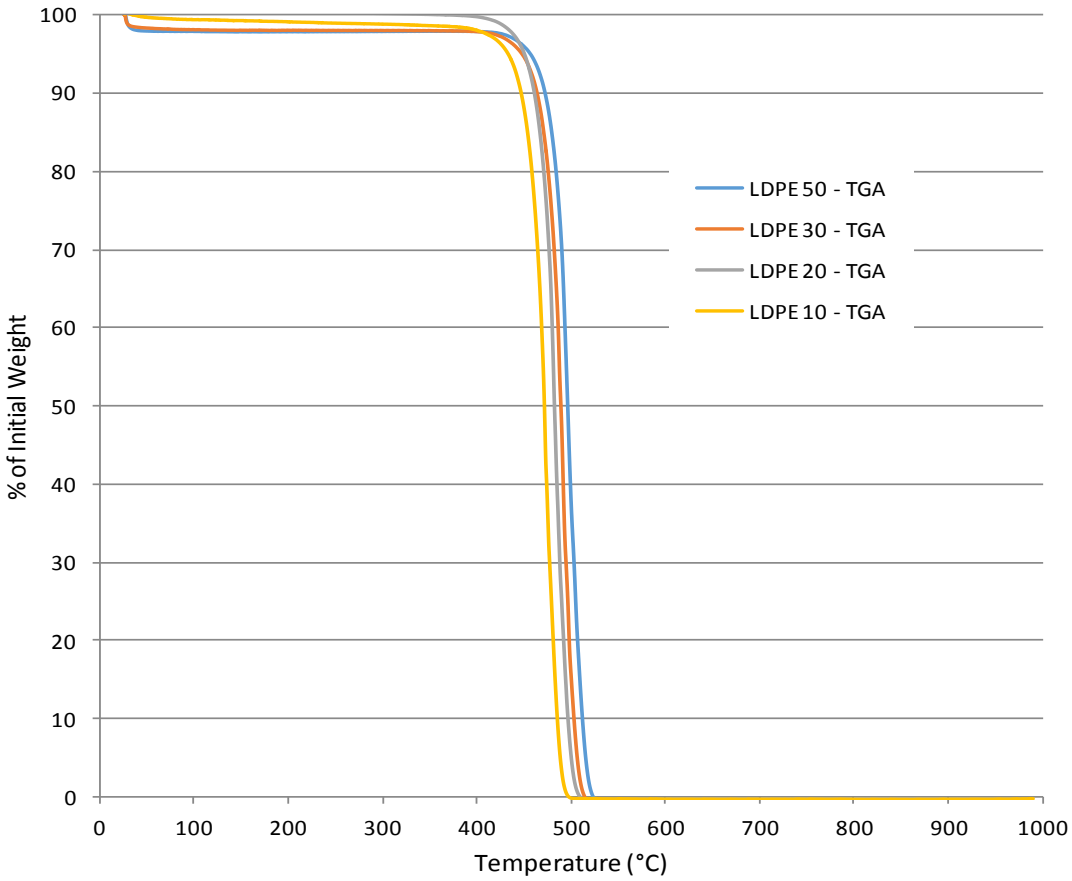

Figure B.2.3: Comparison of the Weight loss of LDPE at Different Heating Rates

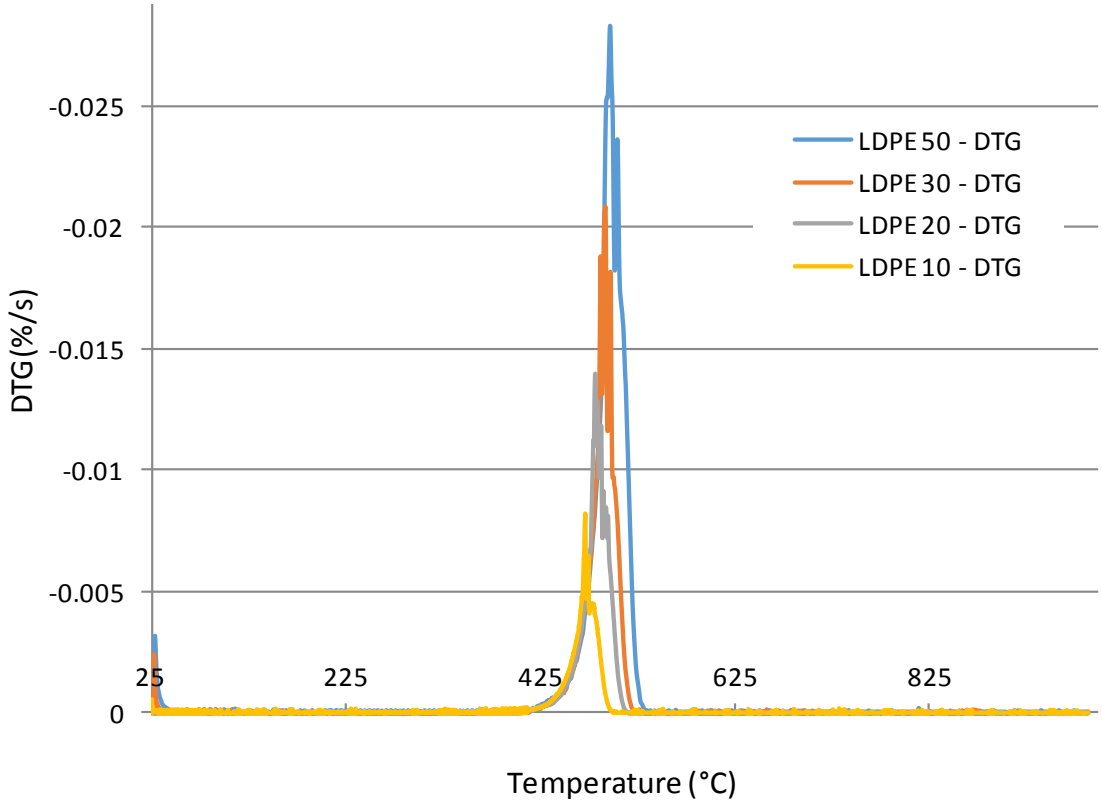

Figure B.2.4: Comparison of the Rates of Weight loss of LDPE at Different Heating Rates

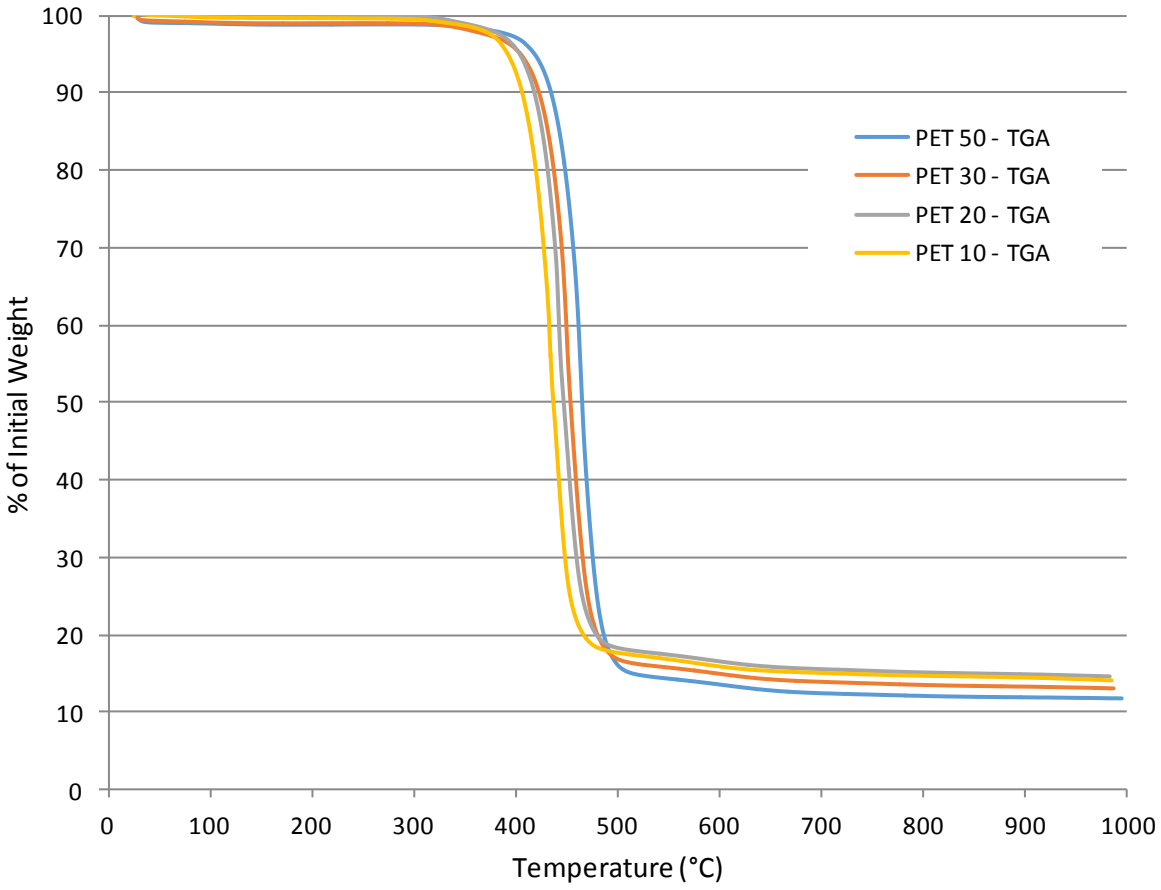

Figure B.2.5: Comparison of Weight loss of PET at Different Heating Rates

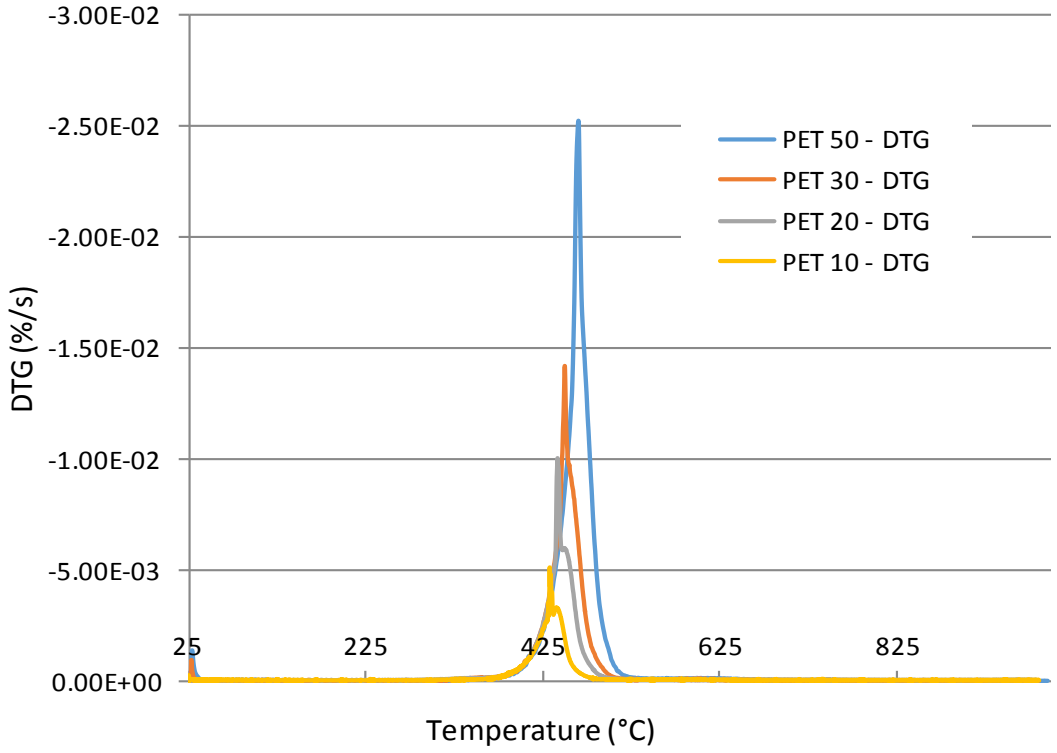

Figure B.2.6: Comparison of the Rates Weight loss of PET at Different Heating Rates

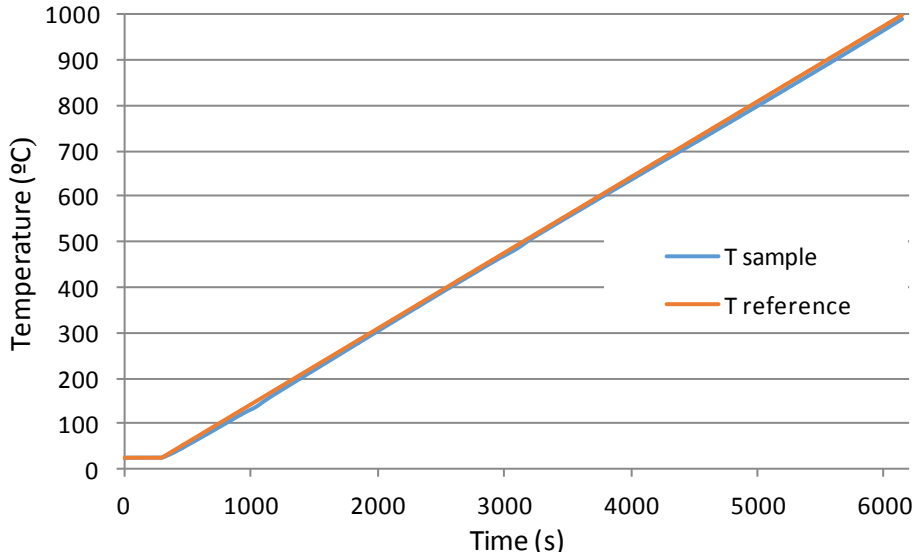

Figure B.2.7: TGA Furnace Thermal Lag Verification Example (HDPE 10K/min)

Appendix C: Activation energy and pre-exponential factor plots- paper

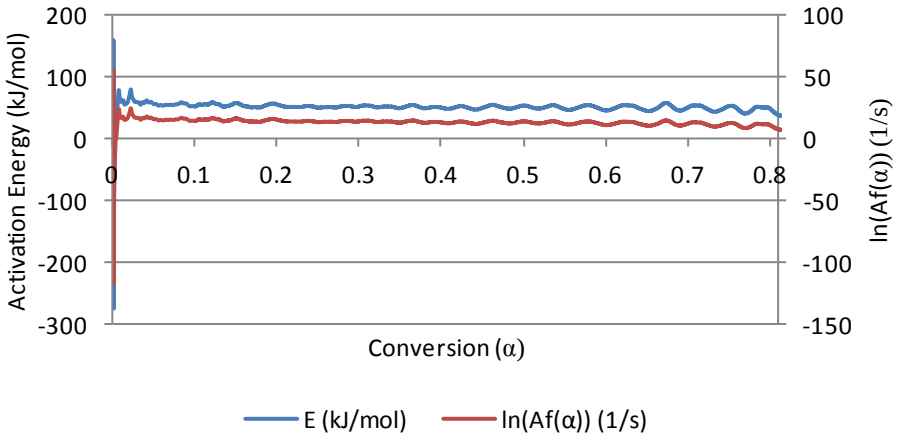

Figure C1 Activation Energy and ln(Af(α)) Dependence on Specific Conversion for Glossy Paper Step 1

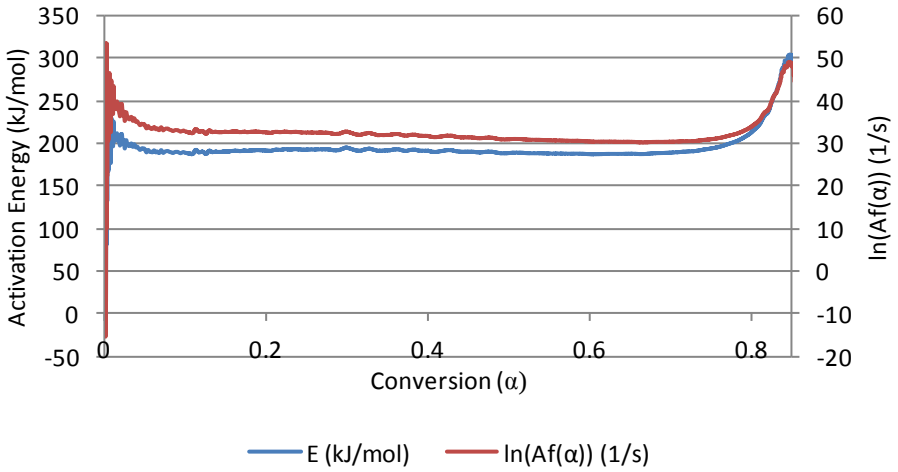

Figure C2: Activation Energy and ln(Af(α)) Dependence on Specific Conversion for Glossy Paper Step 2

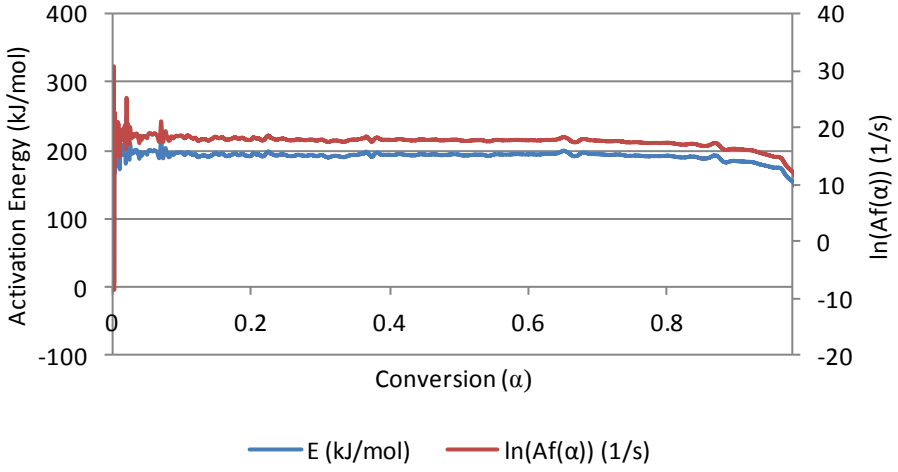

Figure C3: Activation Energy and ln(Af(α)) Dependence on Specific Conversion for Glossy Paper Step 3

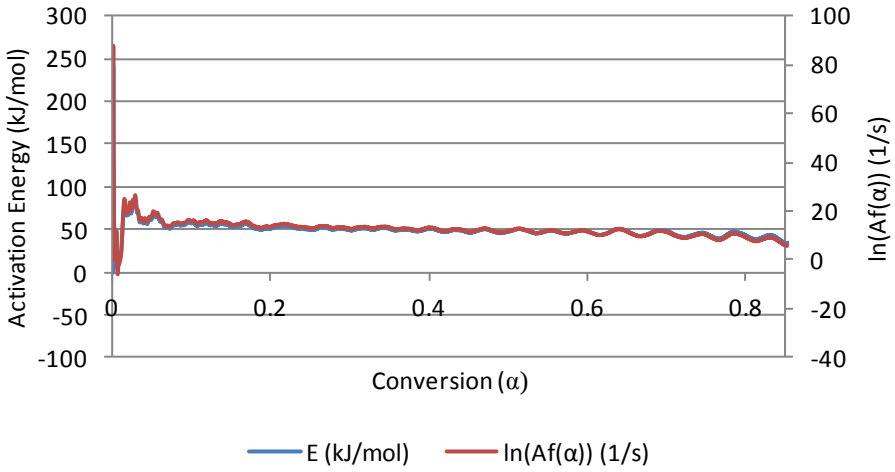

Figure C4: Activation Energy and ln(Af(α)) Dependence on Specific Conversion for Newspaper Step 1

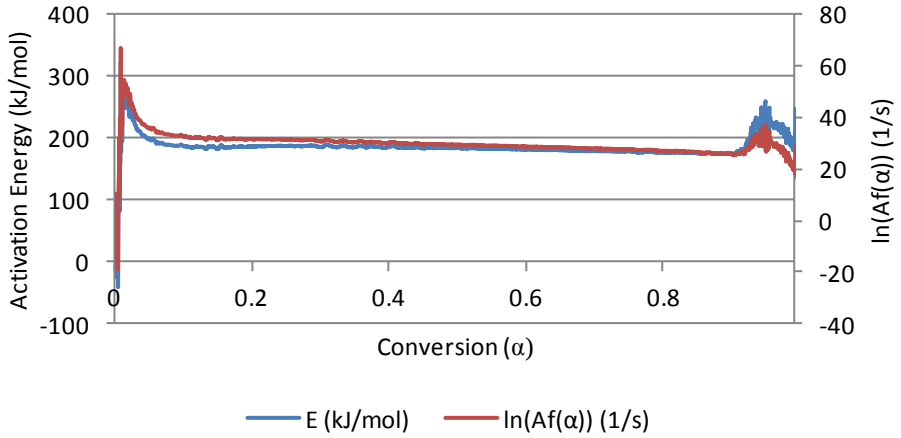

Figure C5: Activation Energy and ln(Af(α)) Dependence on Specific Conversion for Newspaper Step 2

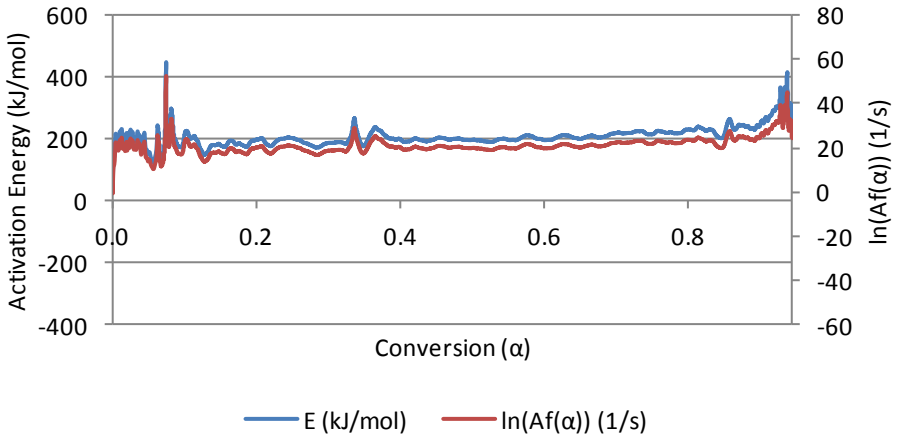

Figure C6: Activation Energy and ln(Af(α)) Dependence on Specific Conversion for Newspaper Step 3

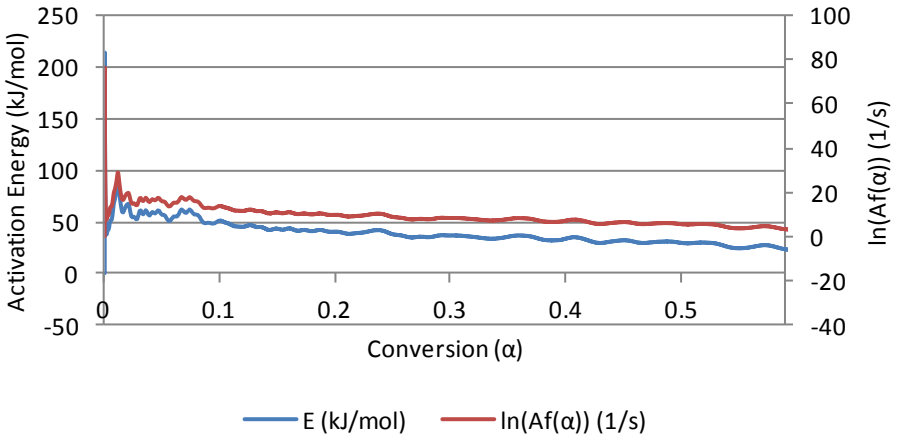

Figure C7: Activation Energy and ln(Af(α)) Dependence on Specific Conversion for Office Paper Step 1

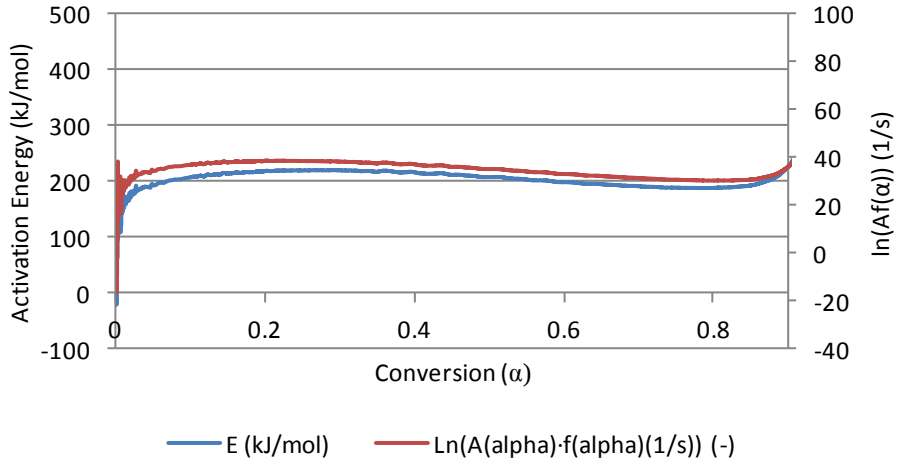

Figure C8: Activation Energy and ln(Af(α)) Dependence on Specific Conversion for Office Paper Step 2

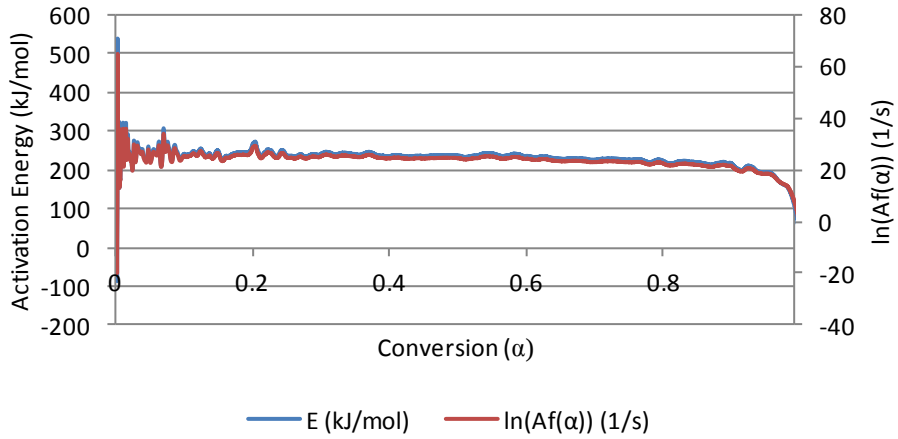

Figure C9: Activation Energy and ln(Af(α)) Dependence on Specific Conversion for Office Paper Step 3

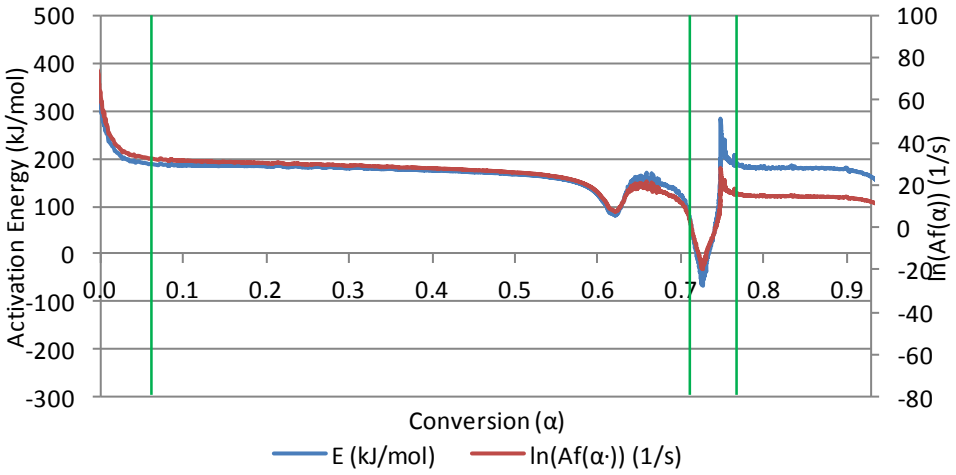

Figure C10: Glossy Paper Overall Degradation Showing Degradation Events with Breaks in Correlation

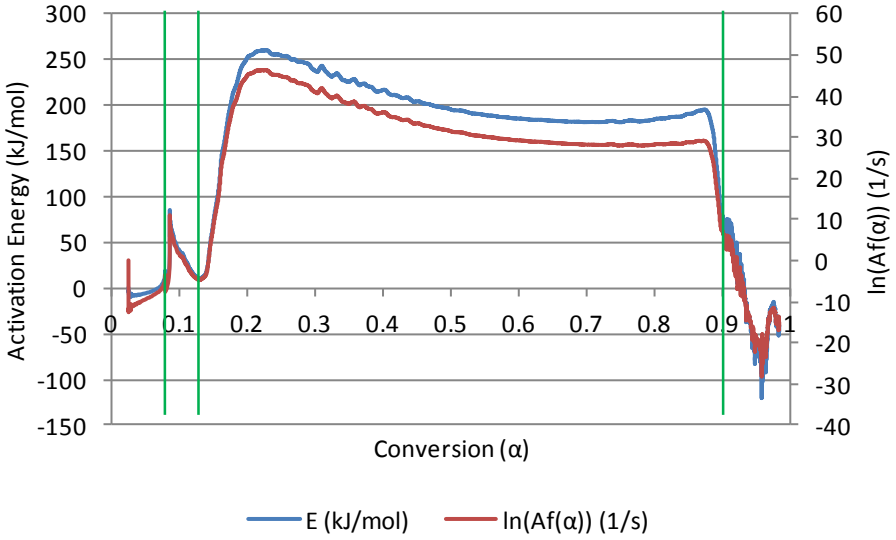

Figure C11: Newspaper Overall Degradation Showing Degradation Events with Breaks in Correlation

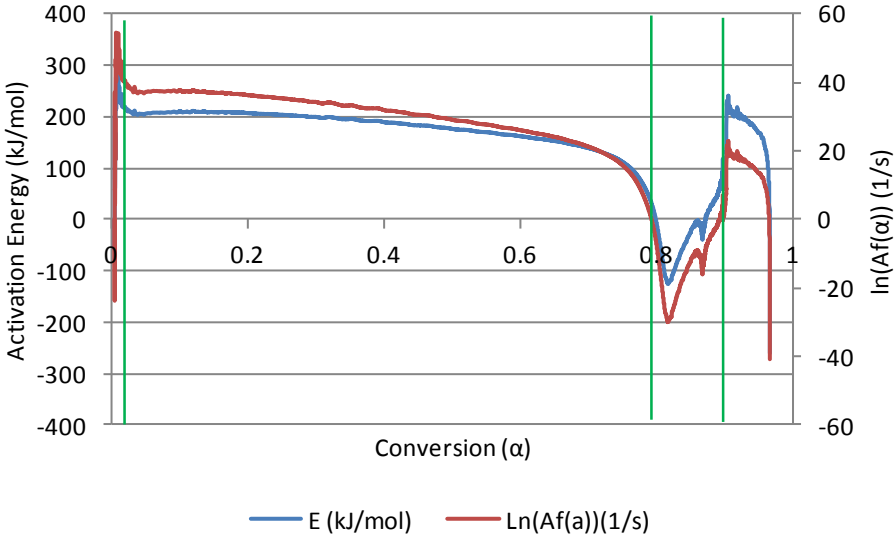

Figure C11: Office Paper Overall Degradation Showing Degradation Events with Breaks in Correlation

Table C1: Summary of Calculated Rates of Reaction (k) at Maximum Degradation Temperatures

Sample	T (°C)	k (1/s)			
		10 K/min	20 K/min	30 K/min	50 K/min
Plastics					
HDPE	**500**	6.37E-04	8.91E-03	1.72E-02	2.20E-02
LDPE	**500**	3.00E-05	1.40E-04	1.09E-02	2.41E-02
PET	**450**	2.81E-03	6.93E-03	1.61E-02	1.06E-02
Glossy Paper					
Step 1	**75**	2.41E-03	4.94E-03	8.66E-03	1.24E-02
Step 2	**350**	2.76E-03	4.77E-03	5.95E-03	7.79E-03
Step 3	**725**	2.38E-03	3.60E-03	4.09E-03	4.64E-03
Newspaper					
Step 1	**75**	2.46E-03	5.62E-03	9.80E-03	1.30E-02
Step 2	**350**	2.11E-03	3.24E-03	4.16E-03	6.15E-03
Step 3	**700**	0.00E+00	5.04E-04	8.17E-03	1.30E-03
Office Paper					
Step 1	**75**	3.36E-03	5.34E-03	8.27E-03	1.42E-02
Step 2	**350**	2.99E-03	5.56E-03	7.27E-03	1.01E-02
Step 3	**650**	1.75E-03	1.94E-03	2.19E-03	2.01E-03

Appendix D: Initial mass spectroscopic scans and ions tracked

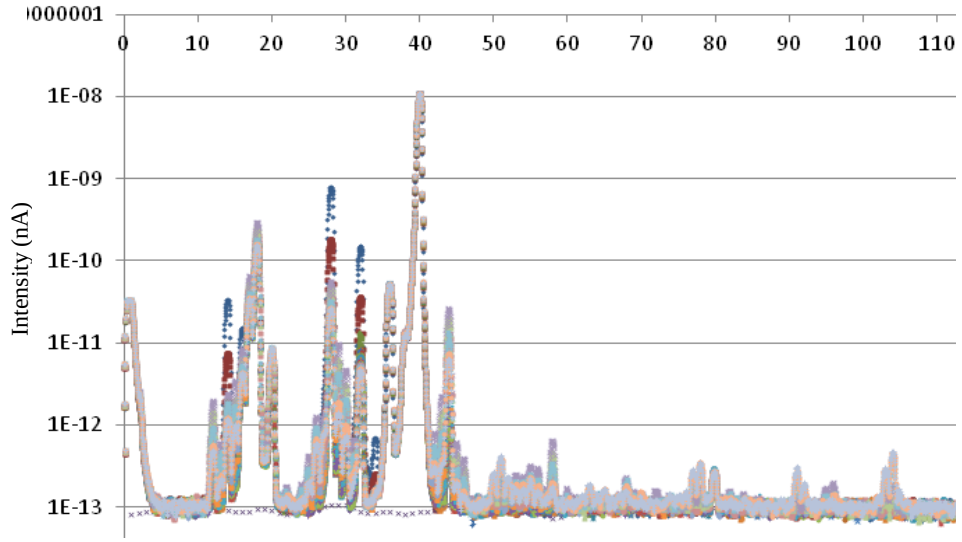

Figure D1: MS Scan for Glossy Paper Degradation

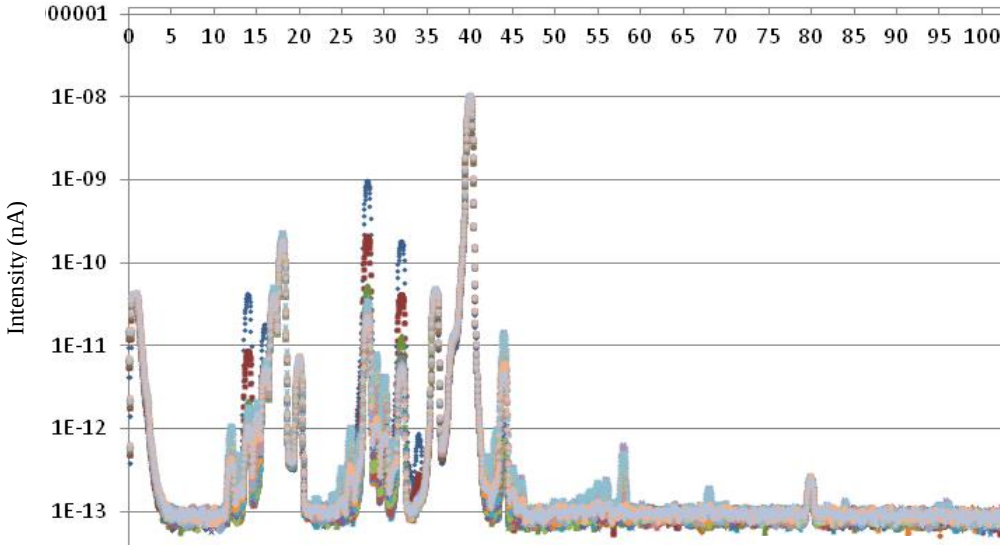

Figure D2: MS Scan for Newspaper Degradation

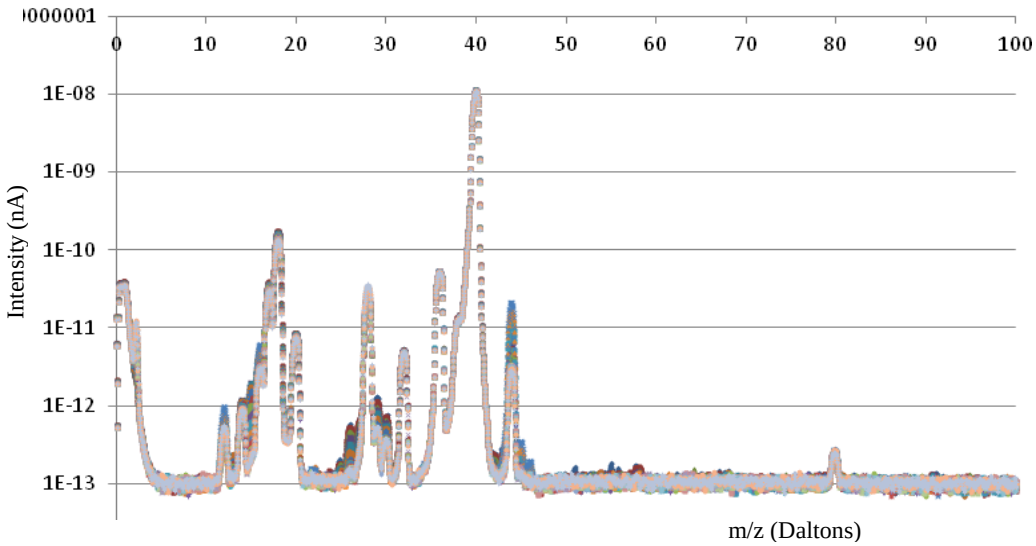

Figure D3: MS Scan for Office Paper Degradation

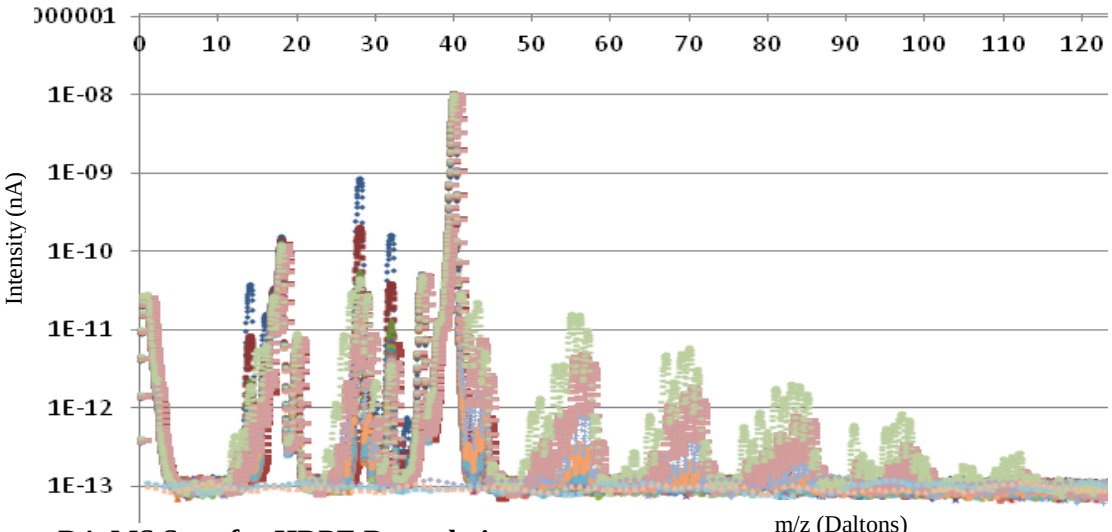

Figure D4: MS Scan for HDPE Degradation

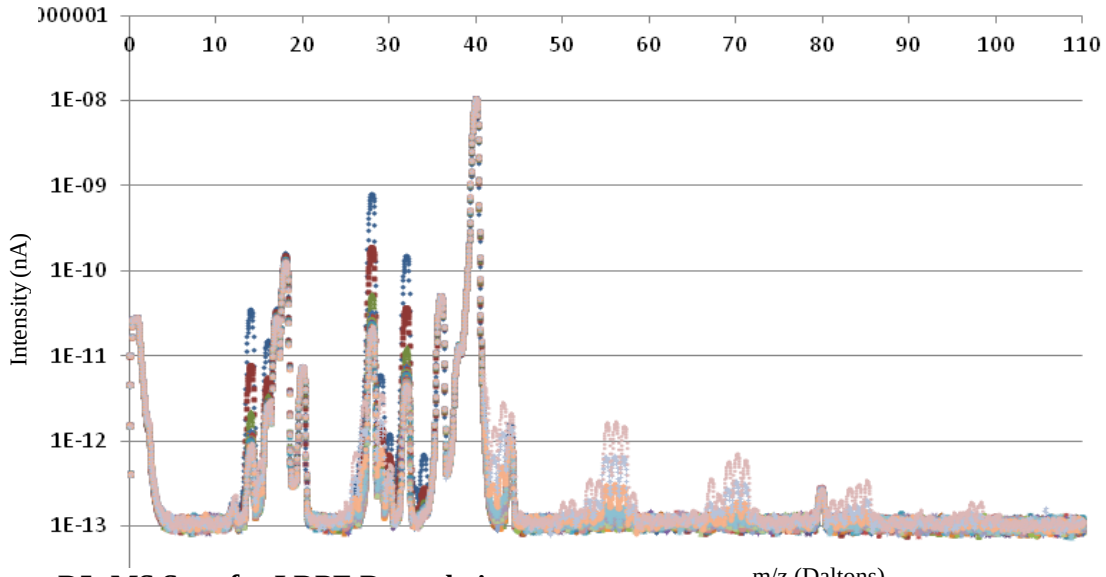

Figure D5: MS Scan for LDPE Degradation

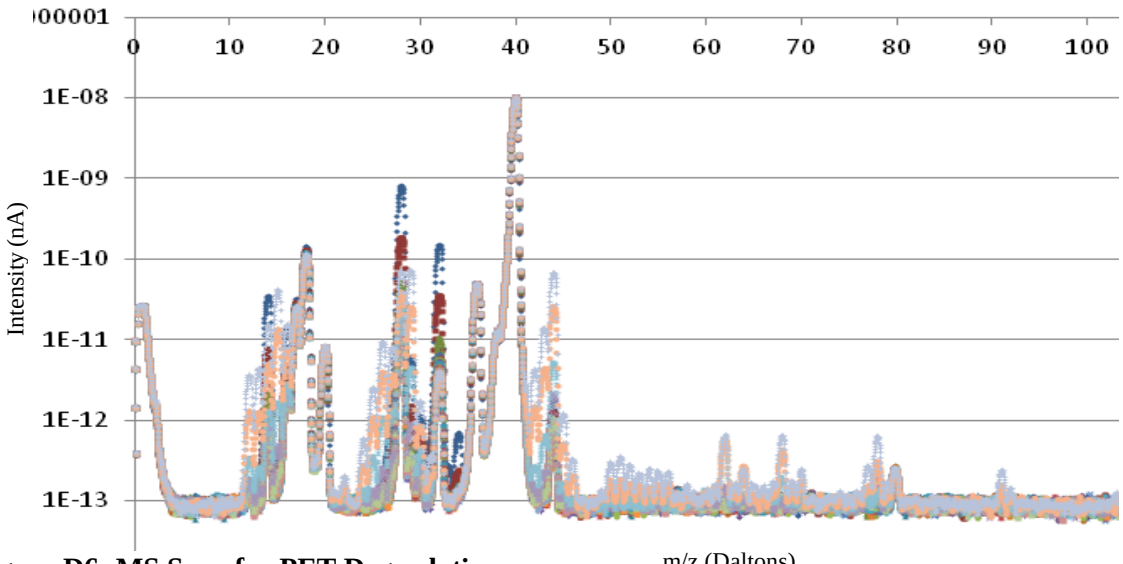

Figure D6: MS Scan for PET Degradation

Table D1: List of m/z Ion Fragments Tracked for Each Sample

Paper Samples			Plastic Samples		
Glossy Paper	**Newspaper**	**Office Paper**	**HDPE**	**LDPE**	**PET**
***m/z* Tracked**					
2	2	2	2	2	2
12	12	12	14	14	14
14	14	14	15	15	15
15	15	15	17	17	17
16	16	16	18	18	18
17	17	17	20	20	20
18	18	18	28	28	28
20	20	20	32	32	36
28	28	26	36	40	40
32	36	28	40	44	42
36	40	32	43	56	44
40	44	36	44	57	55
44	68	40	55	69	64
55	80	44	67	70	68
58		58	70	71	70
78		80	84	80	78
104			97		80
					91

Appendix E: Laboratory scale pyrolysis of glossy paper and HDPE

Table E1: Mass Balances for the Slow Pyrolysis of Glossy Paper and HDPE

Slow	Glossy Paper				HDPE			
	Run 10	Run 11	Run 12	Run 13	Run 14	Run 15	Run 16	Run 17
Heating Rate	20 K/min		10 K/min		20 K/min		10 K/min	
Sample Size (g)	42.09	42.05	40.14	42.45	41.02	40.66	41.31	41.41
Initial Moisture Content	1.41%	1.41%	1.41%	1.41%	0.12%	0.12%	0.12%	0.12%
Initial Water (g)	0.593	0.593	0.566	0.599	0.049	0.049	0.050	0.050
Total Oil (g)	9.11	11.09	8.71	9.74	26.78	27.55	21.73	25.95
Cond 1 - 4 (GP) Cond 1 (HDPE) (g)	3.19	4.3	5.37	5.37	1.21	0.3	7.23	7.84
Moisture Content %	87.63 %	90.28 %	77.71 %	87.22 %	-	-	-	-
Atm Cond (g)	5.12	4.96	2.54	3.61	16.53	17.6	10.55	15.46
Moisture Content %	60.47 %	57.51 %	42.88 %	50.07 %	-	-	-	-
Total Water (g)	5.891	6.734	5.262	6.491	-	-	-	-
Total Pyro Water (g)	5.298	6.141	4.696	5.892	-	-	-	-
Total Char (g)	20.53	20.07	19.46	20.26	6.78	5.51	10.23	5.55
Total Gas (g)	12.45	10.89	11.97	12.45	7.46	7.6	9.35	9.91

Table E2: Mass Balances for the Vacuum Pyrolysis of Glossy Paper and HDPE

Vacuum	Glossy Paper				HDPE			
	Run 2b	Run 3b	Run 4b	Run 5c	Run 6b	Run 7C	Run 8b	Run 9b
Heating Rate	20 K/min		10 K/min		20 K/min		10 K/min	
Sample Size (g)	40.19	38.67	40.66	40.14	41.43	41.3	40.06	40.15
Initial Moisture Content	1.41%	1.41%	1.41%	1.41%	0.12%	0.12%	0.12%	0.12%
Initial Water (g)	0.57	0.55	0.57	0.57	0.05	0.05	0.05	0.05
Total Oil (g)	14.94	13.57	14.92	15.32	35.8	33.5	35.62	36.97
ATM Cond	2.58	3.21	3.59	3.65	23.6	23.01	24.18	28.63
Moisture Content % (KF)	5.00%	5.11%	4.37%	4.47%	-	-	-	-
Moisture (ATM Cond)	0.13	0.16	0.16	0.16	-	-	-	-
Cond 1	5.64	2.7	3.86	3.39	3.17	1.43	2.96	3.82
Moisture Content % (KF)	40.01%	41.65%	37.35%	36.48%	-	-	-	-
Moisture (Cond. 1)	2.25	1.12	1.44	1.24	-	-	-	-
Cond 2, 3 + 4	5.45	6.46	6.72	7.04	1.83	1.93	2.06	1.41
Moisture Content % (KF)	81.57%	81.17%	79.21%	81.51%	Cannot Measure			
Moisture (Cond. 2, 3, 4)	4.45	5.24	5.32	5.74				
Total Water (g)	6.83	6.53	6.92	7.14				
Total Pyro Water (g)	6.26	5.99	6.35	6.57				
Total Wax (g)	-	-	-	-	33.97	31.54	35.54	35.52
Total Char (g)	14.55	13.18	15.86	15.77				
Total Gas (g)	10.7	11.92	9.88	9.05	3.8	7.8	4.44	2.57

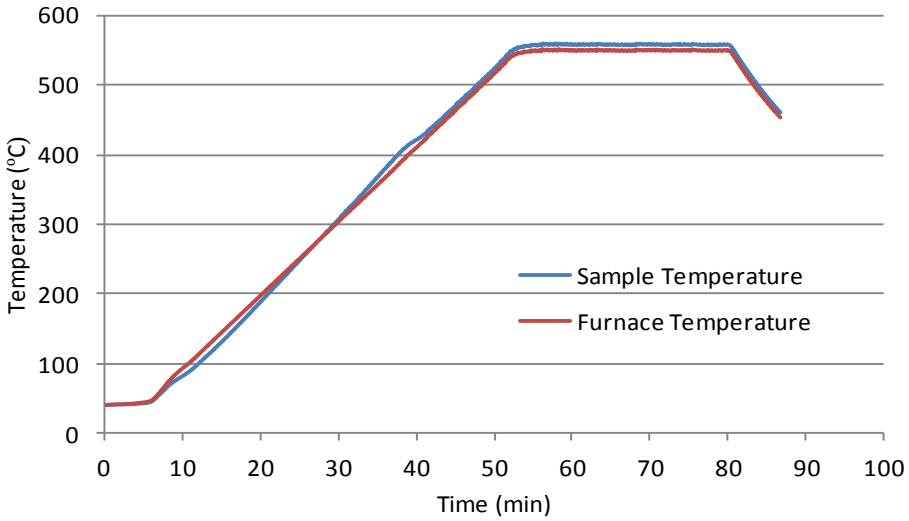

Figure E1: Temperature Profile Example for Slow Pyrolysis: Run 12 - Glossy Paper 10K/min

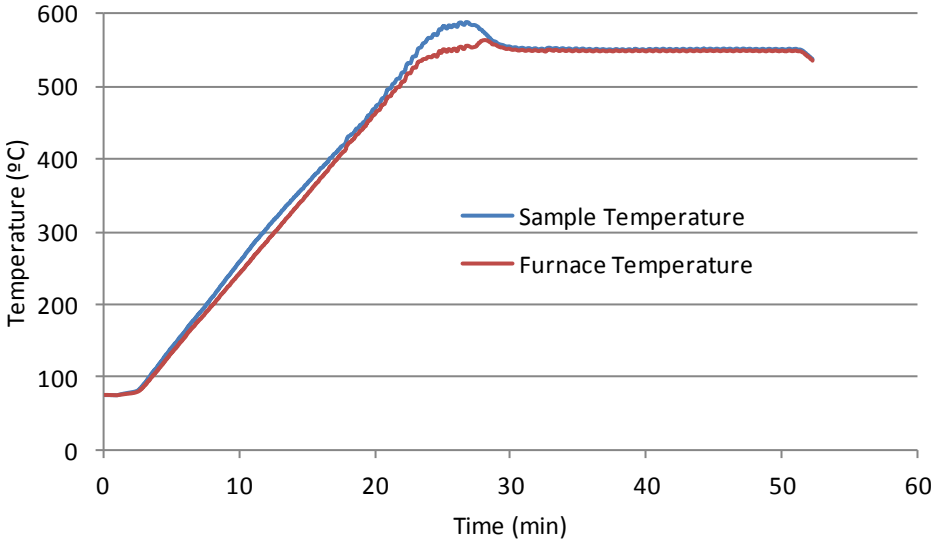

Figure E2: Temperature Profile Example for Slow Pyrolysis: Run 14 - HDPE 10K/min

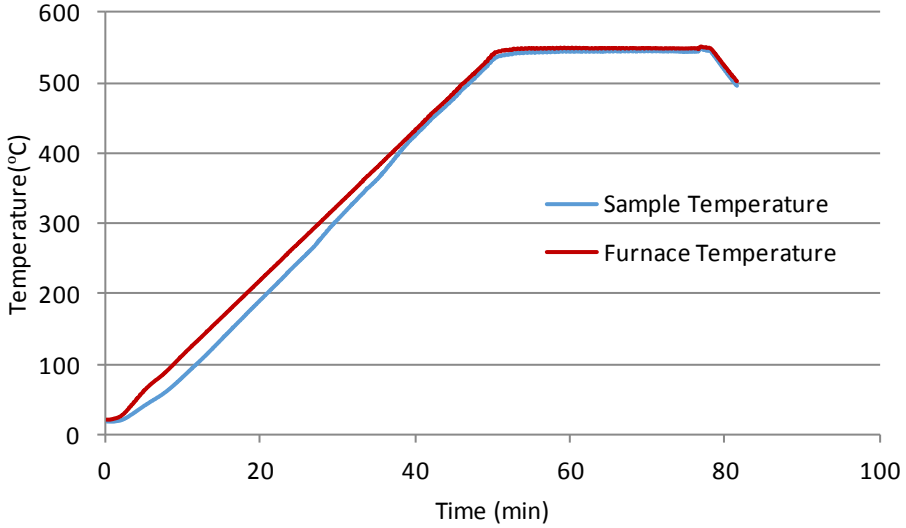

Figure E3: Temperature Profile Example for Slow Pyrolysis: Run 4 – Glossy Paper 10K/min

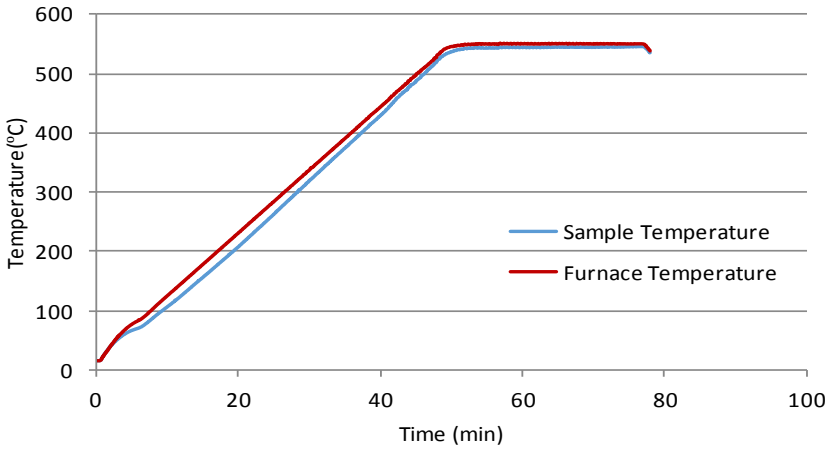

Figure E4: Temperature Profile Example for Slow Pyrolysis: Run 8 – HDPE 10K/min

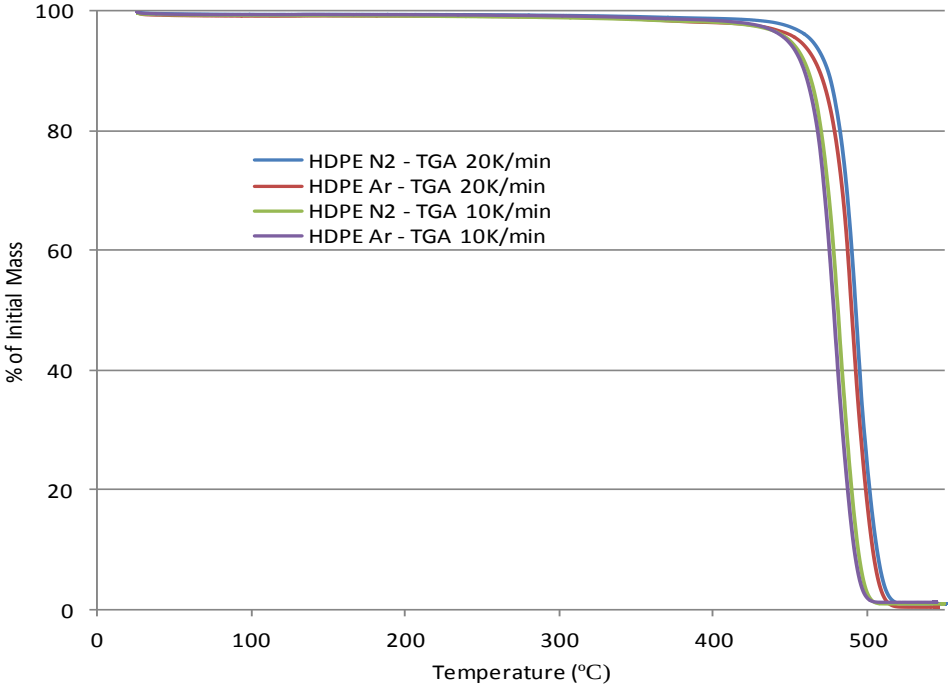

Figure E5: Comparison of Nitrogen and Argon Purge Gases on HDPE Degradation

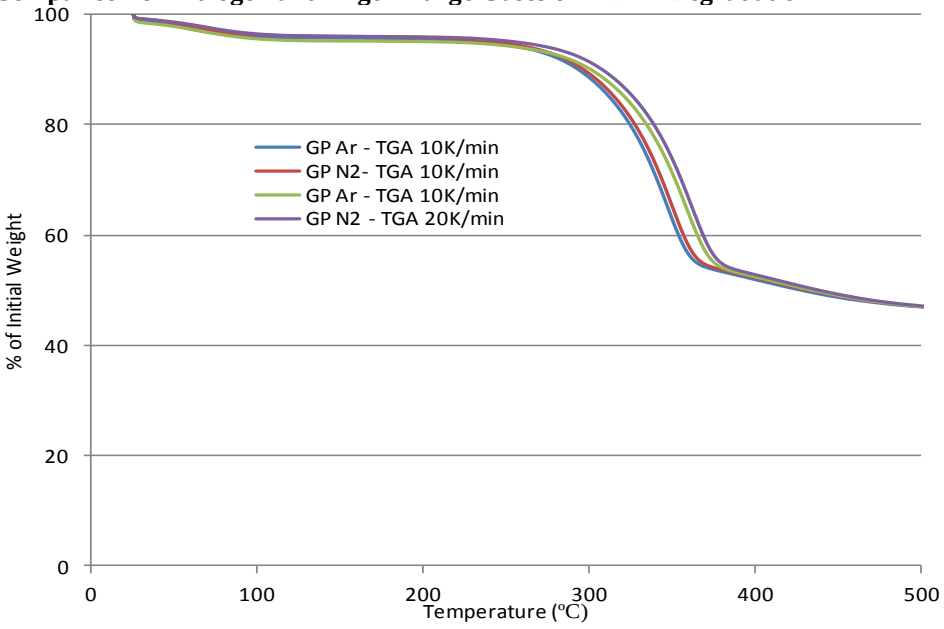

Figure E6: Comparison of Nitrogen and Argon Purge Gases on Glossy Paper Degradation

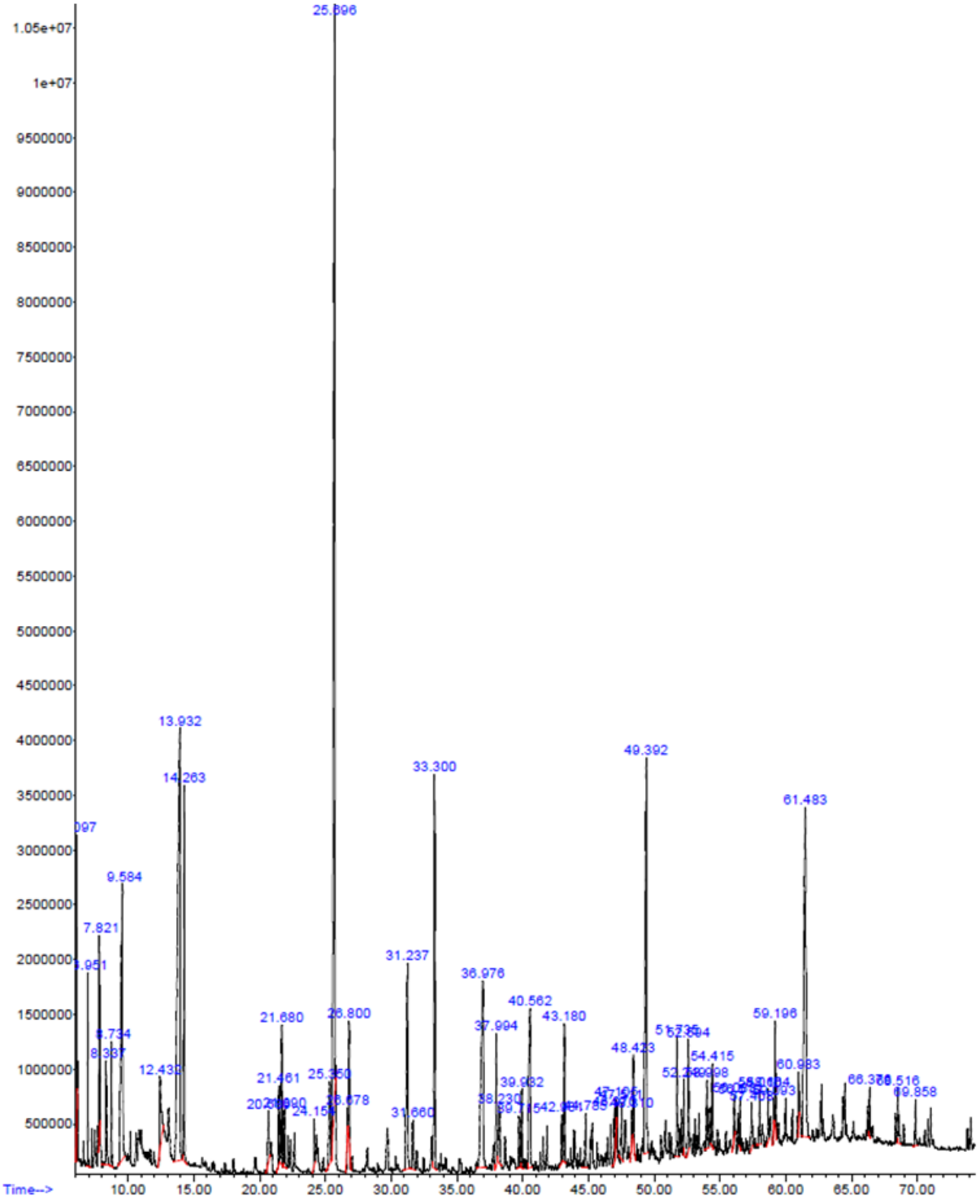

Figure E7: GC-MS Chromatogram (Abundance vs. Retention Time (min)) for TGA Gas Capture for Glossy Paper

Table E3: GC-MS Results for TGA Gas Capture at 20k/min for Glossy Paper
(Greater than 80% Quality of Fit (QoF) in NIST Library of Peaks at Retention Times (RT) in min)

Peak No.	RT	Area%	Library/ID	Molec. Wt.	QoF
6	6.951	0.87	Furan, 2-methyl-	82.1	94
10	7.821	0.83	2,3-Butanedione	86.09	80
12	8.339	0.97	3-Pentanone	86.13	86
13	8.735	0.68	Benzene	78.11	95
17	9.584	4.61	Acetaldehyde, hydroxy-	60.05	72
32	12.432	1.75	Acetic acid	60.05	72
35	13.93	9.36	2-Propanone, 1-hydroxy-	74.08	86
36	14.261	2.62	Toluene	92.14	95
72	21.681	1.07	Ethylbenzene	106.2	91
89	25.349	1.04	Succindialdehyde	86.09	86
90	25.696	13.05	Styrene	104.2	97
95	26.798	0.82	Furfural	96.08	91
117	31.238	2.68	2-Furanmethanol	98.1	97
125	33.298	3.42	.alpha.-Methylstyrene	118.2	95
143	36.978	3.9	1,2-Cyclopentanedione	98.1	90
159	40.564	2.26	2(5H)-Furanone	84.07	94
175	43.181	1.15	2-hydroxy-3-methyl-2-Cyclopenten-1-one,	112.1	91
233	52.595	0.78	1,4:3,6-Dianhydro-.alpha. d-glucopyranose	144.1	96
246	54.413	0.81	5-Hydroxymethyldihydrofuran-2-one	116.1	81
275	59.194	0.72	Benzene, 1,1'-(1,3-propanediyl)bis 5	196.3	97
291	61.481	6.48	.beta.-D-Glucopyranose, 1,6-anhydro 3	162.1	80

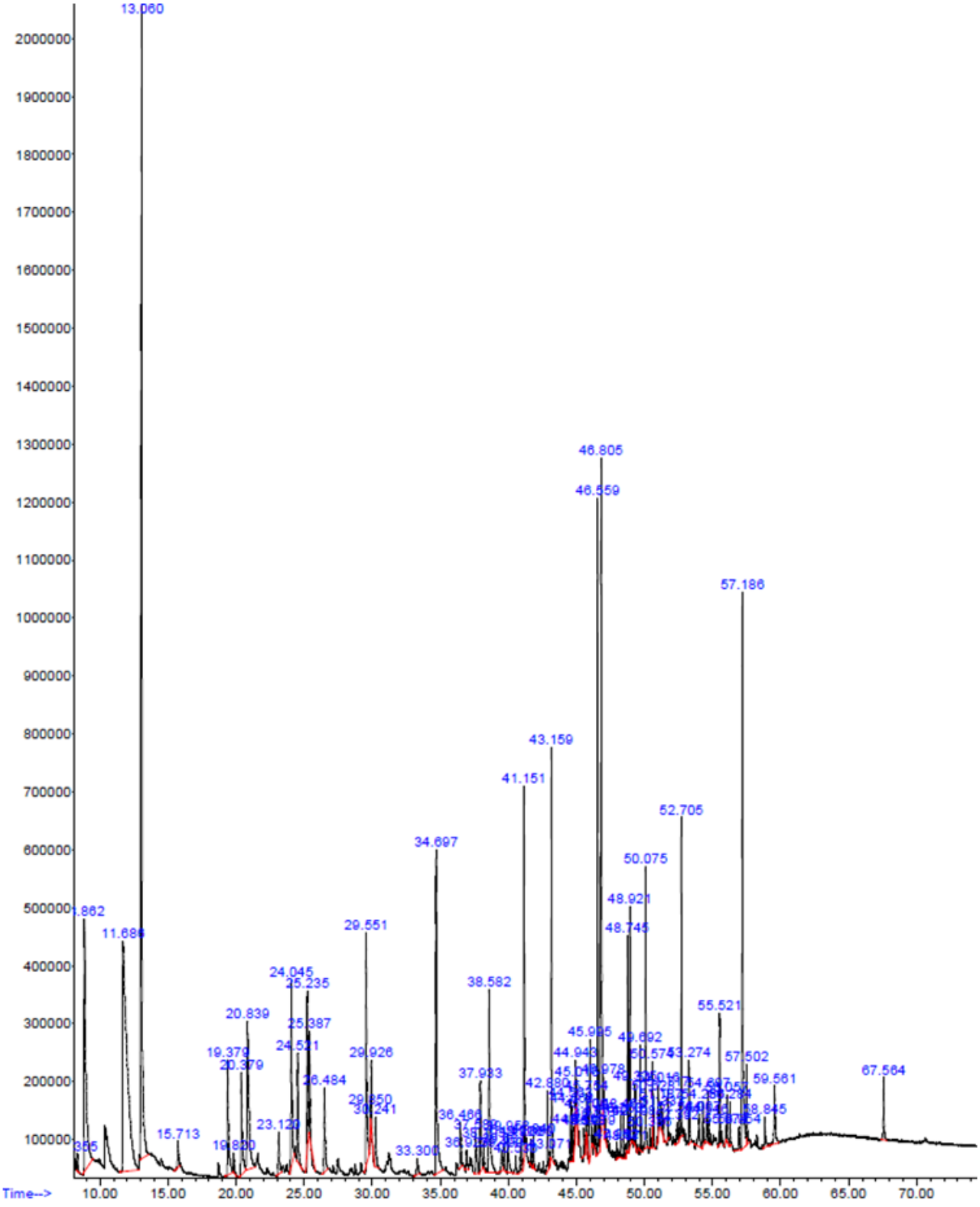

Figure E8: GC-MS Chromatogram (Abundance vs. Retention Time (min)) for New Bio-Oil from Glossy Paper

Table E4: GC-MS Results for New Bio-Oil at 20k/min for Glossy Paper

(Greater than 80% Quality of Fit (QoF) in NIST Library of Peaks at Retention Times (RT) in min)

Peak No.	RT	Area%	Library/ID	Ref#	CAS#	QoF
3	8.864	4.68	Acetaldehyde, hydroxy-	268	000141-46-8	72
6	11.684	10.42	Acetic acid	263	000064-19-7	91
7	13.061	14.89	2-Propanone, 1-hydroxy-	819	000116-09-6	90
11	19.38	1.44	Propanoic acid	811	000079-09-4	95
13	20.377	1.23	1-Hydroxy-2-butanone	2038	005077-67-8	90
20	24.046	2.08	Succindialdehyde	1662	000638-37-9	78
23	25.235	1.19	2-Cyclopenten-1-one	1176	000930-30-3	94
24	25.39	0.68	Furfural	2735	000098-01-1	91
31	29.554	2.57	2-Furanmethanol	3079	000098-00-0	97
34	30.243	0.54	2-Heptanone, 3-methyl-	12508	002371-19-9	78
40	34.699	3.68	1,2-Cyclopentanedione	3095	003008-40-0	72
42	36.468	0.54	2-Furancarboxaldehyde, 5-methyl-	5771	000620-02-0	94
46	37.591	0.63	2-Cyclopenten-1-one, 3-methyl-	2821	002758-18-1	91
47	37.933	0.96	Butyrolactone	1646	000096-48-0	94
49	38.583	2.28	2(5H)-Furanone	1341	000497-23-4	94
55	41.15	2.78	1,2-Cyclopentanedione, 3-methyl-	6411	000765-70-8	94
62	42.88	0.64	Phenol	2591	000108-95-2	94
64	43.16	2.75	Phenol, 2-methoxy-	10419	000090-05-1	95
82	46.559	3.62	Creosol	17270	000093-51-6	97
95	48.746	1.03	Phenol, 4-ethyl-2-methoxy-	25988	002785-89-9	91
103	50.074	1.51	2-Methoxy-4-vinylphenol	24419	007786-61-0	91
118	52.707	1.51	Phenol, 2-methoxy-4-(1-propenyl)-,	33448	005912-86-7	98
123	53.274	0.64	Vanillin	25794	000121-33-5	97
130	55.522	0.64	1-(4-Acetoxy-3-methoxyphenyl)-2-pr	78819	1000308-75-0	72
137	57.185	4.34	.beta.-D-Glucopyranose, 1,6-anhydro-	32447	000498-07-7	80
138	57.505	0.63	Homovanillic acid	47719	000306-08-1	81

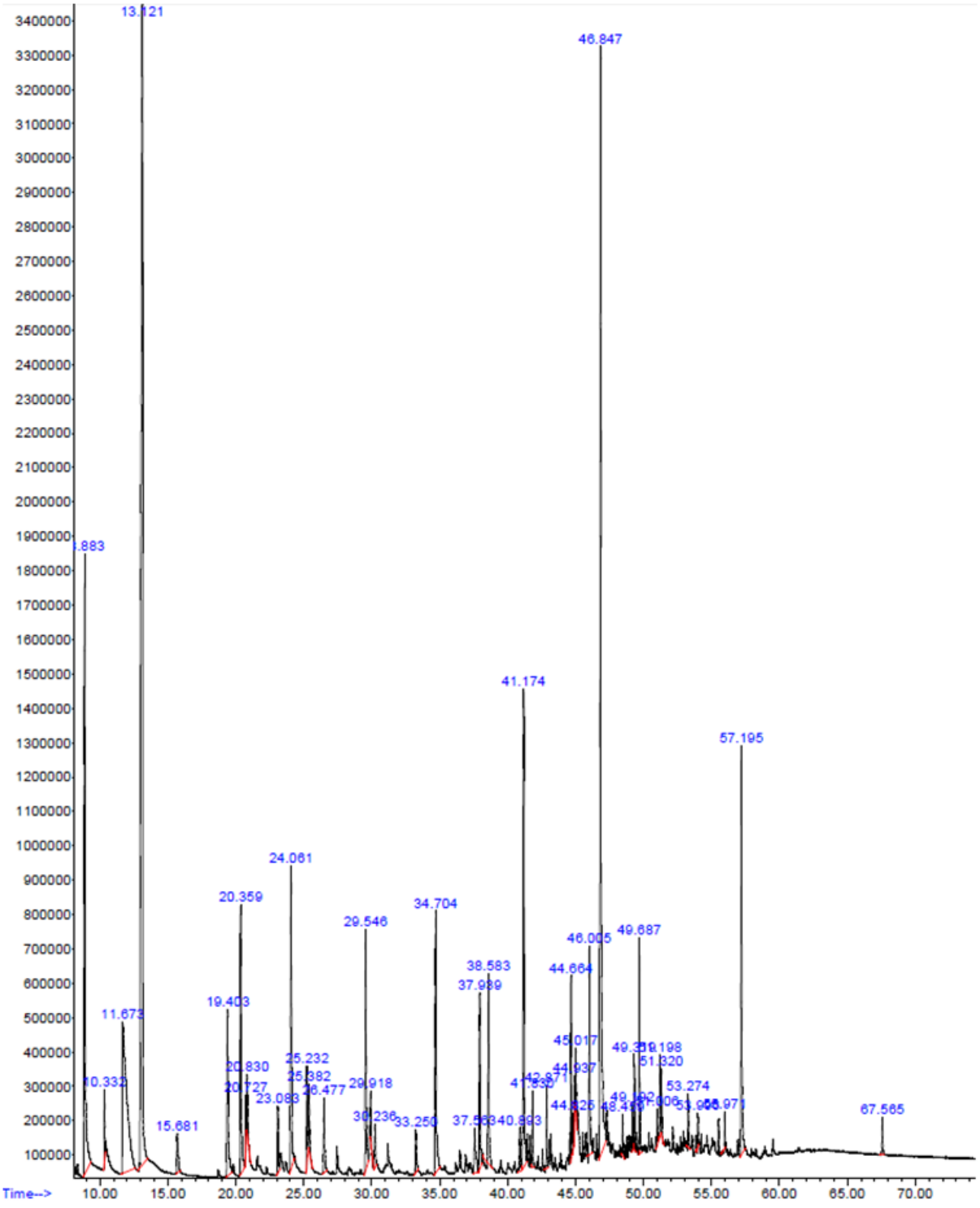

Figure E9: GC-MS Chromatogram (Abundance vs. Retention Time (min)) for Old Bio-Oil from Glossy Paper

Table E5: GC-MS Results for Old Bio-Oil at 20k/min for Glossy Paper

(Greater than 80% Quality of Fit (QoF) in NIST Library of Peaks at Retention Times (RT) in min)

Peak No.	RT	Area %	Library/ID	Ref#	CAS#	QoF
3	8.886	7.92	Acetaldehyde, hydroxy-	268	000141-46-8	72
4	10.334	0.56	Acetaldehyde, methoxy-	816	010312-83-1	83
5	11.673	7.5	Acetic acid	263	000064-19-7	91
6	13.122	21.56	2-Propanone, 1-hydroxy-	819	000116-09-6	90
7	15.683	0.7	Acetoin	2006	000513-86-0	78
9	19.401	2.16	Propanoic acid	811	000079-09-4	95
11	20.36	2.69	1-Hydroxy-2-butanone	2038	005077-67-8	90
19	24.062	3.35	Succindialdehyde	1662	000638-37-9	83
20	25.23	0.67	2-Cyclopenten-1-one	1176	000930-30-3	94
22	26.475	0.89	Butanoic acid	2020	000107-92-6	90
28	29.548	2.49	2-Furanmethanol	3079	000098-00-0	97
40	34.705	3.43	1,2-Cyclopentanedione	3095	003008-40-0	90
47	37.563	0.75	2-Cyclopenten-1-one, 3-methyl-	2824	002758-18-1	94
48	37.938	1.83	Butyrolactone	1649	000096-48-0	91
51	38.583	2.05	2(5H)-Furanone	1341	000497-23-4	94
57	41.177	4.18	1,2-Cyclopentanedione, 3-methyl-	6411	000765-70-8	94
61	41.827	0.52	2-Cyclopenten-1-one, 2-hydroxy-3,4-dimethyl-	11213	021835-00-7	87

77	44.664	1.01	2-Cyclopenten-1-one, 3-ethyl-2-hydroxy-	11198	021835-01-8	94
85	46.003	1.38	Hexanoic acid, 2-tetrahydrofurylmethyl ester	60982	002217-34-7	64
107	49.688	1.41	1,4:3,6-Dianhydro-.alpha.-d-glucopyranose	20631	1000098-14-8	96
152	57.196	3.56	.beta.-D-Glucopyranose, 1,6-anhydr0-	32447	000498-07-7	80